



PHD

Quinoline-8-carboxamide N-oxides as (bio)reductively-activated prodrugs of radiosensitisers and chemosensitisers

Lord, Anna-Marie

Award date:
2007

Awarding institution:
University of Bath

[Link to publication](#)

Alternative formats

If you require this document in an alternative format, please contact:
openaccess@bath.ac.uk

General rights

Copyright and moral rights for the publications made accessible in the public portal are retained by the authors and/or other copyright owners and it is a condition of accessing publications that users recognise and abide by the legal requirements associated with these rights.

- Users may download and print one copy of any publication from the public portal for the purpose of private study or research.
- You may not further distribute the material or use it for any profit-making activity or commercial gain
- You may freely distribute the URL identifying the publication in the public portal ?

Take down policy

If you believe that this document breaches copyright please contact us providing details, and we will remove access to the work immediately and investigate your claim.

Quinoline-8-carboxamide N-oxides as (bio)reductively-activated prodrugs of radiosensitisers and chemosensitisers

submitted by
Anna-Marie Lord
for the degree of PhD
of the University of Bath
2007

The research work in this thesis has been carried out in the Department of Pharmacy and Pharmacology, under the supervision of Dr Michael D. Threadgill and Dr Matthew D. Lloyd.

COPYRIGHT

Attention is drawn to the fact that copyright of this thesis rests with its author. This copy of the thesis has been supplied on condition that anyone who consults it is understood to recognise that its copyright rests with its author and that no quotation from the thesis and no information derived from it may be published without the prior written consent of the author.

This thesis may not be consulted, photocopied or lent to other libraries without the permission of the author for three years from the date of acceptance of the thesis.

..29th November 2007 ✓

.....*A.M.L.*.....

UMI Number: U491957

All rights reserved

INFORMATION TO ALL USERS

The quality of this reproduction is dependent upon the quality of the copy submitted.

In the unlikely event that the author did not send a complete manuscript and there are missing pages, these will be noted. Also, if material had to be removed, a note will indicate the deletion.



UMI U491957

Published by ProQuest LLC 2013. Copyright in the Dissertation held by the Author.
Microform Edition © ProQuest LLC.

All rights reserved. This work is protected against
unauthorized copying under Title 17, United States Code.



ProQuest LLC
789 East Eisenhower Parkway
P.O. Box 1346
Ann Arbor, MI 48106-1346

UNIVERSITY OF BATH
LIBRARY

40 - 4 AUG 2003

PhD.

Abstract

Poly(ADP-ribose) polymerase-1 (PARP-1) is a nuclear enzyme which is involved in control of DNA excision repair. PARP-1 is implicated in the resistance of tumour cells to radiotherapy or DNA-damaging chemotherapeutic agents. Inhibitors of PARP-1 may therefore be of use in the treatment of cancer as potentiators of radiotherapy and chemotherapy. Most potent inhibitors of PARP-1 are analogues of the nicotinamide of the substrate NAD^+ and contain a carboxamide group in which the amide is constrained in an *anti*-conformation to the aromatic ring.

Viable cells in hypoxic tissue present in many tumours are relatively resistant to radiotherapy and chemotherapeutic strategies. Previous studies have examined bioreductively-activated cytotoxins and prodrug systems which release drugs selectively in hypoxic tissue. The aim of the project was to develop novel hypoxia-activated N-oxide prodrugs of PARP-1 inhibitors. Synthetic approaches to 3- and 2-substituted quinoline-8-carboxamides and their corresponding N-oxides were studied.

A wide range of 3-substituted quinoline-8-carboxamides have been synthesised using 3-iodoquinoline-8-carboxamide as a precursor to palladium-catalysed coupling reactions, such as, Suzuki-Miyaura coupling, Stille coupling, and Sonogashira coupling. The intramolecular hydrogen-bond required for PARP-1 activity between the carboxamide N-H and the nitrogen of the quinoline was demonstrated by ^1H NMR spectroscopy and X-ray crystallography.

Suzuki-Miyaura coupling and Stille coupling of 2,8-dibromoquinoline proceeded in high regioselectivity for the 2-position. Lithium-bromine exchange, followed by quenching with trimethylsilylisocyanate led to the target 2-substituted quinoline-8-carboxamides.

A PARP-1 prodrug was designed based on N-oxide bioreduction. N-Oxidation of 3-phenylquinoline-8-carbonitrile with urea hydrogen peroxide complex and trifluoroacetic anhydride gave 8-cyano-3-phenylquinoline-1-oxide. Subsequent hydration with alkaline hydrogen peroxide gave the target 8-carbamoyl-3-phenylquinoline-1-oxide. Attempts to form 8-carbamoylquinoline-1-oxide and 8-carbamoyl-2-phenylquinoline-1-oxide are also discussed.

Quinoline-8-carboxamide and representative examples in the 3-substituted and 2-substituted quinoline-8-carboxamide series were evaluated for their inhibitory activity against recombinant human PARP-1. Seven compounds displayed inhibitory activity

equal or better than our lead compound 5-aminoisoquinolin-1-(2*H*)-one (5AIQ), the most potent inhibitor being 2-methylquinoline-8-carboxamide ($IC_{50} = 0.5 \mu\text{M}$). 8-Carbamoyl-3-phenylquinoline-1-oxide displayed inhibitory activity approximately equal to that of its non-oxide analogue 3-phenylquinoline-8-carboxamide.

Acknowledgements

First and foremost I would like to thank my supervisors, Dr Mike Threadgill and Dr Matthew Lloyd, for their patience, encouragement and enthusiasm throughout my PhD.

I would like to thank Dr Steve Black and Dr Tim Woodman for their NMR services, Mr Chris Cryer and Mr James Amato for the provision of Mass Spectra, Dr Mary Mahon for X-ray crystallography, Dr Andy Thompson for molecular modelling and also to all the postdoctoral and postgraduates in labs 3.11 and 3.14 for their help and advice.

I would like to acknowledge the Association for International Cancer Research for their generous funding.

I thank the postdoctoral and postgraduate colleagues I have worked with in 3.5/3.7, in particular Annika, Archana, Christian, Dan, Pete, Sabela, Vanja and Victoria, for their advice and friendship.

Thank you to Bernard Stricker (Nuffield A-level Bursary student) for assistance with some of the syntheses in this project.

I especially thank my parents and friends for their love and support throughout the course of my PhD.

Contents

Abstract		ii
Acknowledgements		iv
Contents		v
List of Figures, Schemes and Tables		ix
Abbreviations		xv
Chapter 1	Introduction	
1.1	Cancer	1
1.2	Tumour hypoxia	2
1.2.1	Hypoxia and Radioresistance	3
1.2.2	Hypoxia and Chemoresistance	5
1.2.3	Hypoxia-Inducible Factor-1	6
1.3	Bioreductive Prodrugs	9
1.3.1	Bioreductive activation	10
1.3.2	Nitroaromatics	12
1.3.3	Aromatic N-oxides	15
1.3.4	Aliphatic N-oxides	16
1.3.5	Quinones	18
1.4	Poly(ADP-ribose) polymerase	20
1.4.1	PARP-1 activation and catabolism	21
1.5	The PARP superfamily	24
1.5.1	PARP-2	24
1.5.2	PARP-3	25
1.5.3	Vault PARP	26
1.5.4	Tankyrases	26
1.5.5	PARP-7	27

1.6	PARP-1 inhibitors as chemosensitising and radiosensitising agents in cancer therapy	28
1.6.1	Future clinical implications of the inhibition of PARPs in cancer therapy	31
1.7	The role of PARP-1 inhibitors in other pathophysiological conditions	33
1.7.1	Regulation of cell survival and death by PARP	33
1.7.2	Role of PARP in ischaemia-reperfusion injury	34
1.7.3	Role of PARP-1 in inflammation	36
1.8	Current status of clinical trials on PARP inhibitors	38
1.9	PARP inhibitors	40
1.9.1	Nicotinamide and benzamide	40
1.9.2	Dihydroisoquinolinones and isoquinolinones	41
1.9.3	Benzoxazoles and benzimidazoles	43
1.9.4	Phthalazinones and quinazolinones	44
1.9.5	Quinoxalines	46
1.9.6	PARP inhibitors acting at the zinc fingers	47
1.10	Pharmacophore and structure-activity relationship (SAR) studies	47
1.11	Bioreductive prodrugs of PARP-1 inhibitors	49
Chapter 2	Aims and Objectives	
2.1	Design of substituted quinoline-8-carboxamides as novel PARP-1 inhibitors	53
2.2	Design of hypoxia-activated N-oxide prodrugs of substituted quinoline-8-carboxamide PARP-1 inhibitors	54
Chapter 3	Results and Discussion	
3.1	Route (I): 3-Substituted quinoline-8-carboxamides	56
3.1.1	Retrosynthetic analysis	56
3.1.2	Attempted syntheses of 3-aryl-8-methylquinolines	57
3.2	Route (II): 3-Substituted quinoline-8-carboxamides	59
3.2.1	Retrosynthetic analysis	59

3.2.2	Route (II): Synthesis of 3-aryl-8-substituted quinolines	60
3.3	Route (III): 3-Substituted quinoline-8-carboxamides	68
3.3.1	Route (III): Synthesis of 3-phenylquinoline-8-carboxamide	68
3.4	Route (IV): 3-Substituted quinoline-8-carboxamides	70
3.4.1	Route (IV): Synthesis of 3-iodoquinoline-8-carboxamide	70
3.4.2	The Suzuki-Miyaura coupling reaction	76
3.4.3	Suzuki-Miyaura coupling of 3-iodoquinoline-8-carboxamide with aryl and heteroaryl boronic acids	79
3.4.4	Attempted Suzuki-Miyaura coupling of 3-iodoquinoline-8-carboxamide with alkylboronic acids	86
3.4.5	Stille coupling reaction	87
3.4.6	Sonogashira coupling reaction	91
3.4.7	Palladium-catalysed cyanation of 3-iodoquinoline-8-carboxamide	97
3.5	2-Substituted quinoline-8-carboxamides	100
3.5.1	Attempted synthesis of 8-cyanoquinolin-2-yl trifluoromethanesulfonate	100
3.5.2	Synthesis of 2-aryl and 2-alkyl-quinoline-8-carboxamides	103
3.6	Quinoline-8-carboxamide N-oxides	110
3.6.1	Attempted synthesis of quinoline-N-oxides <i>via</i> reductive cyclisation of (<i>E</i>)-methyl 2-nitro-3-(3-oxo-2-phenylbut-1-enyl)benzoate.	110
3.6.2	Attempted syntheses of 8-carbamoylquinoline-1-oxide by direct N-oxidation	112
3.6.3	Attempted synthesis of 8-carbamoyl-2-phenylquinoline-1-oxide	116
3.6.4	Synthesis of 8-carbamoyl-3-phenylquinoline-1-oxide	118
Chapter 4	Biological Evaluation	
4.1	PARP-1 activity assay	125
4.1.1	Inhibition of PARP-1 activity by inhibitors	127
4.1.2	Structure activity relationship (SAR) studies of 3-substituted and 2-substituted quinoline-8-carboxamides as PARP-1 inhibitors	130

4.1.3	Structure activity relationship (SAR) studies of 8-carbamoyl-3-phenyl-quinoline-1-oxide	133
4.2	Sirtuins and NAD⁺ metabolism	135
4.2.1	SIRT1 activity assay	139
Chapter 5	Structural studies and molecular modelling	
5.1	Structural studies of quinoline-8-carboxamides	144
5.2	X-ray crystallography of 3-phenylquinoline-8-carboxamide and 2-(3-(trifluoromethyl)phenyl)quinoline-8-carboxamide	148
5.3	Molecular modelling studies of 8-carbamoyl-3-phenylquinoline-1-oxide	151
Chapter 6	Conclusions	153
Chapter 7	Experimental	156
References		202
Appendices		218

List of Figures, Schemes and Tables

Figures

Figure 1.	Mechanism of radiation cell killing.	3
Figure 2.	Mechanisms and consequences of HIF- α overexpression in cancer.	8
Figure 3.	General features of prodrugs.	10
Figure 4.	Mechanism of prodrug activation under hypoxia.	11
Figure 5.	Schematic view of the three functional domains of PARP-1.	21
Figure 6.	ADP-ribosylation of a protein acceptor. The ADP-ribose moiety conjugated to the protein can act as an acceptor for the addition of another ADP-ribose by PARP.	23
Figure 7.	Comparison of the domain structures of seven PARP isoforms.	25
Figure 8.	Potential clinical implications of vPARP and TANK-1 inhibitors.	32
Figure 9.	Intensity of DNA-damaging stimuli determines the fate of cells: survival, apoptosis or necrosis.	34
Figure 10.	Representation of the restriction of the carboxamide group into either the <i>anti</i> - or <i>syn</i> - conformation.	42
Figure 11.	Consensus pharmacophore for PARP-1 inhibition.	48
Figure 12.	Interactions of 2-(3-methoxyphenyl)benzimidazole-4-carboxamide with the NAD ⁺ binding domain, indicating the likely positioning of a substituent within the cavity.	49
Figure 13.	General structure of potential quinoline-8-carboxamide PARP-1 inhibitors.	54
Figure 14.	Partial HMBC spectrum of 8-nitro-3-phenylquinoline 62 .	63
Figure 15.	Electronic and steric properties of the 'SPhos' ligand.	84
Figure 16.	Structure of compound 111 and proton coupling constants (<i>J</i>).	90
Figure 17.	Assignment of ¹³ C NMR signals of 3-phenylquinoline-8-carbonitrile, 68 (top), and its N-oxide 176 (bottom).	122
Figure 18.	Structure of biotinylated NAD ⁺ .	126
Figure 19.	PARP-1 standard curve.	126
Figure 20.	Colourimetric readout of PARP-1 activity assay.	127
Figure 21.	PARP-1 inhibition curves for quinoline-8-carboxamide 80 and 5-AIQ.	128

Figure 22.	Proposed enzyme-inhibitor interactions between the PARP-1 active site and quinoline-8-carboxamides.	132
Figure 23.	Proposed binding interactions of EX527 (S-enantiomer) with the SIRT1 active site.	138
Figure 24.	Reaction Scheme of the SIRT1 Fluorescent Activity Assay.	140
Figure 25.	Proposed functional interplay between PARP-1 and SIRT1.	143
Figure 26.	Comparison of the N-H signals of 3-phenylquinoline-8-carboxamide in CDCl ₃ (top) and (CD ₃) ₂ SO (bottom).	145
Figure 27.	¹ H- ¹ H COSY spectrum of 3-phenylquinoline-8-carboxamide 69 .	146
Figure 28.	¹ H NMR spectrum of 3-(3-(trifluoromethyl)phenyl)quinoline-8-carboxamide 94 in (CD ₃) ₂ SO.	146
Figure 29.	¹ H NMR spectrum of 8-carbamoyl-3-phenylquinoline-1-oxide 175 in (CD ₃) ₂ SO.	147
Figure 30.	X-ray crystal structure of 3-phenylquinoline-8-carboxamide 69 .	149
Figure 31.	Intermolecular and intramolecular hydrogen bonding present in crystals of 69 .	149
Figure 32.	X-ray crystal structure of 3-(2-(trifluoromethyl)phenyl)quinoline-8-carboxamide 96 , showing intramolecular hydrogen-bonding interactions.	150
Figure 33.	Calculated enantiomeric minimum-energy conformations of 175 .	152

Schemes

Scheme 1.	Reductive activation of nitroaromatic prodrugs.	12
Scheme 2.	Proposed mechanism for the reductive elimination of aspirin from (1-methyl-2-nitroimidazol-5-yl) methyl 2-acetoxybenzoate.	13
Scheme 3.	Proposed mechanism for the release of a cyclophosphoramidate moiety from a nitroquinoline prodrug under hypoxic conditions.	14
Scheme 4.	Bioreductive activation of prodrug 4 .	14
Scheme 5.	Bioreductive activation of tirapazamine.	15
Scheme 6.	Mechanism of activation of AQ4N.	17
Scheme 7.	Reductive activation of a quinone bioreductive system.	19
Scheme 8.	Schematic representation of poly(ADP-ribosyl)ation.	22
Scheme 9.	Reductive release of isoquinolin-1-one 34 from the prodrug 32 .	50
Scheme 10.	Reductive release of 5-bromoisoquinolinone 37 from the prodrug 35 .	51
Scheme 11.	Proposed mechanism of reductively triggered release of drugs from dioxindole-3-methyl prodrugs.	51
Scheme 12.	Route (I) retrosynthetic analysis of 3-arylquinoline-8-carboxamides.	56
Scheme 13.	Attempted synthesis of 3-bromo-8-(bromomethyl)quinoline.	58
Scheme 14.	Attempted synthesis of 3-hydroxy-8-methylquinoline 52 .	59
Scheme 15.	Retrosynthetic analysis of 3-arylquinoline-8-carboxamides.	60
Scheme 16.	Electrophilic bromination and iodination of 8-nitroquinoline.	61
Scheme 17.	Route (II) synthesis of 3-phenylquinoline-8-carboxamide 69 .	64
Scheme 18.	Proposed mechanism for the synthesis of quinoline-8-carbonitrile 72 .	65
Scheme 19.	Proposed mechanism for the hydrolysis of 3-phenylquinoline-8-carbonitrile 68 using H ₂ O ₂ and NaOH.	66
Scheme 20.	Route (III) synthesis of 3-phenylquinoline-8-carboxamide 69 .	69
Scheme 21.	Synthesis of 3-iodoquinoline-8-carboxamide 77 .	71
Scheme 22.	Proposed mechanism of palladium-catalysed cyanation of aryl triflates in the presence of a copper iodide co-catalyst.	72

Scheme 23.	Proposed formation of iodine trifluoroacetate active species.	74
Scheme 24.	Proposed mechanism for the Lewis acid-catalysed iodination of quinoline-8-carboxamide with NIS as the iodinating reagent.	75
Scheme 25.	Proposed palladium-catalysed cross-coupling reactions with 3-iodoquinoline-8-carboxamide 77 .	76
Scheme 26.	General catalytic cycle for the Suzuki-Miyaura coupling of aryl halides with arylboronic acids.	77
Scheme 27.	Reported Suzuki-Miyaura coupling of 84 with the electron deficient 2,3-difluorophenylboronic acid.	78
Scheme 28.	Reported synthesis of 6-[4-(4-fluorophenoxy)phenyl]pyridine carboxamides.	78
Scheme 29.	Proposed mechanism for the formation of compound 103 .	83
Scheme 30.	Reported Heck coupling of 3-bromoquinoline with styrene.	84
Scheme 31.	Photo-induced conversion of 102a to 102b .	86
Scheme 32.	Proposed mechanism for the Stille coupling reaction between 3-iodoquinoline-8-carboxamide 77 and tetramethylstannane.	88
Scheme 33.	Synthesis of tributylbenzylstannane 110 .	90
Scheme 34.	Proposed mechanism for the copper effect on the Stille coupling of tributylethynylstannane with 3-iodoquinoline-8-carboxamide 77 .	91
Scheme 35.	Formation of by-product 115 from the Sonogashira coupling of 3-iodoquinoline-8-carboxamide 77 with alkyne 114 .	92
Scheme 36.	Reported synthesis of 3-ethynylquinoline.	92
Scheme 37.	Proposed mechanism for the Sonogashira coupling between 3-iodoquinoline-8-carboxamide 77 and trimethylsilylethyne.	94
Scheme 38.	Proposed mechanism for the Ag ⁺ -catalysed deprotection of 3-((trimethylsilyl)ethynyl)quinoline-8-carboxamide 120 .	95
Scheme 39.	Synthesis of 3-ethynylquinoline-8-carboxamide 114 and subsequent reduction to 3-ethylquinoline-8-carboxamide 123 .	96
Scheme 40.	Sonogashira coupling of 3-ethynylquinoline-8-carboxamide 114 with 4-iodotoluene.	97
Scheme 41.	Palladium-catalysed cyanation of 3-iodoquinoline-8-carboxamide 77 with CuCN.	98

Scheme 42.	Attempted synthesis of 8-cyanoquinolin-2-yl trifluoromethanesulfonate 131 .	101
Scheme 43.	Proposed mechanism for the Friedel-Crafts-like cyclisation of <i>E</i> - <i>N</i> -(2-bromophenyl)-3-phenylpropenamide 128 using AlCl ₃ in chlorobenzene.	102
Scheme 44.	Regioselective Suzuki-Miyaura coupling of 2,8-dibromoquinoline 133 with arylboronic acids.	105
Scheme 45.	Reported regioselective couplings of 2,4-dibromoquinoline.	106
Scheme 46.	Attempted synthesis of 8-bromo-2-((trimethylsilyl)ethynyl)quinoline 137 .	106
Scheme 47.	Regioselective Stille coupling of 2,8-dibromoquinoline 133 and organostannanes.	107
Scheme 48.	Synthesis of 8-bromo-2-methylquinoline 139 .	108
Scheme 49.	Synthesis of 2-substituted quinoline-8-carboxamides.	108
Scheme 50.	Attempted synthesis of substituted quinoline-8-carboxamide-1-oxides.	111
Scheme 51.	Attempted syntheses of 8-carbamoylquinoline-1-oxide 158 .	116
Scheme 52.	Attempted synthesis of 8-carbamoyl-2-phenylquinoline-1-oxide 168 .	117
Scheme 53.	Attempted synthesis of 8-carbamoyl-3-phenylquinoline-1-oxide 175 .	119
Scheme 54.	Synthesis of 8-carbamoyl-3-phenylquinoline-1-oxide 175 .	120
Scheme 55.	Mechanism of SIRT-catalysed deacetylation.	135

Tables

Table 1.	PARP inhibition in animal models of ischaemia-reperfusion injury.	36
Table 2.	PARP inhibitors in clinical trials.	38
Table 3.	PARP-1 inhibitory activities of benzoxazoles and benzimidazoles.	44
Table 4.	PARP-1/2 inhibitory activities of quinazolinones.	45
Table 5.	PARP-1/2 inhibitory activities of phthalazinones.	46
Table 6.	PARP-1/2 inhibitory activities of quinoxalines.	46
Table 7.	Suzuki-Miyaura coupling of 60 and 61 with arylboronic acids.	62
Table 8.	The iodination properties of ICI and NIS in combination with various Lewis acids.	74
Table 9.	Suzuki-Miyaura coupling of 3-iodoquinoline with aryl and heteroaryl boronic acids.	80
Table 10.	Reaction conditions for the attempted cross-coupling of 77 with alkylboronic acids.	87
Table 11.	Stille cross-coupling of 77 with organostannane reagents.	89
Table 12.	Small compound library of 3-substituted quinoline-8-carboxamides.	99
Table 13.	Yields of 2-aryl and 2-alkyl substituted quinoline-8-carboxamides.	109
Table 14.	Attempted N-oxidations of 8-substituted quinoline.	113
Table 15.	Reaction of (1-oxidoquinolin-8-yl)mercury(II) chloride with various electrophiles.	115
Table 16.	Inhibition of PARP-1 activity by quinoline-8-carboxamides and 5-AIQ control.	129
Table 17.	PARP-1 inhibitory activities of the benzimidazole analogues.	131
Table 18.	PARP-1 inhibitory activities of 8-carbamoyl-3-phenylquinoline-1-oxide 175 3-phenylquinoline-8-carboxamide 69 .	133
Table 19.	Summary of mammalian sirtuins, their localisation, activities, interactions and biological functions.	137
Table 20.	Summary of the SIRT1 plate readings for quinoline-8-carboxamide.	141

Abbreviations

AAIS	amino-acid stimulated insulin secretion
3-AB	3-aminobenzamide
Ac	acetyl
AceCS2	acetyl-CoA-synthetase-2
AcOH	acetic acid
5-AIQ	5-aminoisoquinolin-1(2 <i>H</i>)-one
ADEPT	antibody directed enzyme-prodrug therapy
ADP	adenosine diphosphate
ANK	ankyrin
Aq.	aqueous
ARNT	aryl hydrocarbon receptor nuclear translocator
Asp	aspartic acid
ATP	adenosine triphosphate
BRCA	breast cancer gene
BRCT	breast cancer susceptibility protein, BRCA1, C-terminus
Bu	butyl
BSA	bovine serum albumin
CF	catalytic fragment
Calcd	calculated
CHO	Chinese hamster ovary
COSY	correlation spectroscopy
C_q	quaternary carbon
d	day(s)
Da	daltons
dba	dibenzylideneacetone
DBD	DNA binding domain
DCM	dichloromethane
DIPA	diisopropylamine
DMF	<i>N,N</i> -dimethylformamide
DMSO	dimethyl sulphoxide
DNA	deoxyribonucleic acid
DPPF	1,1'-bis(diphenylphosphino)ferrocene
DSB	double strand breaks
ES	electrospray
EtOAc	ethyl acetate

EtOH	ethanol
FAB	fast atom bombardment
FGI	functional group interconversion
FOXO	forkhead box O transcription factor
g	gram(s)
GDEPT	gene-directed enzyme-prodrug therapy
GDH	glutamate dehydrogenase
Gln	glutamine
Gly	glycine
h	hour(s)
HDAC	histone deacetylase
HIF	hypoxia-inducible factor
HIV	human immunodeficiency virus
HMBC	heteronuclear multiple bond correlation
HMQC	heteronuclear multiple quantum coherence
HOMO	highest occupied molecular orbital
HPLC	high pressure liquid chromatography
HRE	hypoxia-response element
I/R	ischaemia reperfusion
IC₅₀	concentration required for 50% inhibition of activity
IR	infrared
J	coupling constant
K_i	inhibition constant
Lit.	literature
LPS	lipopolysaccharides
LRP	lung resistance-related protein
LUMO	lowest unoccupied molecular orbital
Lys	lysine
M	molar
Me	methyl
2ME2	2-methoxyoestradiol
MeOH	methanol
MCPBA	<i>meta</i> -chloroperoxybenzoic acid
MDR1	multidrug resistance gene
min	minute(s)
mL	millilitre(s)
MNNG	<i>N</i> -methyl- <i>N'</i> -nitro- <i>N</i> -nitrosoguanidine

mol	mole(s)
mp	melting point
MPTP	1-methyl-4-phenyl-1,2,3,6-tetrahydropyridine
MS	mass spectrum
MTO	methyltrioxorhenium
MVP	major vault protein
<i>m/z</i>	mass to charge ratio (mass spectroscopy)
NAD⁺	nicotinamide adenine dinucleotide
NADPH	reduced nicotinamide adenine dinucleotide phosphate
NBS	<i>N</i> -bromosuccinimide
NIS	<i>N</i> -iodosuccinimide
NLS	nuclear localisation signal
NMP	<i>N</i> -methylpyrrolidinone
NMR	nuclear magnetic resonance
NuMA	nuclear mitotic apparatus
OER	oxygen enhancement ratio
PARG	poly(ADP-ribose) glycohydrolase
PARP	poly(ADP-ribose) polymerase
PBS	phosphate-buffered saline
Ph	phenyl
PHD	prolyl-4-hydroxylase domain
PID	poly(ADP-ribose) polymerase inhibitory dose
PI3K	phosphatidylinositol-3-kinase
ppm	parts per million
Pro	proline
PTEN	phosphatase and tensin homologue
R_f	retention factor
RNA	ribonucleic acid
RNP	ribonucleoprotein
SAM	sterile alpha motif
SAR	structure activity relationship
SEM	standard error of the mean
Ser	serine
ySir2	yeast silent information regulator 2
SIRT	sirtuin
S_N2	bimolecular nucleophilic substitution
SSB	single strand breaks

Strep-HRP	streptavidin horseradish peroxidase
STZ	streptozotocin
TANK	tankyrase
TCA	trichloroacetic acid
TCCD	tetrachlorodibenzodioxin
TF1	telomeric repeat binding factor 1
TFA	trifluoroacetic acid
TFAA	trifluoroacetic anhydride
THF	tetrahydrofuran
TLC	thin layer chromatography
TMS	trimethylsilyl
TMZ	temozolomide
Tyr	tyrosine
UHP	urea hydrogen peroxide complex
UV	ultraviolet
VEGF	vascular endothelial growth factor
VHL	von Hippel-Lindau protein
vPARP	vault poly(ADP-ribose) polymerase
vRNA	vault ribonucleic acid

1. Introduction

1.1 Cancer

Cancer is a disease caused by the uncontrolled division of the body's cells. Cancer cells may invade the surrounding tissue, or metastasise through the bloodstream or lymphatic system to other parts of the body. Cancer is the main cause of mortality in developed countries, with one person in three estimated to develop the disease in their lifetime. The most widely used cancer therapies are radiotherapy, surgery and chemotherapy. The effectiveness of these treatments is limited by the toxicity to normal cells in the body.

Surgical procedures are used to remove malignant tissue physically. The complete removal of cancer by surgery is only successful if the disease has not metastasised to other sites in the body prior to the surgical procedure. Consequently, a non-surgical procedure is often also required in the treatment of cancer.

During radiation therapy, cancer cells are exposed to ionising radiation and the resulting damage causes the death of the cell when it tries to divide. The radiation is focused like a beam of light on the treated area called a radiation field, but cancer cells that are outside of the irradiated area will not be damaged. The specific target of radiation damage is DNA. The radiation causes either single or double strand breaks in the DNA and cells are most susceptible to damage during the mitotic or actively dividing stage of the cell cycle. Both cancer cells and normal cells use the same mechanisms for cell division. Therefore, radiotherapy kills malignant cells as well as rapidly dividing normal cells. This results in acute side effects of radiotherapy, and cells that divide as fast as cancer cells are very sensitive, such as hair follicles, bone marrow and gut epithelia.

The use of chemotherapy began in the 1940's with the discovery of nitrogen mustards as an effective treatment for cancer. Like radiotherapy, chemotherapy is designed to kill proliferating cells. However, chemotherapy has the advantage that it is a systemic treatment and therefore can be used to treat distant metastasis. A considerable number of anti-cancer drugs have been developed and all cell cycle phases can be targeted. Chemotherapeutic agents have been successful in improving the prognosis of many malignant conditions such as acute leukaemia, Hodgkin's disease and testicular cancer.¹ The disadvantage of these cytotoxic agents is their limited selectivity

towards cancer cells, which leads to the common side effects associated with cancer chemotherapy. Slow growing solid tumours such as carcinomas of the breast and lung respond poorly to chemotherapy, as the tumour cells are not dividing rapidly.

Investigators have made progress in understanding the basic cellular and molecular mechanisms of cancer therapy resistance. Many of these investigative efforts have focused on intrinsic cellular characteristics, such as the multi-drug resistance phenomenon, gene amplification, and radiation sensitivity. However, there is a second aspect of cancer treatment resistance that is related to the physiological state of the cell and not to intrinsic cellular properties. The physiology of solid tumour tissue is sufficiently different from that of normal tissue, mainly due to differences in the tumour vasculature. These physiological differences create both problems and opportunities in cancer treatment.

1.2 Tumour hypoxia

Thomlinson and Gray² first discovered and described tumour hypoxia. Tumours become hypoxic because the new blood vessels they develop cannot sufficiently supply oxygen and other nutrients to the cells. The normal vasculature is organised with vessels close to cells to ensure an adequate oxygen supply. In comparison the tumour vasculature is often highly irregular, with leaky vessels and sluggish blood flow. The first type of hypoxia is known as chronic or diffusion hypoxia.³ At a distance of about 150 μm from the capillary, cells tend to be well oxygenated. Beyond this distance, the oxygen tension becomes effectively zero and cells become necrotic. Hypoxic cells tend to occur at the interface regions between the well-oxygenated tissue and necrotic zones. Hypoxic cells are viable but sufficiently hypoxic to make them resistant to radiation. The second type of hypoxia is known as transient or perfusion hypoxia and occurs due to the opening and closing of blood vessels, placing sections of tissue under hypoxia for shorter time periods.⁴ Perfusion-limited hypoxia leads to 'reoxygenation injury' and results in an increase in free-radical concentrations, tissue damage and activation of stress-response genes.

The pioneering work of Hockel *et al.*⁵ demonstrated that low oxygen tension in tumours was related to increased metastasis and poor survival in patients suffering from squamous tumours of the head and neck, cervical or breast cancers. They studied measurements of tumour oxygen levels using oxygen electrodes. More efficient, less invasive methods to measure tumour hypoxia *in vivo* have been developed. These

include magnetic resonance imaging techniques,⁶ positron emission tomography scanning with ¹⁸F-labelled hypoxia-activated drugs,⁷ and radiolabelled hypoxia-activated bioreductive drugs.⁸

1.2.1 Hypoxia and Radioresistance

Ionising radiation kills cells by causing damage to the DNA, particularly DNA double strand breaks. Firstly, the target DNA radical (DNA·) is produced, either by direct ionisation or from radiolysis of neighbouring water molecules. Under aerobic conditions, reaction with oxygen (O₂) produces a peroxy radical (DNA-OO·), which causes irreversible damage to the DNA. Under hypoxic conditions, reducing species, such as thiols (-SH), can react with the target radical by hydrogen (H·) donation, resulting in the restoration of the DNA to its original state (Figure 1). The ability of oxygen to act as a sensitising agent is described by the oxygen enhancement ratio (OER). The OER is quantified as the factor by which the dose in the presence of oxygen should be multiplied in order to obtain the same surviving fraction of cells for hypoxic conditions. Mammalian cells irradiated in the presence of air are 2.5-3.0 times more sensitive than are cells irradiated under conditions of severe hypoxia (low oxygen concentration). Consequently, hypoxic cells require a dose three times higher to kill them, which the surrounding normal cells cannot tolerate.

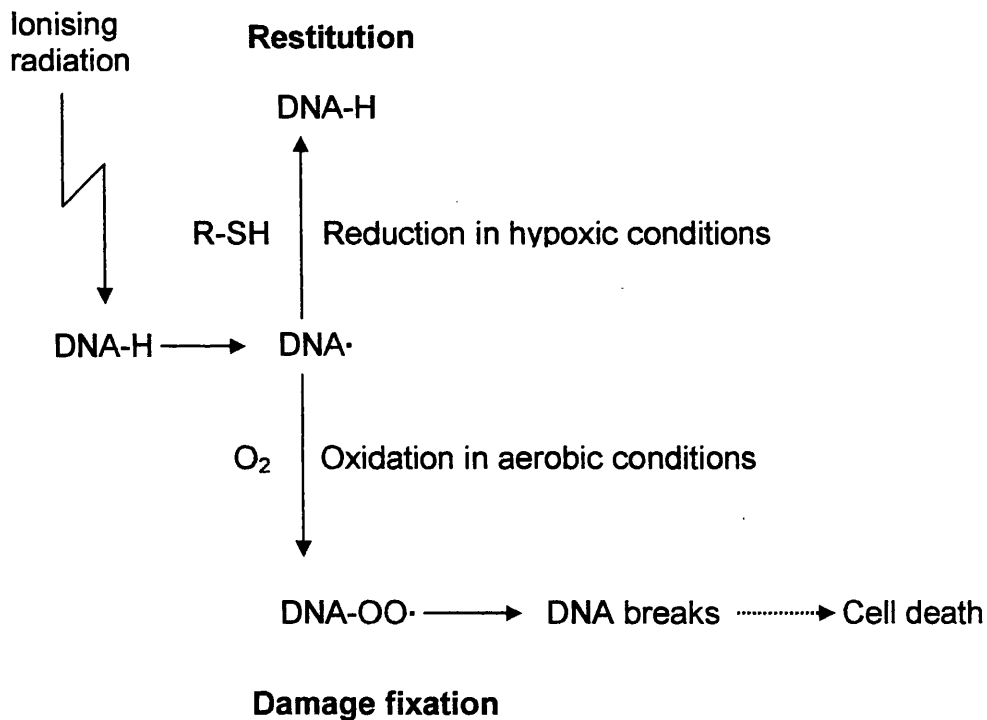
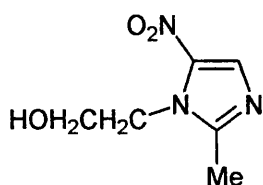


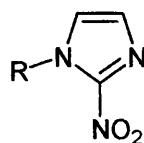
Figure 1. Mechanism of radiation cell killing.³

Hyperbaric oxygen chambers were first used 50 years ago to increase oxygen delivery to tumours and thus to overcome hypoxia as a cause of radioresistance. The approach involves the administration of 100% oxygen at a pressure greater than 1 atmosphere (atm).⁹ Clinical trials using hyperbaric chambers have only had moderate success. However, significant benefit was found with head and neck cancer¹⁰ and carcinoma of the cervix.¹¹

Another approach to target radioresistant hypoxic cells is the use of radiosensitising drugs. These drugs are given shortly before a patient receives radiotherapy and interact with short-lived radicals that are produced during radiation. Radiosensitisers are designed to mimic the sensitising effect of oxygen and act to restore the radiosensitivity of hypoxic cells. These drugs are capable of diffusing further than oxygen from the vascular capillaries and can penetrate hypoxic regions of tumour cells. The radiosensitising efficiency of a compound towards hypoxic cells has been demonstrated to be dependent on the one-electron reduction potential.¹² The first clinical trial data published on hypoxic radiosensitisation used the electron-affinic nitroimidazole metronidazole **1**, which was found to have an E^1_7 reduction potential of -486 mV. Urtasun *et al.*¹³ showed enhanced survival rates of patients with glioblastoma due to radiosensitisation of hypoxic cells. The large amount of this drug required to produce adequate enhancement ratios *in vivo* led to the search for more active nitroimidazoles. A more potent radiosensitising drug called misonidazole **2** was soon developed, which was found to have an E^1_7 reduction potential of -389 mV. In addition, misonidazole was found to be superior to metronidazole both *in vitro* and *in vivo* studies. Unfortunately, in clinical trials misonidazole was observed to have a dose-limiting neurotoxicity, limiting the dose of drug that could be used in radiotherapy.¹⁴ Brown and co-workers¹⁵ developed a series of analogues of misonidazole with the same electron affinity but with reduced lipophilicity. The optimum compound chosen was SR 2508 (etanidazole, **3**) due to its favourable *in vitro* radiosensitisation and toxicity properties. However, Phase III clinical trials comparing radiotherapy of head and neck cancer with or without etanidazole failed to show any significant benefits.¹⁶



1



2 R = CH₂CH(OH)CH₂OCH₃

3 R = CH₂NHCO(CH₂)₂OH

1.2.2 Hypoxia and Chemoresistance

In solid tumours, a number of factors associated with tumour hypoxia contribute to resistance to drugs. Hypoxia can be a direct cause of therapeutic resistance because some anti-cancer agents require cellular oxygen to be maximally cytotoxic. For example, Teicher *et al.*¹⁷ demonstrated that tumour cells in aerobic conditions were more sensitive to melphalan, in contrast to their hypoxic counterparts. Hypoxia can also cause cells to stop or slow their rate of progression through the cell cycle.¹⁸ The rate of cell proliferation decreases with increasing distance from the tumour vasculature. Most anti-cancer drugs are selective at killing rapidly proliferating cells. Therefore, non-proliferating cells or slowly proliferating cells remain resistant to treatment. Furthermore, anti-cancer agents act mainly during DNA synthesis by causing damage to DNA. Studies by Walker *et al.*¹⁹ demonstrated that DNA-damaging anti-cancer agents had a reduced efficacy due to an increased activity of DNA repair enzymes under hypoxic conditions.

Anti-cancer agents reach their target through the circulatory system. The fluctuating blood flow present in tumours due to arteriovenous shunts and dysfunctional blood vessels, which close and re-open, results in poor perfusion and a disordered blood supply. Subsequently, any cells surrounding closed blood vessels will be exposed to lower levels of anti-cancer drugs than those surrounding blood vessels with normal flow.⁴ In order for anti-cancer drugs to be therapeutically effective they must be able to access all viable cells within the tumour. As mentioned previously, solid tumours contain hypoxic cells that are usually located some distance away from the nearest microcapillary.²⁰ The location of these cells creates a challenge to the physical delivery of anti-cancer drugs, as the large chemotherapeutic agents need to penetrate several layers of tissue to reach their target and cause lethal toxicity. The penetration of anti-cancer drugs into tumour tissue has been studied by autoradiography and fluorescence. These studies demonstrated poor penetration for doxorubicin, vinblastine and methotrexate.²⁰

There are also other ways in which hypoxia might contribute to drug resistance. Comerford and co-workers²¹ identified the P-glycoprotein as a pathway for tumour drug resistance and proposed that the multi-drug resistance gene (MDR1) was hypoxia-responsive. It has also been demonstrated that stress conditions, such as glucose starvation, hypoxia and low pH that induce stress proteins, are seen in most solid

tumour cells. Hypoxic stress proteins appear to be responsible for cellular resistance to anti-cancer drugs, such as etoposide,²² doxorubicin,²³ and cisplatin.²¹

1.2.3 Hypoxia-Inducible Factor-1

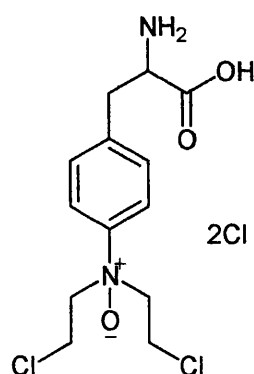
Mammalian cells respond to hypoxic conditions through the hypoxia-inducible transcription factor 1 (HIF-1). HIF-1 is a heterodimeric DNA-binding complex and consists of the hypoxic response factors HIF-1 α and HIF-1 β . HIF-1 acts as global regulator of oxygen homeostasis.²⁴ HIF-1 β is an aryl hydrocarbon receptor nuclear translocator (ARNT) and its activity is independent of concentration of oxygen. Expression of HIF-1 α is induced by cellular hypoxia and is maintained at low levels in most cells with normal concentrations of oxygen. The molecular recognition of oxygen by HIF-1 is primarily determined by the α -subunit.²⁵ The most widely studied mechanism of HIF-1 α protein regulation is the pathway mediated by the von Hippel-Lindau protein (VHL). Under normal oxygen concentrations, HIF-1 α is rapidly and continuously degraded by ubiquitination and proteosomal degradation. Degradation of HIF-1 α is dependent on binding with von Hippel-Lindau protein, which is mediated by hydroxylation of two specific proline residues (Pro402 and Pro564) by a prolyl-4-hydroxylase domain (PHD). PHDs are dioxygenases that require oxygen, Fe²⁺, and 2-oxoglutarate as substrates. Under low oxygen concentrations, the HIF proline residues remain unmodified, preventing binding of the von Hippel-Lindau protein, and HIF-1 α levels increase. HIF-1 α translocates to the nucleus, where it dimerises with HIF-1 β and activates transcription genes. These genes contain a hypoxia-response element (HRE) to which the HIF dimer binds. The activation of hypoxia-response genes enables cells to respond to hypoxic conditions by controlling metabolism, cell growth and angiogenesis.²⁶

The von Hippel-Lindau protein pathway is not the only mechanism controlling levels of HIF-1 α . The MDM2 ubiquitin protein ligase is recruited to HIF-1 α by binding of the tumour suppressor p53, which results in a decrease in HIF-1 α levels. The loss of p53 in tumour cells enhances HIF-1 α levels and promotes neovascularisation and growth of tumour xenografts in nude mice.²⁷ The control of HIF-1 by oncogenic signalling has also been demonstrated. For example, the phosphatidylinositol-3-kinase (PI3K) pathway increases HIF-1 α -mediated transcription of the vascular endothelial growth factor (VEGF) in tumour cells lines.²⁸

Overexpression of HIF-1 α has been shown in a number of cancers and has been linked with poor prognosis of patients receiving cancer treatment. Zhong *et al.*²⁹ analysed HIF-1 α in 179 tumour specimens using immunohistochemical techniques. They demonstrated that HIF-1 α was overexpressed in 13 out of 19 common cancers in comparison to normal tissue. These included colon, breast, gastric, lung, skin, ovarian, pancreatic, prostate, and renal carcinomas. HIF-1 α protein was also expressed in pre-malignant tissue, such as colonic adenoma, breast ductal carcinoma *in situ*, and prostate intraepithelial neoplasia. This suggests that HIF-1 α may represent an early biomarker for aggressive disease.

HIF-1 α overexpression can occur due to hypoxia independent mechanisms. HIF-1 α is expressed in the majority of tumour cells in haemangioblastoma, despite the highly vascularised nature of this tumour. It has also been demonstrated that mutations in oncogenes and loss of function in tumour-suppressor genes, VHL, PTEN or p53 are associated with higher HIF-1 α expression in human cancers. For instance in renal cancer, mutations in VHL resulted in an accumulation of HIF-1 α .^{30,31} Overall, hypoxia-induced expression of HIF-1 appears to be essential for vascularisation and other aspects of tumour progression (Figure 2).

There is currently interest in the use of HIF-1 α as a target for the development of cancer therapy. A variety of anti-cancer drugs that directly and indirectly inhibit HIF-1 have been reported. One approach to selectively targetting HIF-1 signalling is to inhibit HIF-1 α transcription or translocation.³² PX-478, a novel inhibitor of HIF-1 α , decreases cellular HIF-1 α protein levels under hypoxic and non-hypoxic conditions. PX-478 showed anti-tumour activity against a variety of human xenografts characterised by marked tumour regressions and prolonged tumour growth delays.³³



PX-478

Echinomycin, a cyclic peptide of the family of quinoxaline antibiotics, inhibits HIF-1 α DNA binding, thus inhibiting its ability to target genes transcriptionally. However, it has not been established whether echinomycin has potential therapeutic benefits *in vivo*.³⁴

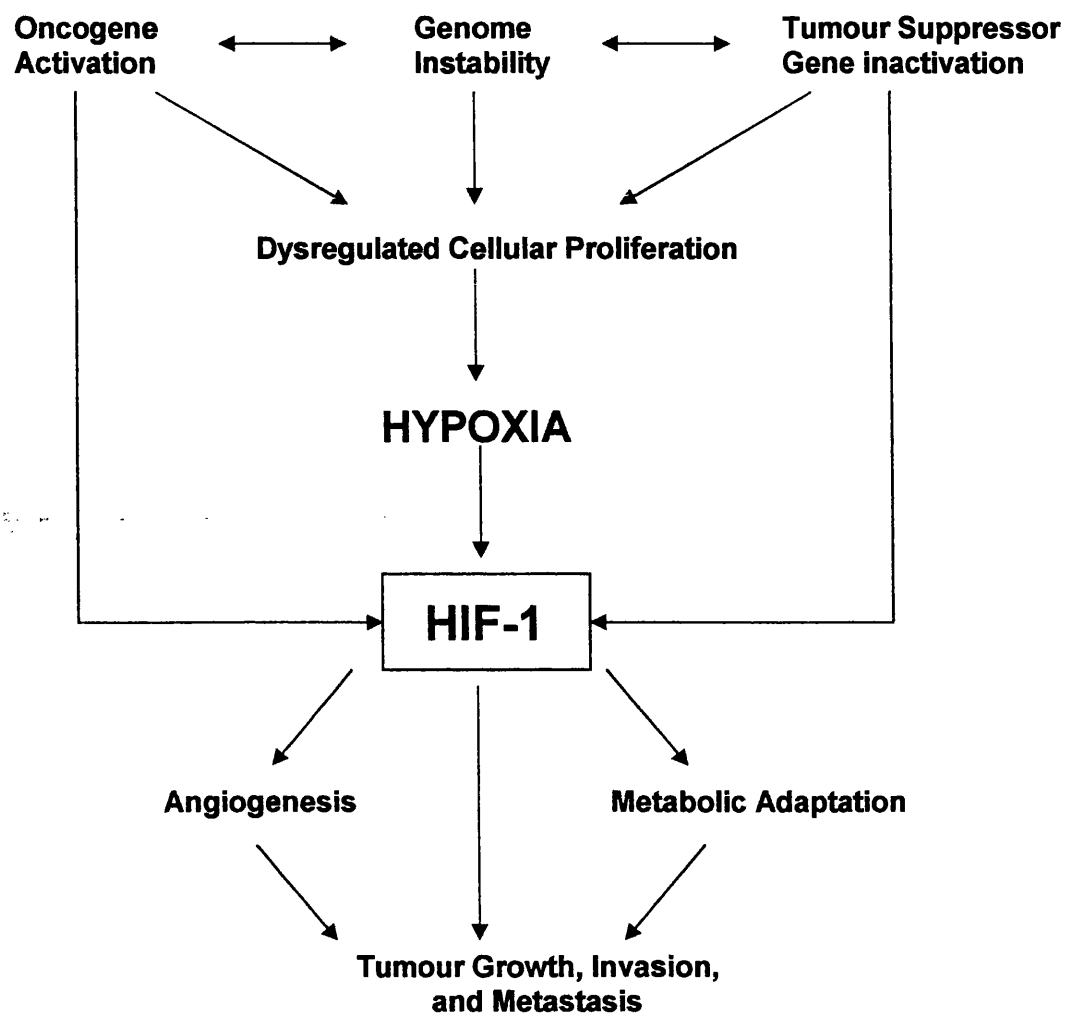


Figure 2. Mechanisms and consequences of HIF-1 α overexpression in cancer.³⁵

The National Cancer Institute's drug library revealed that several camptothecan analogues, including topotecan, blocked expression of HIF-1 α . Studies have indicated that topotecan does not affect the half-life of the HIF-1 α protein or accumulation of mRNA but inhibits translation.³⁶ Yeo *et al.*³⁷ showed that YC-1 [3-(5'-hydroxymethyl-2'-furyl)-1-benzylindazole] demonstrated anti-tumour and antiangiogenic effects. YC-1 decreases HIF-1 α levels and shows anti-tumour activity against human tumour xenografts.

Another class of compounds that affect HIF-1 activity are known as thioredoxin inhibitors. These compounds inhibit redox signalling by inhibiting Trx-1. Thioredoxin inhibitors decrease expression of HIF-1 α , tumour VEGF, and tumour angiogenesis in human tumour xenografts in mice.³⁸

Finally, 2-methoxyoestradiol (2ME2) a microtubule-targeting agent has been reported to inhibit HIF-1 α stability. Majeesh *et al.*³⁹ demonstrated that these microtubule agents inhibit the expression of HIF-1 α in normoxic and hypoxic cancer cells. It was also demonstrated that 2ME2 inhibits the expression of VEGF and other HIF-1 target genes. Overall, it seems that none of the anti-cancer drugs mentioned selectively target HIF-1.

1.3 Bioreductive Prodrugs

Adrien Albert first introduced the prodrug concept in 1958.⁴⁰ A prodrug is defined as an inactive compound that is converted in the body by metabolism or spontaneous chemical breakdown to form a pharmacologically active species.⁴¹ There has been much interest in the use of bioreductive prodrugs in cancer therapy. The majority of clinically used anti-cancer drugs are not selective for cancer cells, and their therapeutic efficacy is limited by the damage they cause to normal cells in the body. The hypoxic cells in solid tumours exist in an environment that can be used to generate reduced derivatives of a variety of chemical groups, and bioreductive prodrug compounds have been developed to exploit such environments.⁴² In order to achieve success a bioreductive prodrug must meet four basic criteria:

- (1) The prodrug must be able to distribute effectively to hypoxic regions in tumours.
- (2) The bioreductive drug should have a half-life that allows diffusion to the surrounding non-transfected cells that may lack the ability to activate the prodrug (bystander effect).
- (3) The prodrug must have minimal toxicity to aerobic cells and be stable to metabolism under aerobic conditions.
- (4) The prodrug must undergo selective activation to release a cytotoxic species.

The general principles involved in the design of bioreductive prodrugs are shown in Figure 3. Bioreductive prodrugs can be considered as comprising of three domains that are the trigger, the effector and the linker.⁴¹ The trigger unit serves as a substrate for tumour specific enzymes or a physiochemical activating event. If tumour-specific enzymes activate the prodrug, the trigger needs to show selectivity, so that the

cytotoxic effector is generated only in hypoxic cells. If the prodrug is activated by radiation, the trigger must also act as a reducing agent. An important design feature of the trigger unit is its one-electron reduction potential. Compounds that are good trigger units include nitro-compounds, quinones, aliphatic N-oxides, aromatic N-oxides and transition metal complexes. The effector is the active species, which must be potent and kill cells rapidly under all cell conditions. A linker unit joins the trigger and effector. The main function of the linker is to deactivate the prodrug until metabolism of the trigger. The linker must be designed so that it quickly releases the active drug after activation of the prodrug.



Figure 3. General features of prodrugs. [https://doi.org/10.1002/9781118134222.ch13](#)

1.3.1 Bioreductive activation

Bioreductive prodrugs require reductive activation in order to be functional. Bioreductive drugs act as substrates for various endogenous reducing enzymes in almost all cells.⁴³ Initially the one-electron reductases add an electron to the non-toxic prodrug, converting the prodrug into a free radical. In oxygenated cells, the unpaired electron in the prodrug radical is transferred to molecular oxygen, forming a superoxide radical. This futile oxygen cycle regenerates the non-toxic prodrug and inhibits drug reduction in normal tissues. In hypoxic conditions, the prodrug radical undergoes spontaneous chemical breakdown or further metabolism to generate the cytotoxic species. The position of the equilibrium in Figure 4 depends on cellular oxygen levels and the one-electron reduction potential. Compounds that are more electron-affinic can be reduced to the one-electron adduct more easily. This has been demonstrated in the comparisons for the bioreduction of metronidazole with that of the more electron-affinic nitrofurazone.⁴⁴

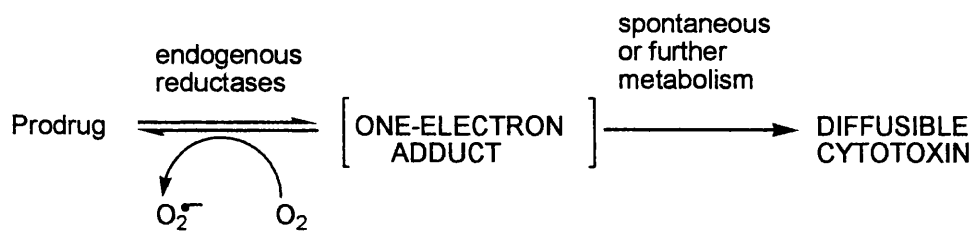


Figure 4. Mechanism of prodrug activation under hypoxia.⁴⁵

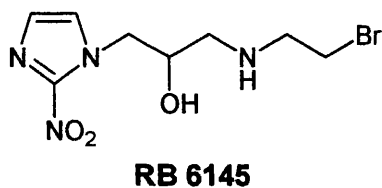
Recently, the focus has turned to the activation of bioreductive prodrugs by endogenous but tumour-specific enzymes. The enzyme-directed approach of activating bioreductive prodrugs looks at factors such as enzyme-substrate specificity and relative patterns of enzyme expression in tumour and normal cells. Robertson *et al.*⁴⁶ showed that the indolequinone EO9 was selectively activated by the oxygen-independent two-electron reductase, DT-diaphorase.

NAD(P)H:cytochrome P450 reductase is a one-electron reductase which is believed to play a vital role in the activation of certain cytotoxins. The activity of cytochrome P450 reductase is significantly higher in tumour tissue than in normal tissue. Studies by Workman and colleagues demonstrated that P450 reductase was important for the hypoxic activation of nitro-heterocyclic compounds and tirapazamine.^{47,48} Other activating enzymes include the one-electron reducing enzymes xanthine oxidase / xanthine dehydrogenase, and the one or two electron reducing enzyme carbonyl reductase.^{49,50}

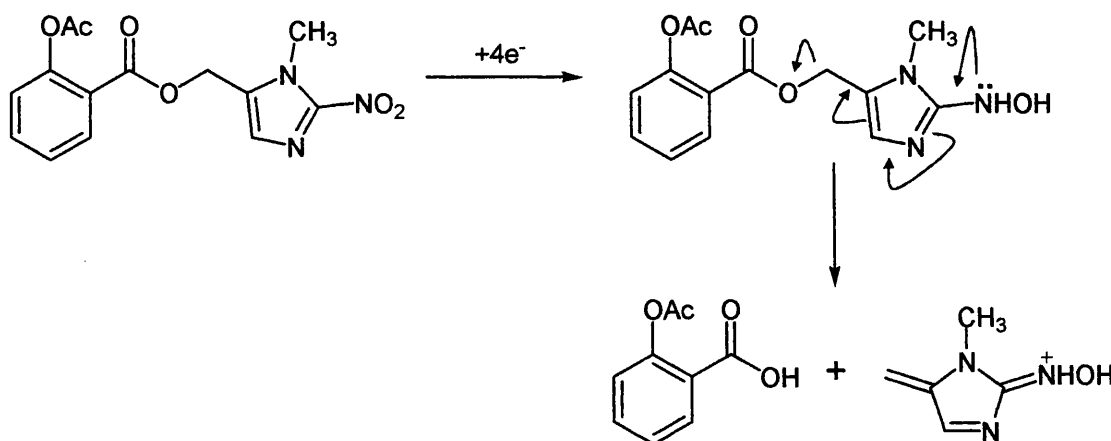
The use of exogenous (non-human) enzymes to activate prodrugs has been investigated. One approach is antibody-directed therapy (ADEPT) where an exogenous enzyme is attached to a tumour-associated antigen. A prodrug is then administered that is a good substrate for the non-human enzyme, and is catalytically activated in tumour cells. Gene-directed enzyme prodrug therapy (GDEPT) is a similar approach that uses a foreign gene in order to generate the enzyme selectively.

Bioreductive prodrugs can also be activated by ionising radiation *via* the reducing species produced from the radiolysis of water. The advantage of this radiation-activated approach is that selectivity can be achieved by restricting the radiation field on the tumour. The radiation-activated approach is a one-electron process and is independent of the expression levels of reductive enzymes in tumour cells. A number of bioreductive prodrugs that are efficiently activated by ionising radiation under hypoxic conditions have been developed, these include cobalt mustard complexes,

trials, RB6145 was shown to cause irreversible retinal damage and the compound was not taken forward for clinical evaluation.⁵⁷



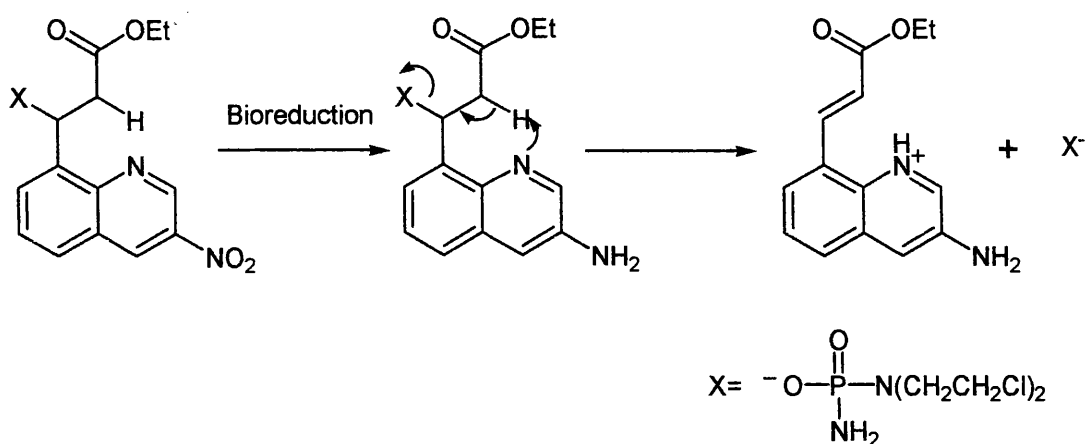
Everett *et al.*⁵⁸ demonstrated the potential delivery of cytotoxins to hypoxic tissue using 2-nitroimidazole as a reductively activated 'trigger' (Scheme 2). Studies showed the reductive elimination of aspirin and salicylic acid from the 2-nitroimidazol-5-methylene moiety. The 2-nitroimidazoles were reduced by a one-electron donor, CO_2^- , which was generated radiolytically. The reaction kinetics revealed that the salicylic acid and aspirin conjugates required a four-electron reduction and subsequent elimination from a hydroxylamine intermediate.



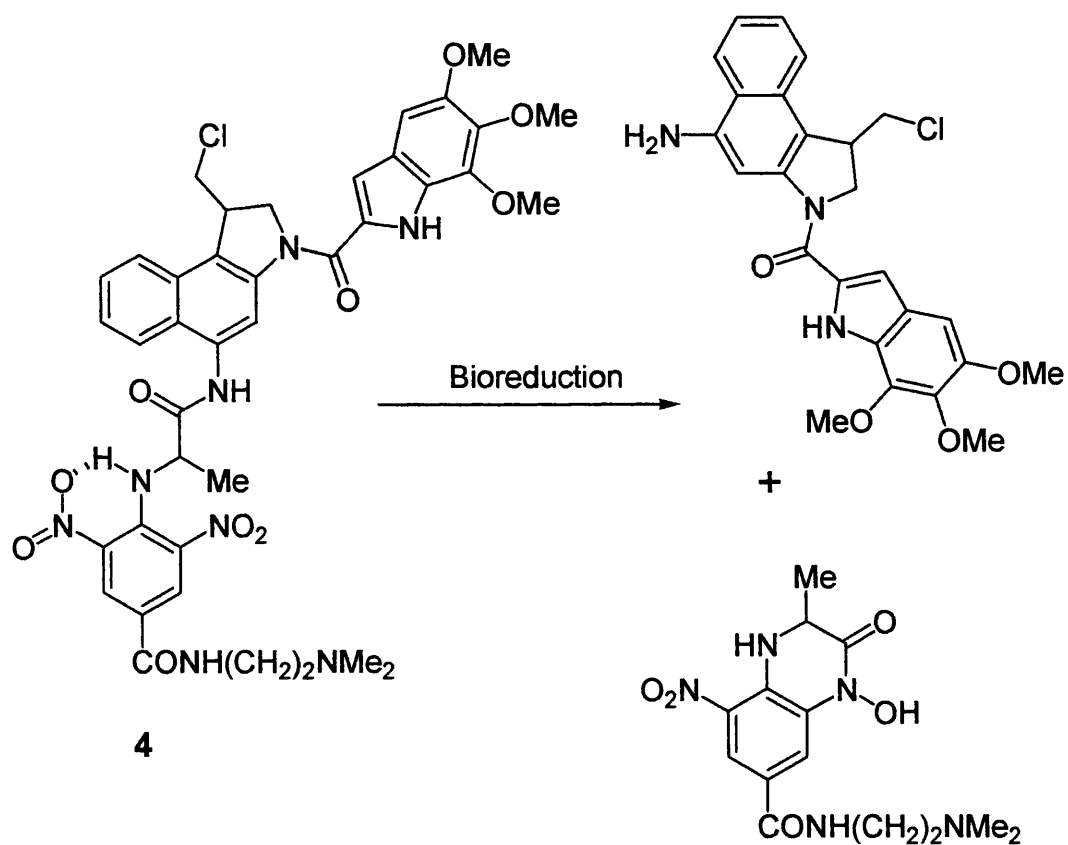
Scheme 2. Proposed mechanism for the reductive elimination of aspirin from (1-methyl-2-nitroimidazol-5-yl) methyl 2-acetoxybenzoate.⁵⁸

In an attempt to improve nitroaromatic trigger efficacy, various other heterocyclic compounds have been explored. Firestone *et al.*⁵⁹ outlined the synthesis and *in vitro* evaluation of a bioreductively-activated nitroquinoline phosphoramidate mustard. The mechanism for the activation of the nitroquinoline prodrug under hypoxic conditions is shown in Scheme 3. The cytotoxicity of the target compound was assessed against HT-29 human colon carcinoma and was found to be 11-fold more toxic under hypoxic

conditions compared with aerobic conditions. Additional studies by Mulcahy *et al.*⁶⁰ reported the use of phosphoramidite-deactivated mustards in combination with a nitrobenzyl trigger.



Scheme 3. Proposed mechanism for the release of a cyclophosphoramidate moiety from a nitroquinoline prodrug under hypoxic conditions.⁵⁹

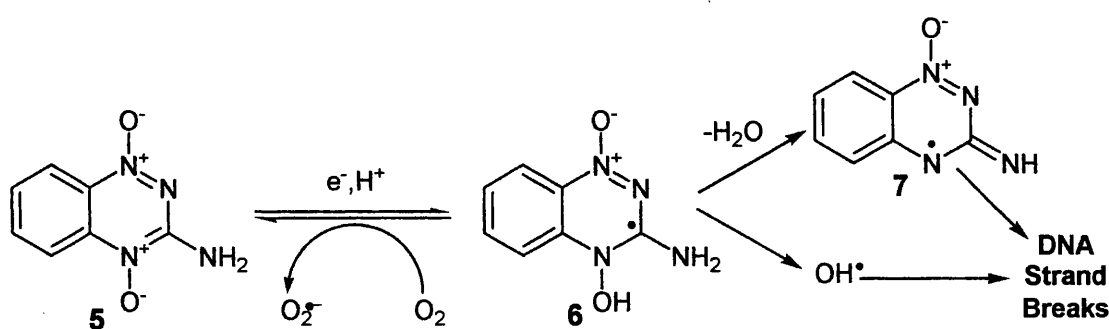


Scheme 4. Bioreductive activation of prodrug **4**.⁶¹

Sykes *et al.*⁶¹ reported a reductively activated prodrug based on a *N*-(2,6-dinitrophenyl)amino trigger system (Scheme 4). Compounds such as **4** were designed to release effectors by a cyclisation-extrusion process. In compound **4**, the *ortho* nitro group can form an hydrogen bond with the neighbouring N-H group, this locks the molecule in the correct conformation, accelerating the rate of cyclisation. Compound **4** did not show significant activity against hypoxic cells in RIF-1 tumours but was significantly activated by ionising radiation at low doses.

1.3.3 Aromatic N-oxides

Tirapazamine (TPZ, **5**) is the lead compound in a class of potent hypoxic cell toxins, which shows highly selective hypoxic cell toxicity.³ The mechanism of activation of tirapazamine under hypoxia is shown in Scheme 5. Tirapazamine is reduced by NAD(P)H:cytochrome P450 reductase to the tirapazamine radical (TPZ[•], **6**), which leads to DNA strand-breaks by a mechanism which is only partly understood. It was first thought that the DNA damaging species was the TPZ radical itself. Recently, it has been proposed that, under hypoxic conditions, the TPZ radical undergoes spontaneous decay to an oxidising hydroxyl radical (OH[•]) or an oxidising benzotriazinyl radical (BTZ[•], **7**) and two-electron reduction product SR4317. Hydrogen-abstraction by the oxidising radical (OH[•] or BTZ[•]) gives rise to DNA double-strand breaks. In the presence of oxygen, the TPZ radical is back-oxidised to regenerate the parent compound. Tirapazamine is highly selective for hypoxic cells (100-200 fold) and cell killing extends over a wide range of oxygen concentrations.⁶²

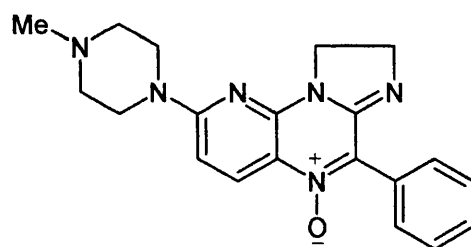


Scheme 5. Bioreductive activation of tirapazamine.³

Tirapazamine-based chemoradiotherapy has been studied in head and neck cancer and Phase II trials show promising results.⁶³ Currently, the use of tirapazamine in combination with the chemotherapeutic drug cisplatin is being investigated. Phase III clinical trials in non-small-cell lung cancer showed an improved survival rate in the group treated with a combination of tirapazamine and cisplatin, compared with those treated with cisplatin alone.⁶⁴

Monge *et al.*⁶⁵, in 1995, developed a series of quinoxalinecarbonitrile 1,4-di-N-oxides as selective hypoxia-activated prodrugs. These compounds replace the 2-nitrogen in the benzotriazine ring of tirapazamine with a cyano group. It was shown that the presence of the cyano group in the second position of the quinoxaline ring was important for biological activity. 7-(4-Nitrophenyl)-2-quinoxalinecarbonitrile 1,4-di-N-oxide was found to be 150-fold more toxic to hypoxic cells than is tirapazamine *in vitro*.

Pyrazine mono-N-oxides have also been reported as hypoxia-activated prodrugs.⁶⁶ RB90740 undergoes reduction by P450 reductase and cytochrome *b5* reductase to generate one-electron-reduced free radicals. The radicals cause single, and possibly some double stranded breakage in DNA. RB90740 was found to be more toxic under hypoxic than aerobic conditions in cell culture.⁶⁷

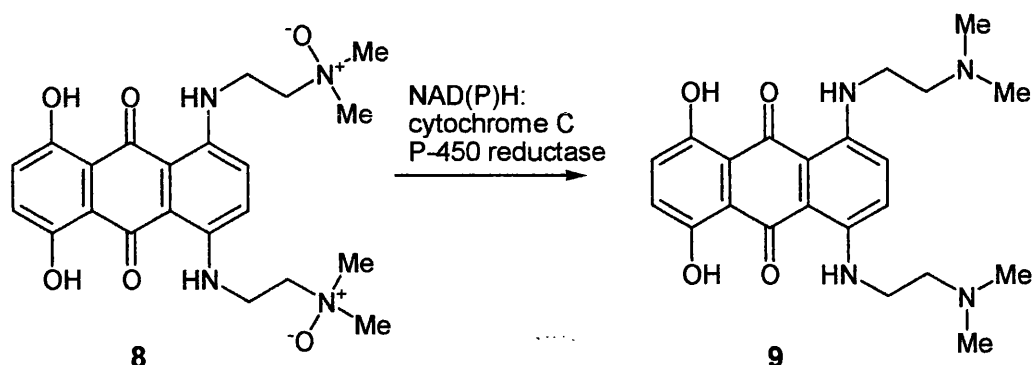


RB90740

1.3.4 Aliphatic N-oxides

Aliphatic amine N-oxides have long been identified as non-toxic metabolites of DNA binding agents bearing cationic tertiary amine side-chains. Enzymatic reduction of the N-oxide trigger unit will generate the active parent amine. This principle has been adopted to develop the di-N-oxide **8** (AQ4N), a prodrug of the metabolite 1,4-bis[2-(dimethylaminoethyl)-amino]5,8-dihydroxyanthracene-9,10-dione **9** (AQ4). AQ4 is a potent DNA intercalator / topoisomerase poison and is at least 100-fold more cytotoxic than **8**.⁶⁸ AQ4N is selectively metabolised under hypoxic conditions by the CYP3A isozyme of NAD(P)H:cytochrome C (P450) reductase (Scheme 6).⁶⁹ This selectivity is

not due to back oxidation of the initial metabolite but rather by direct competition between oxygen and the drug at the enzyme active site. In AQ4N the N-oxide functionality masks the cationic charge of the anti-tumour intercalators and prevents DNA binding. Removal of the N-oxide gives a cationic amine, which can form crucial electrostatic interactions with phosphates of the DNA backbone.⁶⁸ AQ4 can bind very tightly to DNA and is very cytotoxic because of its interference with the action of the topoisomerase II enzyme.⁷⁰



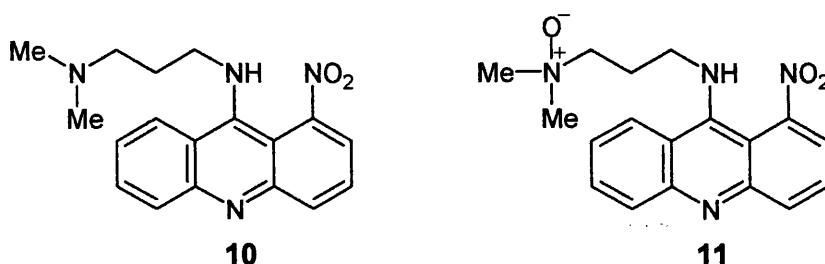
Scheme 6. Mechanism of activation of AQ4N.³

Combination studies of AQ4N and ionising radiation in a series of murine solid tumours *in vivo* showed that the prodrug potentiated the effects of radiation in a dose-dependent manner.⁷¹ Further evidence of the bioreductive nature of AQ4N was shown using the murine tumour *in vivo*; the anti-tumour effect was enhanced with AQ4N when administered in combination with cyclophosphamide. AQ4N is currently undergoing Phase I clinical trials.⁷²

N-Oxide derivatives of other cationic DNA-intercalating agents have also been investigated. Wilson *et al.*⁷³ reported a novel nitracrine-N-oxide as a bioreductively-activated prodrug. Nitracrine **10**, is a potent DNA intercalator that is activated to form a cytotoxic agent by reduction of the nitro group. However, nitracrine does not show significant activity against hypoxic cells in solid tumours, probably because of its limited extravascular diffusion into hypoxic zones.⁷³ The N-oxide derivative was developed to provide a prodrug with a lower DNA binding affinity and improved extravascular properties. Nitracrine N-oxide, **11** can be considered as being a 'bis-bioreductive' compound, with reduction of both nitro and N-oxide moieties needed for full activation under hypoxia. The requirement of two reduction steps for full activation provides exceptional (ca. 1300-fold) selectivity toward AA8 cells in culture. However, compound **11** shows activity against hypoxic cells in KHT tumours only above the maximum

tolerated dose. Studies with multicellular spheroids also suggest the extravascular diffusion of **11** is still restricted, possibly because of high rates of drug metabolism.⁷⁴ Modifications to stabilise either or both of the nitroaromatic and N-oxide redox centres against cellular metabolism were studied, but neither approach resulted in significant improvements of activity *in vivo*.^{74,75}

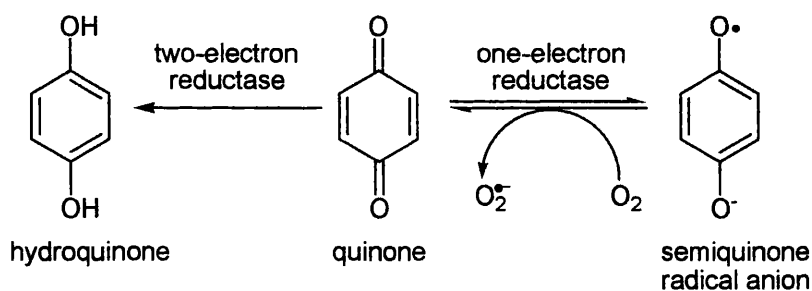
Even more recently, Yin *et al.*⁷⁶ reported a novel series of tertiary amine N-oxides of naphthalimides as potential anti-cancer agents against hypoxic solid tumours. The N-oxides showed hypoxic selectivity in A375 cell cultures.



1.3.5 Quinones

Certain quinones are able to act as bioreductively-activated prodrugs. The representative compound is the natural product mitomycin C **12**, which cross-links DNA following enzymatic reduction of the quinone moiety and spontaneous elimination of the tertiary methoxy and C-10 carbamate groups.⁷⁷ Mitomycin C is then able to bind to the N-2 of guanine in DNA *via* the C-1 site or *via* both the C-1 and C-10 reactive sites.⁷⁸ However, mitomycin C only shows marginal hypoxic selectivity. The analogue porfiromycin **13** shows higher preferential cytotoxicity to hypoxic cells than mitomycin C. Clinical trials have shown a benefit with concurrent use of porfiromycin and radiation therapy in the management of head and neck cancers.⁷⁹

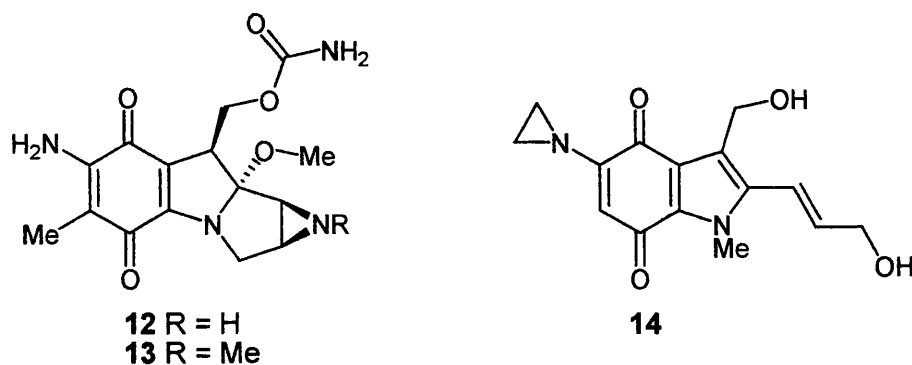
The general mechanism for the activation of quinone-based bioreductively-activated prodrugs is shown in Scheme 7. Quinone analogues can undergo a one-electron reduction by cytochrome C P-450 reductase to the semiquinone radical anion and / or a two-electron reduction to give the hydroquinone species. The latter occurs following reduction with DT-diaphorase, where the hydroquinone is formed *via* hydride transfer.⁸⁰ The semiquinone can be back-oxidised by molecular oxygen to the parent compound, suppressing activation in well perfused cells.



Scheme 7. Reductive activation of a quinone bio-reductive system.⁵⁴

Similar bio-reductive activating processes are involved in the activation of simple benzo- and naphthoquinones whereby the release of the therapeutic drug is attained *via* a methide intermediate. These compounds show selective toxicity towards hypoxic cells *in vitro*.⁸¹

The indolequinone EO9 **14**, represents a related class of quinone-based hypoxia-activated prodrugs. Under aerobic conditions, EO9 is primarily activated by DT-diaphorase to form the hydroquinone. However, it is suggested that the hypoxic selectivity of the prodrug is due to activation by cytochrome P450 reductase. In order for the indolequinones to undergo fragmentation selectively in hypoxic environments a balance needs to be established between the reactivities of both the semiquinone and hydroquinone and their redox-properties. Everett *et al.*⁸² reported that it was possible to control the rate of reductive fragmentation through 3-carbinyl substitution and ideal fragmentation rates were achieved with compounds such as 5-methoxy-1,2-dimethyl-3-[1-(4-nitrophenoxy)-1-(2-thienyl)-methyl]indole-4,7-dione and 5-methoxy-1,2-dimethyl-3-[1-(4-nitrophenoxy)ethyl]indole-4,7-dione. The indolequinone EO9 possesses selective toxicity towards hypoxic cells *in vitro*, and activity *in vivo* against syngeneic mouse neoplasm and human xenografts.⁸³ However, EO9 did not show clinical activity as a single agent in Phase II clinical trials.⁸⁴



1.4 Poly(ADP-ribose) polymerase

Poly(ADP-ribose) polymerase-1 (PARP-1), also known as poly(ADP-ribose) synthetase (PARS), is a multifunctional enzyme present in eukaryotic cells and is the major isoform of an expanding family of poly(ADP-ribose) polymerases (PARPs).⁸⁵ PARP-1 is present in great abundance in organisms ranging from plants to mammals but is absent in yeast.⁸⁶ The enzyme is predominantly found in the nucleus, where it is tightly bound to the chromatin. PARP-1 is involved in locating and repairing single and double DNA strand breaks. Activated PARP-1 catalyses the transfer of ADP-ribose units from its substrate nicotinamide adenine dinucleotide (NAD⁺) to nuclear acceptor proteins such as histones, topoisomerases, DNA polymerases, DNA ligases and PARP-1 itself. Current research has implicated PARP-1 activity in areas such as DNA replication, differentiation, sister chromatid exchange, cellular proliferation and cell death. In addition, studies *in vivo* have demonstrated the therapeutic benefits of pharmacological inhibition of PARP-1, against numerous pathophysiological diseases.

PARP-1 is a 116 KDa multifunctional protein that consists of three functional domains (Figure 5). These are the 46 KDa N-terminal fragment, the central 22 KDa fragment and the 54 KDa C-terminal fragment.

The N-terminal DNA-binding domain (DBD) contains two zinc finger motifs FI and FII, the first interacting with double strand DNA breaks and the second with nicks.⁸⁷ Zinc fingers are regions in the protein where zinc coordinates cysteine and histidine residues to form a loop in the polypeptide chain.⁸⁸ They are responsible for DNA-binding and protein-protein interactions. Gradwohl *et al.*⁸⁸ demonstrated that damage of the first zinc finger resulted in complete loss of enzymatic activity whatever the type of DNA break, whereas destruction of the second zinc finger resulted in avoidance of PARP-1 activation in response to single strand breaks. The DBD also contains a nuclear location signal (NLS), which is responsible for the transportation of PARP-1 into the nucleus.

The central region of the PARP-1 enzyme contains the automodification domain, which includes fifteen highly conserved glutamate residues that are thought to be involved in PARP-1 automodification.⁸⁹ This domain contains regions for dimerisation, which may modulate the interaction of PARP-1 to DNA through its zinc fingers and the association with PARP-1 to proteins. Miwa and co-workers⁹⁰ have identified a leucine zipper motif in the automodification domain of *Drosophila* PARP and proposed that this motif could

be responsible for the homo- and hetero-dimerisation of PARP-1. This domain also contains the terminus motif of the breast cancer susceptibility protein C (BRCT). This domain is common in many DNA and cell cycle proteins. PARP-1 forms several protein-protein interactions through the BRCT motif.⁹¹

The catalytic domain of PARP-1 is located in the C-terminal region of the enzyme and contains the active site. The active site also known as “the PARP signature” is formed by a sequence of 50 amino-acids that is highly conserved in eukaryotes. The C-terminal region can be cut down to a 40 KDa C-terminal polypeptide (PARP-CF) without losing the basal activity.⁹² This region is responsible for the catalytic activities such as NAD⁺ hydrolysis, initiation, elongation and branching involved in the synthesis of poly(ADP-ribose).

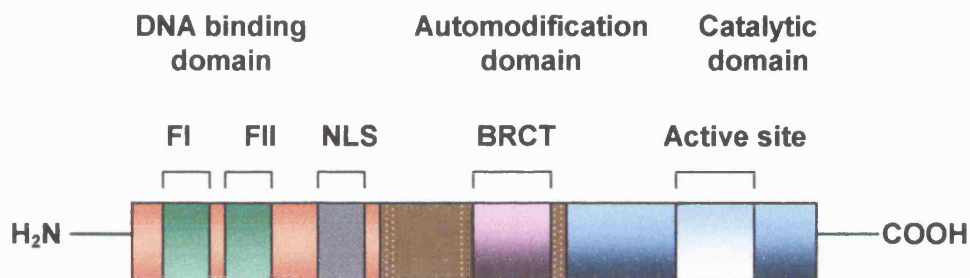
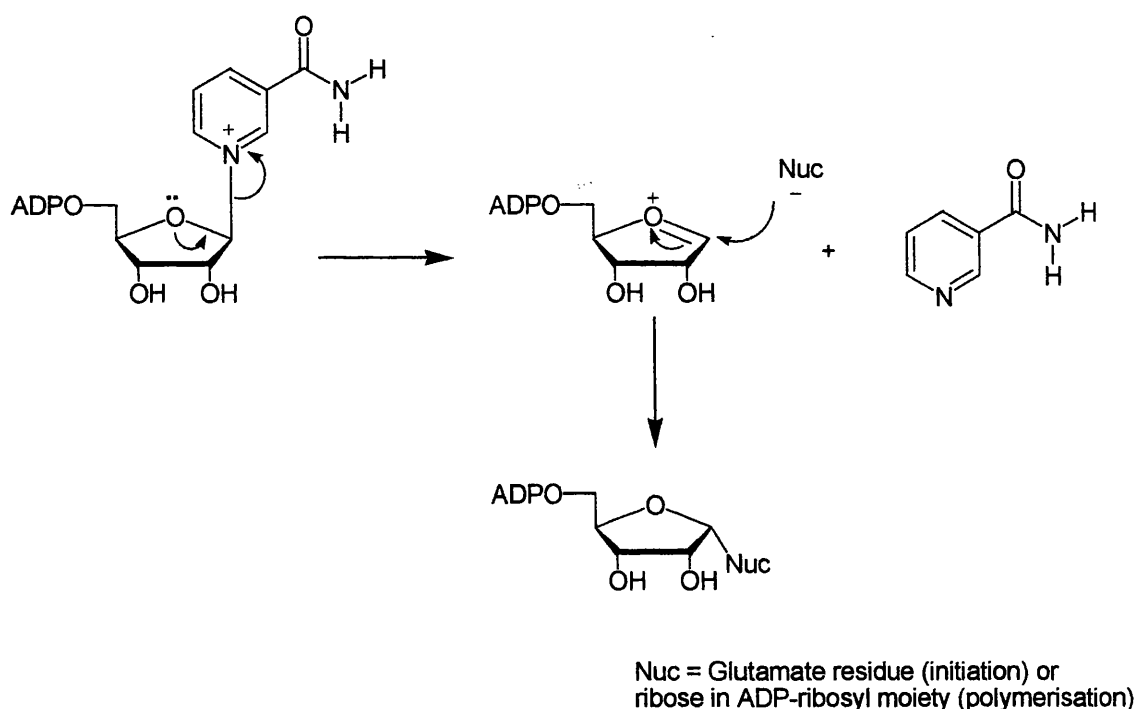


Figure 5. Schematic view of the three functional domains of PARP-1.⁸⁹

1.4.1 PARP-1 activation and catabolism

PARP-1 is activated by strand breaks in DNA, caused by ionising radiation, alkylating agents as well as processes such as DNA repair, replication and recombination. Upon activation PARP-1 binds rapidly and specifically through the second zinc finger to single strand breaks (SSB) in DNA and the enzyme covers seven nucleotides symmetrically on each side of the break.⁹³ This interaction stimulates the catalytic activity of PARP-1. The activation of PARP-1 induced by double strand breaks (DSB) is significant but less important than activation due to SSB.⁸⁹ It has been shown by kinetic studies of the automodification reaction of PARP that the catalytically-active species of the enzyme is a homodimer.⁹⁴ Therefore, two PARP-1 molecules concurrently interact with the site of DNA damage and simultaneously catalyse the synthesis of poly(ADP-ribose). The process of poly(ADP-ribosylation) consists of three stages: initiation, elongation and branching. Initially, the substrate NAD⁺ associates with the NAD⁺-

binding domain on the enzyme.⁹⁵ It is thought that the carbonyl and amino moieties of the nicotinamide carboxamide group make important hydrogen-bond interactions with acceptor and donor residues in the enzyme active site. PARP-1 catalyses the cleavage of the N-glycosidic bond in NAD⁺, this is probably facilitated by the adjacent oxygen lone pair and leads to the formation of an intermediate oxocarbenium ion (Scheme 8). Nicotinamide is released in this process and the resulting ADP-ribose moiety forms an ester bond with a nucleophilic site (invariably a glutamate residue). This may be PARP-1 itself (automodification) or nuclear proteins involved in DNA repair (heteromodification), such as histones, topoisomerases, DNA polymerases and ligases.⁸⁹



Scheme 8. Schematic representation of poly(ADP-ribosylation).⁹⁵

In the elongation stage, the anomeric carbon of an ADP-ribosyl moiety forms a α -(1''-2') glycosidic bond between the 2'-OH group of a growing ADP-ribosyl residue bound to an acceptor protein (Figure 6). Eventually, a branched structure is formed through (1'''-2'') glycosidic bonds between ribose residues. The ADP-ribose polymerisation reaction can catalyse linear polymers with up to 200 residues and with five to seven branching reactions.

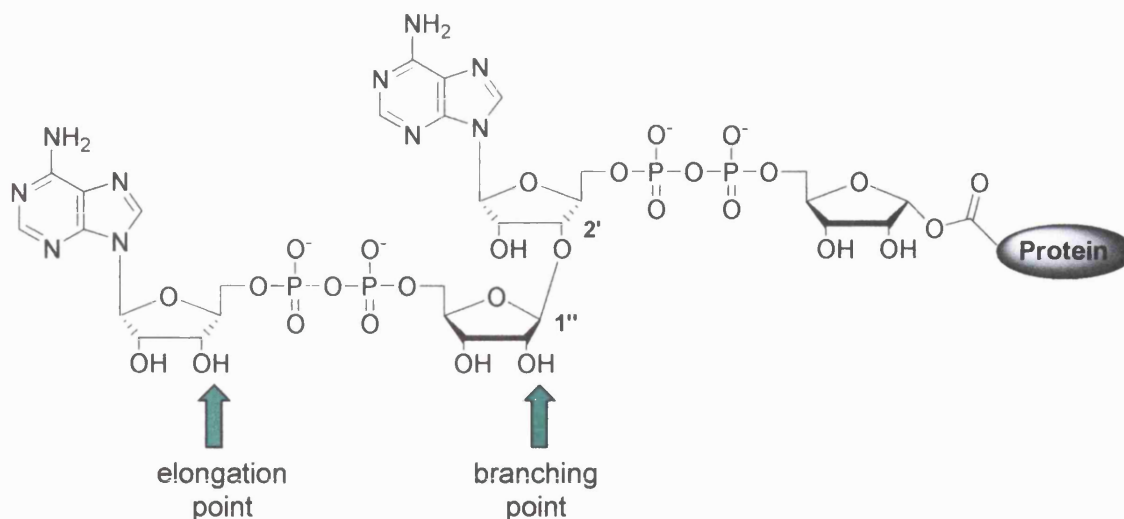


Figure 6. ADP-ribosylation of a protein acceptor. The ADP-ribose moiety conjugated to the protein can act as an acceptor for the addition of another ADP-ribose by PARP.⁸⁹

DNA damage is the most important element in the regulation of poly(ADP-ribosyl)ation reactions. During PARP automodification, the enzyme progressively becomes more negatively charged, resulting in electrostatic repulsion between DNA and the ADP-ribose polymers linked to the enzyme. This leads to the release of the automodified PARP from the DNA strand break and subsequent inactivation of the enzyme. This exposes the damaged site of DNA to repair processes. When DNA is moderately damaged, PARP-1 participates in DNA repair processes and the cell survives. However, in the case of extensive DNA damage PARP-1 overactivation occurs. This leads to a rapid depletion of NAD^+ and ATP levels. The cell then attempts to resynthesise NAD^+ that results in energy crisis and ultimately, cell death by necrosis.⁸⁹

PARP-1 activation eventually results in autoinhibition through poly(ADP-ribosyl)ation. Removal of inhibitory poly(ADP-ribose) units from the automodification domain of PARP-1 is needed in order to reactivate the enzyme and allow for continuous NAD^+ turnover. Poly(ADP-ribose) glycohydrolase (PARG) is the most important enzyme for the catabolism of poly(ADP-ribose) polymers. PARG cleaves bonds between ADP-ribose units of linear and branched poly(ADP-ribose). The K_m value of PARG is much lower for larger (ADP-ribose) polymer units than smaller ones. Therefore, the enzyme probably removes bigger polymer units first by endoglycosidic cleavage and then switches to exoglycosidic cleavage to remove ADP-ribose units one by one. The proximal ADP-ribose monomer portion of poly(ADP-ribose) is removed from acceptor proteins by ADP-ribosyl protein lyase.⁹⁶

1.5 The PARP superfamily

Since the discovery of PARP in 1963 by Chambon *et al.*⁹⁷, it was generally accepted that there was only one type of PARP in each species. Shieh *et al.*⁹⁸, in 1998 discovered that PARP-1 deficient cells were able to synthesise ADP-ribose polymers in response to DNA damage caused by *N*-methyl-*N'*-nitro-*N*-nitroguanidine (MNNG). These findings indicated that PARP-1 is not the only enzyme capable of synthesising ADP-ribose polymers. In the last few years, an exhaustive research of the non-redundant protein database from the National Centre for Biotechnology identified eighteen members of the PARP superfamily.⁹⁹ Currently, very little information is available on the structure and function of the non-classical PARPs. However, the biochemical and enzymatic properties of seven isoforms have been investigated: PARP-1, PARP-2, PARP-3, PARP-4 (also known as vault PARP (vPARP)), tankyrases I and II, and PARP-7 (Figure 7). PARP-1, the founding family member, has been the most extensively studied and this isoform is responsible for the synthesis of 90% of poly(ADP-ribose) in cells.⁸⁶

1.5.1 PARP-2

PARP-2 bears the strongest resemblance to PARP-1 and is the only other isoform known to be activated by DNA-strand interruptions.¹⁰⁰ PARP-2 was discovered as a result of the presence of residual DNA-dependent PARP activity in embryonic PARP-1 knockout mouse fibroblasts. The PARP-2 is a 62 KDa protein and is localised on chromosome 14q11.2, which contains a number of genes involved in apoptosis, chromosome end maintenance and the immune system.¹⁰¹

The central automodification domain is absent from PARP-2. The DBD of PARP-2 is distinct from that of PARP-1 and could indicate different substrate specificities for PARP-2. Interestingly, despite the lack of zinc-finger motifs, PARP-2 is capable of binding to DNA that has been treated with DNase I and catalyses the formation of poly(ADP-ribose) polymers.¹⁰² The basic amino-acid residues present within the N-terminal of PARP-2 may facilitate DNA binding properties and / or nuclear targetting of the protein. PARP-2 can poly(ADP-ribosyl)ate itself (automodification) or histones (heteromodification). PARP-2 preferentially modifies histone H2B, whereas PARP-1 uses histone H1 as its main substrate.⁹⁹

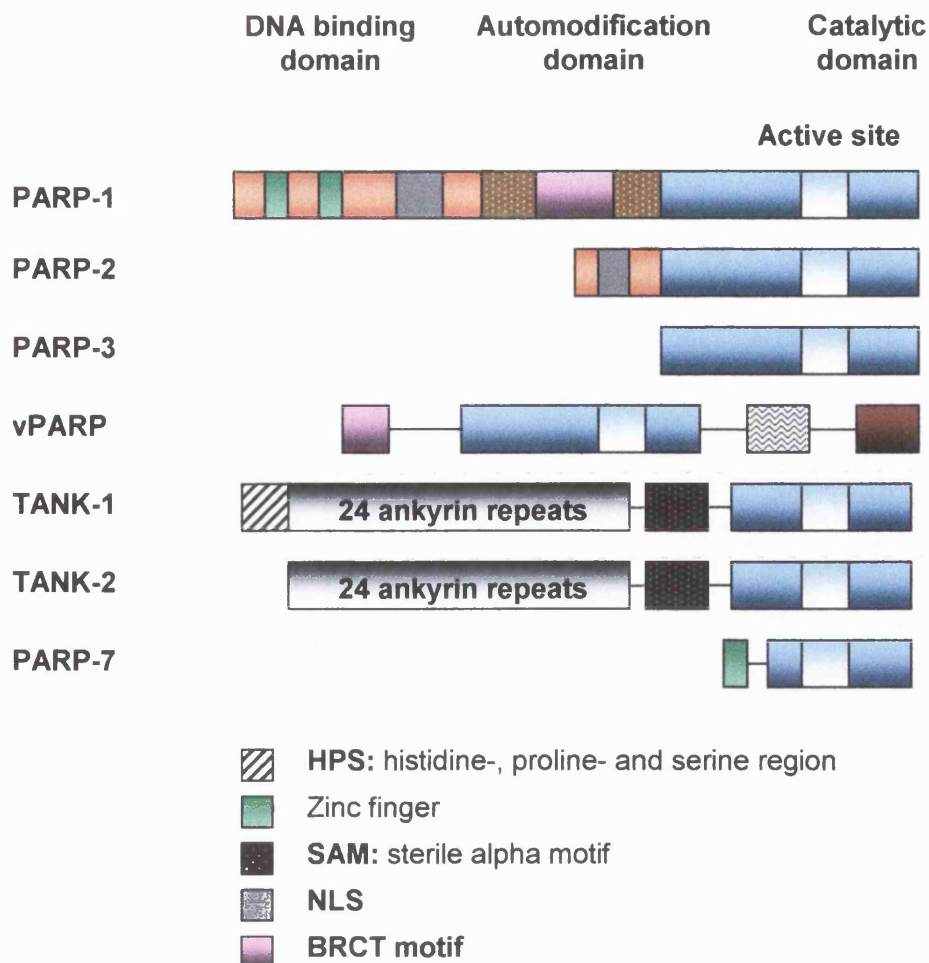


Figure 7. Comparison of the domain structures of seven PARP isoforms.⁸⁵

1.5.2 PARP-3

Human PARP-3 is a 540 amino-acid protein that comprises of a 54 amino-acid N-terminal domain and a catalytic domain of 489 amino-acids that has 39% identity (61% similarity) with the human catalytic domain of PARP-1. PARP-3 can catalyse the synthesis of poly(ADP-ribose) *in vitro* and in purified centrosome preparations.¹⁰³ The N-terminal of PARP-3 is unique and contains a targeting motif that is able to localise the enzyme to the centrosome. The centrosome is a vital organelle in animal cells as it directs the nucleation and organisation of microtubules.¹⁰⁴ Many human tumour cells, including those lacking the tumour suppressor p53, have an abnormally high number of centrosomes. Augustin *et al.*¹⁰⁵ reported that overexpression of PARP-3 or its N-terminal domain in HeLa cells interfered with the G₁/S cycle transition, but had no effect on centrosomal duplication or amplification. Therefore, PARP-3 might function in the maturation of the daughter centriole until the G₁/S restriction point. Kanai *et al.*,¹⁰³ in 2003, demonstrated localisation of human PARP-1 to the centrosome. It has been

suggested that PARP-1 and PARP-3 monitor the eventual presence of broken DNA that originate from tension forces between two daughter cells experiencing unbalanced chromosome segregation through a detection signalling pathway.

1.5.3 Vault PARP

Vault PARP, also known as PARP-4, is a 193 KDa protein and was identified as a component of the vault complex, a cytoplasmic ribonucleoprotein (RNP). Mammalian vaults have a unique barrel-shaped structure and consist of the 100 KDa major vault protein (MVP), the 240 KDa telomerase-associated protein (TEP1), and 193 KDa of untranslated vault RNA (vRNA). At present the biological role of the vault particle is unknown. Kickhoefer *et al.*,¹⁰⁶ in 1996, proposed that vaults play a role in cellular transport. Vaults have also been implicated in multi-drug resistance and as prognostic markers for cancer chemotherapy failure. Overexpression of MVP has been shown in many non-P-glycoprotein tumour cells lines, such as lung cancer and breast cancer cell lines.¹⁰⁷ Scheffer *et al.*¹⁰⁸ showed that overexpression of MVP, is not sufficient alone to confer a drug-resistant phenotype, implying that there is a requirement of additional mechanisms for vault-mediated drug resistance.

The N-terminal domain of vault PARP contains a BRCT motif similar to the central automodification domain of PARP-1. The catalytic domain of vault PARP is a region of 350 amino-acids that shares 29% identity with the catalytic subunit of PARP-1, and is capable of catalysing the poly(ADP-ribosyl)ation of MVP and to a lesser extent itself.

1.5.4 Tankyrases

Tankyrase-1 was first identified through its interaction with the telomeric repeat binding factor 1 (TRF1), a negative regulator of telomere length. Telomeres, which are located at the end of chromosomes and contain simple repeat DNA sequences, are essential for chromosome maintenance and stability. They are maintained by telomerase, a specialised reverse transcriptase. The gene coding for tankyrase-1 is found on chromosome 8 and the protein consists of 1327 amino-acids and a molecular weight of 142 KDa. The N-terminal of tankyrase-1 contains the HPS domain, which contains runs of histidine, proline and serine residues, and, so far, no work has been done to establish how important this domain is. The central domain contains 24 ankyrin (ANK) repeats, a 33-amino-acid motif that is responsible for interactions with proteins such as TRF1, nuclear mitotic apparatus (NuMA) and Golgi-associated GLUT4 vesicles.¹⁰⁹ These

tankyrase-binding proteins play an important role in cellular processes, such as telomere and spindle organisation, Golgi dynamics and apoptosis. Adjacent to the ANK domain is the sterile alpha motif (SAM). The SAM domain is responsible for protein-protein interactions. The SAM domain can self-associate to form multiproteins.¹¹⁰ Tankyrase function does not depend on DNA processes or the presence of DNA strand breaks but seems to be regulated by the phosphorylation state of the protein.¹¹¹ Tankyrase activity is best understood at telomeres, where it appears to act as a telomere-length regulator.¹¹² TF1 has a binding specificity for TTAGGGTTAG sequences in DNA. It binds to the telomere and inhibits the function of telomerase, therefore contributing to the shortening of telomeres during replication. It is suggested that tankyrase-1 releases TF1 from telomeres by adding negatively charged ADP-ribose polymers, allowing access to telomerase. Overexpression of TF1 in a telomere-expressing cell line caused telomeres to shorten gradually and partial inhibition resulted in lengthening of the telomere.

Recently, the 127 KDa protein tankyrase-2 encoded by chromosome 10, has been discovered. The sequence of this protein exhibits 85% identity to the ankyrin repeats, SAM, and PARP catalytic domain of tankyrase-1 but lacks the HPS domain. Tankyrases 1 and 2 show remarkable functional overlap. They both exhibit PARP activity and bind to the same proteins. However, overexpression of tankyrases-2, but not tankyrases-1, caused cell death by necrosis, demonstrating that the two proteins differ in regulation of activity and substrate specificity.¹¹³

1.5.5 PARP-7

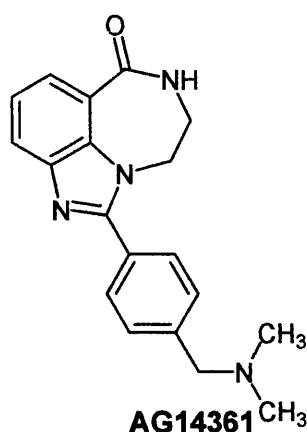
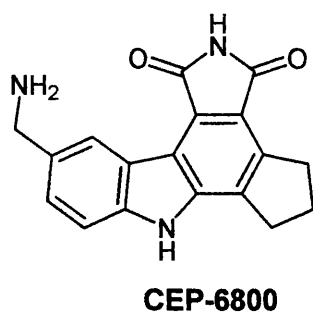
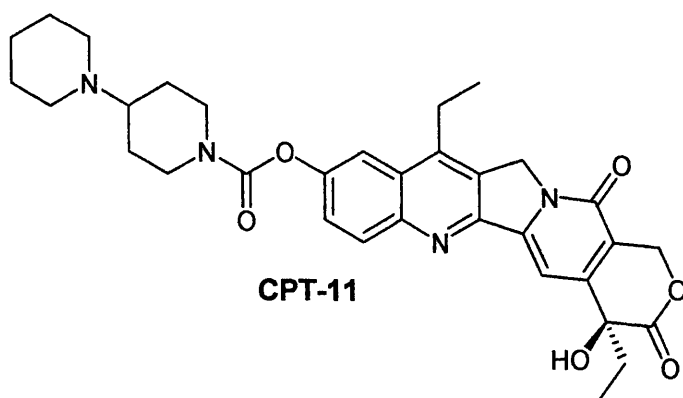
Tetrachlorodibenzodioxin (TCDD) is a prototype for a class of dioxins and causes many adverse effects in mammalian species.¹¹⁴ A TCDD-inducible member of the PARP family (PARP-7) was recently identified. The human PARP-7 gene, consisting of six exons, is located on chromosome 3q25.31. The PARP-7 protein consists of a CCCH-zinc finger (a putative RNA binding module), a WWE domain (protein-protein interaction motif) and a PARP catalytic domain. The exact function of PARP-7 remains unclear. It appears to be involved in T-cell function and its induction by TCDD contributes to tumour promotion.¹¹⁴ The *in vitro* transcribed / translated protein exhibits PARP activity towards histones.

1.6 PARP-1 inhibitors as chemosensitising and radiosensitising agents in cancer therapy

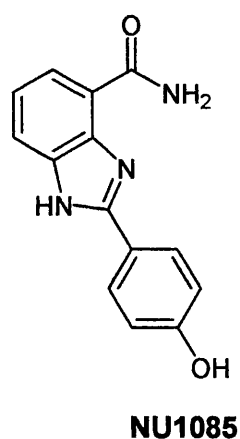
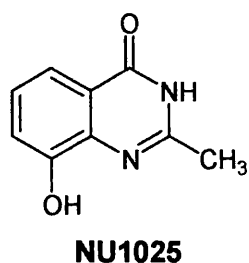
Current therapeutic strategies for the treatment of cancer exploit the hypothesis that sufficient amounts of DNA damage will result in the killing of cancer cells. Most chemotherapeutic agents and radiotherapy lack selectivity, meaning that many rapidly dividing normal cells, such as bone marrow and gastrointestinal epithelial cells, are damaged along with the cancer cells. A general feature of many successful cancer treatments is their ability to damage DNA directly. It is, therefore, not surprising that there has been considerable focus on the pathways of DNA repair as potential targets for improving cancer therapy. Due to the involvement of PARP-1 in base-excision repair of DNA, PARP-1 inhibitors have been investigated as radio- and chemosensitisers for cancer treatment. In regard to the involvement of PARP-1 in DNA repair, most studies have looked at monofunctional alkylating agents or ionising radiation, as these are the most potent activators of PARP-1.

The development of 3-substituted benzamides as inhibitors of PARP-1 in the 1980's has enabled the investigation of the effects of DNA damaging agents in PARP-1-inhibited cells. The PARP-1 inhibitor 3-aminobenzamide (3-AB) has been shown to enhance the anti-tumour activity of bleomycin,¹¹⁵ cisplatin,¹¹⁶ chloroambucil,¹¹⁷ and cyclophosphamide¹¹⁸ against a variety of tumour cell lines *in vivo*. However, the benzamides lack specificity and potency and have been shown to modulate the cytotoxicity of some anti-cancer agents by PARP-independent mechanisms. The doses of 3-AB used to achieve chemopotentialisation *in vivo* are ~500 mg kg⁻¹. The use of such large doses of 3-AB significantly complicates interpretation of the data, because of the potential hypothermic effects of such doses.¹¹⁹ A chemosensitising effect is also observed when PARP-1 is absent from PARP (-/-) cells. However, it is still not clear what effects other PARP homologues have in decreasing cell susceptibility to DNA damaging agents.

A potential combination currently under evaluation is the application of PARP-1 inhibitors to enhance the cytotoxicity of DNA topoisomerase I poisons, such as irinotecan (CPT-11) and topotecan. In pre-clinical studies, the potent PARP inhibitor CEP-6800, potentiated the cytotoxicity of CPT-11 in HT-29 colon carcinoma.¹²⁰ In addition, *in vivo* efficacy of PARP inhibition to potentiate CPT-11 against colon cancer was confirmed by another study using AG14361.¹²¹



Researchers at the University of Newcastle identified quinazolin-4-[3H]ones (e.g. NU1025) and benzimidazole-4-carboxamides (e.g. NU1085) derivatives as two new classes of PARP inhibitors.¹²² NU1025 and NU1085 have been shown to potentiate the cytotoxicity of camptothecin (a topoisomerase I poison) but not etoposide (a topoisomerase II poison) in L1210 cells.¹²³ In addition, NU1025 and NU1085 have been reported to potentiate the cytotoxicity of topotecan, a topoisomerase I inhibitor, in a panel of twelve human tumour cell lines.¹²⁴



Numerous studies *in vivo* have evaluated the potential role of PARP-1 inhibitors when used in combination with the monofunctional DNA-alkylating agent temozolomide (TMZ). TMZ is an agent of clinical interest with promising anti-tumour activity against brain primary tumours and metastases.¹²⁵ In the first *in vivo* pre-clinical study, Tentori *et al.*¹²⁵ demonstrated that the anti-tumour activity of TMZ against brain lymphoma is enhanced by the use of intracerebral injection of the PARP-1 inhibitor NU1025. The drug combination enhanced the survival of lymphoma-bearing mice with respect to the treatment with TMZ only. However, when delivered systemically, NU1025 does not improve the efficacy of TMZ, owing to its limited CNS penetration. Therefore, in order for a PARP inhibitor to increase TMZ efficacy, it needs to be able to cross the blood-brain barrier. It was found that intravenous administration of GPI 15427, a novel PARP-1 inhibitor (Guilford Pharmaceuticals), enhances the efficacy of TMZ against glioblastoma multiforme, brain lymphoma and intracranial malignant melanoma.¹²⁶ Curtin and colleagues¹²¹ developed the PARP-1 inhibitor AG14361 (Pfizer/Agouron Pharmaceuticals) and showed that intraperitoneal administration of the inhibitor enhances the effects of TMZ, and radiation therapy in LoVo colorectal cancer cells.

Cancer cells have also shown increased sensitivity to radiation therapy in the presence of PARP inhibitors. Benzamides have been shown to sensitise tumour cells *in vivo* to both single and fractionated doses of radiation.¹²⁷ Clinical studies of nicotinamide with carbogen breathing in combination with radiotherapy have been conducted for the treatment of malignant gliomas.¹²⁸ However, the effectiveness of this treatment modality is limited due to the occurrence of toxic side effects.

A series of potent dihydroisoquinolinone PARP inhibitors, developed by Suto and co-workers¹²⁹ increased the radiation sensitivity of mammalian cells, by affecting both the shoulder and slope of the survival curve.

Recently, radiopotentiality by INO-1001, a potent PARP inhibitor, has been investigated in rodent and human cell lines. Combination treatment of INO-1001 and a single dose of radiation resulted in significant radiosensitisation of human fibroblasts, murine sarcoma line (SaNH), and Chinese hamster ovary AA8 cells (CHO). Enhancement ratios of 1.4 to 1.6 were obtained at 10 μ M concentration of INO-1001. In addition, it was reported that CHO cells treated with fractionated doses of 4.0 Gy irradiation allowed sublethal radiation damage to be repaired by a factor of 5.3. In

comparison, the treatment of CHO cells with fractionated doses of 4.0 Gy irradiation and 10 μ M concentration of IN-1001, reduced the recovery ratio to 2.2.¹³⁰

Current research has indicated that PARP inhibitors might be beneficial in cancer treatment as a single agent. BRCA-1 and BRCA-2 are important for DNA double strand break repair by homologous recombination. Farmer *et al.*¹³¹ demonstrated that BRCA-1 or BRCA-2 dysfunction sensitises cells to the inhibition of PARP activity, resulting in cell cycle arrest and apoptosis. The PARP inhibitors KU0058684 and KU0058948 (KuDOS Pharmaceuticals) were used to treat BRCA-2 deficient cells and wild type cells. BRCA-2 deficient cells were extremely sensitive to KU0058684 and KU0058948 compared with heterozygous or wild type cells. Therefore, suggesting that PARP inhibitors may play a role in the treatment of ovarian, breast and other malignancies that exhibit BRCA-1 and BRCA-2 mutations.¹³¹

1.6.1 Future clinical implications of the inhibition of PARPs in cancer therapy

As described previously, increased levels of MVP expression, vault-associated vRNA, and vaults have been linked directly to multi-drug resistance. The multi-drug resistant protein LRP is a major vault protein and is overexpressed in tumour cell lines that are resistant to chemotherapeutic agents such as doxorubicin, vincristine, and taxol.¹³² It has been suggested that LRP may be responsible for sequestration and subsequent exocytosis of drugs from the cell.¹⁰⁸ Tentori *et al.*,¹²⁵ in 2002, indicated that inhibition of vault PARP might be a possible strategy to counteract multi-drug resistance due to up-regulation of vault proteins (Figure 8).

Inhibition of telomerase has also been proposed as a strategy for cancer treatment. Most cancer cells exhibit increased telomerase activity that is normally inactive in most somatic cells. This is a very attractive target for cancer treatment, as inhibition would lead to shortening of telomeres and eventual replicative senescence of cells. However, the time and number of cell divisions required to inhibit cell growth make it unlikely that telomerase inhibition will be effectively used as a single agent in cancer treatment. Therefore, it is more likely, that repression of telomerase would represent a novel strategy of cancer therapy following conventional treatment with surgery, chemotherapy or radiotherapy.¹³³ Tankyrase-1 plays a major role in regulating telomere length, its inhibition would greatly impair poly(ADP-ribosyl)ation of TF1. TF1 is the tankyrase binding partner at telomeres and is involved in the negative feedback mechanism that stabilises telomere length.¹³⁴ Inhibition of poly(ADP-ribosyl)ation of

TF1 prevents the binding of telomerase to telomeres and the consequent telomere elongation (Figure 8).

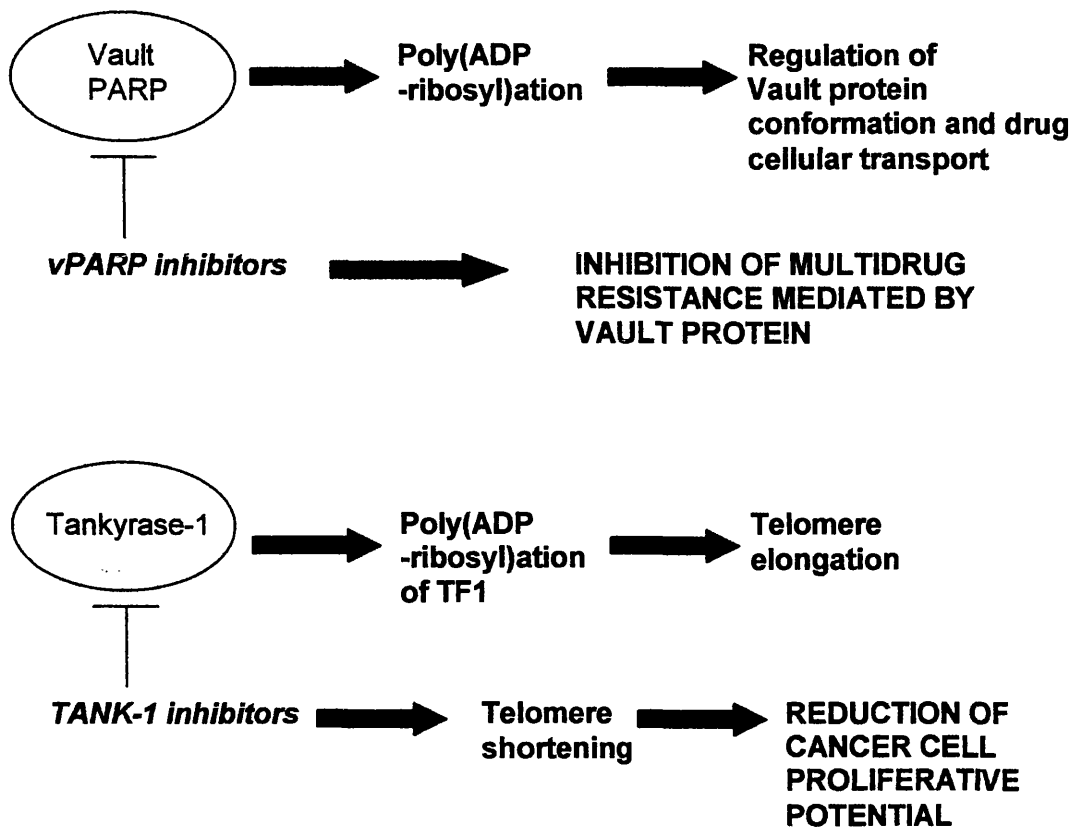


Figure 8. Potential clinical implications of vPARP and TANK-1 inhibitors.¹²⁵

1.7 The role of PARP-1 inhibitors in other pathophysiological conditions

1.7.1 Regulation of cell survival and death by PARP

PARP-1 is involved in two main mechanisms of cell death: apoptosis and necrosis, the mode of cell death being determined by the level of NAD⁺ and ATP. Cells that are exposed to DNA-damaging agents can enter three routes, based on the severity of DNA damage (Figure 9). In the first route, PARP-1, activated by mild genotoxic stimuli, facilitates DNA repair by interacting with DNA repair enzymes and DNA-dependent protein kinase. As a consequence, DNA damage is repaired and cells survive without the risk of passing on mutated genes. In the second route, more severe DNA damage induces apoptotic cell death, during which caspases inactivate PARP-1 by cleaving it into two fragments (p89 and p24). This pathway allows cells with severe DNA damage to be eliminated in a safe and efficient manner. The third route is induced by extensive DNA breakage that is usually caused by oxidative or nitrosative stress. The overactivation of PARP-1 leads to the rapid depletion of the substrate NAD⁺. As a result, the rates of glycolysis and mitochondrial respiration slow down, leading to an energy crisis. The severely compromised cellular energetic state prevents cell death *via* the apoptotic pathway and, ultimately, cell death occurs by necrosis. This final route also known as the “PARP suicide hypothesis” has been proposed to occur in a wide range of pathophysiological conditions. In conclusion, it appears that PARP can function as a switch between life and death by controlling energy metabolism of the cell in response to DNA damage. The suicide response acts as a safety mechanism, which prevents cells with severe DNA damage from attempting to repair themselves and consequently surviving with malignant transformations.

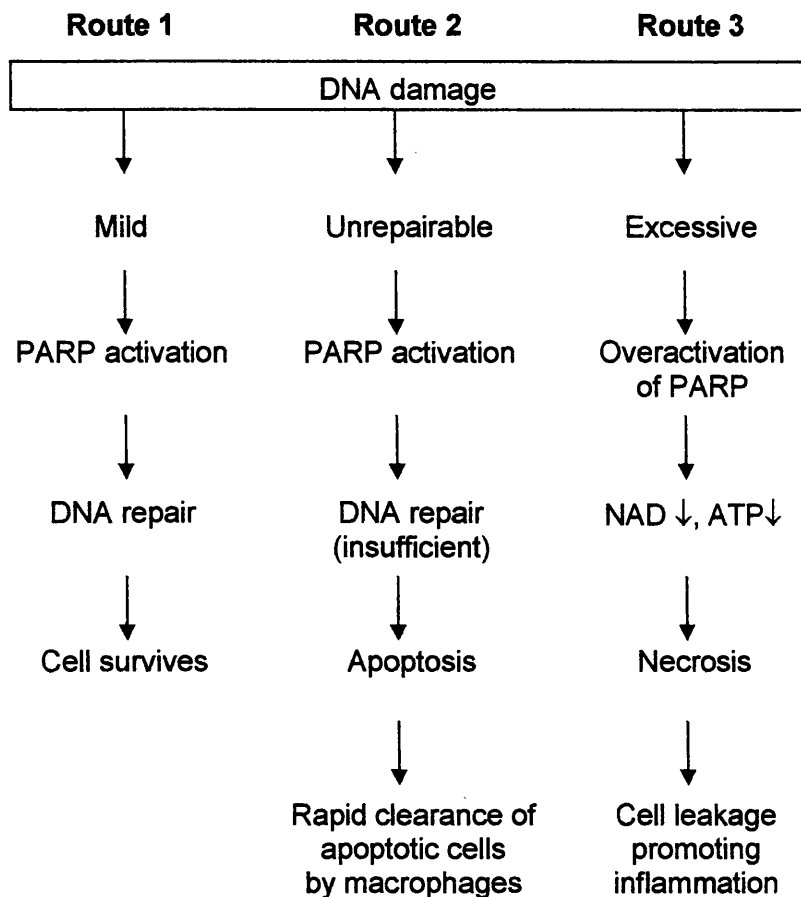


Figure 9. Intensity of DNA-damaging stimuli determines the fate of cells: survival, apoptosis or necrosis.¹³⁵

1.7.2 Role of PARP in ischaemia-reperfusion injury

Ischaemia is the condition suffered by tissues and organs when deprived of blood flow. Reperfusion injury refers to the tissue damage caused when blood flow is restored after an ischaemic period of more than about ten minutes. Ischaemia-reperfusion injury is a complex phenomenon that often occurs during surgery.

Reperfusion triggers the generation of multiple oxidants and free radicals, which include nitric oxide, hydroxyl radical and superoxide. These reactive species, in turn, lead to the generation of peroxynitrite (a highly reactive oxidant produced from the reaction between nitric oxide and superoxide). Peroxynitrite cytotoxicity occurs via multiple pathways involving the oxidative modification and inactivation of proteins and the generation of DNA single strand damage, with consequent activation of PARP-1. PARP-1 overactivation appears to be crucial in ensuing cell death. Ischaemic-reperfusion diseases where PARP-1 activation plays a pathogenic role include haemorrhagic shock, myocardial infarction, stroke and acute renal failure. The

mechanism proposed for the protective action of PARP inhibition in ischaemia-reperfusion injury is the preservation of intracellular NAD⁺ and ATP levels through the interruption of the energy-consuming cycle of DNA damage / PARP overactivation. PARP-mediated reperfusion injury has been extensively studied in the heart and brain. Thiernemann *et al.*¹³⁶ demonstrated that the PARP inhibitor 3-AB reduced the infarct size caused by ischaemia-reperfusion of the heart and skeletal muscle in rabbit models. These results highlight the potential of PARP-1 inhibitors as cardioprotective agents. The inhibition of PARP-1 or PARP-1 genetic inactivation reduces myocardial necrosis in the acute and delayed stages of myocardial infarction.^{137,138} Zingarelli *et al.*¹³⁹ have indicated that PARP-1 inactivation resulted in suppression of neutrophil infiltration and a decrease in inflammatory cytokines. The application of the novel PARP inhibitor PJ34 was assessed after reversible hypothermic ischaemia in a heterotopic rat heart transplantation model. It was demonstrated that inhibiting PARP activity significantly reduced the size of myocardial infarcts.¹⁴⁰

Eliasson *et al.*¹⁴¹, discovered in 1997 that PARP-1 *-/-* mice were resistant to brain ischaemia. The PARP *-/-* mice showed reduced histopathological injury and improved functional outcome, as compared to the PARP *+/+* counterparts. Cosi *et al.*¹⁴² showed that PARP is activated in glutamate-induced death of cerebellar granule neurons in culture. In this study, the PARP inhibitors 3-AB and 3-aminophthalhydrazide were shown to possess neuroprotective potential *in vivo*. Cosi *et al.*¹⁴³ also demonstrated that PARP inhibitors (benzamide and 3-AB) were neuroprotective *in vivo* against 1-methyl-4-phenyl-1,2,3,6-tetrahydropyridine (MPTP)-induced neurotoxicity in C57BL/6N mice. MPTP is a neurotoxin that replicates the motor signs observed in Parkinson patients and produces loss of dopaminergic neurons. Mandir *et al.*¹⁴⁴ showed that mice lacking the PARP-1 gene were resistant to MPTP-induced dopamine neurotoxicity, suggesting novel strategies for the treatment of Parkinson's disease.

More recently, Genovese *et al.*¹⁴⁵ investigated the role of PARP in the tissue injury associated with stroke and neurotrauma. It was demonstrated that the treatment of mice with the PARP inhibitors 3-AB and 5-aminoisoquinolinone (5-AIQ) significantly reduced the degree of spinal cord inflammation, tissue injury, neutrophil infiltration, and apoptosis. These protective effects are associated with the activation of the nuclear factor NF- κ B in the inflamed spinal cord.

The role of PARP-1 in ischaemia-reperfusion is not just confined to the heart and brain. Activation of PARP-1 has also been reported for the reperfused kidney, liver, gut, and eye. Selected ischaemia-reperfusion models are outlined in Table 1.

Table 1. PARP inhibition in animal models of ischaemia-reperfusion injury.

Organ	Disease model	PARP inhibitors	Main result
Gastrointestinal tract	Mesenteric I/R injury	3-AB ¹⁴⁶ NA, ¹⁴⁶ GPI-6150 ¹⁴⁷ 5-AIQ ¹⁴⁸	Protection against histological infiltration and mucosal barrier failure.
Kidney	Reperfusion injury	3-AB ¹³⁶ 5-AIQ ¹⁴⁹	Accelerated recovery of normal renal function.
Liver	I/R	PJ-34 ¹⁵⁰ 5-AIQ ¹⁵¹	Reduction in hepatic necrosis and protection against leukostasis.
Eye	Retinal I/R	3-AB ¹⁵²	Reduction in I/R-induced injury.
Many organs	Haemorrhagic shock	5-AIQ ¹⁵¹	Protection against haemodynamic decompensation and elimination of multiple organ injury and dysfunction.

3-AB, 3-aminobenzamide; NA, nicotinamide; 5-AIQ, 5-aminoisoquinolinone;

PJ-34, *N*-(6-oxo-5,6-dihydro-phenanthridin-2-yl)-*N,N*-dimethylacetamide;

GPI-6150, 1,11b-dihydro-[2H]benzopyrano [4,3,2-*de*]isoquinolin-3-one;

I/R, ischaemia-reperfusion

1.7.3 Role of PARP-1 in inflammation

PARP-1 overactivation plays a role in various experimental models of inflammation, including acute inflammatory diseases such as diabetes and septic shock, as well as chronic inflammation of the gut, joints, and various other organs.

Septic shock is a pathology related to inflammation. Gram-negative bacteria that form endotoxins cause septic shock. Endotoxins are associated with lipopolysaccharides (LPS) that activate NF- κ B/Rel transcription factors, including a number of genes

involved in endotoxic shock.¹⁵³ Endotoxins and the free radicals produced during the inflammation process elicit DNA damage and cause PARP-1 overactivation. Recently, de Murcia and co-workers¹⁵³ demonstrated that PARP-1 deficient mice are resistant to LPS-induced endotoxic shock. In the absence of PARP-1, NF- κ B transcription is impaired and the production of multiple pro-inflammatory mediators is down regulated. It has been demonstrated that septic shock can be prevented by the use of nicotinamide and 3-AB.¹⁵⁴

Type I diabetes of insulin-dependent diabetes mellitus is a chronic disorder resulting in destruction of pancreatic β cells. Destruction of the β cells in diabetes has been attributed to the production of NO and various other free radical oxidant species. Streptozotocin (STZ) selectively destroys insulin-producing pancreatic β -cells and provides a model for type I diabetes. The PARP-1 inhibitor 3-AB prevented the development of diabetes in STZ-mice. Pieper et al.,¹⁵⁵ in 1999, illustrated that PARP-deficient mice are protected from STZ-induced diabetes; therefore, PARP activation may participate in the pathophysiology of type I diabetes. Pharmacological inhibition of PARP-1 also suppresses the development of rheumatoid arthritis¹⁵⁶ and colitis¹⁵⁷ in rodent or mice models.

1.8 Current status of clinical trials on PARP inhibitors

Several PARP inhibitors are currently being evaluated in clinical trials, and their current status is summarised in Table 2.

Table 2. PARP inhibitors in clinical trials.¹⁵⁸

Company	PARP Inhibitor	Application	Clinical status
Abbot Laboratories	ABT-888	Refractory solid tumours and lymphoid malignancies	Phase 0
Pfizer / University of Newcastle	AG014699	Metastatic malignant melanoma	Phase II
Pfizer / University of Newcastle	AG014699	Advanced solid tumours	Phase I
BiPar	BSI-201	Advanced solid tumours	Phase I
AstraZeneca / KuDOS	KU-0059436	Advanced solid tumours	Phase I
Inotek	INO-1001	Melanoma, glioblastoma	Phase I
Inotek	INO-1001	Thoracoabdominal aortic aneurysm	Phase I
Inotek	INO-1001	ST-elevated myocardial infarction	Phase I
Inotek	INO-1001	Ischaemia and reperfusion injury	Phase II
MGI Pharma	GPI 21016	Solid tumours	Phase I planned
Fujisawa Pharmaceutical	FR255595	Parkinson disease	Phase I

ABT-888. ABT-888 is the first PARP inhibitor to be studied in a Phase 0 clinical trial. Phase 0 trials conducted by the National Cancer Institute under an exploratory Investigational New Drug application focus on extensive agent characterisation and target assay development in a limited number of patients.¹⁵⁹ The aim of the Phase 0 study is to determine the dose range at which ABT-888 inhibits PARP activity in tumour samples and peripheral blood mononuclear cells. The study also aims to assess the pharmacokinetics of ABT-888, and the time course of PARP inhibition in peripheral blood mononuclear cells. Phase I clinical trials of ABT-888 in patients with refractory solid tumours or lymphoid malignancies are due to start in 2007.

AG014699. AG014699, a potent tricyclic indole, was the first PARP inhibitor to be evaluated in human cancer clinical trials.¹⁶⁰ The Phase I clinical study combined

AG014699 and TMZ in patients with advanced solid tumours. A PARP inhibitory dose (PID) of AG014699 was determined by measuring the PARP activity in peripheral blood lymphocytes. Patients were treated with escalating doses of AG014699 in combination with TMZ on a five times daily schedule once every four weeks, until the PARP inhibitory dose was determined. Minimal toxicity was observed with the combination of the PARP inhibitory dose of AG014699 ($12 \text{ mg m}^{-2} \text{ d}^{-1}$) and doses of TMZ up to the registered dose of $200 \text{ mg m}^{-2} \text{ d}^{-1}$.¹⁶⁰ AG014699 pharmacokinetic studies indicated that the mean terminal half-life ranged from 7.4-11.7 h with clearance of 25 L/h. In the Phase II study, 40 patients with advanced metastatic melanoma were treated with $12 \text{ mg m}^{-2} \text{ d}^{-1}$ in combination with escalating doses of TMZ to establish the maximum tolerated dose of the combination. There was significant enhancement of TMZ-associated myelosuppression and no toxicity specific to the PARP inhibitor was observed.¹⁶¹

Currently, a Phase II clinical study of AG014699 as a single agent in metastatic breast and ovarian cancer in proven carriers of BRCA-1 and BRCA-2 mutations is in development.

BSI-201. The PARP inhibitor BSI-201 is currently being evaluated in a Phase I clinical trial in patients with solid tumours. There are no published data so far from the ongoing monotherapy trials. BiPAR Sciences announced in a press release (January, 2007) that it is due to begin a Phase Ib study of BSI-201 in combination with four different cytotoxic regimens.

KU-0059436. The KuDOS PARP inhibitor KU-0059436 has a mean IC_{50} of 2 nM against PARP-1 and is currently being evaluated as a single anti-cancer agent.¹⁶² KU-0059436 is targeted at inherited breast and ovarian cancer (BRCA 1 and 2 mutations). The Phase I study initially began with daily dosing of KU-0059436 for 14 days of a 21-day cycle and is now evaluating twice-a-day dosing in patients with advanced solid tumours.¹⁶² Pharmacodynamic studies showed inhibition of PARP functional activity in peripheral blood mononuclear cells.

INO-1001. INO-1001, an indenoisoquinolinone-based PARP inhibitor, is currently being evaluated in a Phase I trial in patients with metastatic melanoma and glioma. A preliminary analysis of the pharmacokinetic data of INO-1001 in combination with TMZ found that the treatment was fairly well tolerated in patients with unresectable stage III/IV melanoma.¹⁶³ INO-1001 is also in clinical trials for the treatment of reperfusion

injury induced by myocardial infarction, cardiopulmonary bypass and thoraco-abdominal aortic aneurysm surgery.

GPI-21016. In pre-clinical studies the PARP inhibitor GPI-21016 was shown to enhance the anti-tumour efficacy of cisplatin in a murine leukaemia model.¹²⁶ The PARP inhibitor was also shown to limit cisplatin-induced neuropathy.¹⁶⁴ A Phase I study is planned to start in 2007.

FR255595. Fujisawa Pharmaceuticals have patented a series of quinazolin-4(3*H*)-one derivatives as PARP inhibitors. The most potent compound 2-{3-[4-(4-chlorophenyl)-1-piperazinyl]propyl}-4(3*H*)-quinazolinone (FR255595) was found to have an IC₅₀ of 10 nM and to be 30 fold more selective to PARP-1 than PARP-2. FR255595 protected against 1-methyl-4-phenyl-1,2,3,6-tetrahydropyridine (MPTP)-induced nigrostriatal dopa-minergic damage in an *in vivo* Parkinson's disease model. FR255595 is currently in Phase I clinical trials for the treatment of Parkinson disease.¹⁶⁵

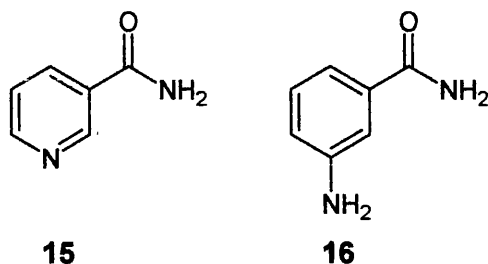
1.9 PARP inhibitors

Most of the PARP inhibitors developed to date are competitive reversible inhibitors that bind to the NAD⁺ binding site of the enzyme. Selectivity for the individual PARP isoforms has not been studied in great detail; however, it is probable that potent PARP inhibitors will inhibit the activity of all the isoforms. Great progress has been made over the last few years in the synthesis of potent PARP inhibitors thanks to a better knowledge of the structure of PARP and its catalytic active site, which has allowed structure-activity relationships to be studied. However, there still remains a need for improvement in potency and selectivity of PARP inhibitors.

1.9.1 Nicotinamide and benzamide

Nicotinamide **15** is a natural compound, which is required for NAD⁺ synthesis and serves as a substrate for NAD⁺ metabolising enzymes. Nicotinamide is a weak PARP inhibitor (IC₅₀ = 210 μM) and has poor selectivity. Nicotinamide behaves as a substrate for metabolising enzymes such as nicotinamide-N-methyltransferase deaminase and phosphoribosyl transferase. Shall *et al.*¹⁶⁶ first showed that benzamide, a structural analogue of nicotinamide, demonstrated inhibition of PARP-1. Purnell and Whish¹⁶⁷ generated a series of benzamides with an electron-donating group at the 3-position. In particular, 3-aminobenzamide **16** (IC₅₀ = 22 μM) was more effective than nicotinamide.

However, the benzamide series have a limited solubility in water as the 1° amide group present in these compounds forms hydrogen-bonded dimers in the crystalline solid. In the benzamide series, alkylation of the carboxamide or replacement with a carboxylic acid group greatly reduced the inhibitory activity. Both nicotinamide and 3-aminobenzamide have been widely used to study the physiological functions of PARP (Section 1.6). These studies have stimulated further research about the specificity of benzamide inhibitors.



1.9.2 Dihydroisoquinolinones and isoquinolinones

The encouraging results obtained in PARP-1 inhibition studies with nicotinamide and the benzamides and the knowledge of the therapeutic benefits of PARP inhibition led to the design of some structurally improved PARP inhibitors.

Ab initio molecular orbital studies carried out by Hong *et al.*¹⁶⁸ provided important information regarding the conformation of the carboxamide group of NAD⁺ in the enzyme active site. The *ab initio* calculations were based on the principle that the carboxamide group of NAD⁺ adopts one of two orientations relative to the catalytic groups within the enzyme's active site (Figure 10). It was found that the conformation of NAD⁺ that binds to PARP-1 has the carboxamide group in an *anti* as opposed to a *syn* conformation. Evidence to support these findings was provided by Suto *et al.*¹²⁹, who designed conformationally restricted compounds. They synthesised a series of rigid benzamides, the 5-substituted dihydroisoquinolinones and isoquinolinones, by closing the amide nitrogen upon the benzene ring with an ethane bridge. The parent compounds **17** and **20**, in which the carboxamide is in the biologically-active *anti*-orientation, were more potent than 3-aminobenzamide with IC₅₀s of 1.5 μM and 6.2 μM respectively. Similarly, it was found that 5-hydroxy-3,4-dihydroisoquinolinone (**18**, IC₅₀ = 0.10 μM) and 5-hydroxyisoquinolin-1-one (**21**, IC₅₀ = 0.15 μM) were potent PARP-1 inhibitors. Studies indicated that, when the substituent in 5-substituted dihydroisoquinolinone was moved to the 6, 7 or 8 position, biological activity decreased. Therefore, Suto and co-workers¹²⁹ concluded that the positioning of substituents on the benzene ring along with the restriction of the carboxamide rotation into the *anti*-

conformation was critical for potent activity. The most potent inhibitor identified in the dihydroisoquinolinone series was 5-methyl-3,4-dihydroisoquinolinone (**19**, PD128763), which was found to be 60-fold more potent than 3-AB against PARP. PD128763 was used to elucidate the tridimensional structure of the catalytic fragment (CF) of chicken PARP.

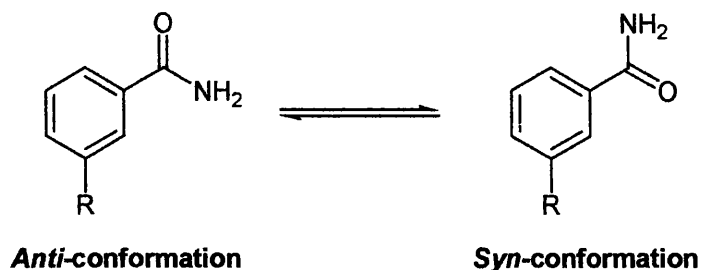
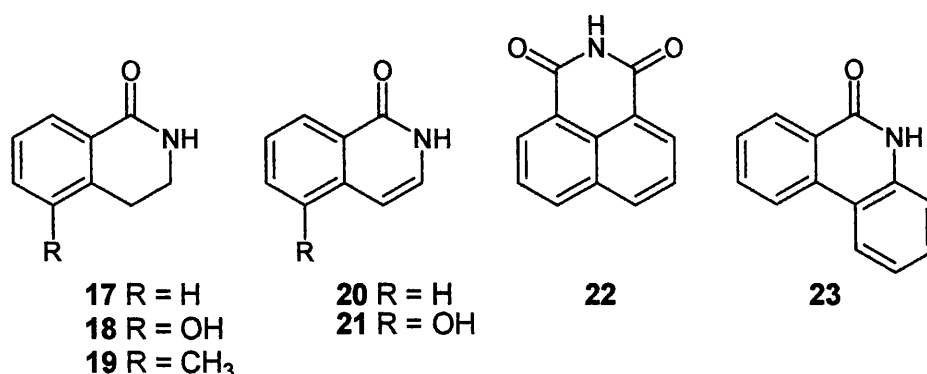


Figure 10. Representation of the restriction of the carboxamide group into either the *anti*- or *syn*- conformation.¹⁶⁸

Banasik and co-workers¹⁶⁹ at Kyoto University screened a large number of compounds and compared their abilities to inhibit PARP. They found that the compounds that had the carboxamide group incorporated within a ring system displayed very potent PARP-1 inhibitory activity. It was proposed that the controlling factor for inhibitory activity was the ability of the oxygen atom of the carboxamide group to donate π -electrons to the enzyme active site. In addition, it was found that all highly potent PARP inhibitors were polyaromatic heterocycles. These heterocycles included the isoquinolinone-related compounds 1,8-naphthalimide **22** and phenanthridinone **23**. The IC_{50} values for the polyaromatic heterocycles varied between 0.18 μ M and 0.39 μ M.

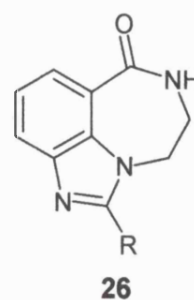
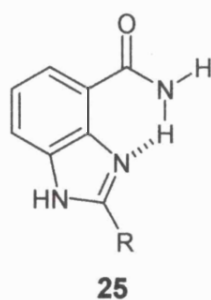
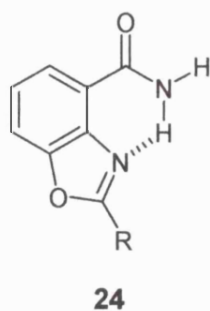


Based on the studies by Banasik *et al.*¹⁶⁹ and on a better understanding of the molecular details of the active site of PARP-1, new highly potent PARP inhibitors have been synthesised.

1.9.3 Benzoxazoles and benzimidazoles

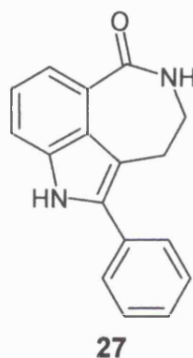
Researchers at the University of Newcastle-upon-Tyne investigated an alternative approach of constraining the carboxamide group in the required *anti*-conformation. They designed a series of benzoxazole-4-carboxamides¹²² and benzimidazole-4-carboxamides¹⁷⁰ with a 6/5 fused ring system, where the carboxamide group was restricted *via* an intramolecular hydrogen bond between the amide proton and the heterocyclic nitrogen. The benzoxazole-4-carboxamide series possessed good donor properties due to the electron-rich heterocycle and demonstrated IC₅₀ values ranging from 2 to 10 μM. 2-Phenylbenzoxazole-4-carboxamide **24c** was the most potent compound with an IC₅₀ value of 2.1 μM. A series of benzimidazole derivatives was then synthesised with alkyl and aryl substituents. The benzimidazole-4-carboxamides **25a** and **25b** showed sub-micromolar activity against PARP-1. A study of the structure-activity relationships (SAR) was carried out for a series of 2-aryl-1*H*-benzimidazole-4-carboxamides. The results showed that PARP-1 tolerates numerous electron-donating and -withdrawing substituents in the 3- and 4- positions on the phenyl ring. 2-(4-(trifluoromethyl)phenyl)-1*H*-benzimidazole-4-carboxamide **25i** was found to be the most active inhibitor. It was also demonstrated that substituents with small groups could be tolerated in the 2 position on the phenyl ring; for example, 2-(2-chlorophenyl)-1*H*-benzimidazole-4-carboxamide **25f** and its isomer **25e** were found to have similar activity. 2-(4-Hydroxyphenyl)-1*H*-benzimidazole-4-carboxamide (NU1085, **25g**, K_i = 6 nM) potentiated the cytotoxic effects of temozolomide and topotecan.¹⁷⁰ These findings indicated that, in the 2-aryl-1*H*-benzimidazole-4-carboxamide series, the intramolecular hydrogen bond constrained the carboxamide in the biologically active conformation and, in addition, the compounds possessed good donor properties due to the presence of an electron-rich heterocyclic ring.

Skalitzky *et al.*¹⁷¹ synthesised tricyclic benzimidazole carboxamide potent PARP-1 inhibitors containing a 5/6/7 fused ring system. In these compounds the intramolecular hydrogen bond is replaced with a covalent bond. The presence of alkyl substituents in the 2-position only had modest activity against PARP-1. The series was extended to include unsubstituted and monosubstituted rings. Of this series compounds **26b**, **26f**, and **26g** were found to be chemopotentiators of temozolomide and topotecan against human lung carcinoma. These studies were extended to include tricyclic indole analogues that restrict the conformation of the carboxamide moiety within a seven-membered ring. The 2-phenyl tricyclic indole **27** has a K_i value of 6 nM suggesting that the lactam N-H participates in a beneficial interaction with the PARP-1 active site.

Table 3. PARP-1 inhibitory activities of benzoxazoles and benzimidazoles.

Compound	R	IC ₅₀ (μM)
24a	CH ₃	9.8
24b	C(CH ₃) ₃	8.4
24c	Ph	2.1

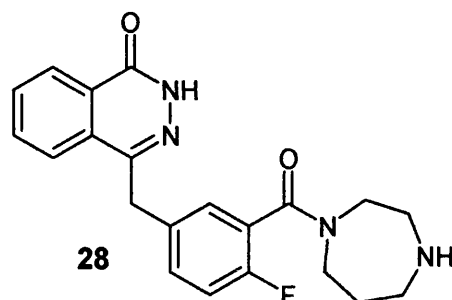
Compound	R	K _i (nM)
25a	H	95
25b	CF ₃	350
25c	Ph	15
25d	4-CN-Ph	4.0
25e	3-Cl-Ph	8.4
25f	2-Cl-Ph	9.4
25g	4-OH-Ph	6.0
25h	4-OMe-Ph	6.8
25i	4-CF ₃ -Ph	1.2
25j	3-CF ₃ -Ph	8.0
26a	Ph	4.1
26b	4-Cl-Ph	5.7
26c	2-Cl-Ph	7.7
26d	3-CF ₃ -Ph	11.2
26e	CH ₃	45
26f		6.3
26g		5.8



1.9.4 Phthalazinones and quinazolinones

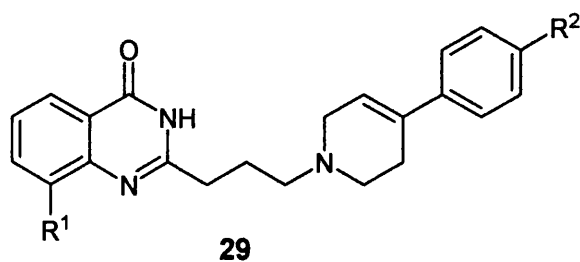
The bicyclic phthalazinone and quinazolinone scaffolds have undergone elaboration in order to achieve better PARP-1 inhibitory activity. KuDOS Pharmaceuticals have been optimising the known 4-aryl-phthalazinones to improve their metabolic stability and potency. KuDOS tested a series of *meta*-substituted 4-benzyl-2*H*-phthalazin-1-one PARP inhibitors. Most of the compounds tested showed low nanomolar inhibitory activity with IC₅₀ values between 5 and 50 nM. Compound **28**, showed low nanomolar inhibitory activity (IC₅₀ = 7 nM) and promising metabolic stability *in vivo*.¹⁷² Griffin *et al.*¹⁷³ reported a series of quinazolin-4-one PARP inhibitors. The most potent compounds were the 8-methyl-quinazolinones, with a 2-phenyl group substituted by a 4-cyano, 4-nitro or 4-methoxy group. 8-Hydroxy-2-methylquinazolin-4-[3*H*]-one

(NU1025) was found have an IC₅₀ of 0.4 μM, and to enhance the action of topotecan and temozolomide in a panel of twelve human tumour cell lines.

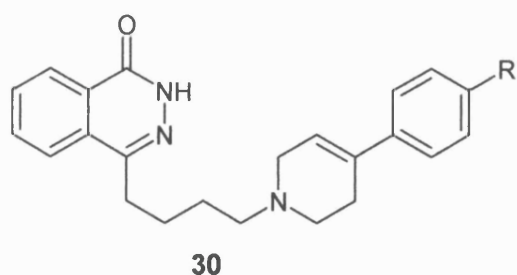


Iwashita and co-workers¹⁷⁴ investigated PARP-1 and PARP-2 inhibitory activity of quinazolinone derivatives *in vitro*. The potency of these derivatives was found to be mostly dependent on the unique linker of the quinazolinone ring. Most of the compounds tested demonstrated high selectivity for PARP-1. Compound **29a** exhibited strong potency against PARP-1 and 30-fold less potency against PARP-2. Phthalazinone derivatives **30a** and **30b** were also investigated.¹⁷⁴ Both compounds showed similar potency for PARP-1 as the quinazolinone derivatives. However, they did not demonstrate selectivity for PARP-1 and PARP-2.

Table 4. PARP-1/2 inhibitory activities of quinazolinones.



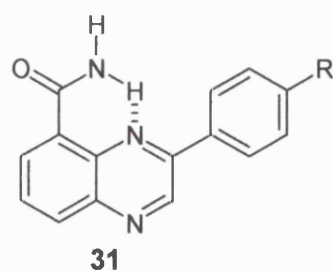
Compound	R ¹	R ²	PARP-1 IC ₅₀ (nM)	PARP-2 IC ₅₀ (nM)	Selectivity PARP-2/1
29a	H	H	21	608	29
29b	Cl	H	23	610	27
29c	Cl	CN	3.0	87	29
29d	Cl	F	13	500	39
29e	Me	F	16	167	10

Table 5. PARP-1/2 inhibitory activities of phthalazinones.

Compound	R	PARP-1 IC ₅₀ (nM)	PARP-2 IC ₅₀ (nM)	Selectivity PARP-2/1
30a	H	120	90	0.8
30b	F	49	84	1.7

1.9.5 Quinoxalines

Iwashita and co-workers¹⁷⁴ synthesised quinoxaline derivatives as selective PARP-2 inhibitors. The quinoxaline series have a 6/6 fused ring system and the carboxamide group is restricted *via* an intramolecular hydrogen bond. Various electron-withdrawing and electron-donating substituents were tolerated in the *para*-position of the terminal phenyl. 3-(4-Chlorophenyl)quinoxaline-5-carboxamide **31b** was shown to be about 5-fold more potent for PARP-2 than for PARP-1. The quinoxaline derivatives are PARP-2 selective, with compound **31b** demonstrating a selectivity of 0.21.

Table 6. PARP-1/2 inhibitory activities of quinoxalines.

Compound	R	PARP-1 IC ₅₀ (nM)	PARP-2 IC ₅₀ (nM)	Selectivity PARP-2/1
31a	H	131	14	0.11
31b	Cl	33	7	0.21
31c	CN	101	8	0.08
31d	CF ₃	118	11	0.09
31e	OMe	71	8	0.11
31f	NH ₂	87	9	0.10

1.9.6 PARP inhibitors acting at the zinc fingers

Rice *et al.*¹⁷⁵ proposed a class of PARP inhibitors that act selectively at one of the two zinc finger sites in the DNA binding domain. A series of C-nitroso substituted compounds was synthesised which uniquely oxidise one of the zinc fingers of PARP, resulting in ejection of the zinc ion. This results in the inactivation of PARP activity without halting the binding of PARP to DNA. Compounds 6-nitroso-1,2-benzopyrone and 3-nitrosobenzamide induce apoptosis in tumour cell lines through depression of a $\text{Ca}^{2+}/\text{Mg}^{2+}$ endonuclease. These compounds have also been shown to inhibit infection of HIV-1 in human lymphocytes without induction of metabolic changes at a concentration of 50 μM .

Bauer *et al.*¹⁷⁶ reported 4-iodo-3-nitrobenzamide (INO_2BA) that can be selectively reduced to the nitroso compound INOBA within the E-ras 20 tumour cell line. It is proposed that the nitroso prodrug induces Zn^{2+} from the asymmetric zinc finger of PARP-1 and subsequently inactivates PARP-1. Studies demonstrated that the action of INO_2BA could be improved by the simultaneous administration of buthionine sulfoxamine (a known inhibitor of glutathione (GSH) synthesis). However, in non-malignant CV-1 cell lines, there was complete lack of reduction of the nitro to the active nitroso prodrug.

1.10 Pharmacophore and structure-activity relationship (SAR) studies

So far it has been established that analogues of NAD^+ , are effective inhibitors of PARP. PARP inhibitory activity appears to be associated with the following structural features:

- (1) An unsaturated aromatic or polyaromatic heterocyclic system.
- (2) The presence of a carboxamide group, which should be restricted to adopt the *anti*-conformation required for hydrogen-bonding with critical residues in the NAD^+ binding site.
- (3) A non-cleavable bond at the 3-position relative to the carboxamide group.
- (4) Presence of at least one amide proton.

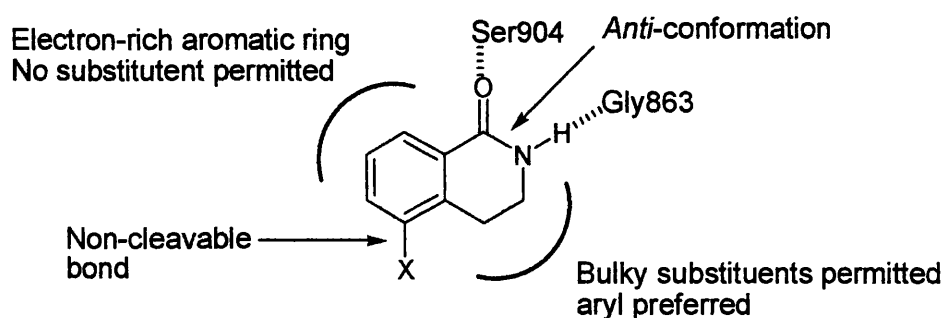


Figure 11. Consensus pharmacophore for PARP-1 inhibition.

The consensus pharmacophore for PARP-1 inhibition is shown in Figure 11. Ruf and co-workers¹⁷⁷ published the first crystal structure of the catalytic fragment of PARP-1 with and without the PARP-1 inhibitor 3,4-dihydro-5-methylisoquinolin-1-one (PD128763). The elucidation of the crystal structure has allowed structure-activity relationships to be understood and binding predictions to be made. The crystal structure showed that the carboxamide group of the inhibitor forms important hydrogen-bond interactions with the amino-acids Gly863 and Ser904. The carboxamide must be in an *anti*-conformation in order for these interactions to occur with the active site. This supports the fact that compounds, in which the amide is constrained in this conformation, are significantly more potent than those with a free amide group. The nitrogen of the carboxamide must carry at least one hydrogen in order for the important hydrogen-bond interactions to occur in the active site. The aromatic portion of the inhibitor also participates in π - π interactions with the phenyl rings of two parallel tyrosine residues (Tyr907 and 896) within the active site forming a “ π -electron sandwich”. This interaction may contribute to the increased activity of large planar fused-ring compounds.

Structure-activity relationship studies of benzimidazole-4-carboxamide with the catalytic domain of chicken PARP revealed that the carboxamide group forms three important hydrogen bonds (Figure 12). It was shown that the carbonyl oxygen of the inhibitor accepted two hydrogen bonds, one from a Gly863 polypeptide amide N-H and the other from the side chain oxygen of Ser904. The amide N-H of the compound is a hydrogen bond donor to Gly863. The benzimidazole part of the molecule was found to lie between Tyr907 and Tyr896. The 2-aryl ring was reported to lie in the NAD⁺ binding pocket, with the substituents in the 3-position having the most available space. Taking into account the mobility of Gln763 side chain space is also available in the 4 and 5 positions.¹⁷⁰

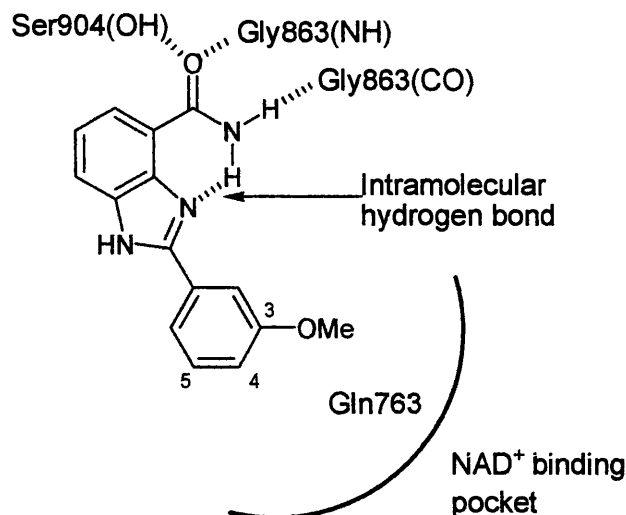


Figure 12. Interactions of 2-(3-methoxyphenyl)benzimidazole-4-carboxamide with the NAD^+ binding domain, indicating the likely positioning of a substituent within the cavity.¹⁷⁰

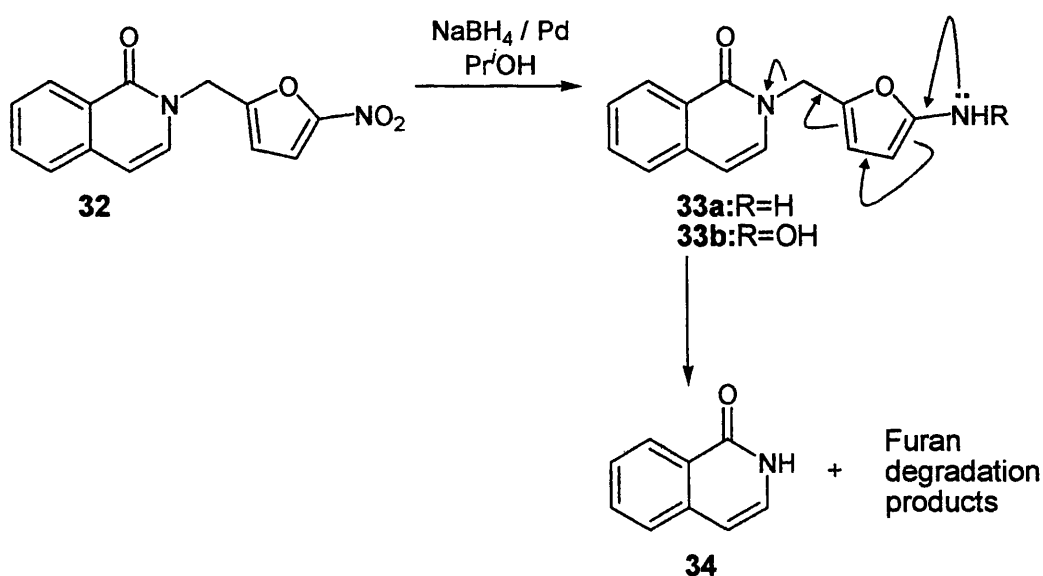
Kinoshita *et al.*¹⁷⁸ reported the crystal structure of the catalytic domain of human recombinant PARP-1 complexed with the inhibitor FR257517 (compound **29e**). The quinazolinone part of the inhibitor binds tightly to the nicotinamide-ribose binding site and the 4-phenyl-tetrahydropyridine moiety provides secondary contacts to the adenosine-binding site. The terminal 4-fluorophenyl ring of the inhibitor induces a conformational change at the bottom of the adenosine-binding site by displacing the side-chain of Arg878.

1.11 Bioreductive prodrugs of PARP-1 inhibitors

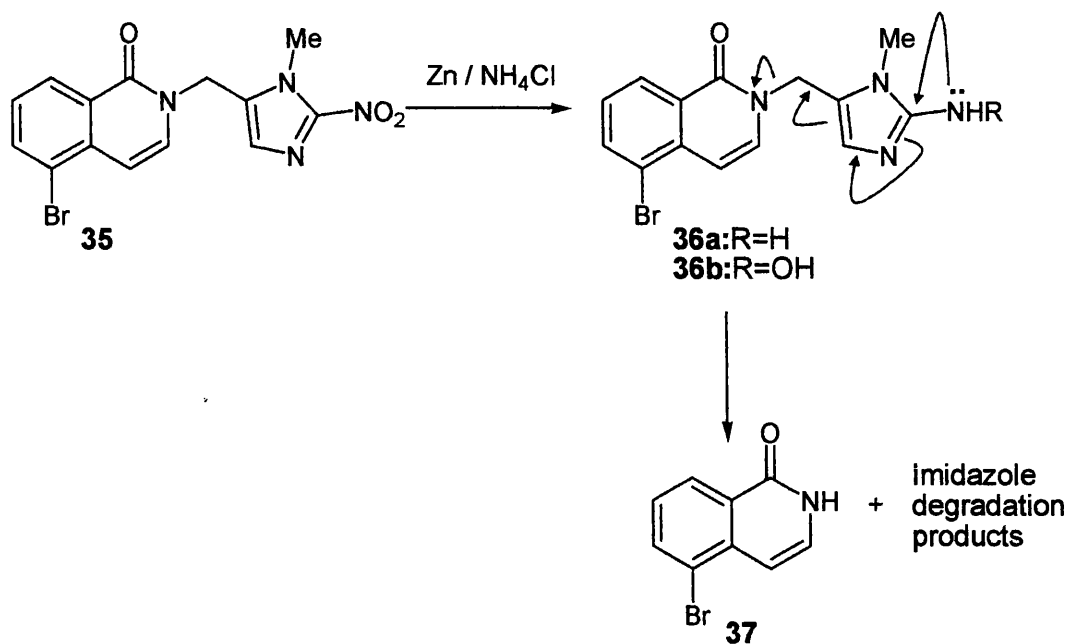
Ideally, PARP-1 inhibitors should be able to demonstrate tissue selectivity. One approach to deliver PARP-1 inhibitors selectively to the desired site of action includes the use of bioreductive prodrugs. Many of the disease states where PARP-1 inhibition is therapeutically beneficial are marked by acute or chronic tissue hypoxia. Such a physiological difference in the concentration of oxygen between normal and hypoxic cells was exploited through the design of hypoxia-activated prodrug systems, which release the PARP-1 inhibitors only in hypoxic cells. Several different redox-sensitive prodrugs have been designed to investigate the bioreductive release of isoquinolin-1-one PARP-1 inhibitors from nitroheterocyclimethyl and 4,7-dioxindole-3-methyl trigger units.

Berry *et al.*,¹⁷⁹ in 1997, first proposed the 5-nitrofuran-2-yl-methyl group as a potential bioreductively-activated prodrug system. The nitro group in the nitrofuran prodrug **32** is selectively reduced to the amine **33a** or hydroxylamine **33b**. The consequential increase in electron-density results in the expulsion of the isoquinolin-1-one drug **34**. In the prodrug **32** the pharmacophore required for activity of the isoquinolin-1-one effector **34** is masked, and PARP-1 inhibitory potency is much weaker. In hypoxic tissue, bioreduction of the prodrug mediated by cytochrome P450 reductase should trigger the release of the effector. The reductant system sodium borohydride / palladium / aqueous propan-2-ol was used to mimic the bioreduction of the nitro group in hypoxic tissue. In these studies, the release of the drug was studied by thin layer chromatography (TLC) and high pressure liquid chromatography (HPLC). It was demonstrated that **34** was rapidly and quantitatively released from the nitrofuran prodrug (Scheme 9).

1-Methyl-2-nitroimidazole-5-yl-methyl prodrugs have also been studied in our laboratory. 5-Bromoisoquinolin-1-one **37** was chosen as the effector to be attached to the nitroimidazole trigger unit.¹⁸⁰ The sodium borohydride / palladium reductive system was not sufficiently selective, in that the trigger released the effector but also caused hydrogenolysis of the C-Br bond. A zinc / ammonium system was used as a mimic for bioreduction and this proved to reduce the nitro group selectively and trigger the release of the intact PARP inhibitor (Scheme 10).

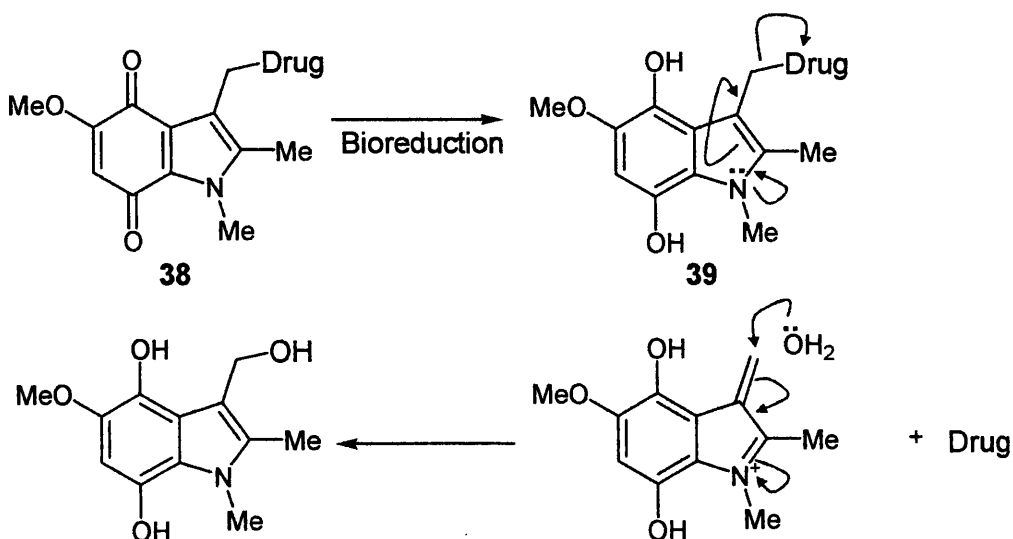


Scheme 9. Reductive release of isoquinolin-1-one **34** from the prodrug **32**.¹⁷⁹



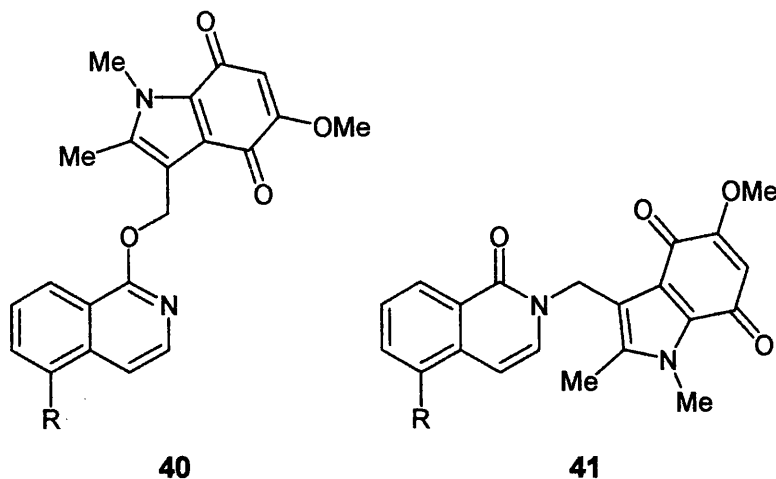
Scheme 10. Reductive release of 5-bromoisoquinolinone **37** from the prodrug **35**.¹⁸⁰

Ferrer *et al.*¹⁸¹ designed 4,7-dioxindole-3-methyl prodrugs of isoquinolin-1-ones. The proposed mechanism for bioreductively triggered release of drugs from 4,7-dioxindole-3-methyl prodrugs is shown in Scheme 11. Prodrug **38** is reduced by two electrons to the dihydroxyindole **39**; the increase in electron-density at the indole nitrogen triggers the release of the isoquinolin-1-one drug.



Scheme 11. Proposed mechanism of reductively triggered release of drugs from dioxindole-3-methyl prodrugs.¹⁸²

Mitsunobu coupling of the trigger unit 1,2-dimethyl-3-(hydroxymethyl)-5-methoxyindole-4,7-dione with various isoquinolin-1-one effectors gave O-linked **40** and N-linked **41** prodrugs.¹⁸¹ In a chemical model system for bioreduction, SnCl₂ in CDCl₃ / CD₃OD triggered release of the corresponding isoquinolin-1-ones from O-linked prodrugs but not from the N-linked prodrugs. These studies have indicated that there is the potential for the design of bioreductive prodrugs that release other structurally related PARP-1 inhibitors.



Thus there has been some research effort on prodrugs for selective delivery of PARP inhibitors based on masking the pharmacophore with an external group. However, there are no reports of prodrugs where the pharmacophore has either been masked by an N-oxide within its structure or by distortion of the pharmacophore by such an N-oxide.

2. Aims and Objectives

The main aim of the research is to develop novel chemo- and radiosensitising drugs and hypoxia-activated N-oxide prodrugs.

2.1 Design of substituted quinoline-8-carboxamides as novel PARP-1 inhibitors

Previous studies have indicated that benzimidazole-4-carboxamides and quinoxaline carboxamides are potent PARP inhibitors. Both these classes of compounds constrain the carboxamide moiety in the *anti*-conformation using an intramolecular hydrogen-bond. On the basis of the structure activity relationship studies carried out on these PARP inhibitors, it is possible to propose quinoline-8-carboxamides as novel PARP-1 inhibitors; a hypothesis for the interaction of the inhibitor with the enzyme active site is shown in Figure 13. Quinoline-8-carboxamides possess structural properties that are essential for significant PARP-1 inhibitory activity. In the quinoline-8-carboxamide targets, the carbonyl group should be a good hydrogen-bond acceptor to the amino-acid residues Ser904 and Gly863 within the NAD⁺ binding domain. The presence of one free amide proton is also important for hydrogen-bonding with the amino-acid residue Gly863. Conjugation to an electron-rich aromatic ring should enhance the acceptor properties of the carbonyl group. The design of the quinoline-8-carboxamides is derived from the concept of using an intramolecular hydrogen bond to control the carboxamide conformation, pioneered by Griffin and co-workers.¹⁷⁰ It is predicted that an intramolecular hydrogen bond will arise between the amide N-H and pyridine nitrogen, forcing the required *anti*-conformation of the carboxamide group. The geometry of the 6/6 fused ring system should be optimal for the formation of the critical intramolecular hydrogen bond.

The synthesis of a series of 2-substituted and 3-substituted quinoline-8-carboxamides will establish whether the postulated hydrogen bond is real and enable the structure activity relationship studies of a variety of substituents to be explored. Studies on benzoxazole, benzimidazole and quinazolinone PARP inhibitors have indicated that a variety of aryl substituents are well tolerated within the enzyme active site (e.g. NO₂, NH₂, OMe, halogen). In the target compounds, R² and R³ will be (substituted) phenyl, (substituted) heterocyclyl, alkyl, alkenyl and alkynyl substituents, carrying solubilising groups if necessary. Individual compounds will carry only one aryl substituent. Groups at R₄ will be used to modify the redox potential of the corresponding N-oxides (see below), and to modify the physicochemical parameters, if necessary. Preliminary

modelling studies show that these substituents will lie in the NAD⁺ binding pocket occupied by the 2-aryl groups in the 2-aryl-1*H*-benzimidazole-4-carboxamide.

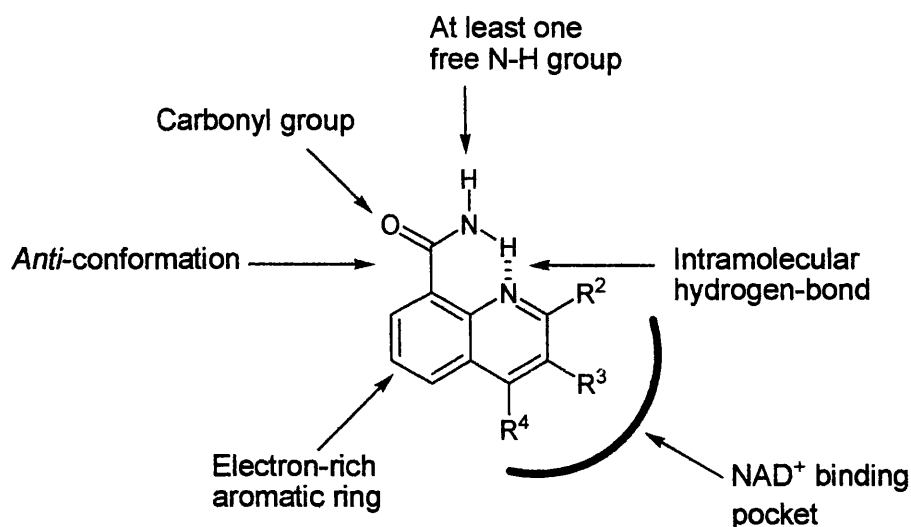
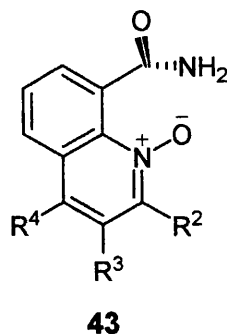
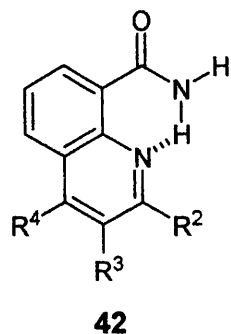


Figure 13. General structure of potential quinoline-8-carboxamide PARP-1 inhibitors.

2.2 Design of hypoxia-activated N-oxide prodrugs of substituted quinoline-8-carboxamide PARP-1 inhibitors

Many disease states where PARP-1 inhibition is therapeutically beneficial are marked by acute or chronic hypoxia. Consequently, there is a requirement for tissue-selective PARP-1 inhibitors. It is proposed that the physiological difference in the concentration of oxygen between normal and hypoxic tissue can be exploited by developing a prodrug system which, when activated under hypoxic conditions, will release inhibitors of PARP-1 selectively in cancer tissue. As previously mentioned, the isoquinolin-1-one PARP inhibitor has been successfully released from the nitroheterocyclymethyl and 4,7-dioxindole-3-methyl redox-sensitive triggers. Studies have shown that aliphatic and aromatic N-oxides can be selectively bioreduced in hypoxic tissue. The concept of combining a PARP-1 inhibitor with an N-oxide trigger is novel. Denny *et al.*⁴³ described the modular nature of the design of prodrugs as comprising of a trigger, linker and effector. The proposed quinoline-8-carboxamide N-oxide targets fulfil the criteria which are considered essential for hypoxia-selective prodrugs. In the N-oxide the severe steric clash should force the carboxamide out of the plane of the quinoline. It is proposed that this steric clash deactivates the effector in aerobic conditions and disrupts the pharmacophore required for PARP-1 inhibition. However, in hypoxic conditions, the N-oxide trigger unit will be selectively metabolised by tumour-specific enzymes. It is hypothesised that, upon bioreduction, there will be a conformational

switch from the N-oxide trigger **43** to the planar active PARP-1 inhibitor **42**. The quinoline-8-carboxamide effector will then sensitise tumour cells to chemotherapeutic and radiotherapeutic treatments.

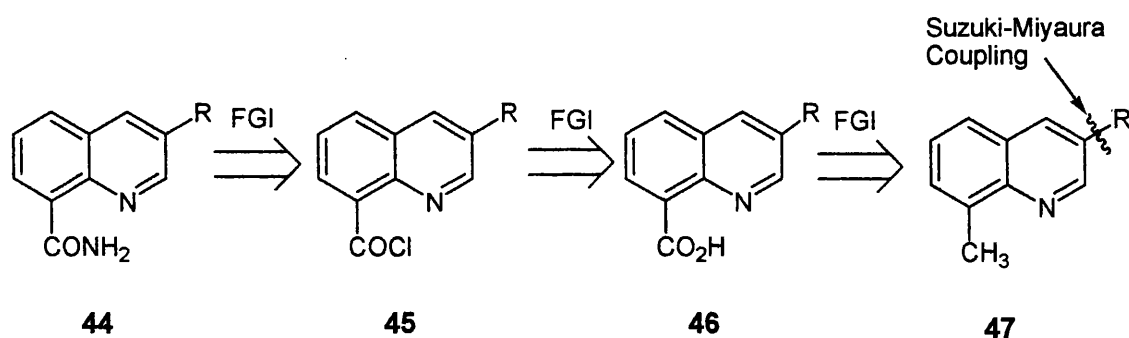


3. Results and Discussion

3.1 Route (I): 3-Substituted quinoline-8-carboxamides

3.1.1 Retrosynthetic analysis

The first target compounds to be investigated were the 3-substituted quinoline-8-carboxamides. The structural core of quinoline has previously been synthesised by various reactions, such as Skraup, Doebner-von Miller, Friedländer, Pfitzinger, Conrad-Limpach and Combes syntheses.¹⁸³ The classical approaches to quinoline compounds are based on the use of mono-substituted or *ortho*-substituted anilines. However, these methods do not allow for adequate diversity and substitution on the quinoline ring system. These synthetic approaches also have considerable drawbacks such as harsh reaction conditions and highly acidic medium, which makes the isolation of products difficult. In designing our synthetic strategies, an effort was made to ensure that a variety of substituents with various electron-withdrawing and -donating groups could be attached at the 3-position *via* a common synthetic approach. Therefore, it was decided to use a quinoline ring system containing a functional group in the 8-position, which could be easily converted to the carboxamide moiety required for PARP-1 inhibitory activity. It was thought that electrophilic substitution of the 8-substituted quinolines would allow for the introduction of substituents in the 3-position *via* organometallic coupling reactions.



Scheme 12. Route (I) retrosynthetic analysis of 3-arylquinoline-8-carboxamides.

The retrosynthetic analysis for route (I) is shown in Scheme 12. We approached our retrosynthesis by first performing three functional group interconversions (FGI) on the target molecule **44** and this led us to the corresponding 3-aryl-8-methylquinoline **47**. The conversion of a carboxylic acid to a carboxamide group is a well-established

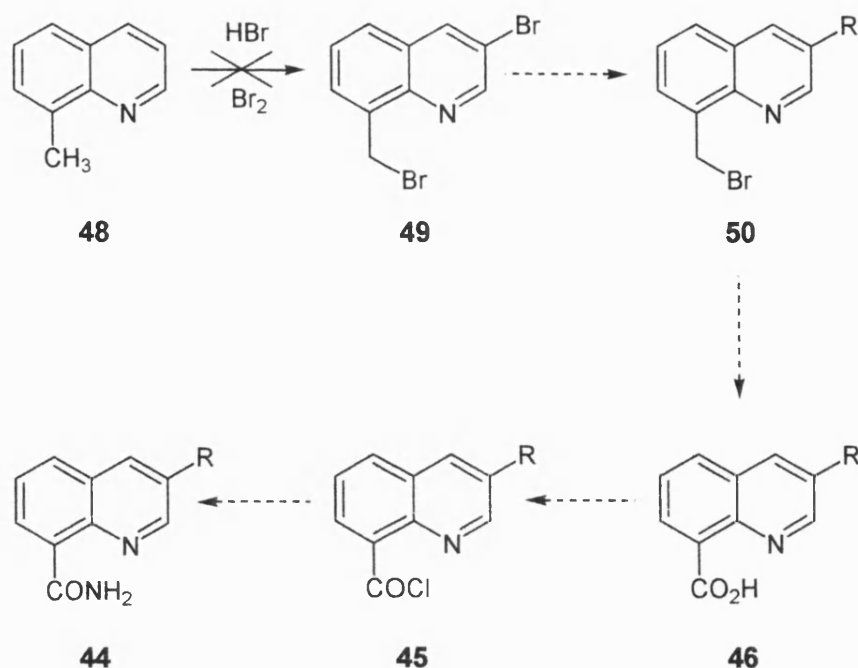
reaction. In our laboratory, the conversion of quinoline-8-carboxylic acid to quinoline-8-carboxamide has been previously reported. Parveen¹⁸⁴ reported the conversion of quinoline-8-carboxylic acid to quinoline-8-carbonyl chloride following treatment with thionyl chloride. Treatment of the quinoline-8-carbonyl chloride with ammonia and CHCl_3 gave quinoline-8-carboxamide in 90% yield.

The carboxylic acid **46** can be made by oxidation of the corresponding 3-aryl-8-methylquinoline **47**. The next step was to devise a strategy for the formation of 3-aryl-8-methylquinoline. A C-C bond disconnection occurs at the biaryl bond, which can be derived from organometallic coupling reactions. It was decided that the Suzuki-Miyaura coupling reaction be used for the synthesis of 3-arylquinoline-8-carboxamides because of its success in the formation of a wide variety of heterocyclic compounds. Many of the previously employed methods for the synthesis of C-C bonds involve the coupling of highly reactive organometallic reagents, such as Grignard, organolithium and organozinc reagents with aryl halides. These reactions usually require anhydrous conditions and an inert atmosphere and only certain functional groups are tolerated.

The Suzuki-Miyaura reaction generally involves the metal-catalysed reaction of an arylboronic acid with an aryl halide, or triflate.

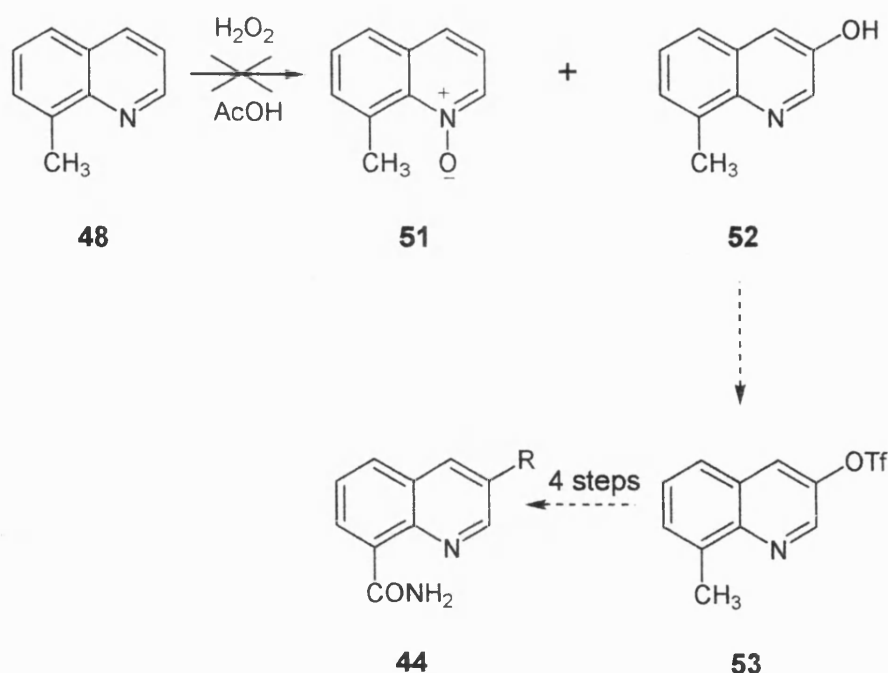
3.1.2 Attempted syntheses of 3-aryl-8-methylquinolines

8-Methylquinoline **48** was chosen as the precursor to the formation of 3-arylquinoline-8-carboxamides. The synthesis of 3-bromo-8-(bromomethyl)quinoline **49** has been reported by Howitz *et al.*¹⁸⁵ This provides compound **49**, in which the bromo is in the required location to add an aromatic substituent to the C(3)- position of the quinoline *via* Suzuki-Miyaura cross-coupling (Scheme 13). The reaction also converts the 8-methyl group into a CH_2Br *via* a radical bromination reaction. Further reaction at this position was planned to give the carboxylic acid **46** and the acid chloride **45** and finally the carboxamide **44**. However, two attempts to repeat the 1906 method of Howitz *et al.*¹⁸⁵ were unsuccessful and after heating at 200°C for 2 h, the ^1H NMR spectrum showed only starting material.



Scheme 13. Attempted synthesis of 3-bromo-8-(bromomethyl)quinoline.

An alternative approach to introduce an aromatic substituent in the 3-position was investigated. The oxidation of 8-methylquinoline **48** to prepare 3-hydroxy-8-methylquinoline **52** has previously been reported by Nakashima and co-workers.¹⁸⁶ This reaction also gives the N-oxide **51** as a by-product. Oxidation gives the hydroxy group in the required 3-position to allow for further reaction. The hydroxy group can then be converted to a triflate group using trifluoromethanesulfonic anhydride. It was hoped that conversion to the triflate **53** and subsequent Suzuki-Miyaura coupling would give compounds such as **44** where R is a (substituted) phenyl group (Scheme 14). 8-Methylquinoline **48** was treated with hydrogen peroxide and acetic acid. TLC analysis showed two spots, neither of which corresponded to the starting material. It proved impossible to isolate either of these new compounds. It was decided that this route would not be convenient for the production of 3-substituted quinoline-8-carboxamides.

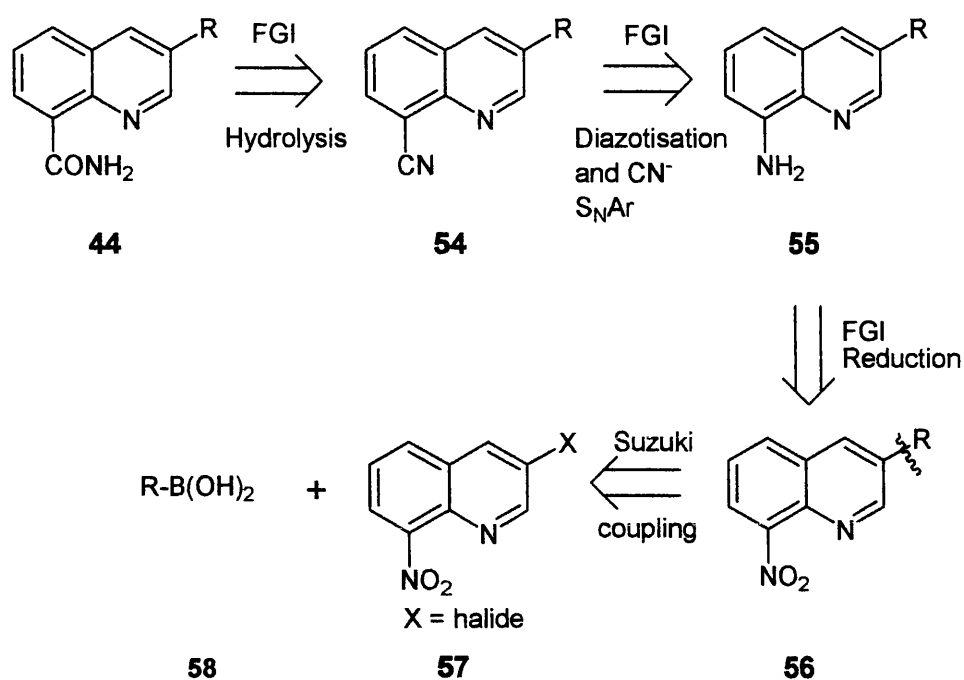


Scheme 14. Attempted synthesis of 3-hydroxy-8-methylquinoline **52**.

3.2 Route (II): 3-Substituted quinoline-8-carboxamides

3.2.1 Retrosynthetic analysis

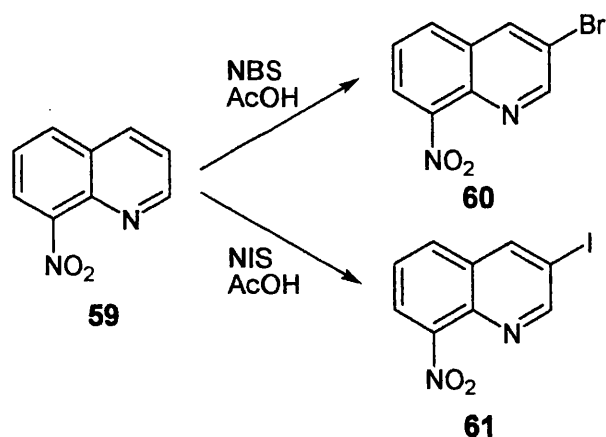
After the failure of converting 8-methylquinoline to the halide or triflate precursors required for the Suzuki-Miyaura cross-coupling reaction, a different approach was sought. The presence of electron-withdrawing groups in the halide substrate is known to aid the Suzuki-Miyaura reaction. Therefore, it was felt that a quinoline with a nitro group in the 8-position would be a suitable precursor for the formation of 3-arylquinoline-8-carboxamides. Retrosynthetic analysis of our 3-arylquinoline-8-carboxamide targets gave route (II) (Scheme 15). Initially, three functional group interconversions (FGI) were carried out on the target molecule to give 3-aryl-8-nitroquinoline **56**. The amine compound **55** can be synthesised by the reduction of the nitro group in **56** (e.g. *via* hydrogenation and acid / metal reduction). The carboxamide moiety is introduced into the 8-position of the quinoline ring by the conversion of the amine group in **55** to the nitrile compound **54** (*via* diazotisation and nucleophilic substitution), followed by hydrolysis to afford the final target **44**. Disconnection of the aryl substituent in **56** gives the major synthons **57** and **58**, which possess the requisite functionality to allow Suzuki-Miyaura cross-coupling reactions.



Scheme 15. Retrosynthetic analysis of 3-arylquinoline-8-carboxamides.

3.2.2 Synthesis of 3-aryl-8-substituted quinolines

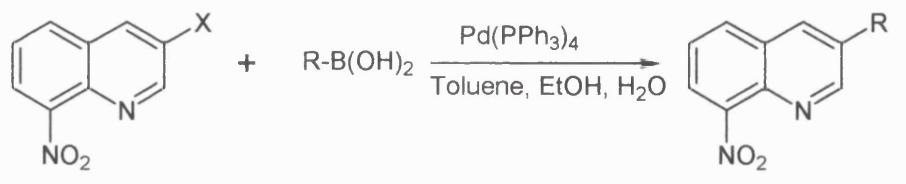
The initial approach to the synthesis of 3-arylquinoline-8-carboxamides was made using 3-bromo- and 3-iodo-8-nitroquinoline as the requisite precursors to the Suzuki-Miyaura coupling reaction. The first step in the synthesis was the electrophilic halogenation of 8-nitroquinoline **59**. The presence of a nitro group should deactivate the benzene ring in the quinoline system, so that the C-(3) position has a higher electron-density and therefore more susceptible to electrophilic attack. Initially, a bromination reaction was attempted using Br₂ in 1,2-dichlorobenzene or Br₂ in nitrobenzene. Neither set of reaction conditions proved successful and harsher conditions were considered. The use of N-bromosuccinimide (NBS) as an electrophile in hot acetic acid gave 3-bromo-8-nitroquinoline **60** in a modest yield (51%). Evidence for the formation of **60** was provided by the fact that the 3-H was no longer present in the ¹H NMR spectrum. Due to the problems encountered in the synthesis of 3-bromo-8-nitroquinoline **60**, the iodination of compound **59** was explored. The synthesis of 3-iodoquinoline-8-nitroquinoline **61** has previously been reported by the reaction of **59** with N-iodosuccinimide (NIS) in acetic acid. Regioselective iodination of the C-(3) position was easily achieved in good yield (71%). Evidence for the formation of compound **61** was obtained using Fast Bombardment Mass Spectroscopy (FAB). In the mass spectrum, a protonated molecular ion was observed at *m/z* 301.9522 (M+H), and the peak (*m/z* 255) is the result of the elimination of iodine.

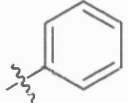
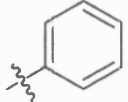
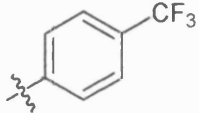
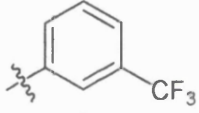
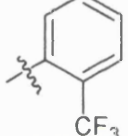


Scheme 16. Electrophilic bromination and iodination of 8-nitroquinoline.

The reactions of **60** and **61** with phenylboronic acid in the presence of tetrakis-(triphenylphosphine)palladium(0), and potassium carbonate gave 8-nitro-3-phenylquinoline **62** in 68 and 97% yield respectively. In order to ensure high yields in subsequent Suzuki-Miyaura coupling reactions, it was decided to proceed with the iodo electrophile, as the bromo electrophile was less efficient. Miyaura *et al.*¹⁸⁷ proposed that oxidative addition of heterocyclic halides is the rate determining step, and relative reactivity decreases in the order of I>OTf>Br>>Cl. The mechanistic study of the Suzuki-Miyaura reaction will be discussed further in Section 3.4.2. The next step was to investigate the tolerance of the iodide precursor for the cross-coupling with electron-deficient boronic acids. The Suzuki-Miyaura coupling reactions of **61** with *para*-, *meta*- and *ortho*- trifluoromethylphenylboronic acids were explored (Table 7). The *para*- and *meta*-trifluoromethylphenylboronic acids coupled to **61** in similar yields to phenylboronic acid. The steric hindrance of the arylation of **61** with *ortho*-trifluoromethylphenylboronic acid was sufficient to reduce the coupling rate and a moderate yield of 8-nitro-3-(2-(trifluoromethyl)phenyl)quinoline **65** was obtained. Interestingly, in the ¹H NMR spectra of 8-nitro-3-(4-(trifluoromethyl)phenyl)quinoline **63** and 8-nitro-3-(3-(trifluoromethyl)phenyl)quinoline **64** the 2-H is observed at δ 9.30. In contrast, in the *ortho* derivative **65** the 2-H shifted upfield by *ca.* 0.3 ppm due to the inductive effects of the nearby CF₃ group.

It was decided to carry out a pilot study on 8-nitro-3-phenylquinoline **62** to investigate whether it was possible to convert the nitro group to the amine, nitrile and finally carboxamide.

Table 7. Suzuki-Miyaura coupling of **60** and **61** with arylboronic acids.

Compound number	X	R	Yield of products (%)
62	I		97
62	Br		68
63	I		74
64	I		97
65	I		66

The synthesis of compound **62** was confirmed using long range ^1H - ^{13}C COSY also known as Heteronuclear Multiple Bond Connectivity (HMBC) characterisation, as the ^1H and ^{13}C NMR spectra proved insufficient. The long-range ^1H - ^{13}C COSY pulse sequence gives a two dimensional spectrum with ^{13}C chemical shifts on one axis and ^1H chemical shifts on the other. In the HMBC spectrum, the time delay in the pulse sequence is set to correspond to $\frac{1}{2}J$ where J is in the region of 10 Hz. This means that the ^{13}C shifts are correlated with the chemical shifts of protons separated from them by two or three bonds. The partial HMBC spectrum is shown in Figure 14. Analysis of an exemplary proton (4-H) at δ 8.39 shows that it is three bonds from the 2-C (δ 152.3), 5-C (δ 132.5), and 8a-C (δ 138.5), it also has two-bond cross peaks with the 3-C (δ 135.7) and the quaternary carbon 4a-C (δ 129.0). Full assignments of the ^1H and ^{13}C NMR spectra of compound **62** are given in the Experimental Section.

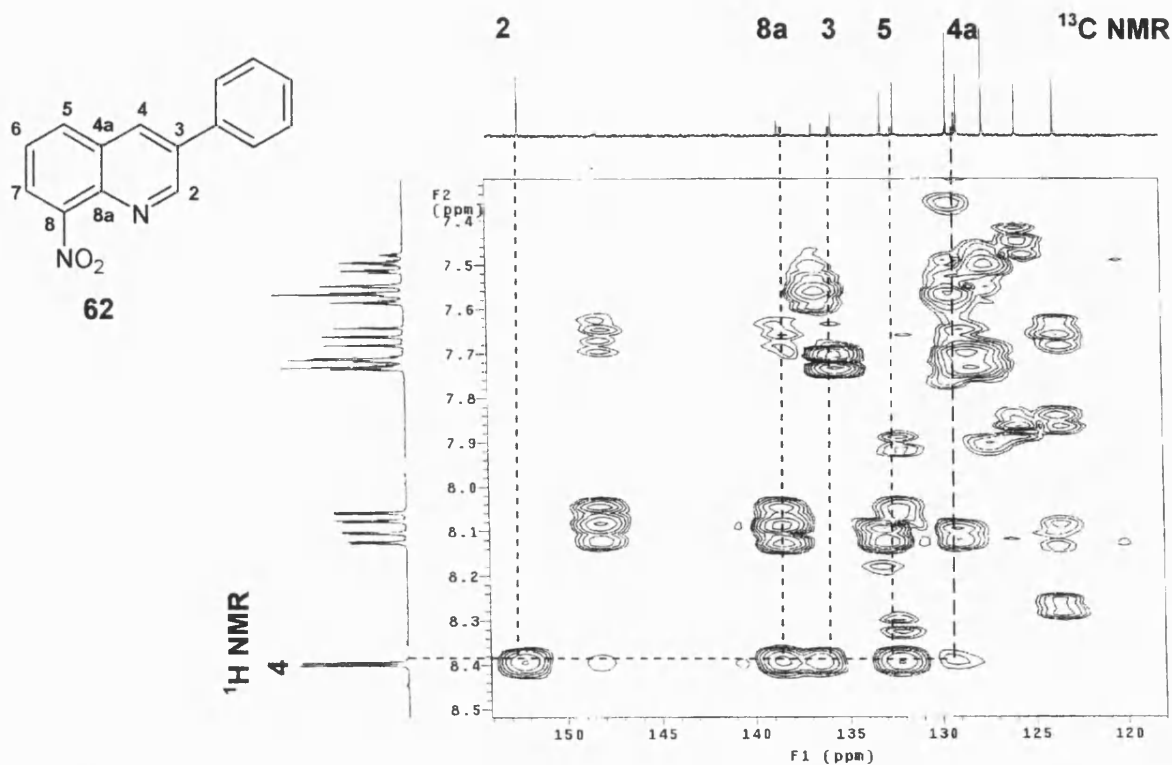
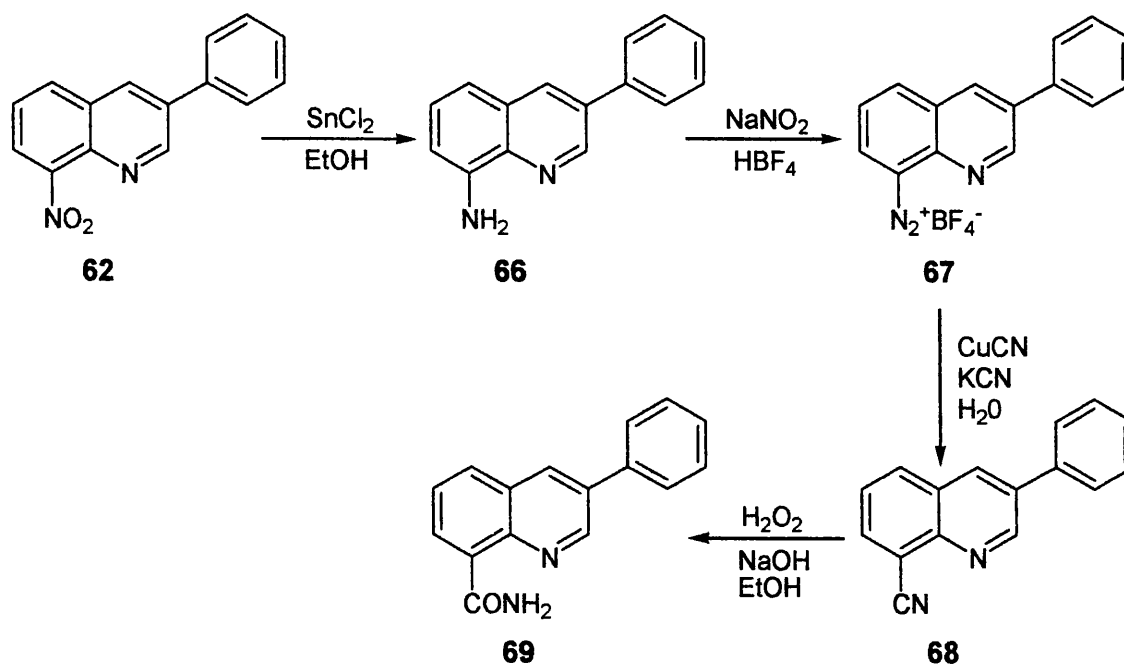


Figure 14. Partial HMBC spectrum of 8-nitro-3-phenylquinoline **62**.

The next step in the synthesis involved the conversion of the nitro group to the amine group. Many reducing agents have been used to reduce heterocyclic nitro compounds; for example, the catalytic hydrogenation of 8-nitro-4-quinolinol to the corresponding 8-amino-4-quinolinol has been demonstrated.¹⁸⁸ Price *et al.*¹⁸⁹ have reported the use of tin(II) chloride in ethanol for the reduction of 5-chloro-8-nitroquinoline. Parveen *et al.*¹⁸⁰ used a zinc / ammonium chloride system to reduce the nitro group in 5-bromo-2-((1-methyl-2-nitroimidazol-5-yl)methyl)isoquinolin-1-one. The nitro group of 8-nitro-3-phenylquinoline **62** was unaffected when palladium / carbon and hydrogen conditions were used. This may be due to quinoline being a known poison of palladium metal catalysts, as in the Lindlar catalyst.¹⁹⁰ An alternative method reported by Price *et al.*¹⁸⁹ as mentioned previously used tin(II) chloride in ethanol. Treatment of **62** with tin(II) chloride in ethanol gave the product 3-phenylquinolin-8-amine **66** in 82% yield. The ¹H NMR spectrum of **66** showed a broad singlet at δ 4.96 corresponding to the amino group. A marked upfield chemical shift was observed for the 5-H and 7-H in comparison to the corresponding nitro compound **62**, due to the shielding effect of the nearby amino group.

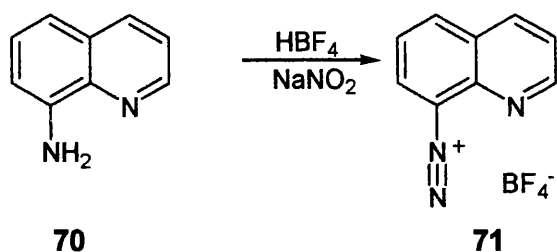


Scheme 17. Route (II) synthesis of 3-phenylquinoline-8-carboxamide **69**.

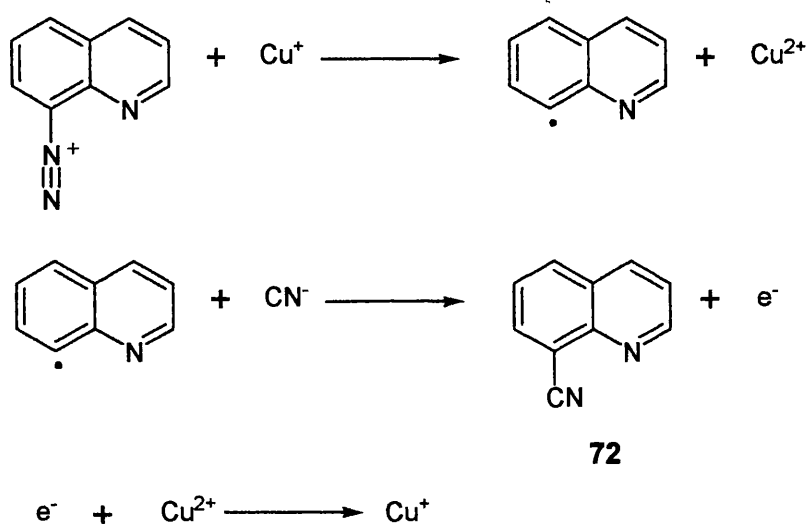
Conversion of the amine to 3-phenylquinoline-8-carbonitrile **68** was first attempted by diazotisation of compound **66** with aqueous hydrochloric acid and sodium nitrite, followed by treatment with copper(I) cyanide, via a Sandmeyer reaction. Monitoring the reaction by TLC showed numerous by-products and it was decided not to proceed any further with these reaction conditions. Interestingly, Fieser and Hershberg¹⁹¹ were unable to prepare quinoline-8-carbonitrile using the same Sandmeyer conditions on 8-aminoquinoline, as only tars were obtained. It is speculated that the failure of the Sandmeyer reaction to provide any desired product may be caused by the poor thermal stability of the diazonium salt. Roe *et al.*¹⁹² reported the synthesis of 8-fluoroquinoline via a Balz-Schiemann reaction. They demonstrated that the intermediate 8-quinolinediazonium tetrafluoroborate salt could be isolated in 74% yield and was relatively stable. It was proposed that the Balz-Schiemann reaction might have applications in the synthesis of 3-phenylquinoline-8-carbonitrile. In our laboratory, a model Balz-Schiemann reaction was carried out on 8-aminoquinoline **70**. The first step in the synthesis involved the diazotisation of **70** using fluoroboric acid and sodium nitrite. The resulting diazonium tetrafluoroborate salt **71** was isolated in 54% yield. Due to the high reactivity of compound **71**, the intermediate was used without further purification. The second step in the reaction involved the decomposition of the diazonium salt, which was achieved by reaction of the diazonium salt with copper(I) cyanide and potassium cyanide. Therefore, in two simple and reliable steps quinoline-8-carbonitrile **72** was synthesised in 50% yield. In the IR spectrum of compound **72** a

peak at 2232 cm^{-1} was observed, corresponding to the nitrile group. The mechanistic details of this reaction are not completely understood. Presumably the reaction proceeded via a radical mechanism as shown in Scheme 18.

(i) Diazotisation reaction



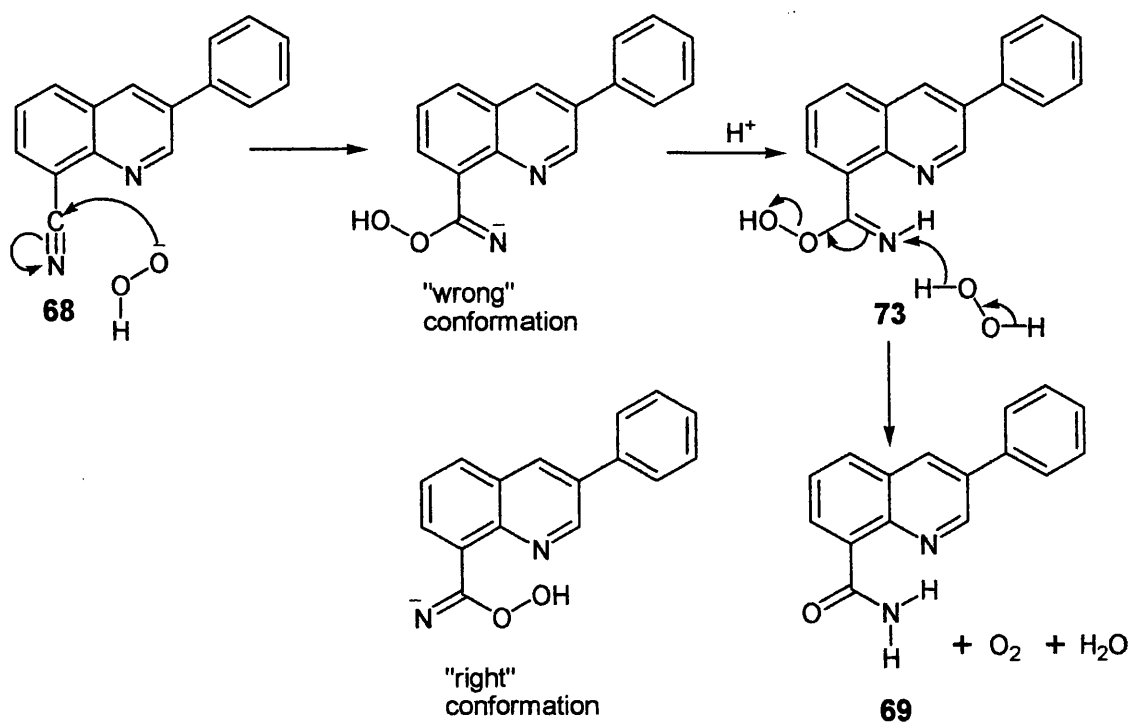
(ii) Decomposition of diazonium salt via copper (I) catalyst



Scheme 18. Proposed mechanism for the synthesis of quinoline-8-carbonitrile **72**.

The Balz-Schiemann reaction mentioned above was repeated on 3-phenylquinolin-8-amine **66**. The solid intermediate **67** was easily isolated and was treated with copper(I) cyanide and potassium cyanide. The absence of the broad NH_2 peak in the ^1H NMR spectrum demonstrated the loss of starting material **66**. Furthermore, the signals for the quinoline 7-H and 5-H were changed most distinctly from the starting compound **66**, with downfield shifts of δ 1.2 and δ 0.9 respectively; this is due to the deshielding effect of the nearby nitrile group. An additional peak in the nitrile region of the ^{13}C NMR spectrum also confirmed the formation of compound **68**.

Nitrile compounds can be hydrolysed to give either amides or carboxylic acids. Formation of the amide **69** is possible using sodium hydroxide and hydrogen peroxide. This method ensures that there is no further hydrolysis to the carboxylic acid. The controlled hydration of compound **68** was achieved using these conditions affording the target molecule 3-phenylquinoline-8-carboxamide **69** in 60% yield. A mechanism for this reaction is shown in Scheme 19. Initially, there is a nucleophilic addition of the hydroperoxide ion to the C≡N group followed by transfer of a hydride ion from a second molecule of peroxide to the intermediate peroxyimine **73**, giving the amide **69**, molecular oxygen, and water. Surprisingly, this reaction only gave the desired product without the formation of any by-products. In theory, the quinoline nitrogen could have been oxidised by hydrogen peroxide providing easy access to the N-oxides required later. The lack of formation of 8-carbamoyl-3-phenylquinoline-1-oxide is probably due to the “wrong” conformation of the peroxyimine intermediate being adopted, hence preventing the N-oxidation reaction.



Scheme 19. Proposed mechanism for the hydrolysis of 3-phenylquinoline-8-carbonitrile **68** using H_2O_2 and NaOH .

In 3-phenylquinoline-8-carboxamide **69**, a chemical shift difference of ca. 5 ppm was observed between the two N-H protons of the carboxamide moiety. This indicates that the rotation of the NH_2 group is restricted and that the carboxamide moiety is constrained in the *anti*-conformation. Thus, the lone pair of the quinoline nitrogen

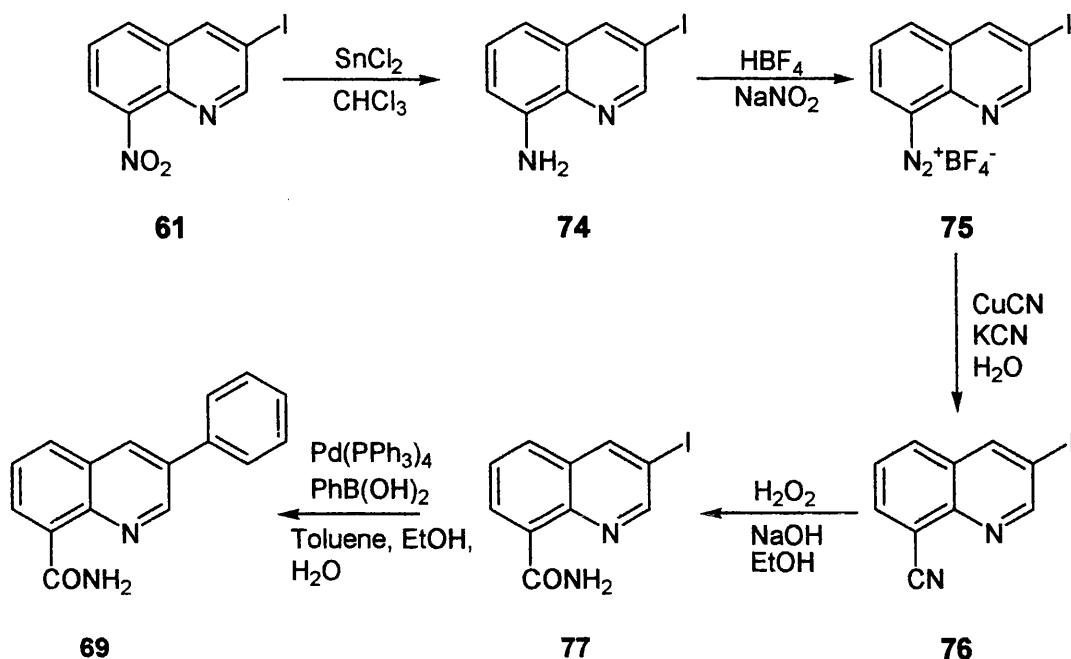
serves as a good hydrogen-bond acceptor. The chemical shift of δ 10.95 is assigned to the N-H involved in the intramolecular hydrogen bond. The upfield chemical shift of δ 6.17 is assigned to the N-H which is not hydrogen-bonded to the quinoline nitrogen. This supports the hypothesis outlined in the research aims (Section 2.1). In addition, the 7-H was observed as a doublet of doublets due to the *ortho* coupling being observed with the 6-H and *meta* coupling being observed with the 5-H. The 7-H signal shifted downfield in comparison to the spectrum of the nitrile **68**, this may be due to anisotropic effects of the carbonyl and suggests that the carboxamide is in plane with the heterocycle. The 2-H of **69** was assigned to the signal at δ 9.20, *i.e.* downfield due to the electron-withdrawing effect of the heteroaromatic ring nitrogen.

Route (II) was beneficial in producing the first target PARP-1 inhibitor 3-phenyl-quinoline-8-carboxamide. The main drawback of this route is that the addition of the 3-substituent *via* Suzuki-Miyaura coupling occurs at the start of the reaction sequence. Ideally, diversification should occur at a late stage of the synthesis to avoid tedious repetition of synthetic steps. In order to efficiently synthesise a wide variety of 3-substituted quinoline-8-carboxamides efforts were focused on developing an alternative strategy.

3.3 Route (III): 3-Substituted quinoline-8-carboxamides

3.3.1 Route (III): Synthesis of 3-phenylquinoline-8-carboxamide

Route (II) was not a very efficient strategy for the production of compound libraries. An alternative synthetic strategy to the synthesis of 3-phenylquinoline-8-carboxamides **69** was investigated (Scheme 20). This strategy allowed for the introduction of diversity at a later stage in the synthesis, utilising phenylboronic acid in the final cross-coupling step. The first stage in the synthesis of 3-phenylquinoline-8-carboxamide was the reduction of 3-iodo-8-nitroquinoline **61** to give 8-amino-3-iodoquinoline **74**. Initially, the tin(II) chloride / ethanol conditions previously used in route (II) were employed for the reduction of **61**. However, ^1H NMR analysis indicated not only reduction of the nitro group to give the amine but also reductive removal of the iodine. Therefore, alternative methods were considered. Baik *et al.*¹⁹³ reported the use of bakers' yeast as a biocatalyst for the reduction of aromatic nitro compounds to the corresponding amine compounds. They demonstrated that aromatic nitro compounds containing halide groups showed remarkable selectivity to give the amine product without giving dehalogenation. Treatment of **61** with bakers' yeast did not give the required product. Zinc and ammonium chloride conditions were also unsuccessful and showed no reduction of the nitro compound. The tin(II) chloride method was re-examined and it was decided to investigate the method by ^1H NMR spectroscopy. Trial experiments were set up using CDCl_3 as a solvent and increasing amounts of tin(II) chloride added as a solution in CD_3OD . After 6 h, using 3.5 equivalents of tin(II) chloride, there was complete loss of starting material and signals indicating formation of the product, 8-amino-3-iodoquinoline **74**, were observed. The reaction was successfully repeated on larger scale amounts of 3-iodo-8-nitroquinoline **61**. It is thought that over-reduction of compound **61** was due to limited solubility of the starting material in the original tin(II) chloride and ethanol conditions.



Scheme 20. Route (III) synthesis of 3-phenylquinoline-8-carboxamide **69**.

Diazotisation of compound **74** with tetrafluoroboric acid and sodium nitrite, followed by treatment with copper(I) cyanide and potassium cyanide, gave 3-iodoquinoline-8-carbonitrile **76** in 50% yield. In the ^1H NMR spectrum the absence of the broad NH_2 peak indicated the formation of the product **76**. Treatment of **76** with sodium hydroxide and hydrogen peroxide gave 3-iodoquinoline-8-carboxamide **77**. The ^1H NMR spectrum of **77** showed one N-H peak at δ 6.11 and the other at δ 10.53, indicating the formation of the carboxamide functional group. Cross-coupling of **77** with phenylboronic acid gave pale yellow crystals of **69**. The structure of **69** was confirmed by X-ray crystallography (Section 5.2). ^1H NMR studies of compound **69** confirmed the presence of the intramolecular hydrogen bond between the heterocyclic nitrogen and one of the N-H groups of the carboxamide (Section 5.1).

Route (III) demonstrated that the carboxamide functional group was well tolerated by the Suzuki-Miyaura conditions. However, a poor overall yield of compound **69** was obtained, which was mainly due to the problems encountered in the purification of 3-iodoquinoline-8-carbonitrile **76**.

3.4 Route (IV): 3-Substituted quinoline-8-carboxamides

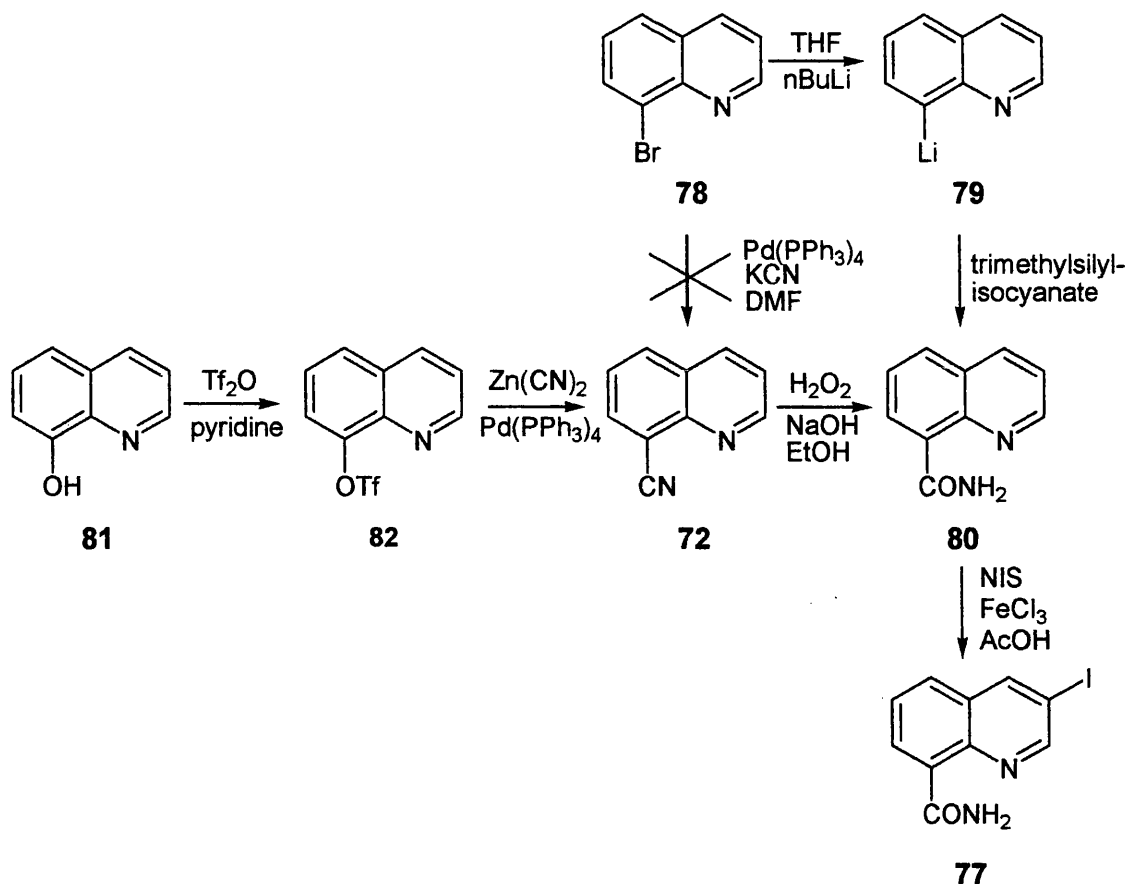
3.4.1 Route (IV): Synthesis of 3-iodoquinoline-8-carboxamide

The disappointing overall yield of 3-phenylquinoline-8-carboxamide obtained by routes II and III, led us to modify our synthetic strategy. Experiments were conducted to investigate alternative methods of introducing the carboxamide functionality into the 8-position of the quinoline ring (Scheme 21).

The first synthetic strategy involved the use of the commercially-available 8-bromoquinoline. It was hoped that the bromo moiety could be easily converted to a nitrile moiety. As demonstrated previously nitrile compounds can be prepared by diazotisation of amines and subsequent Sandmeyer reaction. The main disadvantage of the Sandmeyer reaction is the requirement of stoichiometric amounts of copper(I) cyanide as the cyanating agent, which leads to equimolar amounts of heavy metal waste and results in problematic work-up procedures. A useful alternative for the preparation of nitriles is the palladium-catalysed cyanation of aryl compounds with NaCN or KCN. However, attempts to convert 8-bromoquinoline to compound **72** using Pd(PPh₃)₄ and KCN in DMF failed and only starting material was recovered. It was planned that hydration of compound **72** would give quinoline-8-carboxamide and subsequent iodination would allow the introduction of substituents into the 3-position of the quinoline ring.

An alternative strategy was sought to convert 8-bromoquinoline to quinoline-8-carboxamide. Suggs *et al.*¹⁹⁴ reported the preparation of 8-lithioquinoline **79** via halogen-metal interchange between lithium reagents and 8-bromoquinoline. Subsequent reaction of 8-lithioquinoline with various electrophiles afforded a series of 8-substituted quinoline derivatives. It was proposed that lithiation of 8-bromoquinoline followed by treatment with trimethylsilylisocyanate may afford quinoline-8-carboxamide. It is generally known that the quinoline ring system is easily attacked by nucleophiles, this limits the conditions under which metal-halogen exchange can occur. For example, quinoline itself can add n-BuLi promptly to give excellent yields of 2-butyloquinoline. Consequently, it was decided to use a short reaction time of 10 min and a low temperature of -79°C in the interchange reaction. Treatment of 8-bromoquinoline **78** with n-BuLi, followed by quenching with trimethylsilylisocyanate, gave **80** in 48% yield. Although this method is a direct route to the synthesis of quinoline-8-carboxamide, the 8-bromoquinoline starting material is very expensive. Therefore, we decided to

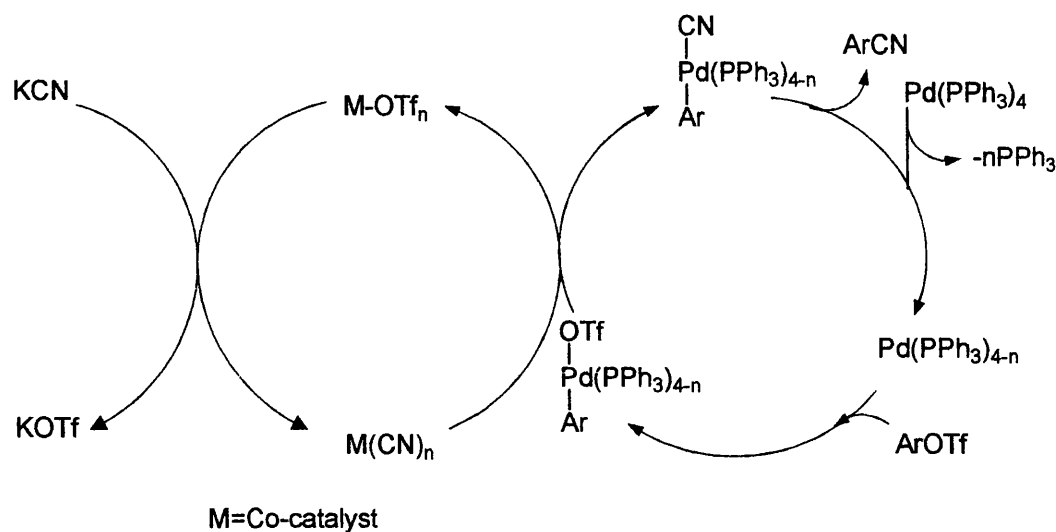
investigate a more cost-effective means of producing large quantities of quinoline-8-carboxamide.



Scheme 21. Synthesis of 3-iodoquinoline-8-carboxamide **77**.

Quinolin-8-yl trifluoromethanesulfonate has previously been synthesised using the cheap commercially available starting material quinolin-8-ol **81**.¹⁹⁵ Furthermore, Anderson *et al.*¹⁹⁶ reported the palladium-catalysed cyanation of quinolin-8-yl trifluoromethanesulfonate, affording quinoline-8-carbonitrile in 87% yield. In our laboratory, trifluoromethanesulfonation of compound **81** was achieved using triflic anhydride and pyridine. A cyanation reaction of triflate **82** was used to obtain the corresponding nitrile **72**. Firstly, we used the previously-reported conditions: $\text{Pd}(\text{PPh}_3)_4$ / KCN / CuI / MeCN . Application of this method gave a low yield of **72** with recovery of significant amounts of unreacted **82** even after prolonged reaction conditions. Varying the solvent from acetonitrile to DMF had little effect on the overall yield. The use of NaCN as the cyanide source also gave a low yield of **72**. A two-cycle process is proposed to explain the role of the copper co-catalyst. In the first cycle, the copper co-catalyst might serve as a carrier which transfers the cyanide ion between KCN and the $\text{Pd}(\text{II})$ intermediate.

The second cycle involves the activation of the substrate through Pd(0)-mediated oxidative addition-transmetallation-reductive elimination (Scheme 22).



Scheme 22. Proposed mechanism of palladium-catalysed cyanation of aryl triflates in the presence of a copper iodide co-catalyst.¹⁹⁶

Takagi *et al.*¹⁹⁷ pointed out that an excess of cyanide ions in solution inhibits the catalytic cycle. The excess cyanide reacts with palladium(II) species, forming inactive Pd(II) cyano compounds, which cannot be reduced to the active palladium(0) species. As a consequence the palladium catalyst is deactivated. It is proposed that the incomplete conversion of triflate **82** to the nitrile **72** was a result of high levels of dissolved KCN in solution, which in turn induced catalyst deactivation.

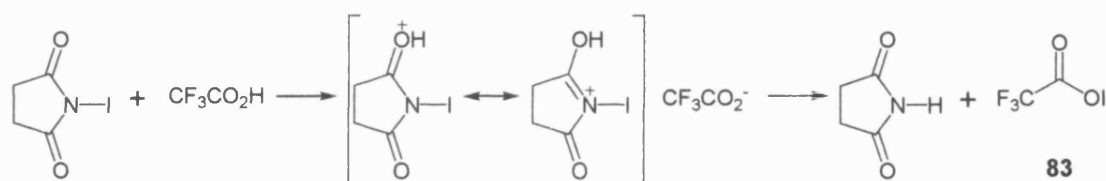
The use of $\text{Zn}(\text{CN})_2$ in cyanation reactions has become widespread, as it is less soluble in DMF than are KCN or NaCN.¹⁹⁸ The reagent system $\text{Zn}(\text{CN})_2$, $\text{Pd}(\text{PPh}_3)_4$ in DMF has recently been shown to be efficient for the cyanation of aryl triflates.¹⁹⁹ The reaction conditions $\text{Zn}(\text{CN})_2$ / $\text{Pd}(\text{PPh}_3)_4$ / DMF / 150°C were employed for the cyanation of compound **82**. The conversion rate of the triflate **82** to the nitrile **72** was significantly improved. Column chromatography gave **72** in 73% yield. It is proposed that the $\text{Zn}(\text{CN})_2$ source might facilitate the cyanation reaction by providing a species which functions more efficiently in the transmetallation step with Pd(II) than does either NaCN or KCN.

Conversion of the nitrile **72** to the corresponding carboxamide **80** was achieved using sodium hydroxide and hydrogen peroxide. With quinoline-8-carboxamide now formed, efforts were focused on transforming **80** into a viable cross-coupling partner for the Suzuki-Miyaura reaction. Initially, quinoline-8-carboxamide was treated with NIS in boiling acetic acid to give **77** in 26% yield. 3-Iodoquinoline-8-carboxamide was synthesised previously in 43% yield in route (III). It was proposed that the low yield of the iodination reaction was due to the deactivating effect of the carboxamide moiety. An optimisation study was carried out on the iodination of quinoline-8-carboxamide and the results are presented in Table 8. Even though iodination of aromatic compounds is a useful reaction for providing the precursors to organometallic species, there are still a limited number of protocols describing the iodination of deactivated aromatic compounds. Due to its low electrophilicity, elemental iodine is sometimes incapable of direct iodination of even electron-rich substrates. In contrast, iodine monochloride (ICl) is reported to be successful in the iodination of electron-deficient aromatic substrates. However, treatment of quinoline-8-carboxamide with ICl in acetonitrile failed to give the required product and only unreacted **80** was recovered from the reaction. Johnsson *et al.*²⁰⁰ reported the mild iodination of aromatic compounds using ICl in combination with the Lewis acid In(OTf)₃. On the basis of these results, we decided to investigate the activating properties of various Lewis acids towards the iodination of quinoline-8-carboxamide. Firstly, quinoline-8-carboxamide was treated with ICl and In(OTf)₃ in acetonitrile at room temperature for 5 h. TLC analysis failed to show the formation of the product spot. Consequently, the reaction mixture was then heated at 80°C for 12 h. However, a ¹H NMR spectrum of the crude mixture indicated that only the starting material was present. Even when InCl₃ and FeCl₃ were used as the Lewis acid catalyst, the iodination reaction failed.

Our attention then focussed on enhancing the electrophilicity of NIS for the reaction with the electron-deficient quinoline-8-carboxamide. Castanet *et al.*²⁰¹ demonstrated that the iodination of electron-rich aromatics could be achieved using a combination of NIS and catalytic amounts of trifluoroacetic acid (TFA). Iodine trifluoroacetate **83** was proposed as the active species for the iodination reaction and was generated *in situ* upon treatment of NIS with TFA (Scheme 23). We were curious if the electrophilic nature of iodine trifluoroacetate could be extended to the iodination of the deactivated quinoline-8-carboxamide substrate. We considered that the highly reactive iodine trifluoroacetate would enhance the iodination of **80** through an electrophilic solvation effect. However, treatment of compound **80** with the NIS/TFA system failed to give the desired product and only unreacted starting material was recovered.

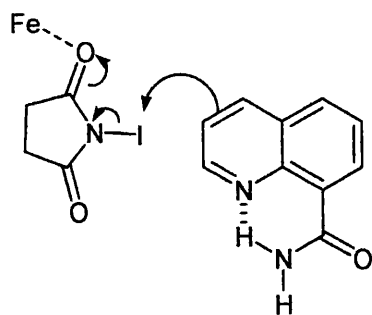
Table. 8 The iodination properties of ICl and NIS in combination with various Lewis acids.

Starting material	Iodinating reagent	Solvent	Catalyst	Product	Yield of products (%)
80	NIS	AcOH	None	77	26
80	ICl	MeCN	None	-	-
80	ICl	MeCN	InCl ₃	-	-
80	ICl	MeCN	In(OTf) ₃	-	-
80	ICl	MeCN	None	-	-
80	NIS	None	TFA	-	-
80	NIS	MeCN	TFA	-	-
80	NIS	AcOH	InCl ₃	77	31
80	NIS	AcOH	FeCl ₃	77	40
80	NIS	AcOH	AlCl ₃	77	34



Scheme 23. Proposed formation of the iodine trifluoroacetate active species.²⁰¹

Finally, the iodinating capability of the NIS/AcOH acid system in combination with various Lewis acids was investigated. Initially, quinoline-8-carboxamide was treated with NIS and 5 mol% of FeCl₃ in AcOH and the reaction mixture was boiled under reflux for 24 h. 3-Iodoquinoline-8-carboxamide was isolated in 40% yield and was fully characterised by NMR spectroscopy. In contrast, reaction of **80** with NIS in the presence of InCl₃ and AlCl₃ gave **77** in 31% and 34% yield respectively. Indicating that the NIS/FeCl₃ system is superior for compound **80**. The success of the reaction may involve the coordination of the Lewis acid (FeCl₃) with the carbonyl oxygen of NIS thereby increasing the reactivity of the iodine atom (Scheme 24).

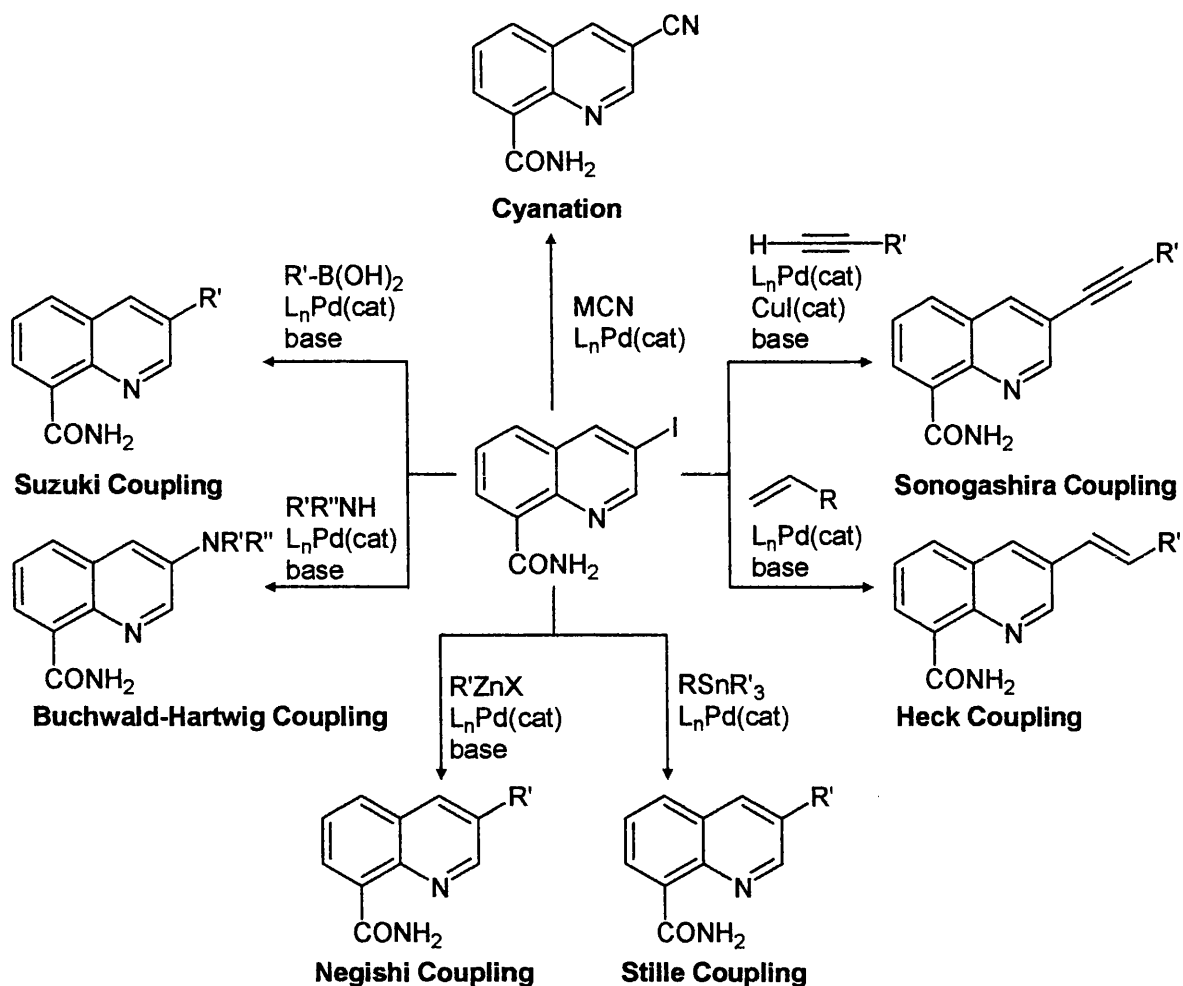


Scheme 24. Proposed mechanism for the Lewis acid-catalysed iodination of quinoline-8-carboxamide with NIS as the iodinating reagent.

3-Iodoquinoline-8-carboxamide serves as a vital synthetic precursor for the formation of C-C bonds through palladium-catalysed cross-coupling reactions (Scheme 25). There are three main advantages of using palladium cross-coupling reactions:

- (1) Ready availability of starting materials.
- (2) Simplicity and generality of the cross-coupling methods.
- (3) The broad tolerance of palladium catalysts towards various functional groups.

Due to the synthetic power of the cross-coupling reactions, we believe that this type of method is well suited for the synthesis of libraries of 3-substituted quinoline-8-carboxamides. A wide diversity of substituents may be introduced into the 3-position *via* organometallic reagents such as organoboranes (Suzuki-Miyaura reaction), organozincs (Negishi reaction) and organostannanes (Stille reaction). It is also possible to cross-couple alkynes (Sonogashira reaction), amines (Buchwald-Hartwig reaction), alkenes (Heck reaction) and cyanide (palladium catalysed cyanation) with aryl iodides.

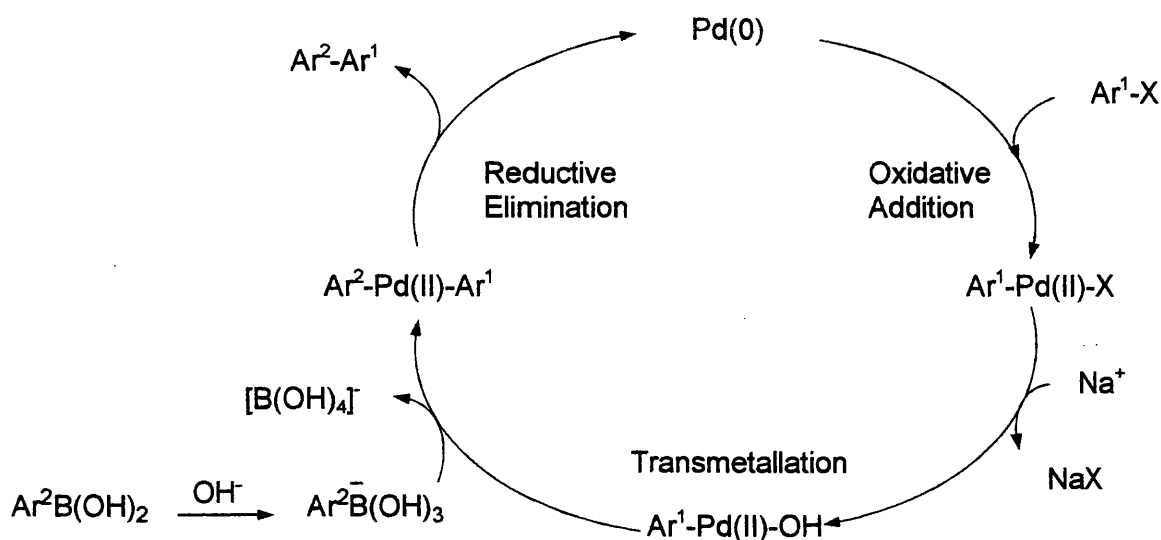


Scheme 25. Proposed palladium-catalysed cross-coupling reactions with 3-iodoquinoline-8-carboxamide **77**.

3.4.2 The Suzuki-Miyaura coupling reaction

As discussed previously in Section 3.2.2, the Suzuki-Miyaura coupling reaction plays a vital role in the synthesis of the 3-substituted quinoline-8-carboxamide targets. It offers the formation of $C_{sp^2}-C_{sp^2}$ bonds through the metal-catalysed reaction of an arylboronic acid with an aryl halide, triflate or sulfonate. The key advantages of the Suzuki-Miyaura coupling reaction are the mild reaction conditions and the commercial availability of the boronic acids that are safer than other organometallic reagents. The inorganic by-products are non-toxic and can be easily removed from the reaction mixture. A catalytic cycle for the transition metal-catalysed cross-coupling of organic halides and organoboranes is shown in Scheme 26, and includes three steps. The first step involves the oxidative addition of the catalyst to the aryl halide to form the organopalladium halide $Ar^1[Pd]X$, and is often the rate-determining step in the catalytic cycle. Secondly, transmetalation of an arylboronic acid gives a diarylated palladium complex $Ar^2[Pd]Ar^1$, and finally reductive elimination forms the biaryl product and the palladium(0) catalyst,

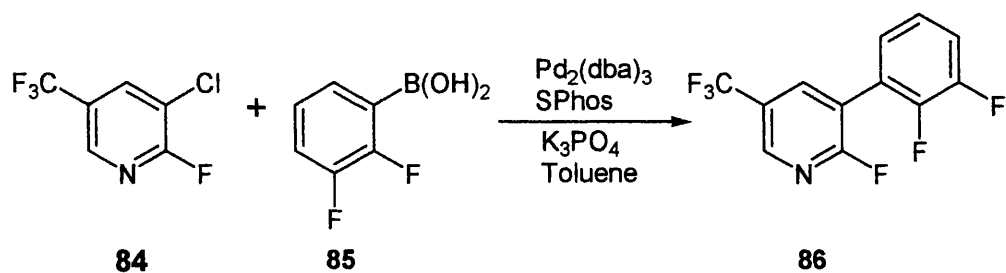
which re-enters the catalytic cycle. It is unlikely that organoboranes participate in the catalytic cross-coupling reaction, since they are only weakly nucleophilic and lack sufficient reactivity to transmetallate to palladium. It is reported that the addition of a base has a remarkable effect on the transmetallation rate of organoboranes. Sodium carbonate is the most commonly used base. However, Na_2CO_3 can be ineffective with sterically demanding substrates and often other bases are used such as K_2CO_3 , Cs_2CO_3 , and Ag_2O .



Scheme 26. General catalytic cycle for the Suzuki-Miyaura coupling of aryl halides with arylboronic acids.²⁰²

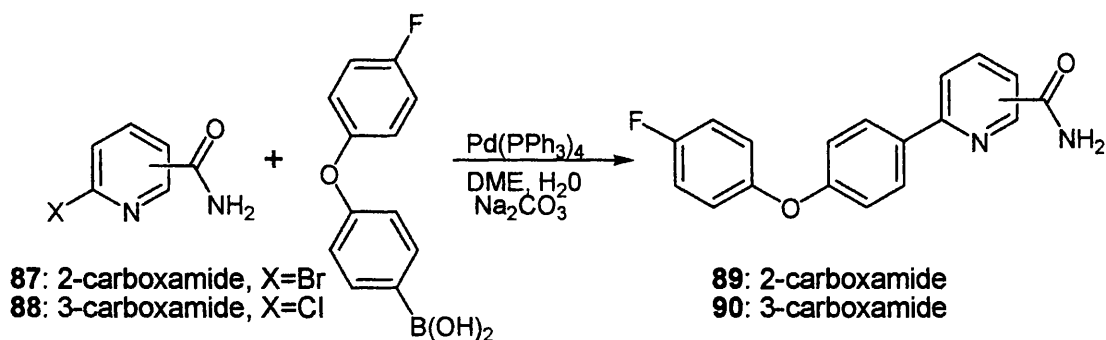
Tetrakis(triphenylphosphine)palladium(0), $\text{Pd}(\text{PPh}_3)_4$, is the most widely used catalyst in Suzuki-Miyaura reactions. Recent advances in Suzuki-Miyaura coupling reactions have focused on increasing the reactivity and stability of the metal catalyst through ligand modification. Examples of catalysts include: tris(dibenzylidene)dipalladium(0) acetone, $\text{Pd}_2(\text{dba})_3$, palladium(II) acetate, $\text{Pd}(\text{OAc})_2$ and [1,1'-bis(diphenylphosphino)-ferrocene] dichloropalladium(II), $\text{PdCl}_2(\text{dppf})$.

Recent improvements in Suzuki-Miyaura coupling reactions have relied on the increased reactivity and stability of metal catalysts by employing supporting ligands. Phosphine-based ligands are the most commonly used, although many other ligands have proved effective for a variety of substrates.¹⁸⁷ A recent publication by Buchwald and co-workers²⁰³ reported that the Suzuki-Miyaura coupling of aryl chloride **84** with the electron-deficient arylboronic acid **85** was aided by the use of the phosphine ligand 2-(2',6'-dimethoxybiphenyl)dicyclohexylphosphine, SPhos.



Scheme 27. Reported Suzuki-Miyaura coupling of **84** with the electron deficient 2,3-difluorophenylboronic acid.²⁰³

A variety of heterocyclic halides have been coupled with boronic acids, including thiophenes, thiazoles, pyridines, quinolines, pyrimidines and pyrazines.²⁰⁴ However, there have only been a small number of reports of Suzuki-Miyaura reactions involving N-heterocyclic systems containing a carboxamide functionality. Shao *et al.*²⁰⁵ reported the synthesis of a series of 6-[4-(4-fluorophenoxy)phenyl]pyridine carboxamides using the Suzuki-Miyaura coupling reaction (Scheme 28). The bromo- and chloro- pyridine carboxamides **87** and **88** were coupled with 4-(4-fluorophenoxy)phenylboronic acid to give compounds **89** and **90** in 18% and 40% yield respectively. In contrast, our quinoline-8-carboxamide precursor contains an iodo substituent that should aid the Suzuki-Miyaura coupling reaction.



Scheme 28. Reported synthesis of 6-[4-(4-fluorophenoxy)phenyl]pyridine carboxamides.²⁰⁵

Recently, Sicre *et al.*²⁰⁶ reported the regioselective Suzuki-Miyaura coupling of aryl and alkenyl boronic acids with 2,4-dibromopyridine. It was demonstrated that oxidative addition to Pd(0) selectively occurred at the 2-position of the pyridine ring. This regioselectivity can be explained by the difference in the electronic properties between the carbon centres with bromine atoms attached (C2 and C4).

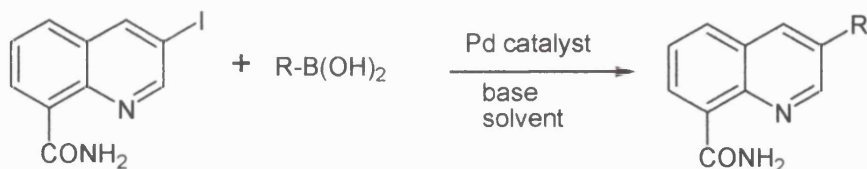
3.4.3 Suzuki-Miyaura coupling of 3-iodoquinoline-8-carboxamide with aryl and heteroaryl boronic acids

For the arylation of 3-iodoquinoline-8-carboxamide **77**, we initially chose a standard Suzuki-Miyaura reaction protocol: reflux in toluene / EtOH / H₂O solution with Na₂CO₃ and Pd(PPh₃)₄. To evaluate the scope and limitations of this protocol, the cross-coupling of **77** with a wide variety of aryl and heteroaryl boronic acids was carried out. The results are shown in Table 9. Arylboronic acids with electron-donating groups such as OCH₃ and CH₃ coupled with compound **77** in excellent yields (65-95%). In comparison, arylboronic acids with electron-withdrawing groups such as Br and CN afforded much slower cross-coupling rates.

The Suzuki-Miyaura coupling reactions with trifluoromethylphenylboronic acids were also successful. The cross-coupling of **77** with both *meta*- and *para*-trifluoromethylphenylboronic acids gave compounds **94** and **95** in 43% and 38% yield respectively. However, the coupling of **77** with *ortho*-trifluoromethylphenylboronic acid gave compound **96** in a much lower yield of 27%. The low yield obtained by the *ortho* substituent was as anticipated. In the transmetalation step of the Suzuki-Miyaura catalytic cycle, the aryl group is transferred from the metal boron to the metal palladium system generating the aryl-Pd-arylB(OH)₂ intermediate. The formation of this intermediate is sterically hindered by the *ortho* substituent of the arylboronic acid and the reaction is reduced. The last step, the reductive elimination, is probably also slowed because of this reason.

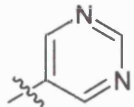
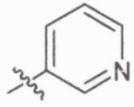
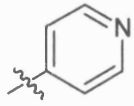
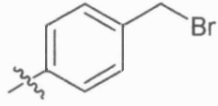
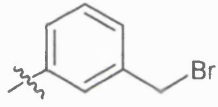
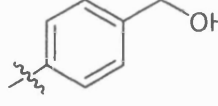
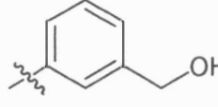
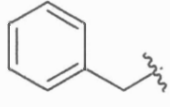
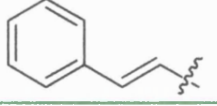
The presence of the CF₃ group in compounds **94-96** was determined using ¹⁹F NMR spectroscopy. Fluorine is monoisotopic with a nuclear spin of $I = \frac{1}{2}$ so that organic fluorine compounds lend themselves to fluorine NMR spectroscopy. The *meta* compound **94** gave a singlet at δ -62.56 which corresponds to the three fluorine atoms in the CF₃ group. Similarly, in the *para* compound **95** a singlet at δ -60.92 was observed. However, the presence of an *ortho* substituent dramatically affected the chemical shift in the ¹⁹F NMR spectrum with a singlet peak observed at δ -56.70. The ¹⁹F chemical shifts for compounds **94-96** suggest that the quinoline nitrogen acts as an electron-withdrawing group and is *meta*-directing. The ¹⁹F chemical shift signal of the *meta* compound **94**, is slightly more downfield than the ¹⁹F chemical shift signals of compounds **95** or **96**. Thus, it appears that the quinoline nitrogen removes electrons from the *ortho* and *para* positions, leaving the *meta* position with the greatest electron density.

Table 9. Suzuki-Miyaura coupling of 3-iodoquinoline with aryl and heteroaryl boronic acids. (-) denotes unsuccessful attempts.



Compound number	R	Reaction conditions	Yield of products (%)
69		Pd(PPh ₃) ₄ , toluene, EtOH, H ₂ O, Na ₂ CO ₃	78
		Pd(OAc) ₂ , SPhos, toluene, K ₃ PO ₄	93
91		Pd(PPh ₃) ₄ , toluene, EtOH, H ₂ O, Na ₂ CO ₃	95
92		Pd(PPh ₃) ₄ , toluene, EtOH, H ₂ O, Na ₂ CO ₃	65
93		Pd(PPh ₃) ₄ , toluene, EtOH, H ₂ O, Na ₂ CO ₃	41
		Pd(PPh ₃) ₄ , K ₂ CO ₃ , THF, H ₂ O	48
		Pd(OAc) ₂ , SPhos, toluene, K ₃ PO ₄	78
94		Pd(PPh ₃) ₄ , toluene, EtOH, H ₂ O, Na ₂ CO ₃	43
95		Pd(PPh ₃) ₄ , toluene, EtOH, H ₂ O, Na ₂ CO ₃	38
96		Pd(PPh ₃) ₄ , toluene, EtOH, H ₂ O, Na ₂ CO ₃	27
97		Pd(PPh ₃) ₄ , toluene, EtOH, H ₂ O, Na ₂ CO ₃	31
98		Pd(PPh ₃) ₄ , toluene, EtOH, H ₂ O, Na ₂ CO ₃	41

Table 9. Ctd

Compound number	R	Reaction conditions	Yield of products (%)
-		Pd(PPh ₃) ₄ , toluene, EtOH, H ₂ O, Na ₂ CO ₃ Pd(PPh ₃) ₄ , DMF, Na ₂ CO ₃	- -
99		Pd(PPh ₃) ₄ , Na ₂ CO ₃ , THF, H ₂ O Pd(PPh ₃) ₄ , DMF, Na ₂ CO ₃	- 26
100		Pd(PPh ₃) ₄ , DMF, Na ₂ CO ₃	40
101		Pd(PPh ₃) ₄ , toluene, EtOH, H ₂ O, Na ₂ CO ₃ Pd(PPh ₃) ₄ , Na ₂ CO ₃ , THF, H ₂ O Pd(PPh ₃) ₄ , K ₂ CO ₃ , THF, H ₂ O	- - 2
-		Pd(PPh ₃) ₄ , K ₂ CO ₃ , THF, H ₂ O Pd(OAc) ₂ , SPhos, toluene, K ₃ PO ₄	- -
-		Pd(PPh ₃) ₄ , K ₂ CO ₃ , THF, H ₂ O Pd(OAc) ₂ , SPhos, toluene, K ₃ PO ₄	- -
-		Pd(PPh ₃) ₄ , K ₂ CO ₃ , THF, H ₂ O	-
-		Pd(PPh ₃) ₄ , toluene, EtOH, H ₂ O, Na ₂ CO ₃ Pd(PPh ₃) ₄ , K ₂ CO ₃ , THF, H ₂ O	- -
102a		Pd(PPh ₃) ₄ , DMF, Na ₂ CO ₃	52

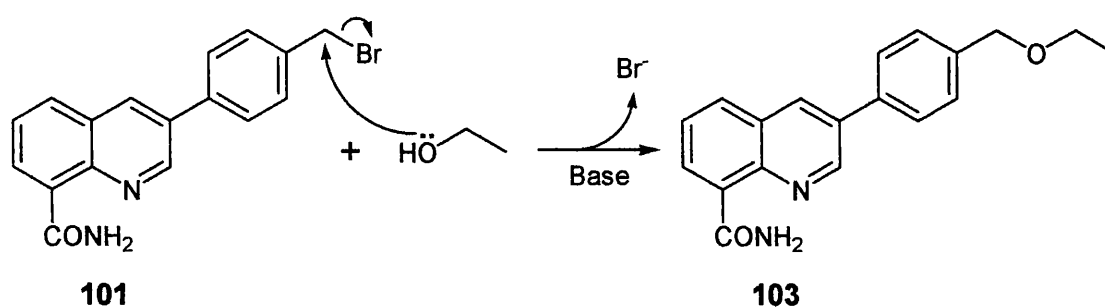
The cross-coupling of **77** with 3- and 4-pyridylboronic acids using the standard reaction conditions failed to give the required products. It appeared that the failure of both these reactions was due to the poor solubility of the pyridylboronic acids in toluene. However, upon switching the solvent to DMF, the desired products were formed in moderate

yields. Treatment of compound **77** with pyrimidine-5-boronic acid, Pd(PPh₃)₄ and Na₂CO₃ in DMF failed to give the desired coupling product. It was expected that the electron-deficient pyridyl and pyrimidine boronic acids would be difficult coupling partners as they are less nucleophilic relative to electron-neutral boronic acids such as phenylboronic acid. Therefore, the transmetallation of the aryl-Pd-I complex is slowed, which, in turn retards the entire catalytic cycle.

In an attempt to investigate further the binding properties of the 3-substituted quinoline-8-carboxamides with the enzyme active site, the standard Suzuki-Miyaura protocol was applied to a series of substituted methylphenylboronic acids. Unfortunately the reaction of compound **77** with 3- and 4-(hydroxymethyl)phenylboronic acids did not give the required products and only starting material was recovered from the reactions. Additionally, we were unable to couple compound **77** with benzylboronic acid and 3-(bromomethyl)phenylboronic acid.

Surprisingly, the Suzuki-Miyaura coupling of **77** with 4-(bromomethyl)phenylboronic acid in toluene / EtOH gave 3-(4-(ethoxymethyl)phenyl)quinoline-8-carboxamide **103** as a white solid. Evidence for the formation of compound **103** was obtained by the presence of the OCH₂ group in the ¹H NMR spectrum, which was observed as a singlet at δ 4.59. The CH₂ protons of the ethyl group in **103** were observed as a quartet at δ 3.60 with a vicinal coupling constant of 7.2 Hz. The CH₃ protons were split into a triplet and were observed at δ 1.28. A possible mechanism for the formation of compound **103** is illustrated in Scheme 29. It is proposed that the Suzuki-Miyaura coupling reaction between 4-(bromomethyl)phenylboronic acid and **77** initially gives 3-(4-bromomethylphenyl)quinoline-8-carboxamide **101**. The ethanol solvent then acts as a nucleophile and attacks the methylene carbon in **101**. Ethanol then replaces bromide and forms the ether **103**. This displacement is facilitated by the presence of the base Na₂CO₃.

The Suzuki-Miyaura reaction conditions were modified, omitting ethanol, in an attempt to overcome this problem. The cross-coupling of 4-(bromomethyl)phenylboronic acid with **77** was repeated using Pd(PPh₃)₄ and K₂CO₃ in THF and water. However, compound **101** was only isolated in 2% yield. However, it was possible to recover 33% yield of unreacted starting material from the cross-coupling reaction.



Scheme 29. Proposed mechanism for the formation of compound **103**.

As mentioned previously, Buchwald and co-workers²⁰³ developed the ligand 'SPhos' which has applications to the Suzuki-Miyaura coupling of difficult substrates, including aryl chlorides, under mild conditions. However, the reaction of 3-(bromomethyl)phenyl and 4-(hydroxymethyl)phenylboronic acids with compound **77** using the Buchwald protocol: SPhos / toluene / Pd(OAc)₂ / K₃PO₄ failed to give the required products and only unreacted starting material was recovered.

Treatment of phenyl and 4-methylphenylboronic acids with **77** using the Buchwald protocol significantly increased the rate of the cross-coupling reaction. An increase from 41% (standard protocol) to 78% (Buchwald protocol) was found for compound **93**. The efficiency of the 'SPhos' ligand in the formation of compound **93** can be explained by both electronic and steric factors (Figure 15). The 'SPhos' ligand contains the electron rich trialkylphosphine PCy₂ moiety which facilitates oxidative addition much more readily than the less electron-rich triarylphosphine ligand. The *ortho* substituents in 'SPhos' may also provide a stabilising interaction between the aromatic π system and one of the palladium d-orbitals, thereby increasing the steric bulk around the palladium metal, which promotes reductive elimination.²⁰³

The Buchwald protocol also has the added advantage that it requires a much lower catalyst loading than the standard Suzuki-Miyaura protocol. There are certain advantages of performing cross-coupling reactions at low catalyst loadings. Firstly, it allows for the more cost-effective use of the Suzuki-Miyaura reaction on a large scale. Secondly, it minimises the effort required for the removal of palladium from the final product.

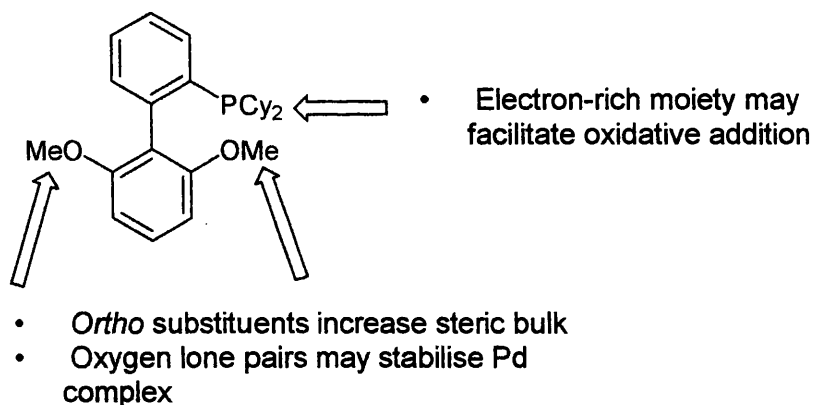
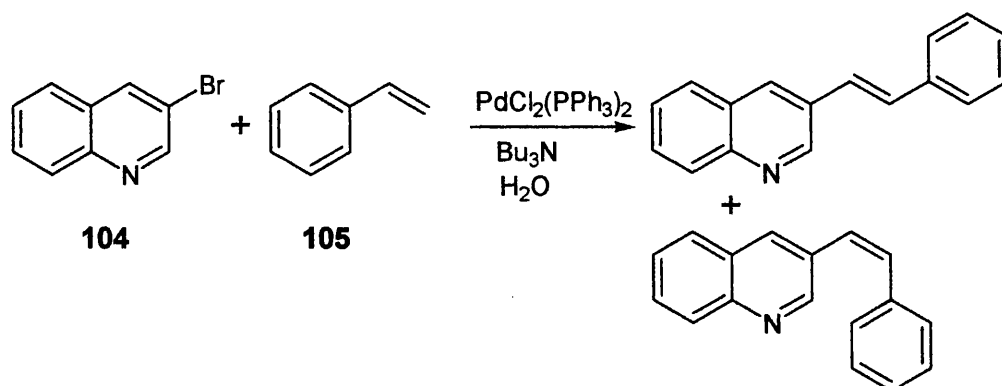


Figure 15. Electronic and steric properties of the 'SPhos' ligand.

Due to the difficulties encountered in the coupling of **77** with benzyl boronic acid, we decided to turn our attention to the synthesis of the alkenyl compound (*E*)-3-(2-phenylethenyl)quinoline-8-carboxamide.

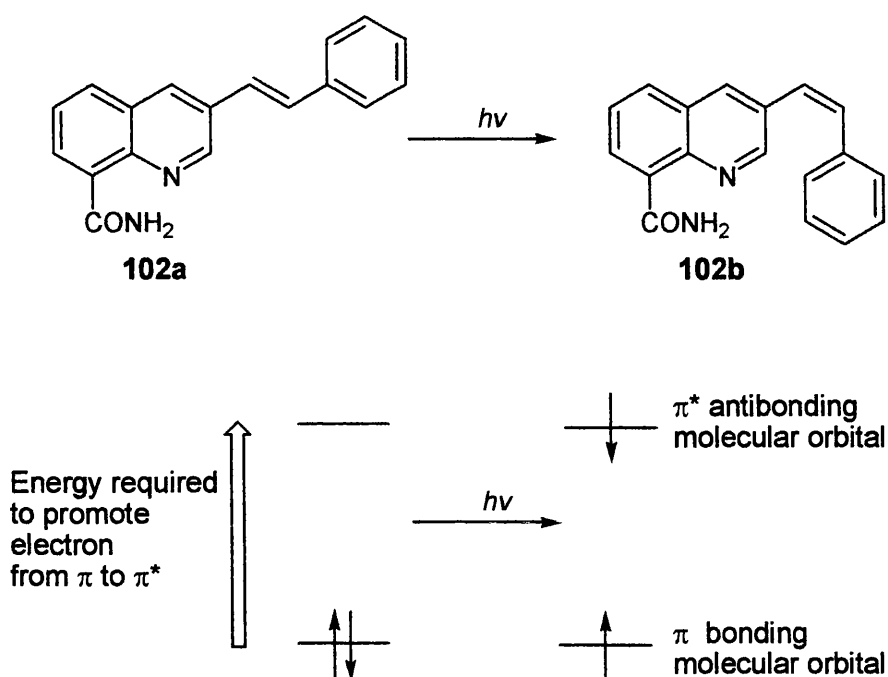
The palladium-catalysed vinylation of aryl halides is most commonly carried out *via* the Heck cross-coupling reaction. The Heck reaction usually proceeds through an addition-elimination cycle such that the reactant and product have sp^2 hybridisation at the site of substitution. However, there is one severe limitation associated with this reaction. During the Heck catalytic cycle, reversible β -hydride elimination can lead to isomerisation of the alkene. Bumagin *et al.*²⁰⁷ discovered that the Heck coupling of 3-bromoquinoline **104** and styrene **105** provided a mixture of *E* and *Z* isomers (Scheme 30). Other authors have also demonstrated the poor selectivity of the β -hydride elimination step. Consequently, the Heck reaction was not chosen for the synthesis of (*E*)-3-(2-phenylethenyl)quinoline-8-carboxamide.



Scheme 30. Reported Heck coupling of 3-bromoquinoline with styrene.²⁰⁷

Recently, there have been publications on the use of the Suzuki-Miyaura reaction for stereospecific cross-coupling of aryl halides with (*E*)-2-phenylethenyl boronic acid. Buchwald and co-workers²⁰³ demonstrated that 2-bromomesitylene could be stereospecifically coupled with (*E*)-2-phenylethenyl boronic acid to give the *trans* product in 99% yield. Due to the promising results obtained by Buchwald and co-workers, we decided to use the Suzuki-Miyaura coupling reaction to synthesise (*E*)-3-(2-phenylethenyl)quinoline-8-carboxamide. It was found that the (*E*)-2-phenylethenyl boronic acid was not soluble in the standard Suzuki-Miyaura reaction conditions and the solvent was switched to DMF. The coupling of **77** with (*E*)-2-phenylethenyl boronic acid gave (*E*)-3-(2-phenylethenyl)quinoline-8-carboxamide **102a** in 52% yield. The ¹H NMR spectrum of the isolated product in CDCl₃ showed doublet peaks at δ 7.28 and δ 7.35 with a mutual coupling constant of 19 Hz, confirming the formation of the *E* isomer. The NMR tube was then left in direct sunlight for two days. Interestingly, when the ¹H NMR spectrum was retaken after this time period, two doublets corresponding to the *Z* isomer **102b** were observed at δ 6.80 with a coupling constant of 10 Hz. By comparison with the original ¹H NMR spectrum, the conversion ratio of **102a** to **102b** was estimated to be 4:1 *E*:*Z*. Column chromatography failed to separate **102a** from **102b**.

It is generally known that the interconversion of *E* and *Z* alkenes is possible by breaking the π-bond allowing rotation to occur. In order to break the π-bond and promote the electron from the HOMO to LUMO, a considerable amount of energy is required. It is plausible that shining direct sunlight onto compound **102a** would provide enough energy to promote an electron from its bonding π molecular orbital to its antibonding π* orbital, consequently breaking the π bond and allowing rotation to occur (Scheme 31). It is known that Suzuki-Miyaura coupling reactions usually progress with complete retention of stereochemistry at the alkene. Therefore, we concluded that the Suzuki-Miyaura coupling reaction stereospecifically gave the *E* isomer **102a** and that the formation of the *Z* isomer **102b** was due to a photoisomerisation reaction.



Scheme 31. Photo-induced conversion of **102a** to **102b**.

3.4.4 Attempted Suzuki-Miyaura coupling of 3-iodoquinoline-8-carboxamide with alkylboronic acids

The Suzuki-Miyaura methodology was extended to investigate the coupling of 3-iodoquinoline-8-carboxamide **77** with alkylboronic acids. Accounts of the Suzuki-Miyaura coupling of alkylboronic acids with aryl halides are sporadic and the reported yields of products are usually very low. A similar situation exists for the coupling of aryl halides with alkylboronic esters, where low yields of products have been obtained unless highly toxic thallium compounds were used as bases in the reaction.²⁰⁸ With alkylboronic acids the most encouraging results have been described with Pd(PPh₃)₄²⁰⁹ or PdCl₂(dppf)²¹⁰ conditions. Zou *et al.*²¹¹ have reported the successful cross-coupling of alkylboronic acids with a variety of aryl and alkenyl halides. They showed that the palladium-catalysed reaction was significantly enhanced by using the additive Ag₂O in combination with K₂CO₃ and PdCl₂(dppf).

Attempts were undertaken to synthesise a variety of 3-alkylquinoline-8-carboxamides using the conditions described in Table 10. Unfortunately, none of the reaction conditions proved sufficient to activate the alkylboronic acids towards the transmetalation reaction.

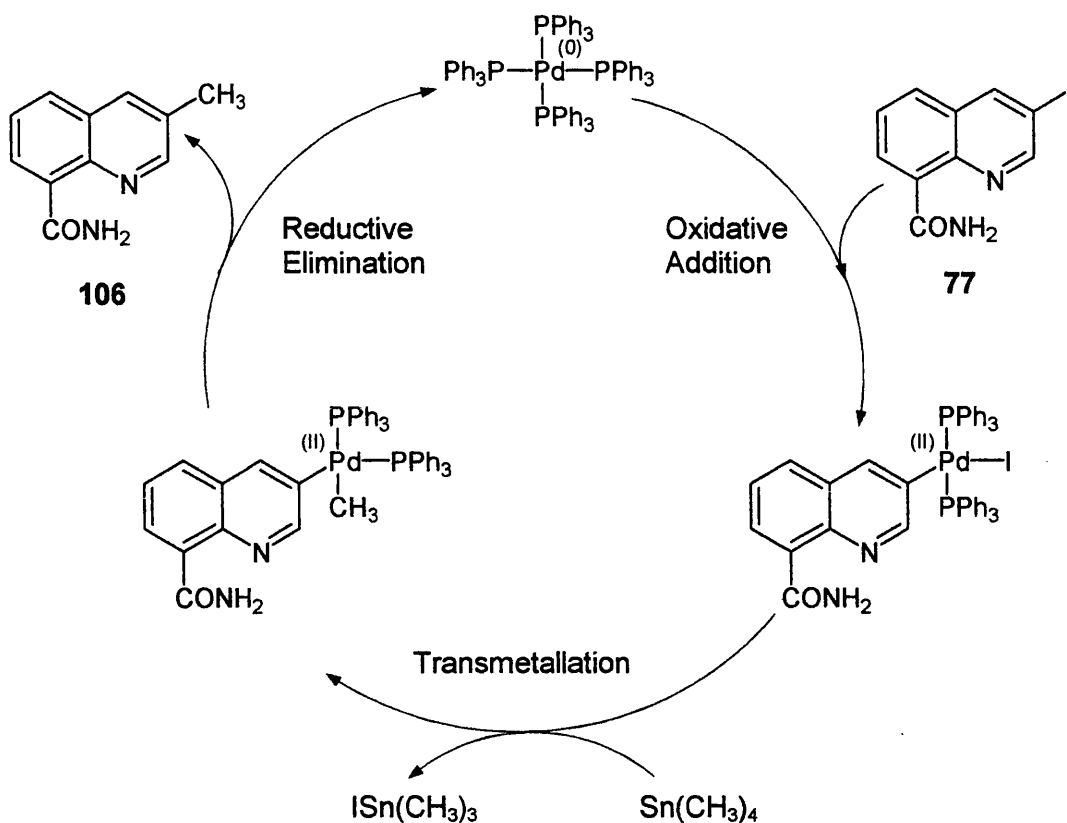
Table 10. Reaction conditions for the attempted cross-coupling of **77** with alkylboronic acids.

Boronic acid	Reaction conditions	Results ^a
Methyl	Pd(PPh ₃) ₄ , toluene, EtOH, H ₂ O, Na ₂ CO ₃	starting material 77
	PdCl ₂ (dppf), Na ₂ CO ₃ , THF, Cs ₂ CO ₃ , H ₂ O	starting material 77
	Pd(PPh ₃) ₄ , 1,4-dioxane, K ₂ CO ₃	decomposition
	Pd(OAc) ₂ , Sphos, toluene, K ₂ PO ₄	decomposition
Isobutyl	Pd(PPh ₃) ₄ , toluene, EtOH, H ₂ O, Na ₂ CO ₃	starting material 77
	PdCl ₂ (dppf), Na ₂ CO ₃ , THF, H ₂ O	starting material 77
	Pd(PPh ₃) ₄ , 1,4-dioxane, K ₂ CO ₃	starting material 77
	Pd(PPh ₃) ₄ , 1, THF, K ₂ CO ₃	starting material 77
	PdCl ₂ (dppf), K ₂ CO ₃ , THF, Ag ₂ O	starting material 77
Isopropyl	Pd(PPh ₃) ₄ , toluene, EtOH, H ₂ O, Na ₂ CO ₃	starting material 77

^a The reactions were monitored by TLC and crude mixtures were analysed by ¹H NMR spectroscopy.

3.4.5 Stille coupling reaction

Due to the failure of the Suzuki-Miyaura reaction to provide a series of 3-alkylquinoline-8-carboxamides, we directed our attention to the use of the Stille cross-coupling reaction. The Stille reaction is a versatile C-C bond forming reaction, which involves the coupling of an aryl or alkenyl halide with an organostannane reagent. The use of the Stille reaction for the construction of substituted heterocyclic compounds has been widely reviewed²¹² and has simplified the synthesis of many medicinal products. However, there are two major drawbacks to the Stille reaction: (1) Removal of tin residues from the product after the reaction can prove tedious (2) Organostannane compounds are quite toxic and special care is needed when handling these compounds. Nevertheless, the use of organostannane reagents in our experiment is advantageous as they are compatible with electrophiles that contain sensitive functional groups, such as carboxamide.



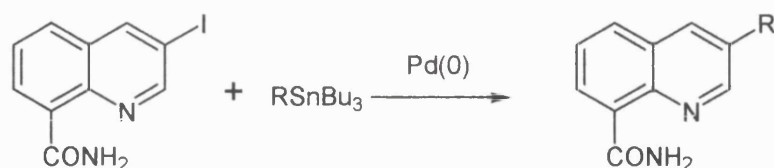
Scheme 32. Proposed mechanism for the Stille coupling reaction between 3-iodoquinoline-8-carboxamide **77** and tetramethylstannane.

The Stille coupling reaction between 3-iodoquinoline-8-carboxamide **77** and tetramethylstannane was therefore attempted. The reaction was carried out in *N*-methylpyrrolidinone (NMP) in the presence of (10 mol%) Pd(PPh₃)₄. Remarkably, the Stille reaction gave 3-methylquinoline-8-carboxamide **106** in 40% yield. The presence of the characteristic N-H peaks at δ 6.20 and δ 10.99 in the ¹H NMR spectrum of compound **106** indicated that the carboxamide functionality was well tolerated in the Stille reaction.

As with the Suzuki-Miyaura reaction, the Stille reaction probably operates by an oxidative addition-transmetalation-reductive elimination mechanism, as illustrated in Scheme 32. A unique feature of the Stille coupling mechanism is that no base is required to activate the organostannane reagent. However, in the Suzuki-Miyaura coupling reaction, the organoboron reagent must be activated, for example with a base, to facilitate the transmetalation process.

The Stille reaction was extended to explore the coupling of **77** with alkynyl, benzyl and alkenyl organostannane reagents (Table 11).

Table 11. Stille cross-coupling of **77** with organostannane reagents. (-) denotes unsuccessful attempts.

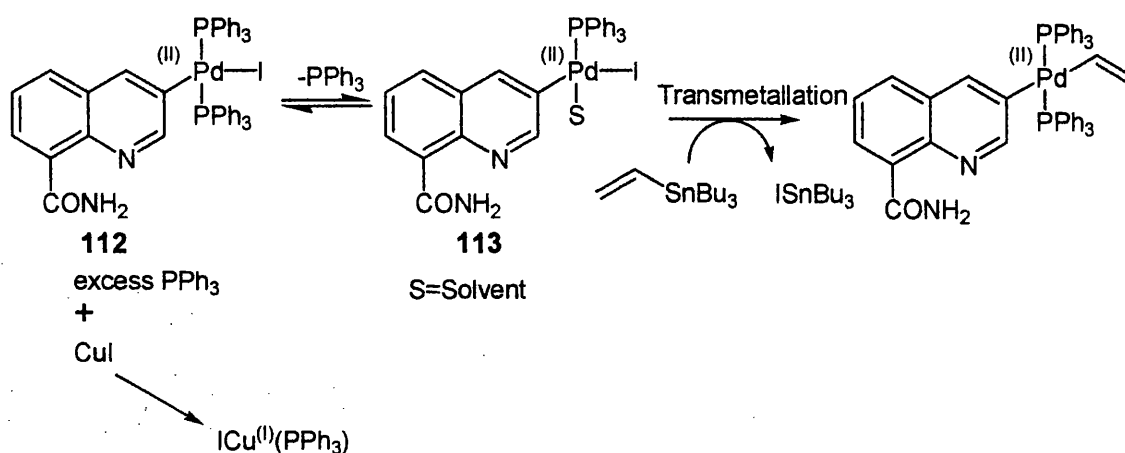


Compound number	R	Reaction conditions	Yield of products (%)
107	MeC≡C	Pd(PPh ₃) ₄ , NMP	39
-		Pd(PPh ₃) ₄ , NMP	-
111	H ₂ C=CH	Pd ₂ dba ₃ , PPh ₃ , CuI, 1,4-dioxane	55

The cross-coupling of **77** with tributyl(prop-1-ynyl)stannane gave **107** in 39% yield. ¹H NMR and TLC analyses of the crude mixture indicated that clean coupling had occurred with only trace amounts of the starting tributyl(prop-1-ynyl)stannane present in the mixture. Analytically-pure **107** was isolated as a pale-buff solid by column chromatography. The IR spectrum of **107** showed a distinct peak at 2363 cm⁻¹ corresponding to the triple bond of the alkyne group. Particularly characteristic in the ¹³C spectrum are the signals of the alkyne carbons at δ 90.6 and δ 118.3. Interestingly, even though the starting organostannane reagent contains four substituents around the tin atom, only the alkynyl group was transferred to the substrate **77**. This can be explained by the rate of ligand transfer which proceeds as follows: alkynyl > alkenyl > allyl = benzyl > alkyl.²¹² Therefore, the tributylstannane group (SnBu₃) is generally transferred intact during the Stille reaction.

Organostannanes can be prepared by the reaction of an organometallic reagent such as lithium or magnesium with an organostannane electrophile. Tributylbenzylstannane was not commercially available and was prepared by the reaction of benzyl magnesium chloride **108** with tributylstannyl chloride **109** (Scheme 33). The mixture was stirred in dry THF for 30 min at room temperature. Aqueous work up and column

The exact role of the copper iodide salt in the Stille coupling reaction is not fully understood. It is proposed that the copper effect could be explained by the 'ligand association mechanism' as demonstrated in Scheme 34. Presumably, the active species **113** is formed by loss of a triphenylphosphine ligand from the initial palladium(II) species **112** that is generated after oxidative addition. The triphenylphosphine ligand is a strong electron donor and allows only minute concentrations of the reactive species **113** at equilibrium. Ligand dissociation from **112** is a key factor in the transmetalation step. Since the copper iodide salt has a high affinity for phosphines, it may function to facilitate the loss of the ligands which would otherwise cause an inhibitory effect.

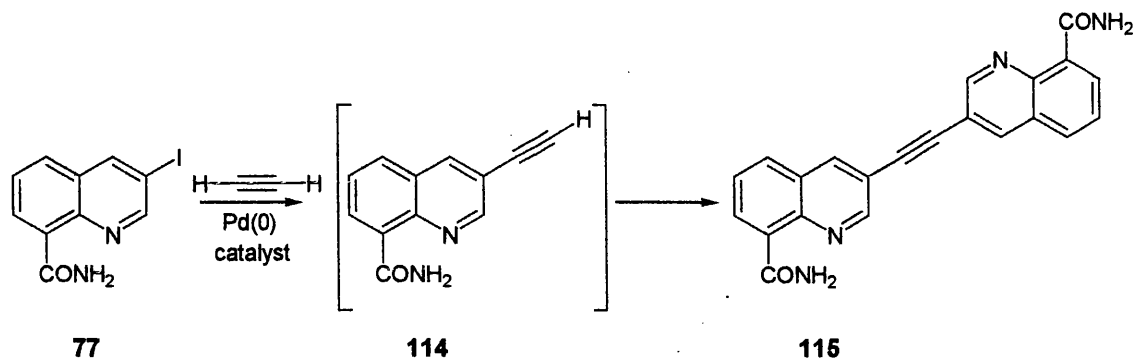


Scheme 34. Proposed mechanism for the copper effect on the Stille coupling of tributylethenylstannane with 3-iodoquinoline-8-carboxamide **77**.²¹³

3.4.6 Sonogashira coupling reaction

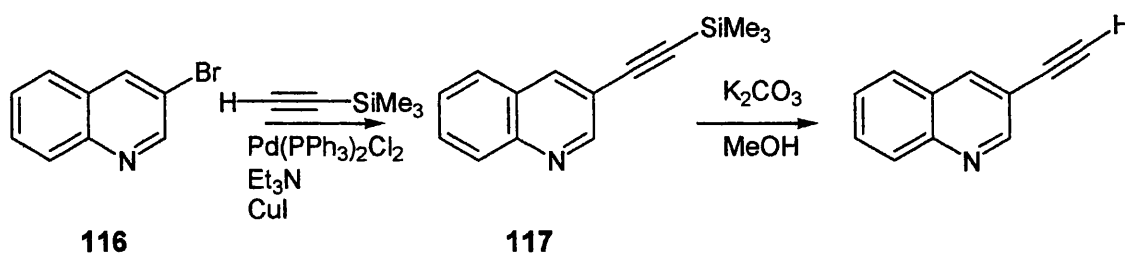
The Sonogashira reaction involves the formation of C_{sp2}-C_{sp} bonds through the reaction of an aryl halide or triflate with terminal alkynes under palladium-catalysed conditions. The electron-rich nature and rigidity of the C_{sp2}-C_{sp} bond make alkynes structurally appealing. The alkyne moiety also provides a point of unsaturation for further transformation and / or derivatisation. A wide variety of heterocyclic compounds has been synthesised using the Sonogashira approach. The reaction is highly versatile and has a great tolerance for a range of functional groups. Consequently, we decided that the Sonogashira reaction would be appropriate for the introduction of alkyne substituents into the 3-position of quinoline-8-carboxamide. In order to establish whether 3-iodoquinoline **77** would be a good coupling substrate in the Sonogashira reaction, it was decided to synthesise 3-ethynylquinoline-8-carboxamide **114**.

A direct synthesis to alkyne **114** would be to couple **77** with ethyne gas. A major drawback to this synthetic strategy is that the alkyne **114** formed in the reaction may be more acidic than ethyne itself. This means that compound **114** may compete with ethyne for the coupling of the substrate **77**. Subsequently, this could lead to the formation of the by-product **115**.



Scheme 35. Formation of by-product **115** from the Sonogashira coupling of 3-iodoquinoline-8-carboxamide **77** with alkyne **114**.

Gulykina *et al.*²¹⁴ reported the synthesis of 3-ethynylquinoline using Sonogashira conditions. They approached their synthesis by first protecting one end of ethyne with a trimethylsilyl (TMS) group. Coupling of the free ethyne end with 3-bromoquinoline **116** afforded **117** in 96% yield. Deprotection of **117** was achieved under basic conditions (Scheme 36). Therefore, an alternative method for the synthesis of alkyne **114** would be to couple **77** with trimethylsilylethyne, followed by TMS-deprotection of the resultant alkyne.



Scheme 36. Reported synthesis of 3-ethynylquinoline.²¹⁴

Sonogashira coupling of **77** with trimethylsilylethyne was performed in the presence of a catalytic amount of bis(triphenylphosphine)palladium(II) chloride $\text{Pd}(\text{PPh}_3)_2\text{Cl}_2$ and copper(I) iodide in diisopropylamine (DIPA) and dry THF. The mixture was stirred at 45°C under argon for 2 h. The catalyst used in this reaction, $\text{Pd}(\text{PPh}_3)_2\text{Cl}_2$ was prepared by treating palladium(II) chloride with two equivalents of triphenylphosphine in

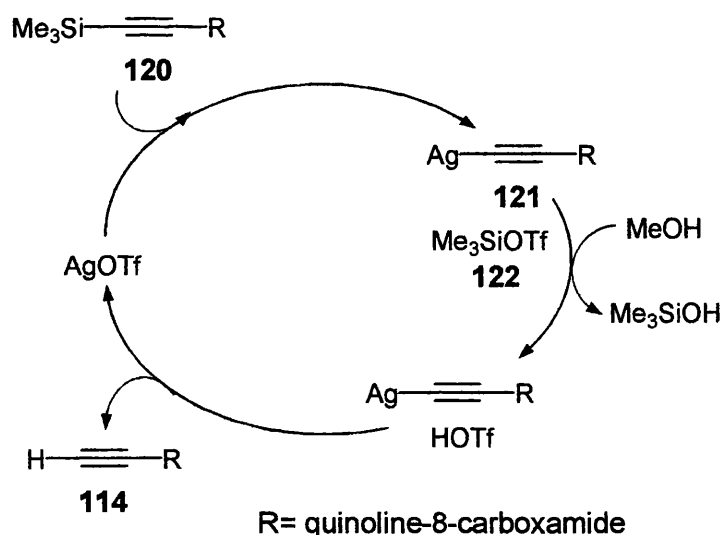
DMF at 80°C for 24 h. Pd(II) complexes are often used in the Sonogashira reaction as they are usually more stable and less sensitive to air than their Pd(0) counterparts. It is known that triphenylphosphine ligands and amines such as DIPA can reduce Pd(II) complexes to the active Pd(0) species. The presence of the copper(I) iodide co-catalyst has been shown to accelerate greatly the Sonogashira reaction, thus enabling performance of the alkynylation under mild reaction conditions.

The exact mechanism of the co-catalysed Sonogashira reaction has yet to be established. However, it is believed that the reaction proceeds through two independent catalytic cycles as shown in Scheme 37. The mechanism is similar to that of the Suzuki-Miyaura and Stille couplings. Initially, the Pd(PPh₃)₂Cl₂ is reduced *in situ* to give the catalytic species bis(triphenylphosphine)palladium(0). Oxidative addition of the aryl iodide **77** to the Pd(0) complex gives the Pd(II) intermediate. The next step is the rate-determining step in which the palladium-cycle connects with the copper co-catalyst cycle. Transmetalation of the Pd(II) intermediate with the copper acetylide species **118** gives the diorgano-Pd(II)-complex **119**. Reductive elimination with coupling of two organic ligands gives the final coupled alkyne **120** with regeneration of the Pd(0) catalyst.

The catalytic copper cycle is still poorly understood. It is believed that the base (DIPA) abstracts the acetylenic proton from the terminal alkyne, thus forming copper acetylide species **118** in the presence of copper(I) iodide. A second proposal is that a π -alkyne-copper complex shown in Scheme 37 is involved in the copper-cycle, thus making the alkyne proton more acidic for easier abstraction.²¹⁵ Mechanistic studies, however, have not been reported yet. The alkyne **120** was obtained in 62% yield. In the ¹H NMR spectrum the TMS group gave a singlet at δ 0.29 integrating for 9 protons. In the IR spectrum a peak at 2164 cm⁻¹ confirmed the formation of the C_{sp2}-C_{sp} bond.

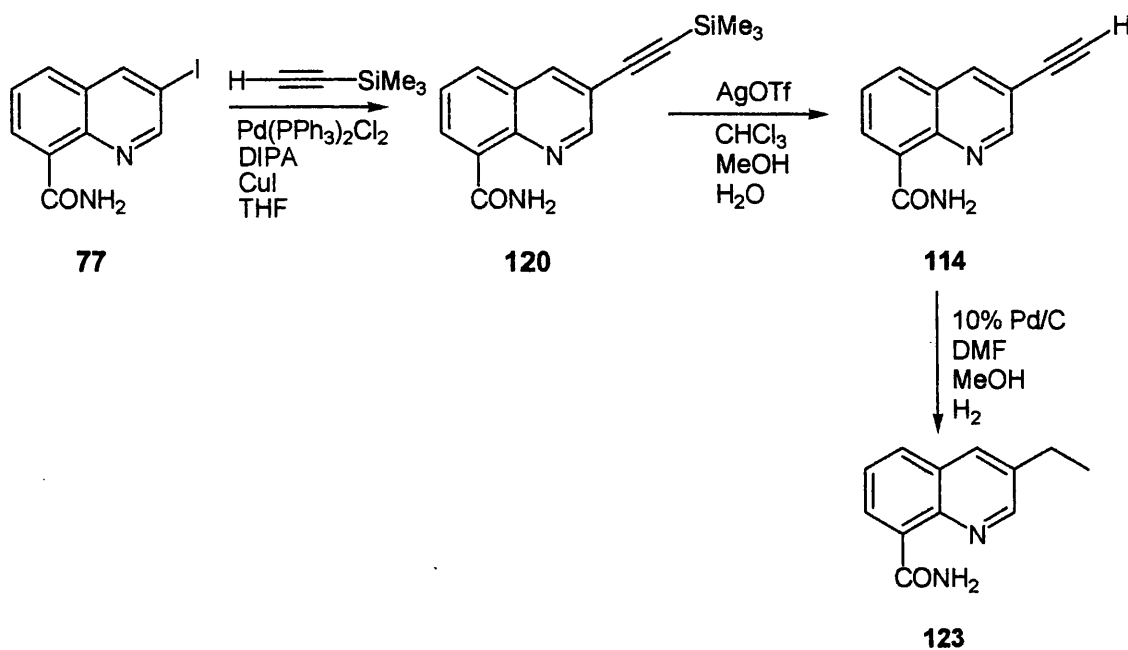
prolonged heating of the electron-deficient methyl 3-nitro-2-(2-trimethylsilylethynyl)-benzoate with silver(I) triflate in a mixture of methanol, water and dichloromethane gave good yields of methyl 2-ethynyl-3-nitrobenzoate. The alkyne **120** was treated with silver(I) triflate in a mixture of methanol, water and dichloromethane at room temperature for 24 h. A TLC analysis indicated that only the starting material was present in the crude mixture. Failure to achieve desilylation of **120** at room temperature led to the employment of harsher reaction conditions. Prolonged heating of **120** with silver(I) triflate in a mixture of methanol, water and chloroform gave **114** in 99% yield. The use of chloroform, methanol and water mixture (4:1:7) as the solvent allowed a relatively high reflux temperature for the reaction. The existence of compound **114** was supported by mass spectrometry. In the electrospray (ES) spectrum a signal corresponding to **114** ($m/z = 197.0702$ M+H) was observed.

The mechanism for the desilylation reaction is not fully understood. It is proposed that the silver counter ion (TfO^-) acts as a nucleophile and attacks the silicon atom of the TMS group upon silver activation. This results in the cleavage of the C-Si bond and to the *in situ* formation of the alkynyl silver species **121** and the silyl-triflate species **122**. In the aqueous methanol solvent, **122** is methanolised leading to a better proton source, strong enough to hydrolyse the alkynyl silver species. Silver ions are released and the catalytic cycle is then regenerated (Scheme 38).



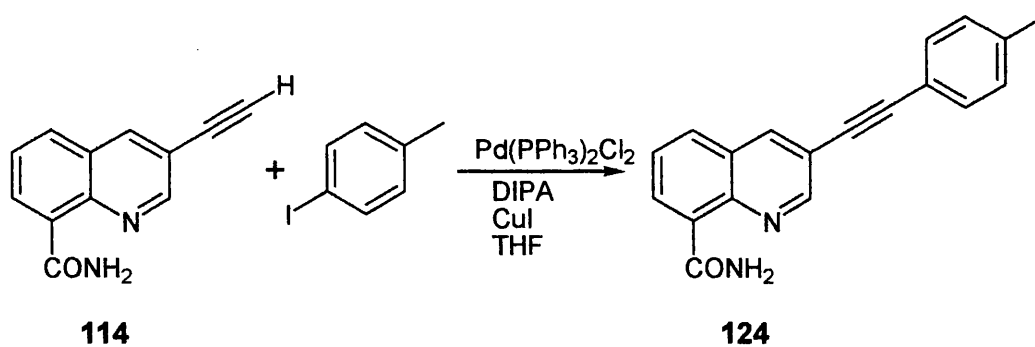
Scheme 38. Proposed mechanism for the Ag^+ -catalysed deprotection of 3-((trimethylsilyl)ethynyl)quinoline-8-carboxamide **120**.²¹⁸

Having established a satisfactory route to the synthesis of **114**, it was decided to reduce the triple bond to give the ethyl compound **123** as an additional PARP inhibitor. The alkyne **114** was reduced to the alkyl compound **123** via catalytic hydrogenation with Pd/C. Surprisingly, the alkyl compound **123** was produced cleanly in 64% yield without the presence of alkene by-products. Evidence for the formation of compound **123** was obtained by the presence of the ethyl group in the ^1H NMR spectrum, which was observed as a quartet at δ 2.88 and a triplet at δ 1.37.



Scheme 39. Synthesis of 3-ethynylquinoline-8-carboxamide **114** and subsequent reduction to 3-ethylquinoline-8-carboxamide **123**.

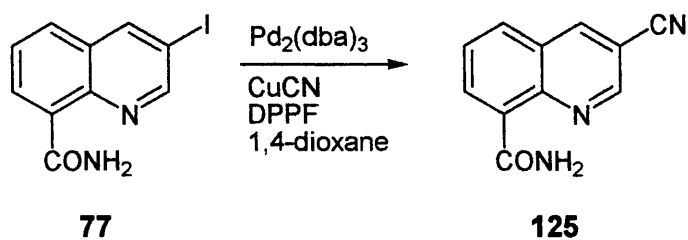
Due to the success of the Sonogashira reaction in the synthesis of alkyne **114**, it was decided to extend the methodology further. It was proposed that **114** could be functionalised by acting as a coupling partner in a second Sonogashira reaction. 4-Iodotoluene was chosen as the substrate for the reaction because it was cheap and commercially available. Alkyne **114** was directly coupled to 4-iodotoluene in the presence of $\text{Pd}(\text{PPh}_3)_2\text{Cl}_2$, CuI, and DIPA in THF. The mixture was stirred at 45°C under argon for 24 h. Purification of the alkyne **124**, was achieved by washing with water and separation using column chromatography. Alkyne **124** was obtained in 12% yield. The reaction was repeated but even after several days and adding fresh reagent, a low yield of 9% was obtained. However, the purification only required the separation of the product from unreacted starting material.



Scheme 40. Sonogashira coupling of 3-ethynylquinoline-8-carboxamide **114** with 4-iodotoluene.

3.4.7 Palladium-catalysed cyanation of 3-iodoquinoline-8-carboxamide

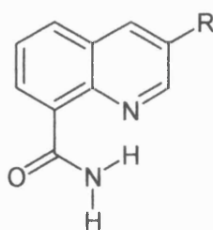
As mentioned previously, the palladium-catalysed cyanation of aryl halides and triflates is a useful modern method to prepare aryl cyanides. Despite the problematic cyanation of quinoline-8-yl trifluoromethanesulfonate **82**, we decided to explore the use of 3-iodoquinoline-8-carboxamide **77** in the palladium-catalysed cyanation reaction. Compound **77** was treated with Zn(CN)₂ and Pd(PPh₃)₄ in DMF and heated at 150°C for 24 h. The ¹H NMR spectrum of the crude mixture indicated that only unreacted starting material was present. Sakamoto *et al.*²²⁰ reported a novel method for the palladium-catalysed cyanation of both π-deficient and π-efficient aryl iodides. In particular, they managed to synthesise quinoline-8-carbonitrile in 91% yield. The reported synthesis of quinoline-8-carbonitrile involved the treatment of 3-iodoquinoline with Pd₂(dba)₃, 1,1'-bis(diphenylphosphino)ferrocene (DPPF), and CuCN in 1,4-dioxane. These reaction conditions were applied to the cyanation of compound **77** (Scheme 41). However, treatment of **77** with CuCN in the presence of Pd₂(dba)₃ and DPPF only gave **125** in 2% yield. In the ¹H NMR spectrum of compound **125** the chemical shift values were very similar to that of the starting material **77**. This was expected as the cyano functional group has a similar electron-withdrawing capacity as the iodo group. The mass spectrum of compound **125** indicated the presence of a pseudo molecular ion at *m/z* 220, corresponding to the molecular mass of **125** plus a sodium ion.



Scheme 41. Palladium-catalysed cyanation of 3-iodoquinoline-8-carboxamide **77** with CuCN.

Overall, we have successfully investigated the reactivity of 3-iodoquinoline-8-carboxamide, under palladium-catalysed cross-coupling conditions, for the synthesis of a series of 3-substituted quinoline-8-carboxamides (Table 12). A variety of different substituents with different electronic properties have been introduced into the 3-position of quinoline-8-carboxamide *via* Suzuki-Miyaura, Stille, Sonogashira and palladium-catalysed cyanation reactions. A selection of these target compounds will be tested for their PARP inhibitory activity *in vitro*. The inhibitory constants and SAR studies of the 3-substituted quinoline-8-carboxamides will be discussed further in Section 4.1.2.

Table 12. Small compound library of 3-substituted quinoline-8-carboxamides.



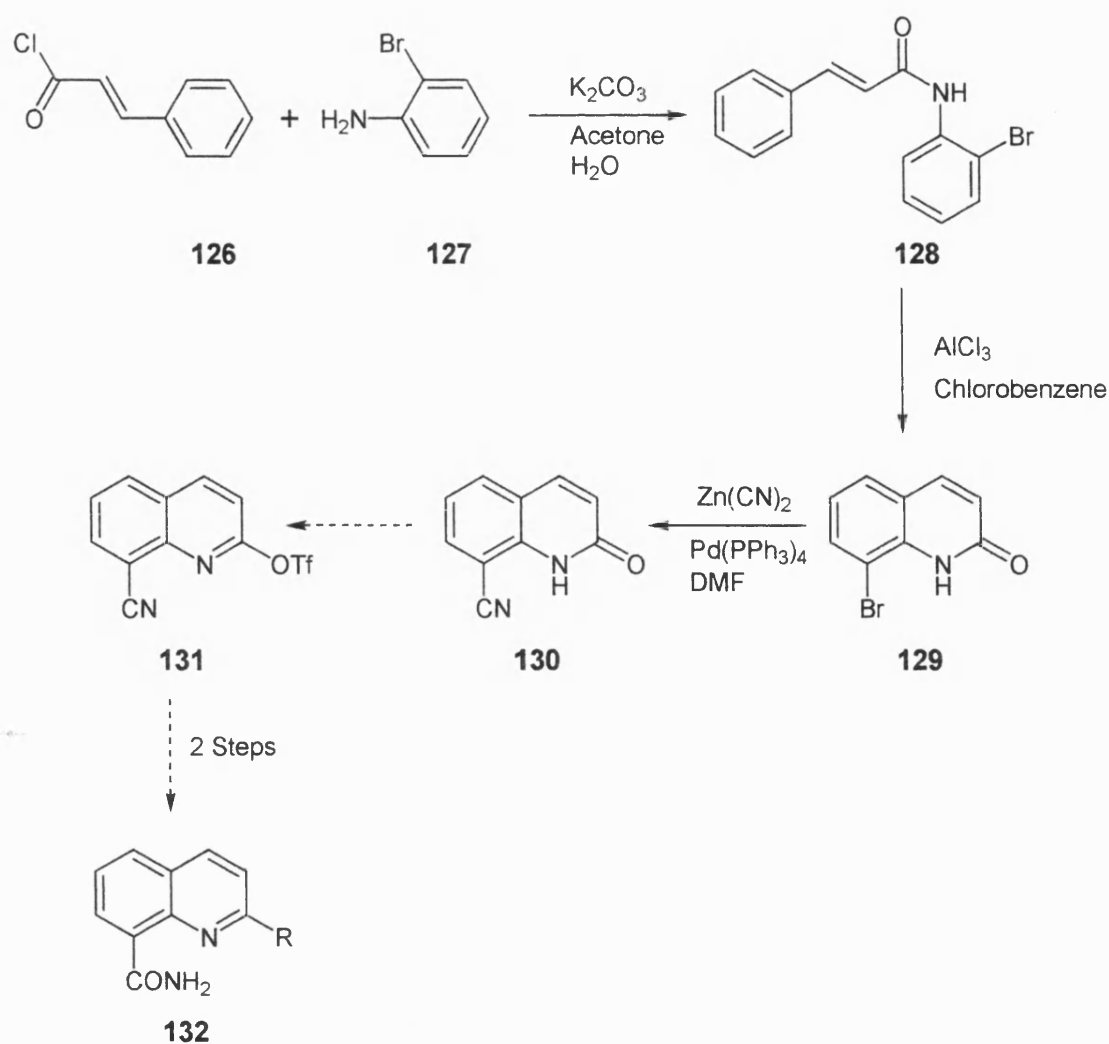
Compound number	R
69	Ph
91	4-MeOPh
92	3,5-Me ₂ Ph
93	4-MePh
94	3-F ₃ CPh
95	4-F ₃ CPh
96	2-F ₃ CPh
97	3-BrPh
98	4-NCPH
99	Pyridin-3-yl
100	Pyridin-4-yl
103	4-EtOCH ₂ Ph
101	4-BrCH ₂ Ph
102a	<i>E</i> -PhCH=CH
106	Me
123	Et
111	H ₂ C=CH
114	HC≡C
124	4-MePhC≡C
107	MeC≡C
125	CN

3.5 2-Substituted quinoline-8-carboxamides

Following on from the successful synthesis of a range of 3-substituted quinoline-8-carboxamides, we decided to direct our attention to the synthesis of 2-substituted quinoline-8-carboxamides. As mentioned previously in Section 1.10 SAR studies by Griffin and co-workers¹⁷⁰ indicated that the PARP-1 enzyme has a relatively large NAD⁺-binding pocket. In addition, SAR studies on quinazolinone PARP-1 inhibitors demonstrated that even bulky substituents such as 4-fluorophenyltetrahydropyridine were well tolerated in the enzyme active site. The 2-substituted quinoline-8-carboxamides are of particular interest because the 2-substituent should occupy the same region of space as the 2-aryl substituent in the benzimidazole-4-carboxamides. Therefore, it is highly probable that 2-substituted quinoline-8-carboxamides will be well tolerated by the active site and may enhance PARP-1 inhibitory activity. Our initial approach to the preparation of 2-substituted quinoline-8-carboxamides focused on extending the synthetic approaches previously employed, such as organometallic synthesis. Thus, allowing us to explore further the synthetic potential of the palladium-catalysed coupling reaction in providing quinoline-8-carboxamide derivatives.

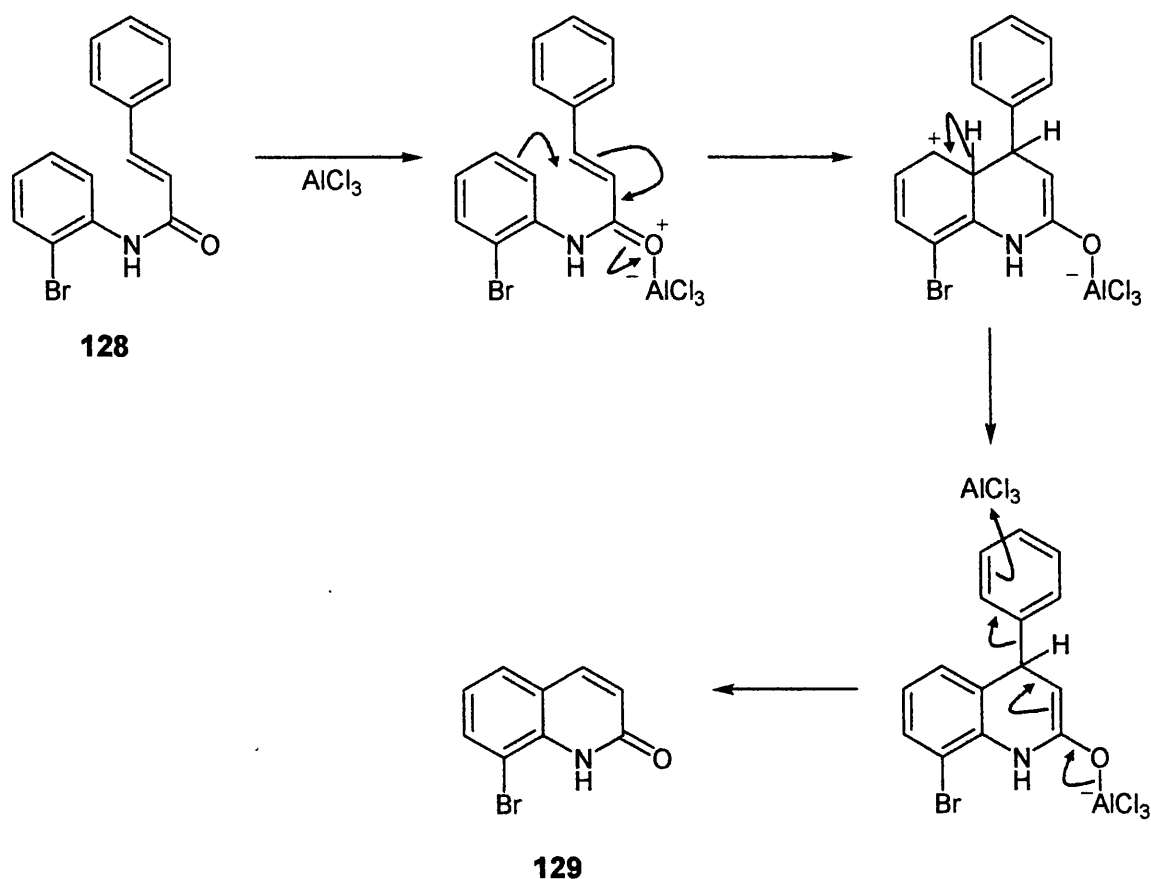
3.5.1 Attempted synthesis of 8-cyanoquinolin-2-yl trifluoromethanesulfonate

Recently, Cottet *et al.*²²¹ reported the synthesis of a series of 2,8-disubstituted quinoline derivatives. In particular, they demonstrated that 8-bromo-2-chloroquinoline could be prepared by treatment of 8-bromoquinolin-2(1*H*)-one with phosphorus oxychloride. 8-Bromoquinolin-2(1*H*)-one **129** emanated from an unusual Friedel-Crafts-like intramolecular cyclisation of *E*-*N*-(2-bromophenyl)-3-phenylpropenamide **128** with aluminium chloride in chlorobenzene. We proposed that compound **129** could be used as an intermediate for the formation of 8-cyanoquinolin-2-yl trifluoromethanesulfonate **131**. The triflate **131** functions as a scaffold through which a diverse range of substituents may be introduced into the 2-position of the quinoline ring *via* palladium-catalysed cross-coupling reactions. Subsequent hydration of the nitrile group should give the necessary carboxamide functionality. Our synthetic strategy for the preparation of 2-substituted quinoline-8-carboxamides is outlined in Scheme 42.



Scheme 42. Attempted synthesis of 8-cyanoquinolin-2-yl trifluoromethanesulfonate **131**.

In our laboratory, compound **129** was synthesised in two steps. The first step was the preparation of *E*-*N*-(2-bromophenyl)-3-phenylpropenamide **128** by the reaction of *E*-3-phenylpropenoyl chloride **126** and 2-bromoaniline **127** to afford **128** in 97% yield. Treatment of **128** with the strong Lewis acid aluminium trichloride at high temperature led to a 41% yield of the required quinolinone **129**. A proposed mechanism for this unusual Friedel-Crafts-like reaction is shown in Scheme 43. Lewis-acid-catalysed addition of the bromobenzene ring into the conjugate electrophile gives the intermediate dihydroquinoline. The heterocycle is aromatised by elimination of a proton and of molecular benzene, a highly unusual leaving group.



Scheme 43. Proposed mechanism for the Friedel-Crafts-like cyclisation of *E*-*N*-(2-bromophenyl)-3-phenylpropenamide **128** using AlCl_3 in chlorobenzene.

A palladium-catalysed cyanation reaction on compound **129** was undertaken. Initially, compound **129** was treated with $\text{Zn}(\text{CN})_2$ and $\text{Pd}(\text{PPh}_3)_4$ and heated to 150°C for 12 h. Although the reaction was successful, 2-oxo-1,2-dihydroquinoline-8-carbonitrile **130** was obtained in only 6% yield. As a result, the reaction was repeated using CuCN as the cyanide source. However, in this procedure, compound **130** was obtained in a lower yield of 5%. Further reaction of **130** was planned to give the triflate **131**. It was hoped that subsequent Suzuki-Miyaura coupling would give compounds where R is a (substituted)phenyl group. However, due to the persistent low yields obtained in the palladium-catalysed cyanation reactions, it was decided to investigate an alternative strategy to the formation of 2-substituted quinoline-8-carboxamides.

3.5.2 Synthesis of 2-aryl and 2-alkyl-quinoline-8-carboxamides

In contemplating ways to synthesise 2-substituted quinoline-8-carboxamides, we found that one possible strategy would be to explore the option of regioselective palladium-catalysed couplings on 2,8-dihaloquinolines.

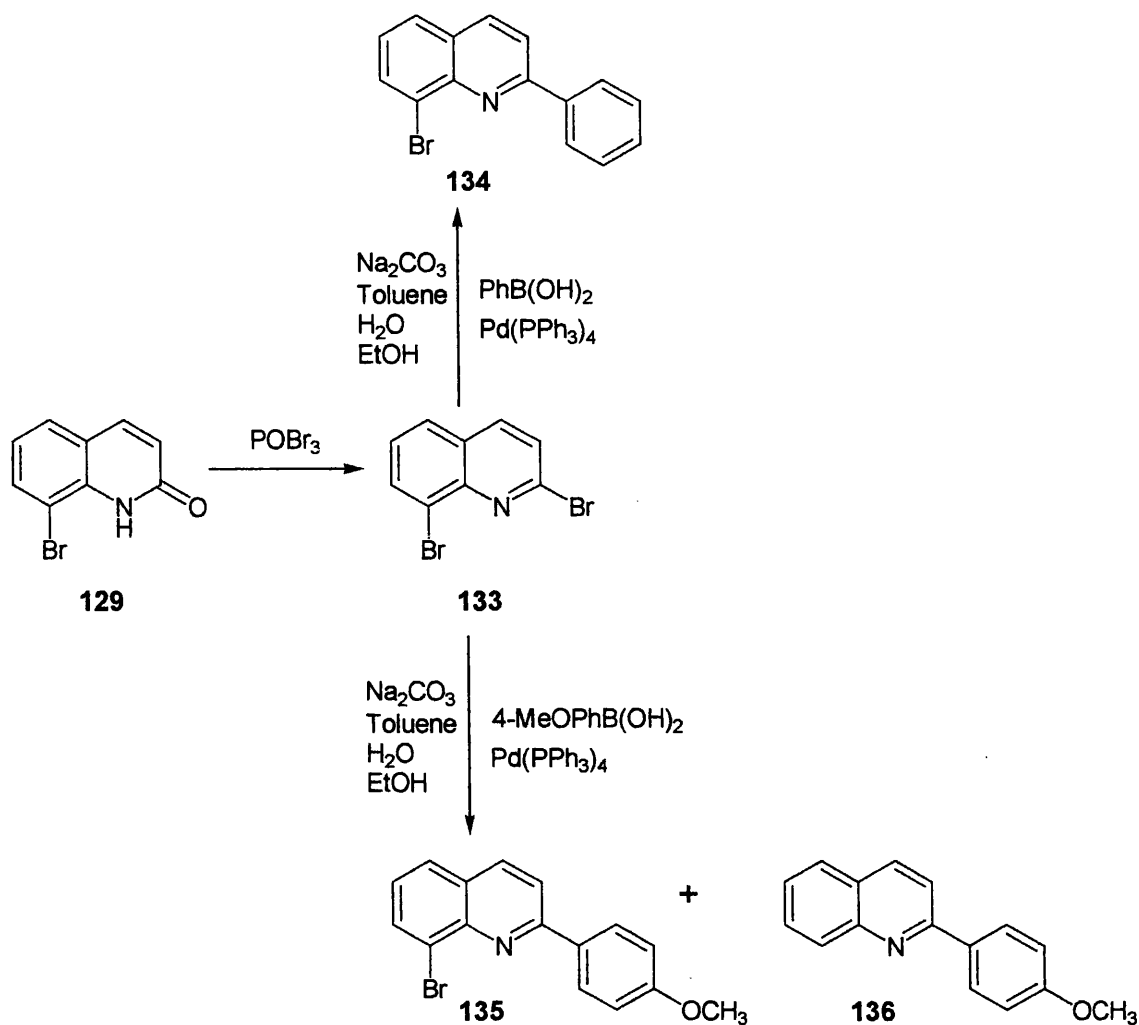
Handy *et al.*²²² described a simple guide for predicting the order and site of coupling (*i.e.* Suzuki-Miyaura, Stille and Sonogashira) in polyhaloheteroaromatics based upon ¹H NMR chemical shift values of the parent non-halogenated heteroaromatics. In addition, the electronic preference for oxidative addition has been reported to parallel that of nucleophilic aromatic substitution in heterocyclic compounds.²²³ Due to the annelated benzene ring, quinolines possess only one highly electrophilic position at the carbon atom 2-C. Therefore, cross-coupling reactions for which the oxidative addition is the rate-determining step should show a preference in favour of the most electrophilic carbon atom in 2,8-dihaloquinolines. Consequently, we decided to exploit the electronic differences between the 2- and 8- positions of 2,8-dibromoquinoline **133**.

Treatment of compound **129** with POBr₃ gave 2,8-dibromoquinoline **133** (synthesised according to the method described by Mao *et al.*²²⁴) in 41% yield. The ¹³C NMR spectrum of **133** demonstrated that the chemical shifts of the carbon atoms bearing a bromo substituent (2-C and 8-C) differ slightly (δ 145.8 and δ 123.6 respectively). Therefore, oxidative addition to Pd(0) should preferentially occur at the 2-carbon, ensuring regioselective coupling. Subsequent lithium-halogen exchange reaction and treatment with trimethylsilylisocyanate should afford the carboxamide functionality in the 8-position.

To investigate the regioselectivity and efficiency of the Suzuki-Miyaura coupling reaction of **133** and arylboronic acids to afford 2-aryl-8-bromoquinoline, the reaction of **133** with phenylboronic acid was chosen as a model (Scheme 44). Treatment of **133** with phenylboronic acid under standard Suzuki-Miyaura conditions gave the monocoupled product **134** in 43% yield. The ¹³C NMR spectrum of **134** showed that the 2-carbon had moved downfield going from 2,8-dibromoquinoline **133** at δ 145.8 to δ 156.8. This is due to the presence of the phenyl substituent in the 2-position. HMBC analysis of compound **134** demonstrated that the phenyl protons (2',6'-H₂) at δ 8.31 showed three bond cross-peaks with the 2-C (δ 156.8) and 4'-C (δ 127.7), confirming the regioselectivity of the Suzuki-Miyaura coupling reaction. In addition, the ¹H NMR and ¹³C NMR spectra of **134** were in agreement with the reported data by Mao *et al.*²²⁴

The exclusive formation of **134** results from the higher reactivity of the bromopyridine compared to bromobenzene. Comins and co-workers²²⁵ suggested that the regioselectivity of coupling at the 2-position of quinoline derivatives could also be due to the pre-coordination of the palladium metal to the quinoline nitrogen.

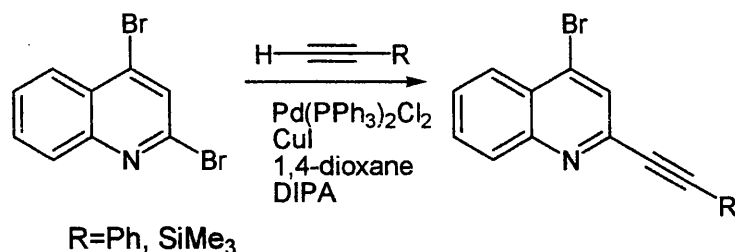
The Suzuki-Miyaura coupling of **133** with 4-methoxyphenylboronic acid was also explored. A TLC analysis of the reaction indicated the formation of two products. Column chromatography afforded the monocoupled product **135** in 84% yield, also isolated was the de-brominated compound **136** in 21% yield. It was thought that the formation of **136** was a result of the replacement of bromine with hydrogen during the Suzuki-Miyaura coupling reaction. Presumably steric retardation of the rate of transmetallation provided an opportunity for bromine-hydrogen exchange to take place. In the ¹H NMR spectrum of **135**, a singlet peak corresponding to the methoxy substituent was observed at δ 3.88. Compound **135** also provided ³J_{CH} couplings available for HMBC correlation, and the 1D ¹H spectrum revealed that the phenyl protons (2',6'-H₂) at δ 8.28 showed three-bond cross-peaks with the 2-C (δ 157.1) and the quaternary carbon 4'-C (δ 161.1). These results, in combination with the ¹³C NMR spectrum, provide a fully assigned structure for quinoline **135**.



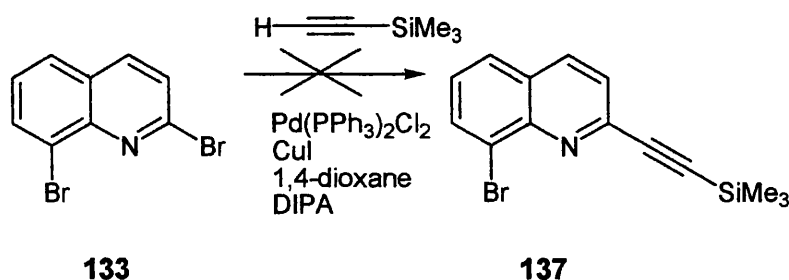
Scheme 44. Regioselective Suzuki-Miyaura coupling of 2,8-dibromoquinoline **133** with arylboronic acids.

Comins and co-workers²²⁵ reported that 2,4-dibromoquinoline could be mono-substituted with various terminal alkynes (Scheme 45). They demonstrated by HMBC analysis that the coupling reactions were selective for the C-2 position of the quinoline ring when one equivalent of the alkyne reagent was used. Accordingly, 2,8-dibromoquinoline should selectively form an alkynyl-carbon bond in the 2-position. The Sonogashira reaction on **133** was briefly examined (Scheme 46). Compound **133** was treated with one molar equivalent of trimethylsilylethyne, with Pd(PPh₃)₄, CuI and DIPA in THF at 45°C for 2 h. TLC and ¹H NMR analyses indicated that the starting material had not been consumed in the reaction and there was no evidence of the formation of the monocoupled product **137**. The reaction was repeated using 1.2 molar equivalents of trimethylsilylethyne. However, a mixture of products was obtained which could not be separated using column chromatography. It is proposed that the 2-alkynylquinolines may be unstable under the Sonogashira reaction conditions, thereby leading to the

formation of a mixture of products through a polymerisation reaction. The identity of the products could not be ascertained from the ^1H NMR spectrum. Due to the sensitivity of the Sonogashira reaction of 2,8-dibromoquinoline it was decided not to progress any further with the 2-alkynylquinoline derivatives.



Scheme 45. Reported regioselective couplings of 2,4-dibromoquinoline.²²⁵



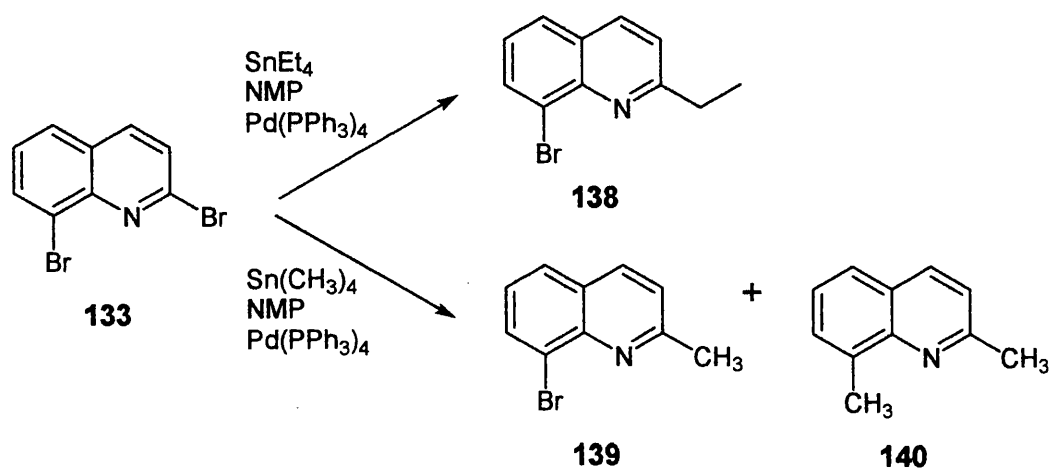
Scheme 46. Attempted synthesis of 8-bromo-2-((trimethylsilyl)ethynyl)quinoline **137**.

Our attention turned to the regioselective Stille coupling of 2,8-dibromoquinoline (Scheme 47). To our knowledge, there have only been a limited number of studies on the regioselective Stille coupling of quinoline derivatives. The coupling of compound **133** with one molar equivalent of tetraethylstannane was conducted using the standard protocol. The reaction was successful and gave the monocoupled product **138** in 50% yield. The ^1H NMR and HMBC analyses also indicated that the coupling reaction had not occurred in the 8-position and was selective for the 2-position.

The methodology was extended to investigate the Stille coupling of **133** with one molar equivalent of tetramethylstannane. Unfortunately, the lower steric bulk of the tetramethylstannane translated into a reduced discrimination between the C-2 and C-8 by the stannane and a mixture of the monocoupled **139** and disubstituted **140** products was obtained. Therefore, it appears that steric hindrance of the organostannane

reagent has a distinct effect on the success of the regioselective coupling reaction. Column chromatography failed to separate **139** from **140**.

According to the experimental results, the Suzuki-Miyaura coupling led to the highest regioselectivity. A similar finding was reported by Pereira *et al.*²²⁶ in the regioselective cross-coupling reactions with 2,3-dibromothiophene. They demonstrated that the Stille coupling of 2,3-dibromothiophene with various organostannanes was less convenient, since the disubstituted thiophenes were obtained in greater proportion than when using the Suzuki-Miyaura coupling. In addition, it was reported that the Sonogashira coupling reactions gave inconsistent results, depending on the structure of the alkyne nucleophile used in the coupling reaction.

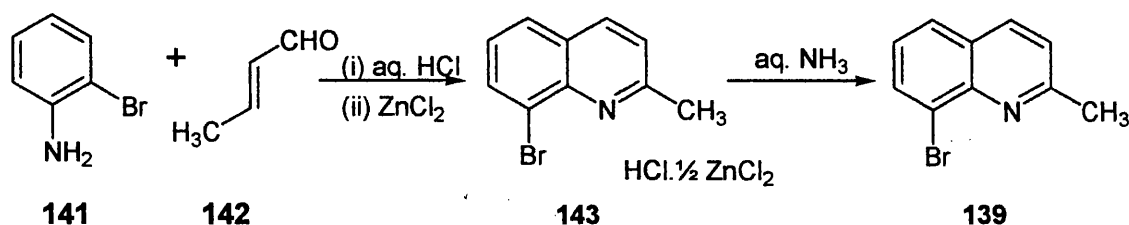


Scheme 47. Regioselective Stille coupling of 2,8-dibromquinoline **133** and organostannanes.

Due to the problems encountered in the Stille coupling reaction of **133** with tetramethylstannane an alternative strategy to provide 2-bromo-8-methylquinoline was explored. The Doebner-Miller reaction was chosen for the synthesis of **139** (Scheme 48). This method utilises a different mechanism to introduce the methyl substituent into the 2-position of the quinoline. The Doebner-Miller reaction, also known as the Skraup-Doebner-Miller quinoline synthesis, involves the reaction of an aniline with an α,β -unsaturated carbonyl to form a quinoline. The serious drawback of the Doebner-Miller reaction is that the acid-catalysed polymerisation of α,β -unsaturated aldehydes lowers the yield of the reaction and makes isolation of the products difficult. Leir²²⁷ designed an improved Doebner-Miller strategy for the synthesis of 8-bromo-2-methylquinoline, which involved the isolation of the quinoline derivative through a zinc chloride complex. Following the reported procedure, 2-bromoaniline **141** and *E*-but-2-enal **142** in 6 M

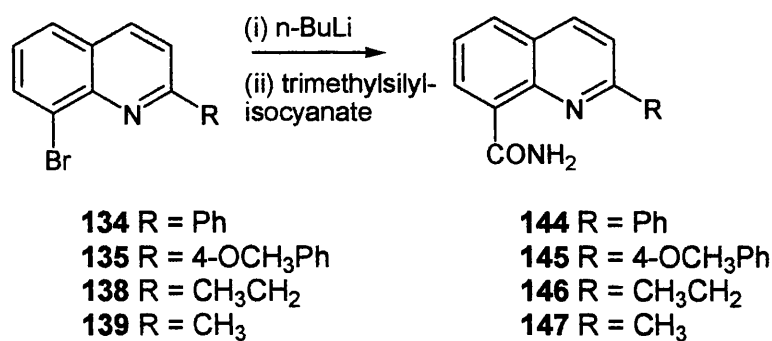
hydrochloric acid were heated under reflux for 1 h. After the Doebner-Miller reaction was complete, an equimolar amount of zinc chloride was added to the reaction mixture, affording **143** as a yellow precipitate. Treatment of **143** with aqueous concentrated ammonia gave the quinoline derivative **139** in 59% yield. The melting point of **139** matched the reported literature value.²²⁷ In the ¹H NMR spectrum of **139**, a singlet integrating for three protons was observed at δ 2.73 corresponding to the methyl group. In addition, the 3-H and 4-H were observed as doublets at δ 7.34 and δ 7.99, respectively, with a coupling constant of 8.2 Hz. Using the ¹H NMR spectrum of **139** it was possible to fully assign the ¹H NMR signals in 2,8-dimethylquinoline **140**.

Presumably, the Doebner-Miller process involves the Michael addition of the aniline **141** to α,β -unsaturated carbonyl **142** followed by cyclisation and aromatisation under acid-catalysed conditions.



Scheme 48. Synthesis of 8-bromo-2-methylquinoline **139**.

What remained to be done was to convert the 8-bromoquinoline derivatives into the corresponding quinoline-8-carboxamides. The 8-bromoquinoline derivatives **134**, **135**, **138**, and **139** were lithiated with *n*-BuLi and quenched with trimethylsilylisocyanate, yielding quinoline-8-carboxamides **144-147**. The synthetic route is illustrated in Scheme 49 and the results are collected in Table 13.



Scheme 49. Synthesis of 2-substituted quinoline-8-carboxamides.

In all experiments, the reaction time and equivalents of n-BuLi and trimethylsilyl-isocyanate reagents were kept constant (12 h, 1 equiv., 3 equiv., respectively). IR, NMR and MS data showed evidence for the formation of the carboxamide group in compounds **144-147**. Although the yields of the 2-substituted quinoline-8-carboxamides were moderate, the synthetic route only involved two steps from the starting 2,8-dibromoquinoline. The PARP-1 inhibitory activity of these compounds was compared with the activity of the 3-substituted quinoline-8-carboxamide series and the results are discussed in Section 4.1.2.

Table 13. Yields of 2-aryl and 2-alkyl substituted quinoline-8-carboxamides.

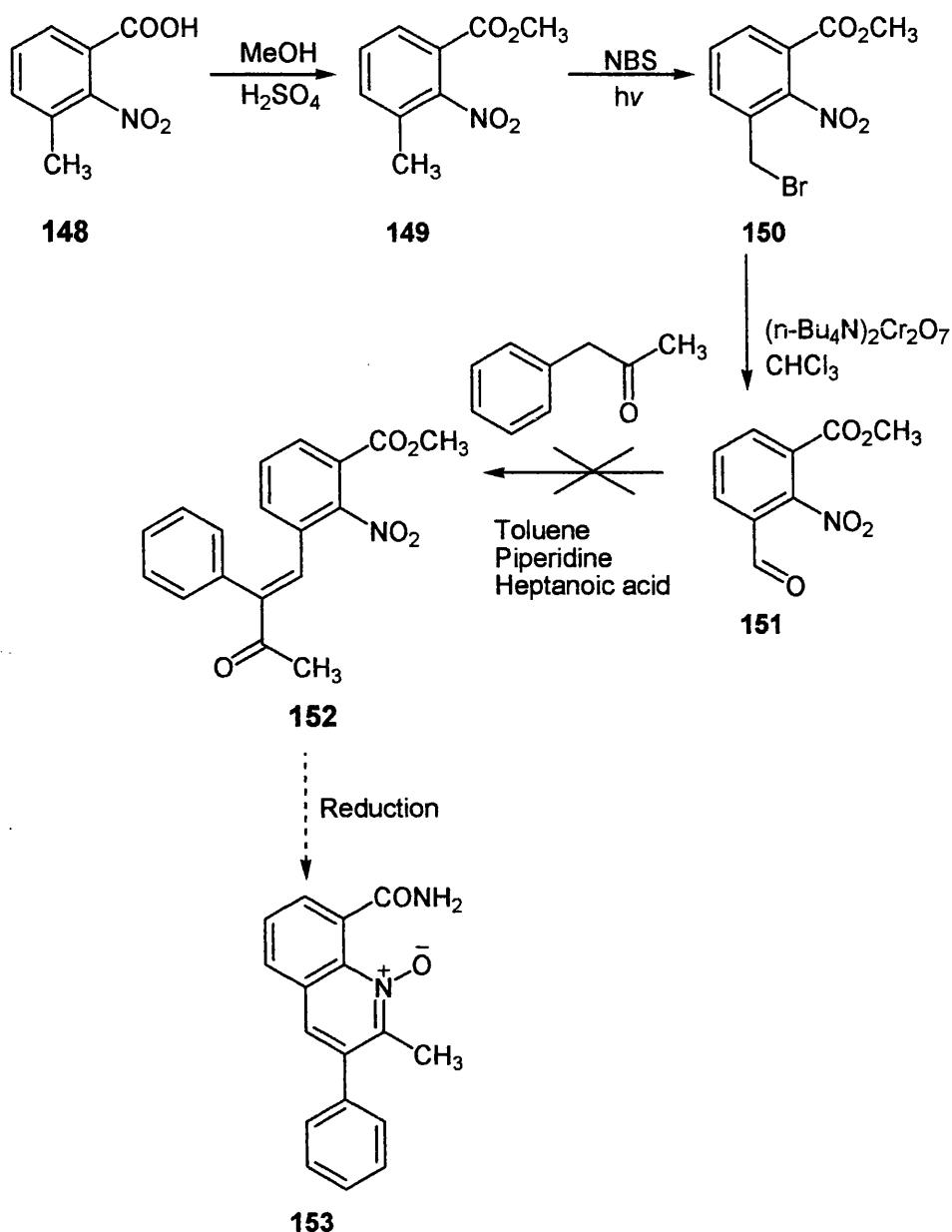
Compound	Yield of products (%)
144	34
145	43
146	43
147	52

3.6 Quinoline-8-carboxamide N-oxides

Quinoline-N-oxides can be prepared by the direct N-oxidation of the quinoline nitrogen or by a cyclisation reaction involving the formation of the quinoline ring containing the N-oxide group. A cyclisation method was considered to be the most appropriate strategy to the synthesis of substituted quinoline-8-carboxamide-1-oxides. It was thought that direct oxidation of quinoline-8-carboxamide may be impeded by the presence of the intramolecular hydrogen bond which was a designed part of the pharmacophore.

3.6.1 Attempted synthesis of quinoline-N-oxides *via* reductive cyclisation of (*E*)-methyl 2-nitro-3-(3-oxo-2-phenylbut-1-enyl)benzoate

One original aim of the project was to synthesise substituted quinoline-8-carboxamides and their corresponding N-oxides. One possible route to the formation of substituted quinoline-8-carboxamide-1-oxides is shown in Scheme 50. The first stage in the synthesis involved the esterification of the starting material 3-methyl-2-nitrobenzoic acid **148** to give the methyl ester **149** in 56% yield. Söderberg *et al.*²²⁸ prepared 2-methyl-1-nitrobenzenes *via* a radical bromination reaction. In the present work, bromination of **149** with NBS, light and a radical initiator gave the product **150**. Attempts to oxidise **150** to the aldehyde **151** with DMSO and mild base in a Swern-like oxidation failed. It was thought that the failure of the reaction might have been due to the hydrolysis of the ester group in the starting material. Mohan *et al.*²²⁹ demonstrated that α -bromo-2-nitro-4-methoxytoluene could be oxidised to 2-nitro-4-methoxybenzaldehyde by a 10-minute exposure to tetrabutylammonium dichromate. The direct oxidation of **150** using tetrabutylammonium dichromate was successful. TLC analysis showed the disappearance of the bromo starting material after 1 h, and the ¹H NMR spectrum showed the presence of a CHO signal at δ 9.90 indicating the formation of the product **151**. However, problems were encountered in the work-up of compound **151**, and eliminating the tetrabutylammonium salts by filtering through silica proved difficult. This may explain the low yield obtained for compound **151**. Condensation of the aldehyde **151** with an aliphatic ketone under basic conditions should give the enone **152**. Baik *et al.*²³⁰ showed that reduction of 2-nitrocinnamaldehyde with bakers' yeast and sodium hydroxide and subsequent cyclisation formed the quinoline-N-oxide. We proposed that reduction of the nitro group in compound **152** to the hydroxylamine using bakers' yeast and subsequent cyclisation should give the N-oxide **153**. This route has the advantage of introducing diversity late in the sequence.



Scheme 50. Attempted synthesis of substituted quinoline-8-carboxamide-1-oxides.

Abramovitch *et al.*²³¹ reported that the condensation reaction of 1-phenylpropan-2-one with benzaldehyde in the presence of piperidine and heptanoic acid took place at the methylene group *i.e.*, through the thermodynamic enolate. It was thought that these reaction conditions might have an application in the synthesis of enone **152**. Aldehyde **151** was treated with methyl benzyl ketone, piperidine and heptanoic acid in toluene. The reaction mixture was heated at 80°C for 24 h. However, only unreacted starting material was recovered from the reaction. It is speculated that the hindered nature of both the ketone nucleophile and aldehyde **151** prevented the condensation reaction.

Due to the failure of this reaction it was decided not to progress any further with this route.

3.6.2 Attempted syntheses of 8-carbamoylquinoline-1-oxide by direct N-oxidation

The failure of the cyclisation reaction to afford substituted quinoline-8-carboxamide-1-oxides led us to investigate methods that would oxidise the N-heterocyclic aromatic system directly. Several oxidising reagents are available for the N-oxidation of N-heterocyclic compounds. Hydrogen peroxide and *m*-chloroperoxybenzoic acid (MCPBA) are the most commonly used reagents. Such peracid-based methods are very reliable for many N-heterocyclics, but usually less so for electron-deficient ones. N-Oxidation of N-heterocyclic compounds that are deactivated by the presence of electron-withdrawing groups usually requires the use of strong oxidants. The hydrogen peroxide urea complex, normally called urea-hydrogen peroxide (UHP), is commercially available and has been successfully employed for the N-oxidation of very deactivated substrates, including heterocyclic quinoline.²³² Zhong *et al.*²³³ have also demonstrated that substituted pyridines could be converted to their corresponding N-oxides using trichloroisocyanuric acid [1,3,5-trichloro-1,3,5-triazine-2,4,6-(1H,3H,5H)-trione] in acetonitrile.

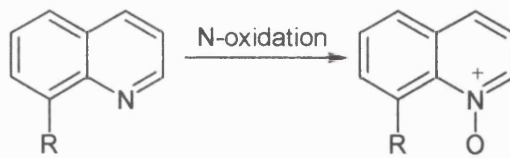
We decided to investigate the following methods for the N-oxidation of various 8-substituted quinoline derivatives.

- **Method A-** 30% Aqueous hydrogen peroxide and acetic acid, reflux, 5 h.
- **Method B-** Trifluoroacetic anhydride (TFAA), urea hydrogen peroxide, Na₂CO₃ in DCM, reflux, 24 h.
- **Method C-** MCPBA in CHCl₃, rt, 24 h.
- **Method D-** Trichloroisocyanuric acid, acetic acid and sodium acetate in acetonitrile.

The results of the N-oxidation experiments are reported in Table 14. As a model, initial attempts involved the oxidation of quinoline-8-carboxamide. However, neither method A or B yielded the corresponding N-oxide. It is proposed that the failure of the reaction was due to deactivation by the very strong hydrogen bond to the pyridine nitrogen which was a designed part of the pharmacophore. Both methods A and B oxidised unsubstituted quinoline to give quinoline-1-oxide **154**. In the ¹H NMR spectrum of quinoline, the 8-H signal was observed at δ 7.70 whereas, in quinoline-1-oxide, the 8-H

signal moved sharply downfield to δ 8.71. This was due to the deshielding effect of the adjacent oxygen.

Table 14. Attempted N-oxidations of 8-substituted quinoline. (-) denotes unsuccessful attempts.



Compound number	R	Method ^a	Yield of products(%)
-	CONH ₂	A	-
		B	-
-	CN	B	-
		C	-
		D	-
-	Br	B	-
154	H	A	26
154	H	B	62

^a Method A = H₂O₂, AcOH; Method B = UHP, TFAA, Na₂CO₃, DCM; Method C = MCPBA, CHCl₃; Method D = Trichloroisocyanuric acid, AcOH, NaOAc, MeCN.

Our attention was then focused on the N-oxidation of quinoline derivatives that contained a functional group in the 8-position which could easily be converted to the corresponding carboxamide. The presence of electron-withdrawing substituents in the 8-position of the quinoline ring proved detrimental to the N-oxidation reaction. This was illustrated by the failure of the N-oxidation reaction for the substrates 8-bromoquinoline and quinoline-8-carbonitrile. These results support the findings by Fieser *et al.*²³⁴, who reported that N-oxides of quinoline derivatives could not be obtained with peracids or hydrogen peroxides, due to the low basicity of the nitrogen atom. In fact, a literature search demonstrated that N-oxides of quinoline and isoquinoline have usually been obtained through N-oxidation of precursors having electron-releasing substituents in the 5- or 8-position. It soon became apparent that the N-oxidation of 8-substituted quinoline derivatives was going to be a major challenge.

8-Hydroxyquinoline-1-oxide **155** is commercially available and it was proposed that this compound would make an ideal precursor for the synthesis of 8-carbamoylquinoline-1-oxide. However, treatment of compound **155** with trifluoromethanesulfonic anhydride

and pyridine failed to give the triflate **156** and only unreacted starting material was recovered from the reaction. Further reaction at the 8-position was planned to give the nitrile **157** and finally the carboxamide **158** (Scheme 51).

Consequently, an alternative route was proposed. Ukai *et al.*²³⁵ claimed that (1-oxidoquinolin-8-yl)mercury(II) chloride could be converted to 8-bromoquinoline-1-oxide by reaction with potassium bromide and bromine. We proposed that treatment of 8-bromoquinoline-1-oxide with CuCN, DPPF, and Pd₂(dba)₃ should give the nitrile **157**, and finally the corresponding carboxamide **158**.

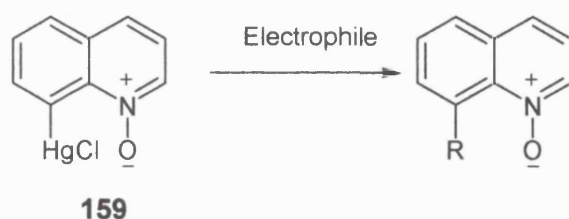
Mercuration at the 8-position of quinoline was achieved by treatment of quinoline-1-oxide **154** with mercury(II) acetate and sodium chloride in acetic acid. The mercurial **159** was obtained in 86% yield. Electrophilic substitution of the chloromercuri group by bromine gave 8-bromoquinoline-1-oxide **160** in 2% yield (Table 15). In performing the experiment, we noticed that no by-products were recovered from the reaction, suggesting that the low yield might be due to difficulties in the isolation of **160**. It should be noted that both the starting material **159** and product **160** demonstrated poor solubility in most organic solvents and water. However, it was possible to dissolve compound **160** in (CD₃)₂SO and this allowed for an NMR spectrum to be taken. In the ¹H NMR spectrum, the 2-H signal was observed downfield at δ 9.03 due to the deshielding effect of the adjacent N-oxide group. Therefore, due to the solubility issues encountered in the bromination reaction we decided to use a different approach. It was found that the mercurial **159** was readily soluble in the highly polar aprotic solvent NMP. The mercurial **159** was treated with one equivalent of iodine in NMP. Due to the high boiling point of the solvent a Kugelrohr distillation apparatus was required to remove any residual NMP. 8-Iodoquinoline-1-oxide **161** was obtained in 44% yield. The molecular formula of **161** was derived as C₉H₇INO from the EI mass spectrum (*m/z* = 271.9567 M+H).

8-Iodoquinoline-1-oxide **161** was treated with CuCN, Pd₂(dba)₃, and DPPF in 1,4-dioxane. A TLC analysis indicated the formation of numerous products, none of which could be isolated by column chromatography. It is believed that the N-oxide **161** may poison the palladium catalyst, thus preventing the cyanation reaction from taking place.

We decided to re-examine the use of (1-oxidoquinolin-8-yl)mercury(II) chloride **159** as a precursor to the formation of 8-carbamoylquinoline-1-oxide. It is known that organo-metallic compounds can be converted to ketones, aldehydes, carboxylic acids and

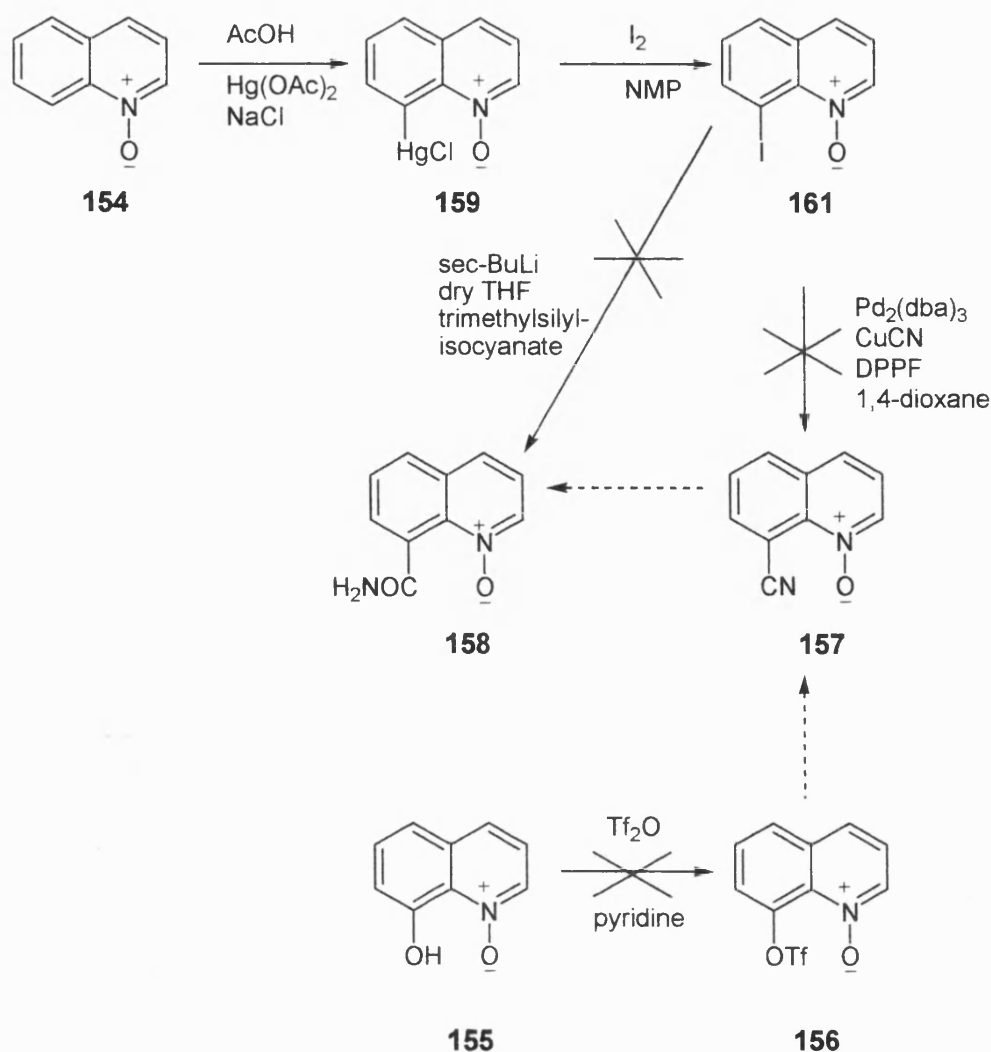
esters by treatment with an appropriate carbon electrophile. In an alternative route, it was decided to investigate the reaction of **159** with various electrophiles. Acylation of **159** with phenylchloroformate failed to give 8-(phenoxy carbonyl)quinoline-1-oxide and only unreacted starting material was recovered. In addition, both the more reactive 4-nitrophenyl chloroformate and cyanogen bromide electrophiles failed to react with the mercurial **159** in NMP (Table 15).

Table 15. Reaction of (1-oxidoquinolin-8-yl)mercury(II) chloride with various electrophiles. (-) denotes unsuccessful attempts.



Compound number	R	Reaction conditions	Yield of products (%)
160	Br	Br ₂ , KBr, rt	2
161	I	I ₂ , NMP, rt	44
-	CN	BrCN, NMP, rt	-
-		phenyl chloroformate, NMP, rt	-
-		4-nitrophenyl chloroformate, NMP, rt	-

An alternative strategy to introduce the carboxamide group into the 8-position without affecting the N-oxide group was also considered. It was proposed that metal-halogen exchange of **161** and treatment with trimethylsilylisocyanate might afford 8-carbamoylquinoline-1-oxide. Disappointingly, treatment of **161** with *n*-BuLi in THF and quenching with trimethylsilylisocyanate resulted in the formation of a complex mixture. This could be due to the competition of metallation at the C-8 position, reduction of the C-I bond, and addition of *n*-BuLi to the quinoline ring.²³⁶ The use of *sec*-BuLi as the lithiating reagent also resulted in the formation of complex mixtures.



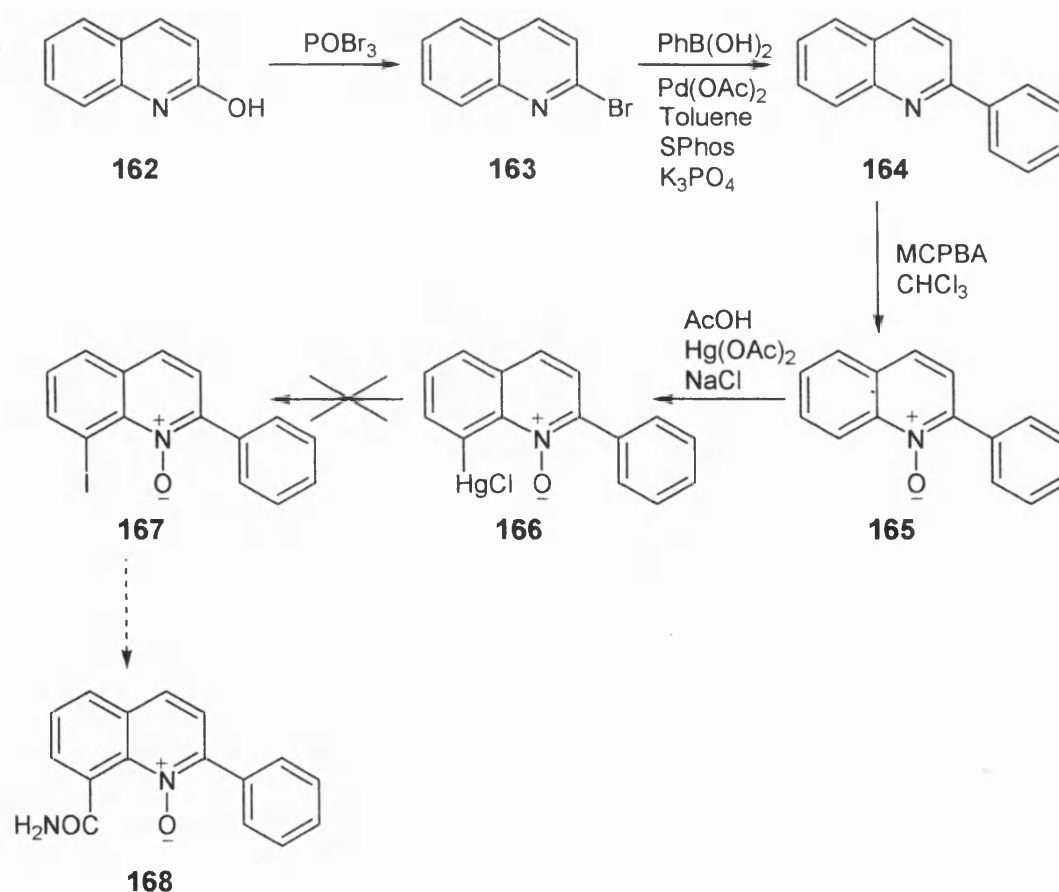
Scheme 51. Attempted syntheses of 8-carbamoylquinoline-1-oxide **158**.

Overall, we have demonstrated that the direct N-oxidation of 8-substituted quinoline derivatives was not a feasible strategy for the synthesis of 8-carbamoylquinoline-1-oxide. In addition, owing to the solubility problems encountered with (1-oxidoquinolin-8-yl)mercury(II) chloride **159** and 8-iodoquinoline-1-oxide **161** it was decided to abandon the synthesis of 8-carbamoylquinoline-1-oxide **158**.

3.6.3 Attempted synthesis of 8-carbamoyl-2-phenylquinoline-1-oxide

Our attention was directed to the synthesis of 2-substituted quinoline-1-oxides. As previously demonstrated the N-oxidation of quinolines is normally inhibited by the presence of bulky or electron-withdrawing substituents in the 8-position, so we decided to design a route in which the 2-substituent was present in the oxidation step but the 8-position contained only hydrogen. It was hoped that the introduction of a 2-substituent

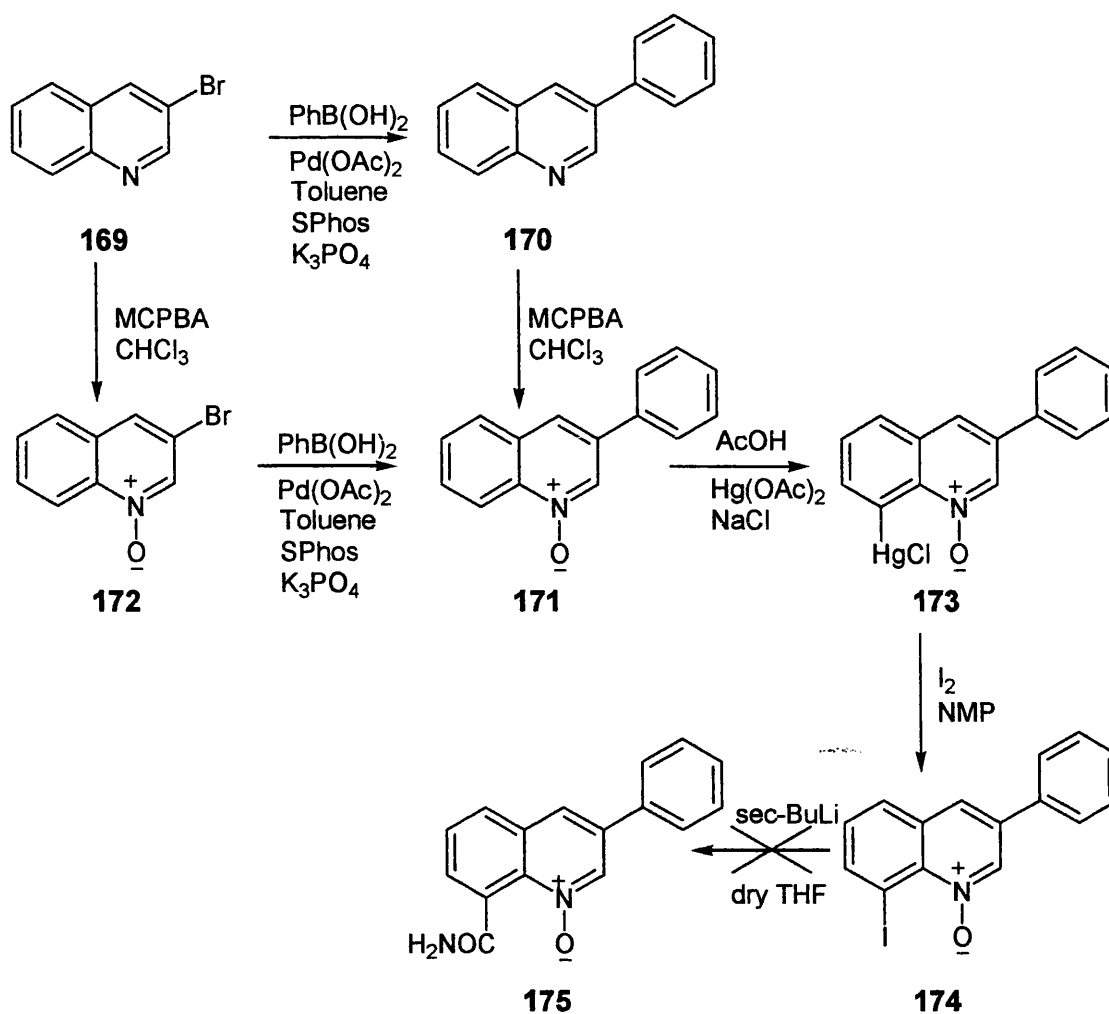
might also improve the solubility and reactivity of the mercurial precursor towards the synthesis of 8-carbamoyl-2-phenylquinoline-1-oxide **168**. A synthetic strategy for the preparation of compound **168** is outlined in Scheme 52. Quinoline-2-one **162** is a cheap and commercially available material and is the starting point in the synthesis of **168**. Treatment of compound **162** by treatment with POBr_3 gave 2-bromoquinoline **163** in 34% yield. A phenyl substituent was added into the 2-position *via* the Suzuki-Miyaura coupling of **163** with phenylboronic acid, giving **164** in excellent yield. The ^1H NMR spectrum and melting point data for compound **164** matched those reported in the literature.²³⁷ N-Oxidation of **164** with MCPBA gave 2-phenylquinoline-1-oxide **165** in 87% yield. Mercuration of compound **165** with mercury(II) acetate and sodium chloride afforded the chloromercuri compound **166**. In the ^1H NMR spectrum of compound **165**, the 7-H signal was evident at δ 7.94 whereas in the mercurial **166** the 7-H signal moved sharply downfield to δ 8.64. In the next stage of the reaction, the mercurial **166** was treated with one equivalent of iodine in NMP. Unfortunately, despite multiple attempts, only unreacted starting material was obtained from the reaction.



Scheme 52. Attempted synthesis of 8-carbamoyl-2-phenylquinoline-1-oxide **168**.

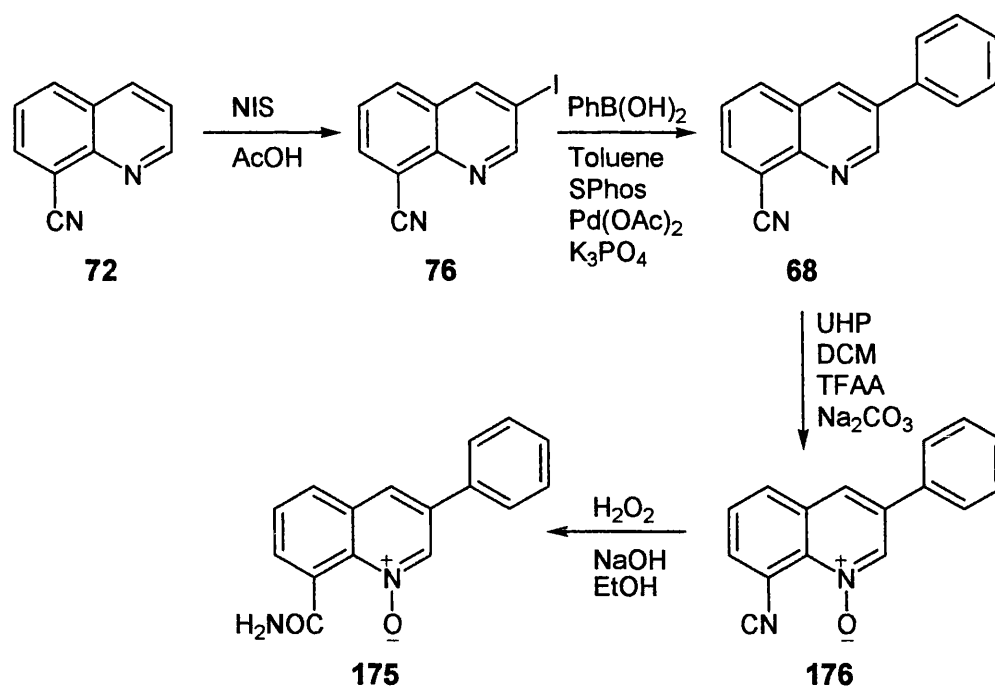
3.6.4 Synthesis of 8-carbamoyl-3-phenylquinoline-1-oxide

Simultaneous efforts were directed to the synthesis of 8-carbamoyl-3-phenylquinoline-1-oxide. The initial approach to the synthesis of 8-carbamoyl-3-phenylquinoline-1-oxide is outlined in Scheme 53. 3-Phenylquinoline-1-oxide **171** was synthesised from commercially available 3-bromoquinoline in two steps. Suzuki-Miyaura coupling of 3-bromoquinoline **169** with phenylboronic acid gave **170** in 75% yield. Subsequent N-oxidation of 3-phenylquinoline provided **171** in 22% yield. In an attempt to improve the yield of 3-phenylquinoline-1-oxide the first two steps in the synthetic strategy were reversed. N-Oxidation of 3-bromoquinoline with MCPBA gave 3-bromoquinoline-1-oxide **172** in 75% yield. A cross-coupling reaction was then carried out between compound **172** and phenylboronic acid affording **171** in 74% yield. The second approach has the advantage that it allows diversification at a later stage in the synthesis. Treatment of **171** with mercury(II) acetate and sodium chloride gave **173** in 75% yield. Replacement of the chloromercuri group in **173** by iodine gave 8-iodo-3-phenylquinoline-1-oxide **174** in 43% yield. Evidence to support the formation of **174** was provided by mass spectrometry. In the ES mass spectrum a signal corresponding to **174** ($m/z = 347.9869$ M+H) was observed, and loss of iodine gave an ion at 221. However, treatment of **174** with *sec*-BuLi and quenching with trimethylsilylisocyanate failed to give the N-oxide **175** and the ^1H NMR spectrum only indicated the presence of starting material, suggesting that the intermediate (1-oxido-3-phenylquinolin-8-yl)lithium had not formed. In addition, solubility problems were encountered with the use of dry THF as the solvent and this may have contributed to the failure of the lithiation reaction.



Scheme 53. Attempted synthesis of 8-carbamoyl-3-phenylquinoline-1-oxide **175**.

Finally, we turned to the direct N-oxidation of 3-phenylquinoline-8-carbonitrile as a promising alternative to the synthesis of 8-carbamoyl-3-phenylquinoline-1-oxide (Scheme 54). We have previously reported the synthesis of 3-phenylquinoline-8-carbonitrile **68** in Section 3.2.2. However, due to the problems encountered with the Sandmeyer reaction it was decided to use an alternative method to synthesise compound **68**. Iodination of quinoline-8-carbonitrile **72** with NIS gave 3-iodoquinoline-8-carbonitrile **76** in 35% yield. Suzuki-Miyaura coupling of **76** with phenylboronic acid gave 3-phenylquinoline-8-carbonitrile **68** in 86%.



Scheme 54. Synthesis of 8-carbamoyl-3-phenylquinoline-1-oxide **175**.

Jain *et al.*²³⁸ reported that sodium peroxycarbonate is an efficient oxygen source for the oxidation of tertiary nitrogen compounds to N-oxides in the presence of catalytic amounts of methyltrioxorhenium (MTO). Interestingly, they reported the synthesis of 4-cyanopyridine N-oxide and quinoline-1-oxide in excellent yields. It was proposed that similarly, it might be possible to oxidise 3-phenylquinoline-8-carbonitrile directly with sodium peroxycarbonate and MTO. However, following treatment with sodium peroxycarbonate and MTO, the ¹H NMR spectrum indicated that only unreacted starting material was present. Oxidation of 3-phenylquinoline-8-carbonitrile with MCPBA also proved unsuccessful and only unreacted starting material was recovered, even after prolonged treatments.

Treatment of compound **68** with urea hydrogen peroxide, sodium carbonate, TFAA in dichloromethane, according to the procedure reported by Phillips,²³⁹ gave 8-cyano-3-phenylquinoline-1-oxide **176** in a low yield. Even after prolonged reaction times and after addition of fresh reagents, yields were still low ranging from 10-14%. However, unreacted starting material could be recovered and was re-used in subsequent reactions. In the ES mass spectrum a signal corresponding to **176** ($m/z = 247.0865$ M+H) was observed, and loss of oxygen gave an ion at 231. In the ¹H NMR spectrum of 3-phenylquinoline-8-carbonitrile **68** the 2-H signal was observed at δ 9.34 whereas in the N-oxide **176** the 2-H signal shifted upfield to δ 8.83. An upfield shift of similar magnitude was also found for the 2-H signal upon N-oxidation of quinoline to quinoline-

1-oxide **154** (Section 3.6.2). In addition, the 4-H signal shifted upfield in the N-oxide **176** by δ 0.45. The ^{13}C NMR spectrum assignments for compounds **68** and **176** were achieved on the basis of HMBC experiments and comparison of the chemical shifts. The N-Oxidation reaction resulted in a significant upfield shift of most of the carbons. However, the 2-C signal deserves particular attention, due to the strong shielding that it undergoes upon N-oxidation. Oxidation of **68** to **176** causes an upfield shift of the 2-C signal from δ 152.1 to δ 139.0 (Figure 17). It also appears that the oxidation of **68** to **176** results in an increase in the π electron density at the 4-carbon centre, thereby shifting the 4-C signal upfield by δ 10.4.

Finally, treatment of 8-cyano-3-phenylquinoline-1-oxide **176** with sodium hydroxide and hydrogen peroxide gave the target compound **175** in 14% yield. Even though a low yield of the N-oxide was obtained the purification of the N-oxide only required the separation of the product from the unreacted starting material. It was thought that the time period of the reaction was insufficient for the hydration of nitrile **176** to the carboxamide **175** to take place. In an attempt to increase the yield of compound **175**, the reaction time was extended to 2 h. However, increasing the reaction time resulted in the formation of 3-phenylquinoline-8-carboxamide. This suggests that the optimum reaction time was in fact 1 h and at a longer reaction period the N-O bond of the N-oxide **175** was cleaved.

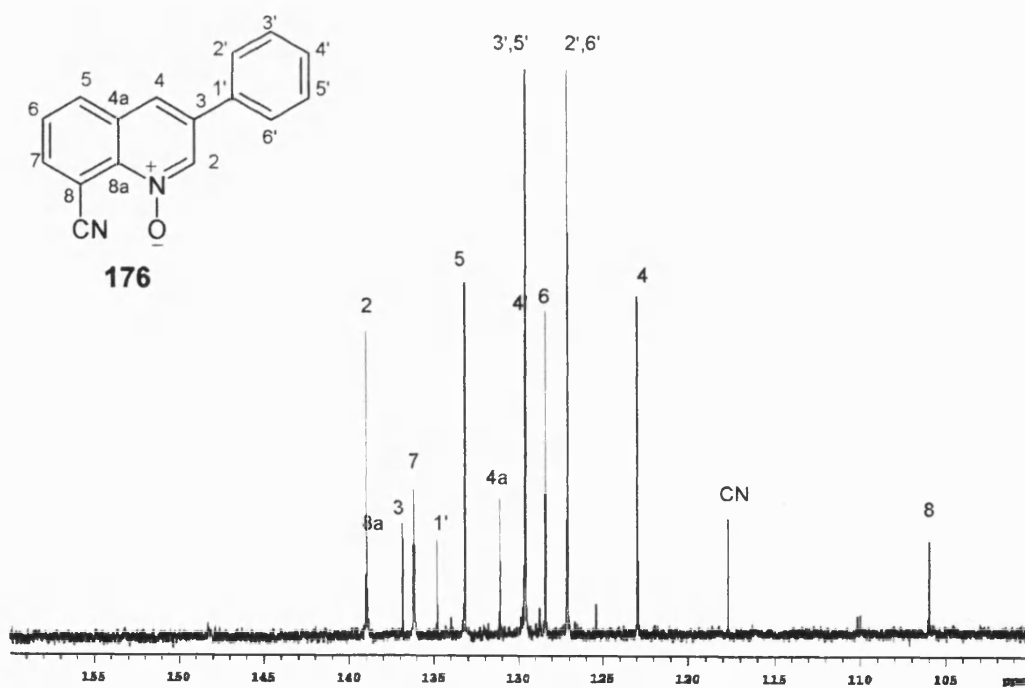
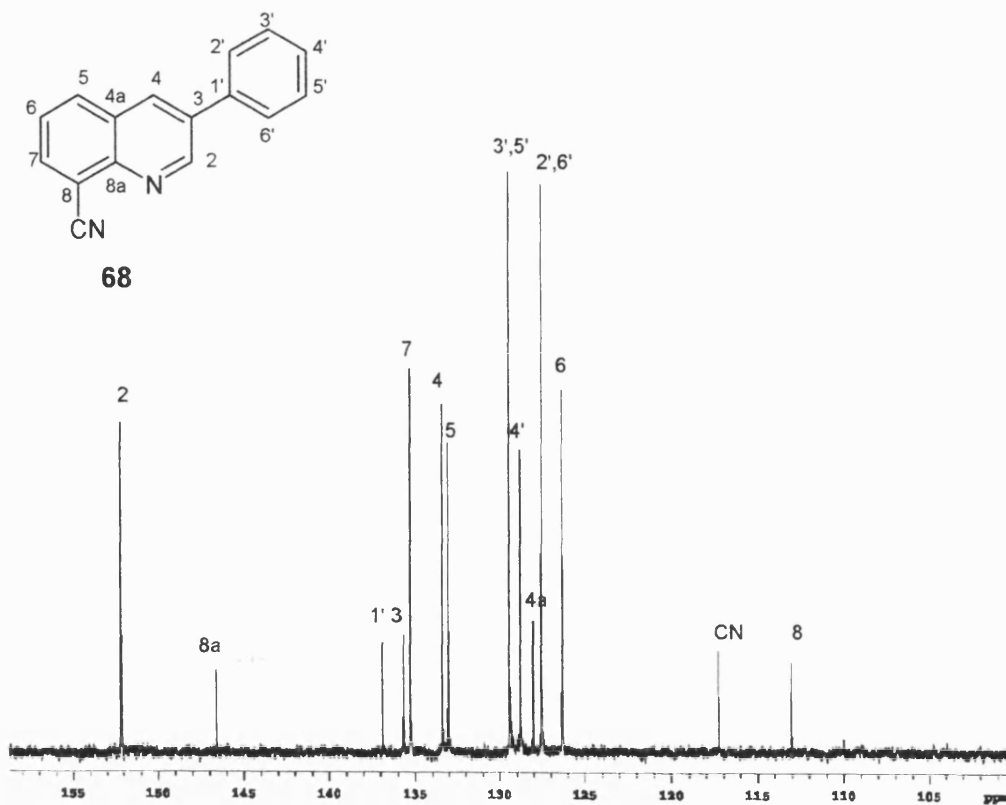


Figure 17. Assignment of ^{13}C NMR signals of 3-phenylquinoline-8-carbonitrile, **68** (top), and its N-oxide **176** (bottom).

The structure of 8-carbamoyl-3-phenylquinoline-1-oxide **175** was characterised by ^1H NMR, ^{13}C NMR, HMQC, HMBC, MS, and CHN analyses. In the ^{13}C NMR spectrum the presence of a peak at δ 170.4 provides evidence for the formation of the carboxamide moiety. In our original research proposal we hypothesised that in the presence of the N-oxide moiety the carboxamide would be tipped out of plane. The carbonyl out of plane should disrupt the pharmacophore required for PARP-1 inhibitory activity.

We have previously demonstrated that the carboxamide moiety is held in a restricted conformation in quinoline-8-carboxamide derivatives (Section 3.2.2). ^1H NMR studies showed that when the carboxamide was in plane, one of the N-H was found to be hydrogen-bonded resulting in the signal being of a low field. The majority of the quinoline-8-carboxamide derivatives previously studied also demonstrated good solubility in many organic solvents and CDCl_3 was predominantly chosen as the NMR solvent. Unfortunately, the N-oxide **175** was not readily soluble in CDCl_3 so $(\text{CD}_3)_2\text{SO}$ was used as the solvent. For comparison, it was decided to obtain a ^1H NMR spectrum of 3-phenylquinoline-8-carboxamide **69** in $(\text{CD}_3)_2\text{SO}$. Significant differences were noticed between the ^1H NMR data of compounds **69** and **175**. For example, in compound **69** the 2-H signal was evident at δ 9.41, whereas in the N-oxide **175** the 2-H signal was evident at δ 8.92, providing evidence that the presence of an N-O moiety induces a sizeable perturbation to the chemical shift of the 2-H signal of the quinoline ring system. The proton chemical shift of the 2-H signal of **175** was assigned easily as it appears at a lower field due to the adjacent pyridine nitrogen. The location of the 2-H was confirmed by a two-dimensional HMBC spectrum. We found that the 2-H signal at δ 8.82 had 3J -HMBC correlations with 4-C (δ 122.2), 1'-C (δ 135.2) and 8a-C (δ 136.2). The 4-H signal at δ 8.31 displayed 3J -HMBC correlations with 2-C (δ 134.4), 1'-C (δ 135.2) and 5-C (δ 129.7). Also the 5-H signal at δ 8.13 demonstrated a 3J -HMBC correlation with 7-C (δ 130.9) and a 2J -HMBC correlation with 6-C (δ 128.7). In the same manner the chemical shifts in the phenyl ring were assigned. In this case, the 2',6' aromatic protons were coupled to 3-C (δ 134.2) and 4'C (δ 131.8). The 3',5' aromatic protons resonated as two-proton triplet at δ 7.56 which correlated with the 1'-C (δ 135.2). On the other hand, the signals of the quaternary carbons 4a-C and 8-C were too weak and could not be assigned unambiguously.

In this section of the project, we found that 8-carbamoyl-3-phenylquinoline-1-oxide could be obtained by the hydration of 8-cyano-3-phenylquinoline-1-oxide. Therefore, we have successfully designed a synthetic route to the preparation of 3-substituted quinoline-8-carboxamide-1-oxides. Regrettably, we were not able to introduce a variety of substituents into the 3-position due to the shortage in time. However, it is proposed that in the synthetic route outlined in Scheme 54 the phenylboronic acid could easily be replaced by alternative aryl substituents to give a library of 3-substituted quinoline-8-carboxamide-1-oxides. The next stage in the project was to evaluate the PARP-1 inhibitory activity of the N-oxide **175** and the results are discussed in Section 4.1.3. Molecular modelling studies were also carried out to investigate the conformation of the N-oxide **175** and the results are presented in Section 5.3.

4. Biological Evaluation

4.1 PARP-1 activity assay

A number of assay methods have been developed for the identification of inhibitors of the enzyme PARP-1. Most commonly, PARP activity is monitored by radioactive methods using either ^{32}P - or ^3H -labelled NAD^+ .²⁴⁰ There are several disadvantages with this methodology, including the requirement of using radioactive reagents and the inefficiency of washing steps to remove any unincorporated radiolabelled NAD^+ from trichloroacetic acid (TCA) precipitates. In an alternative approach, ADP-ribose polymers, the products of the PARP-1 catalysed reaction, can be purified from cells by a tedious procedure involving boronate chromatography and the ADP-ribose polymers can be measured using HPLC analysis.²⁴¹

An ELISA PARP-1 assay has also been developed for the assessment of PARP-1 activation. This assay is more sophisticated than the standard radiolabelled methods and involves the detection of an antibody to poly(ADP-ribose).²⁴²

Recently, a novel colourimetric PARP-1 assay has been developed by Trevigen Inc. (Gaithersburg, USA) for the screening of potential PARP inhibitors. The assay is non-radioactive and utilises a novel substrate 6-biotin-17-nicotinamide-adenine-dinucleotide (biotinylated NAD^+) (Figure 18). We proposed that the commercially available colourimetric PARP-1 assay would be convenient for determining the PARP-1 activity of a selection of quinoline-8-carboxamide compounds *in vitro*. The assay takes advantage of the fact that the PARP-1 enzyme catalyses poly(ADP-ribosyl)ation of histone proteins in the presence of damaged DNA. The principles of the assay are as follows. Briefly, the test inhibitor is pre-incubated with the PARP-1 enzyme on a 96 strip-well plate coated with histone acceptor proteins. A PARP-cocktail reagent, containing biotinylated NAD^+ and activated DNA, is added to the wells to initiate the reaction. Upon activation, PARP-1 cleaves biotinylated NAD^+ into nicotinamide and biotinylated (ADP-ribose) and synthesises biotinylated (ADP-ribose) polymers covalently attached to the acceptor histone proteins. The extent of biotin incorporation is measured using a conjugated streptavidin detection system. The PARP-1 activity of the PARP-1 inhibitors is assessed on the basis of their inhibition of biotinyl-(ADP-ribose) incorporation.

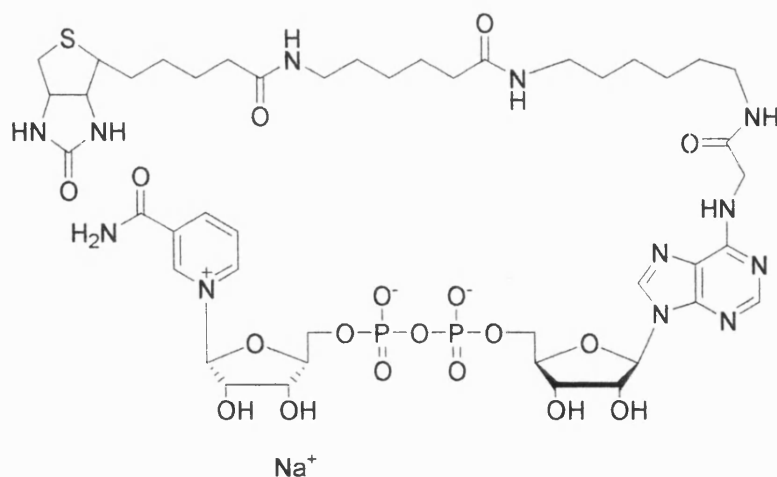


Figure 18. Structure of biotinylated NAD⁺.

Firstly, a standard curve using varying amounts of PARP-1 enzyme was produced for the biotinylated poly(ADP-ribose) polymerisation reaction. As shown in Figure 19, a linear relationship exists between the absorbance at 450 nm and the concentration of the PARP-1 enzyme. From the standard curve, it was established that 0.8 units of PARP-1 enzyme was sufficient to give an absorbance reading in the range of 2.0-2.5 in the absence of any inhibitor. In order to validate the assay, a negative control (no enzyme) was prepared to determine the background absorbance.

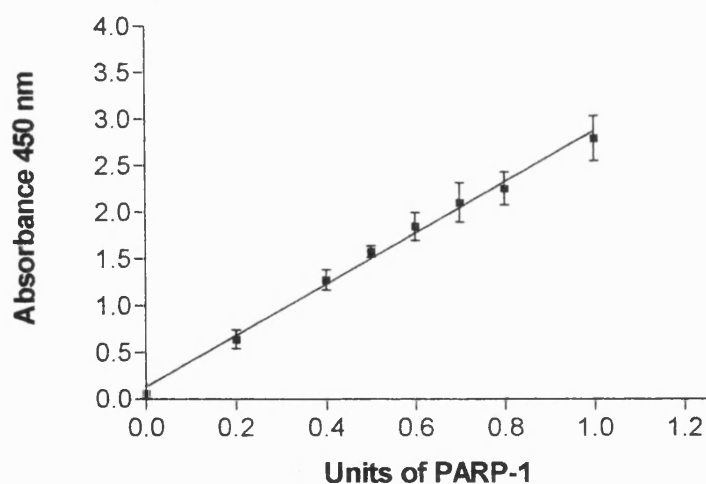


Figure 19. PARP-1 standard curve. Data are the mean of three experiments and are reported as mean \pm standard error of the mean (SEM).

4.1.1 Inhibition of PARP-1 activity by inhibitors

The inhibitory effects of 3-substituted and 2-substituted quinoline-8-carboxamides were examined using the colourimetric assay system. 5-AIQ was used as the benchmark inhibitor. In this evaluation, seven different final concentrations (100, 30, 10, 3, 1, 0.3, 0.1 μM) of each inhibitor were used. The presence of biotinylated poly(ADP-ribose) generated by PARP-1 during the ribosylation of histone proteins layered on the 96-well plate was detected using streptavidin horseradish peroxidase (Strep-HRP) and TACS Sapphire™. The TACS Sapphire™ substrate generates a soluble blue colour in the presence of Strep-HRP with a maximum absorbance of 630 nm. The development of the colourimetric reaction was terminated by addition of 0.2 M hydrochloric acid, generating a yellow colour with an absorption maximum at 450 nm. A representative colourimetric assay plate is shown in Figure 20.

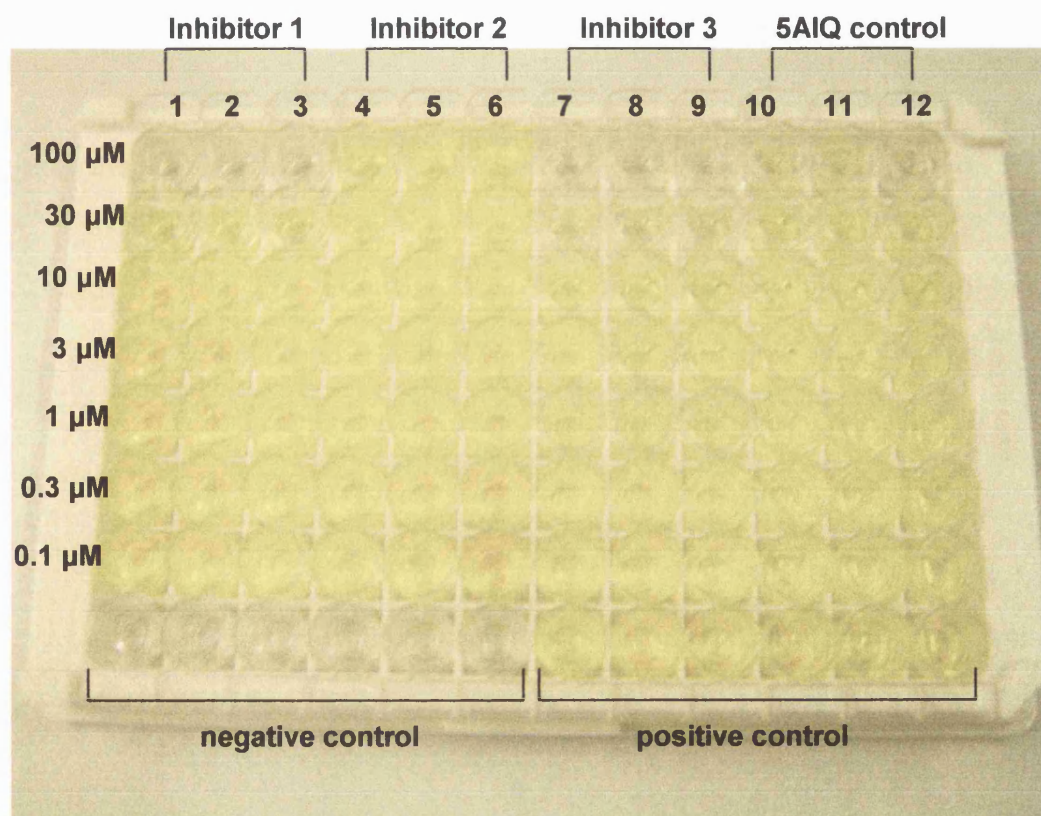


Figure 20. Colourimetric readout of PARP-1 activity assay. Inhibitors 3-phenylquinoline-8-carboxamide (lane 1-3), 8-carbamoyl-3-phenylquinoline-1-oxide (lane 4-6), 2-ethylquinoline-8-carboxamide (lane 7-9), 5-AIQ (lane 10-12) were tested in decreasing concentration starting with the highest concentration 100 μM at the top of the plate.

Determinations for each PARP-1 inhibitor were performed in triplicate and their mean IC_{50} values are summarised in Table 16. The complete results for the evaluation of quinoline-8-carboxamide compounds for activity in the colourimetric assay are contained in the Appendices.

The unsubstituted analogue quinoline-8-carboxamide **80**, which was also an intermediate in the synthesis, was tested for its effect on PARP-1 activity. The mean IC_{50} value of the inhibitor was estimated graphically from a plot of the \log_{10} [inhibitor] versus absorbance. 5-AIQ has previously been reported as a potent PARP-1 inhibitor and was contained in the assay for comparison purposes. Figure 21 shows the PARP-1 inhibition curves of quinoline-8-carboxamide and 5-AIQ. The inhibition calculated for quinoline-8-carboxamide **80** was 1.9 μM . This result demonstrates that quinoline-8-carboxamide is an excellent PARP-1 inhibitor and has comparable activity to 5-AIQ ($IC_{50}=1.8 \mu\text{M}$) using the colourimetric assay conditions.

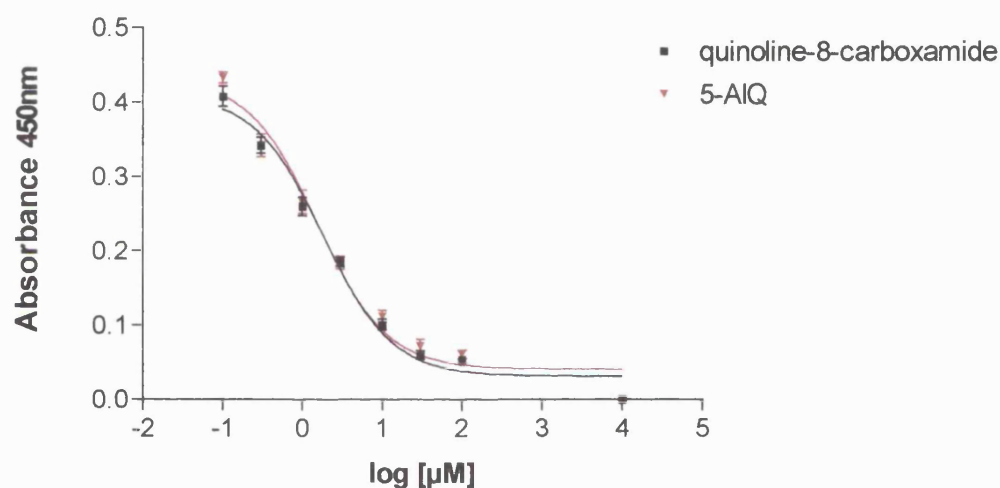
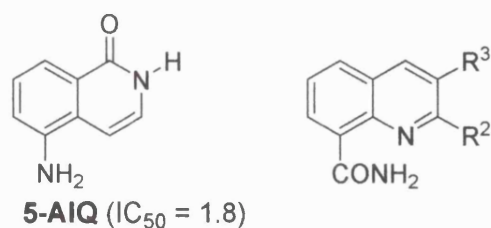


Figure 21. PARP-1 inhibition curves for quinoline-8-carboxamide **80** and 5-AIQ generated using the colourimetric assay, as described in the Experimental Section.

It should be noted that a direct comparison of inhibition constants (IC_{50} , K_i) from different laboratories should be undertaken with caution, since values for the same compound can vary, depending on the assay system employed. Suto *et al.*,¹²⁹ for instance, reported an IC_{50} value of 0.24 μM when 5-AIQ was evaluated using an *in vitro* cell-free preparation consisting of PARP-1 isolated from calf thymus. In contrast, using the PARP-1 colourimetric assay an IC_{50} value of 1.8 μM was obtained which is six-fold higher than the reported literature value. Nevertheless, the literature inhibition constants were used as a means of predicting general trends in PARP-1 activity.

Table 16. Inhibition of PARP-1 activity by quinoline-8-carboxamides and 5-AIQ control.



Compound number	R ²	R ³	IC ₅₀ (μM)	Log IC ₅₀ (μM) ^a
80	H	H	1.9	0.27 ± 0.11
69	H	Ph	15	1.17 ± 0.15
94	H	3-CF ₃ -Ph	52	1.71 ± 0.16
91	H	4-OMe-Ph	62	1.79 ± 0.15
93	H	4-Me-Ph	43	1.63 ± 0.25
98	H	4-CN-Ph	27	1.43 ± 0.14
144	Ph	H	0.9	-0.06 ± 0.33
145	4-OMe-Ph	H	1.1	0.03 ± 0.13
123	H	Et	3.7	0.57 ± 0.05
106	H	Me	3.4	0.53 ± 0.08
111	H	H ₂ C=CH	5.8	0.76 ± 0.07
114	H	HC≡C	2.3	0.36 ± 0.17
107	H	MeC≡C	2.2	0.34 ± 0.10
147	Methyl	H	0.5	-0.30 ± 0.08
146	Et	H	0.8	-0.09 ± 0.10

^a Data are the mean of three experiments and are reported as mean ± standard error of the mean (SEM).

4.1.2 Structure activity relationship (SAR) studies of 3-substituted and 2-substituted quinoline-8-carboxamides as PARP-1 inhibitors

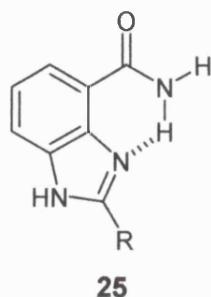
Initially, we decided to investigate the effect of introducing aryl substituents into the 3- and 2-positions of quinoline-8-carboxamide. 3-Phenylquinoline-8-carboxamide **69** was the first compound to be synthesised. The IC_{50} value determined for compound **69** was 15 μ M showing it to be a moderate PARP-1 inhibitor in comparison to the parent quinoline-8-carboxamide **80** (IC_{50} = 1.9 μ M). A series of 3-arylquinoline-8-carboxamides was therefore synthesised to enable the SAR for substituents on the phenyl ring to be explored. A number of substituents, with differing electronic properties were introduced at the 3-position. The results indicated that the introduction of *para* substituents into the phenyl group of 3-phenylquinoline-8-carboxamide was detrimental to PARP-1 inhibitory activity. 3-(4-Methoxyphenyl)quinoline-8-carboxamide **91** was >4 fold less active than compound **69**, suggesting that steric bulk and electron-donating groups in the 3-position are not well tolerated in the enzyme active site. Similarly, 3-(4-methylphenyl)quinoline-8-carboxamide **93** showed poor PARP-1 inhibitory activity.

Griffin and co-workers¹⁷⁰ reported a series of potent PARP-1 inhibitors based on a related benzimidazole scaffold. SAR studies indicated that various aryl substituents were well tolerated in the 2-position of the benzimidazole-4-carboxamides. They reported PARP-1 inhibitory activity at nanomolar concentrations. In contrast to our findings, Griffin and co-workers¹⁷⁰ demonstrated that the presence of *para* substituents on the phenyl group of the 2-phenyl-1*H*-benzimidazole-4-carboxamides, such as cyano, hydroxy, methoxy and trifluoromethyl (compounds **25d**, **25g**, **25h** and **25i**) markedly increased inhibitory potencies. It was also reported that 2-(3-trifluoromethylphenyl)-1*H*-benzimidazole-4-carboxamide **25j** was well tolerated in the active site and was found to be 2-fold more potent than 2-phenyl-1*H*-benzimidazole-4-carboxamide **25c**.

Interestingly, the introduction of a trifluoromethylphenyl group into the 3-position of quinoline-8-carboxamide resulted in loss of potency, as demonstrated by compound **94**, which was >3 fold less potent with respect to compound **69**. This result suggests that the NAD^+ binding pocket is limited in size at the 3-position. 3-(4-Cyanophenyl)-quinoline-8-carboxamide **98** gave an IC_{50} value of 27 μ M, suggesting that electron-withdrawing groups are better tolerated in the 3-position than electron donating groups. In addition, the nitrile substituent is less sterically demanding than the bulky methyl or

methoxy substituent, providing further evidence that there might be a size-limited binding pocket around the 3-position of the quinoline.

Table 17. PARP-1 inhibitory activities of the benzimidazole analogues.¹⁷⁰



Compound	R	K_i (nM)
25c	Ph	15
25d	4-CN-Ph	4.0
25g	4-OH-Ph	6.0
25h	4-OMe-Ph	6.8
25i	4-CF ₃ -Ph	1.2
25j	3-CF ₃ -Ph	8.0

In the case of the 2-aryl substituted derivatives, 2-phenylquinoline-8-carboxamide **144** was found to be >16 fold more active than 3-phenylquinoline-8-carboxamide **69**, suggesting that substitution in the 2-position is preferred. This was supported by the preparation of 2-(4-methoxyphenyl)quinoline-8-carboxamide **145**, which was >56 fold more potent than its 3-aryl counterpart.

Quinoline-8-carboxamides containing alkyl, alkenyl and alkynyl substituents were synthesised to further study the SAR. The introduction of a methyl group into the 3-position of quinoline-8-carboxamide demonstrated a higher affinity to the nicotinamide binding pocket of PARP-1 than the 3-aryl congeners. The 3-ethynyl compound **107** was the most potent inhibitor of the 3-substituted series with an IC_{50} value of 2.2 μ M. It appears that relatively small substituents, which are not sterically demanding, are well accommodated in the enzyme active site. This is demonstrated by the fact that the 3-aryl substituted quinoline-8-carboxamides are >20 fold less active than the 3-alkyl and 3-alkynyl derivatives.

2-Methylquinoline-8-carboxamide **147** (IC_{50} = 0.5 μ M) and 2-ethylquinoline-8-carboxamide **146** (IC_{50} = 0.8 μ M) were slightly more potent than the parent compound **80** and

their 3-alkyl analogues **106** ($IC_{50} = 3.4 \mu\text{M}$) and **123** ($IC_{50} = 3.7 \mu\text{M}$). This demonstrates that substitution in the 2-position is most favourable for improving PARP-1 inhibitory activity.

It is proposed that the quinoline-8-carboxamide inhibitors bind to the nicotinamide sub-site of the NAD^+ -binding domain of PARP-1 (Figure 22). The carboxamide moiety of the inhibitor forms three important hydrogen bonds with the enzyme active site. The inhibitor carbonyl moiety accepts two hydrogen bonds, one from the amino-acid residue Ser904, and the other from the Gly863 polypeptide amide N-H. The third hydrogen bond is formed between the Gly863 carbonyl oxygen and the carboxamide N-H.

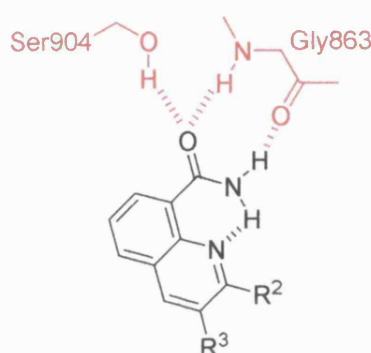


Figure 22. Proposed enzyme-inhibitor interactions between the PARP-1 active site and quinoline-8-carboxamides.

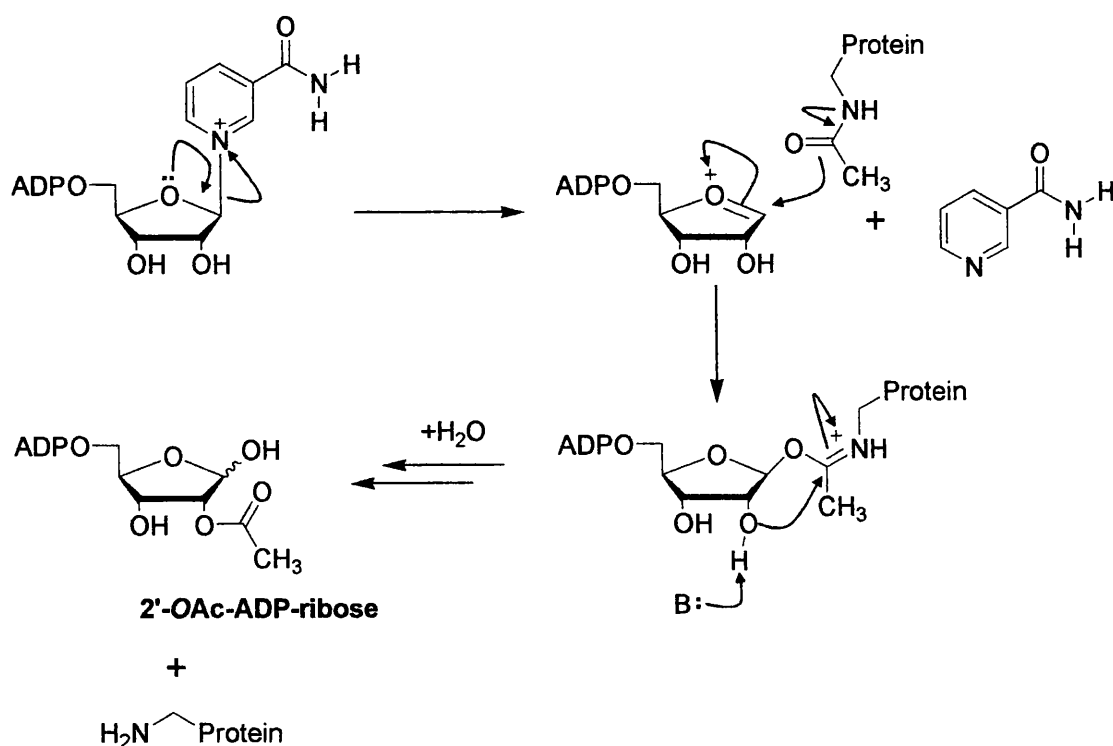
The colourimetric PARP-1 assay identified seven compounds with PARP-1 inhibitory activity equal or better than the lead compound 5-AIQ. Overall several SAR trends were identified:

- (1) Bulky *para*-substituents on the 3-aryl quinoline-8-carboxamides impaired PARP-1 inhibitory activity.
- (2) The most potent compounds in the 3-substituted series were those containing sterically very thin substituents.
- (3) The presence of 2-alkyl or 2-aryl substituents enhanced the potency of the parent compound **80**.

Researchers at the University of Newcastle reported tricyclic benzimidazole carboxamides as potent PARP-1 inhibitors.¹⁷¹ In the tricyclic inhibitors, the carboxamide moiety is held in the *anti*-conformation by incorporation into a seven-membered ring, allowing hydrogen-bond interactions to occur between the lactam ring and Ser904 and Gly863 of the PARP-1 active site. As constraining the carboxamide moiety into the *anti*-conformation by incorporation into a seven-membered ring is beneficial for PARP-1 inhibitory activity, the 8-carbamoyl-3-phenylquinoline-1-oxide **175** may provide a new structural lead for PARP-1 inhibition.

4.2 Sirtuins and NAD⁺ metabolism

The sirtuin family of enzymes, also known as SIRT5, constitute the class III histone deacetylases (HDACs). Yeast Sir2 (ySir2, yeast silent information regulator 2) is the founding member of the sirtuins and is essential for maintaining silent chromatin through the deacetylation of the histones.²⁴³ Sir2 has also been shown to enhance lifespan in yeast, worms and flies.²⁴³ Currently, seven mammalian sirtuins (SIRT1-7) have been identified, with SIRT1 demonstrating the greatest homology to Sir2. Unlike Class I and II HDACS, which remove the acetyl group by hydrolysis to acetate, class III HDACS require NAD⁺ as a co-substrate for deacetylation activity. The sirtuins catalyse the cleavage of the glycosidic bond between the ADP-ribose and nicotinamide moieties of NAD⁺, releasing nicotinamide and forming the positively charged O-alkyl-amidate intermediate. Subsequently, the acetyl group attached to Lys of substrate proteins is transferred to ADP-ribose forming the metabolite O-acetyl-ADP-ribose, as shown in Scheme 55.²⁴⁴ Nicotinamide inhibits the deacetylation reaction and is important for the regulation of sirtuin activity.



Scheme 55. Mechanism of SIRT catalysed deacetylation.²⁴⁴

SIRT1 can also deacetylate non-histone proteins including p53,²⁴⁵ p300,²⁴⁶ NFκB,²⁴⁷ and FOXO proteins.²⁴⁸ The SIRT1 homologue is the most widely studied of the sirtuin family. SIRT1 can be therapeutically applied to a variety of diseases. SIRT1 activators show promise for the treatment of diseases such as diabetes, obesity, age-related disease, and neurodegeneration.^{249,250} On the other hand, SIRT1 inhibition has been suggested for future cancer and anti-HIV treatments.²⁵¹

The therapeutic applications of the other Sir2 genes, SIRT2-7, have only recently begun to emerge. Studies indicate that SIRT2 may play a role in regulating the cell cycle. Dryden *et al.*²⁵² demonstrated that SIRT2 protein levels increase during the mitotic phase of the cell cycle and SIRT2 overexpression delays mitosis. In addition, Hiratsuka *et al.*²⁵³ demonstrated that expression of SIRT2 is down regulated in human gliomas.

SIRT7 is associated with active rRNA genes (rDNA) and is a positive regulator of Po1 I transcription. Recent work has shown that SIRT7 expression is elevated in thyroid cell lines and biopsies.²⁵⁴

SIRT3 has been shown to deacetylate and activate acetyl-CoA-synthetase-2 (AceCS2), a mitochondrial enzyme that catalyses the synthesis of acetyl-CoA from acetate.²⁵⁵ SIRT4 is also located in the mitochondria of mammalian cells and regulates energy usage. Haigis *et al.*²⁵⁶ demonstrated that SIRT4 has an important role in regulating amino-acid stimulated insulin secretion (AASIS) in pancreatic β-cells by ADP-ribosylating and inhibiting glutamate dehydrogenase (GDH). A summary of the biological functions of the mammalian sirtuins is presented in Table 19.

Table 19. Summary of mammalian sirtuins, their localisation, activities, interactions and biological functions.

Sirtuin	Localisation	Activity	Interactions	Biological functions
SIRT1	Nucleus	Deacetylase	p53 FOXO proteins NFκB	Repression; reduced DNA damage; increased cell survival Repression; increased resistance to stress. Increased apoptosis
SIRT2	Cytoplasm	Deacetylase	α-tubulin, G2/M proteins	Cell structure, intracellular transport and mobility. Controls mitotic cell cycle exit.
SIRT3	Mitochondria	Deacetylase	AceCS2	Thermogenesis / metabolism
SIRT4	Mitochondria	ADP-ribosyl- transferase	GDH	Insulin secretion / metabolism
SIRT5	Mitochondria	Deacetylase	Unknown	Unknown
SIRT6	Nucleus	ADP-ribosyl- transferase	DNA Po1β	DNA repair
SIRT7	Nucleolus	Unknown	Po1 I	rDNA transcription

Several crystal structures of sirtuin proteins have been reported, either uncomplexed,²⁵⁷ or bound to substrates such as NAD⁺ and/or acetylated peptides.^{258,259} These crystal structures have provided insights into the catalytic mechanisms of sirtuins, for example, the mechanism by which NAD⁺ cleavage occurs.

As previously mentioned, PARP-1 also uses NAD⁺ as its electrophilic substrate when SSB or DSB activate PARP-1. Therefore, NAD⁺ serves as a substrate for both SIRT1 and PARP-1. Nicotinamide has been identified as a moderately potent SIRT1 inhibitor, with an IC₅₀ < 50 μM. Interestingly, nicotinamide also serves as a PARP-1 inhibitor, albeit at a high IC₅₀ of > 100 μM.

The pharmacophore for PARP-1 inhibition has been widely studied and numerous PARP-1 inhibitors have been developed. In contrast, the pharmacophore inhibition of SIRT1 activity is poorly defined and, as of yet, a crystal structure of SIRT1 has not been published. However, a pharmacophore comparative model for SIRT1 has recently

been constructed using the crystal structure of SIRT2 as the primary template. Huhtiniemi *et al.*²⁶⁰ proposed the binding mode of the indole-based inhibitor EX527 (S-enantiomer) in SIRT1 (Figure 23). EX527 has been reported to be approximately 1000-fold more potent than nicotinamide.²⁶¹ The site of interaction and the ligand conformation were predicted using molecular modelling studies. It was found that the amino NH₂ moiety of EX527 donates a hydrogen bond to the carbonyl group of the D348 residue. In addition, the carbonyl oxygen of EX527 forms hydrogen bonds with the D348 and I347 residues. Therefore, SIRT-1 and PARP-1 appear to have a common pharmacophore, for example, the amide group in nicotinamide contains donor and acceptor functionalities that can bind to the active site of both SIRT1 and PARP-1. The quinoline-8-carboxamide series also contains an amide group that could potentially form binding interactions with the SIRT-1 active site. It is predicted that these compounds may show inhibitory activity towards the SIRT1 enzyme. In order to test this hypothesis, a series of our quinoline-8-carboxamide PARP-1 inhibitors were tested for their inhibitory activity against SIRT1 *in vitro*.

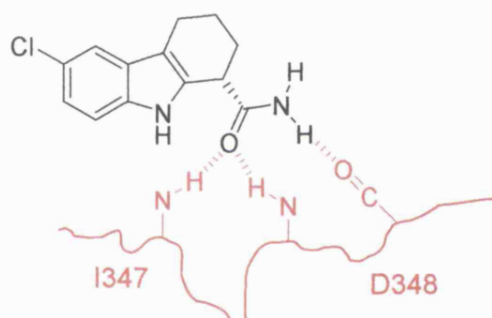


Figure 23. Proposed binding interactions of EX527 (S-enantiomer) with the SIRT1 active site.²⁶⁰

4.2.1 SIRT1 activity assay

The classical assay methods for monitoring sirtuin activity involve the use of either radiolabelled [^3H] acetyl-histone or [^3H]acetyl-peptides as substrates. These assay systems require tedious extraction procedures, using solvents that have a limited capacity to extract the radiolabelled acetate released in the assay, thereby reducing the range of detectable activity.^{262,263} Recently, the detection of human SIRT1 activity, using a commercially available *Fluor de Lys*TM fluorescence-based assay, has been reported. The SIRT1 fluorescent activity kit developed by Biomol[®] (Plymouth, USA) is non-radioactive and utilises a unique *Fluor de Lys*TM Substrate/ Developer system. The *Fluor de Lys*TM substrate is a peptide comprising of amino-acids 379-382 of human p53, which contains an acetylated lysine side chain. The assay system is based on a two-step reaction as shown in Figure 24. The first step involves the NAD^+ -dependent deacetylation of the substrate by recombinant human SIRT1. The second step involves the proteolytic cleavage of the deacetylated substrate by the Developer solution and generation of a fluorophore. Addition of nicotinamide to the assay ensures that the reaction is stopped. The measured fluorescence is directly proportional to the deacetylation activity of SIRT1.

As an initial study, 3-AB, 5-AIQ and several substituted quinoline-8-carboxamides were evaluated for their *in vitro* activity against recombinant human SIRT1. Seven different final concentrations (100, 30, 10, 3, 1, 0.3 and 0.1 μM) of inhibitor were used in the fluorimetric assay. Nicotinamide was also included in the assay as a reference compound. For each inhibitor, three independent determinations were performed and the raw data are presented in Appendix 3. It was found that none of the compounds tested had an inhibitory effect on SIRT1 activity at the micromolar level, although there was some indication that quinoline-8-carboxamide may show activity at higher concentrations (Table 20). 5-AIQ appears not to inhibit SIRT.

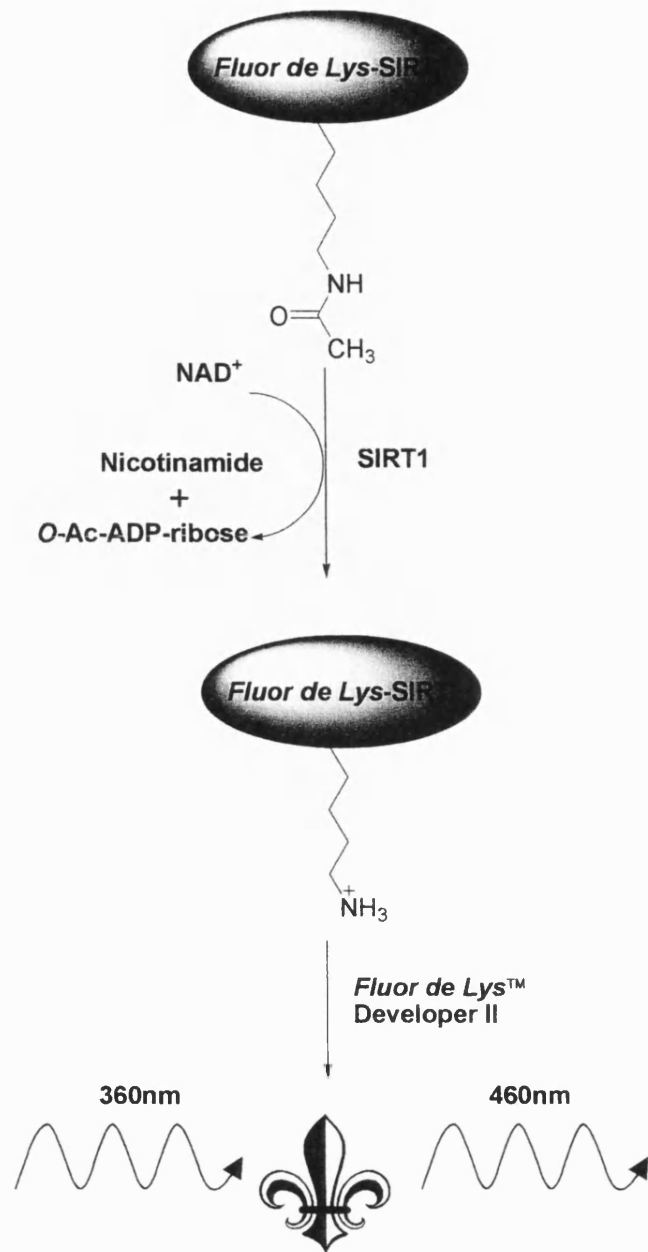


Figure 24. Reaction Scheme of the SIRT1 Fluorescent Activity Assay. Deacetylation of the *Fluor de Lys*[™] substrate sensitises it to the developer, which then generates a fluorophore (symbol).

Table 20. Summary of the SIRT1 plate readings for quinoline-8-carboxamide and 5-AIQ.

Concentration (μM)	Quinoline-8-carboxamide fluorescence readings (460 nm)		
	Run 1	Run 2	Run 3
100	896	781	894
30	1101	1144	1003
10	949	921	909
3	1100	1143	1061
1	1506	1012	895
0.3	1020	1227	1177
0.1	1363	1373	1173

As mentioned previously, the pharmacophore for SIRT1 is poorly defined. Nevertheless, the crystal structures of sirtuins complexed to nicotinamide may provide insights into the likely mode of binding of inhibitors to the SIRT1 active site. Structural studies of the Sir2Af2 and Sir2Tm enzymes show that nicotinamide can bind to sirtuins simultaneously in complex with a peptide, ADP-ribose or NAD^+ that is in a non-productive conformation, thus allowing binding of nicotinamide to the C-pocket of the active site.²⁶⁴ The carboxamide amino of nicotinamide forms a hydrogen bond with the Asp103 residue in the C-pocket of the enzyme active site. In addition, the carboxamide oxygen forms hydrogen bonds with the Ile102 residue. These hydrogen-bond interactions anchor the carboxamide moiety to the enzyme, yet allow the pyridine ring of nicotinamide to rotate around the C-pocket.

The pharmacophore for PARP-1 inhibition requires a carboxamide group that is restricted into the *anti*-conformation. This is so that the carboxamide moiety can form important hydrogen-bond interactions with the amino-acid residues Ser904 and Gly863 in the PARP-1 active site. As the carboxamide moiety in the quinoline-8-carboxamide compounds is in a restricted conformation it cannot freely rotate in the sirtuin active site. Therefore, it is possible that the carboxamide moiety in the quinoline-8-carboxamide compounds is not in the correct conformation in order to form the crucial hydrogen-bond interactions with C-pocket of the sirtuin active site.

Zhang *et al.*²⁶⁵ suggested that there is a functional link between the PARP-1 and sirtuin pathway as both enzymes compete for NAD⁺ (Figure 25). The sirtuin enzyme can be suppressed by NAD⁺ depletion and nicotinamide increase due to PARP activation. The connection between the PARP-1 and sirtuin pathway might play a role in the regulation of cellular processes such as gene expression, DNA repair, cell cycle progression and chromatin remodelling. Recent work has demonstrated that the p53 substrate is shared between PARP-1 and sirtuins. The p53 protein is the product of the tumour suppressor gene and acts as an antiproliferative factor by controlling growth arrest, apoptosis and cell senescence in response to cellular stress. Activation of PARP-1 in response to DNA damage or oxidative stress results in decreased NAD⁺ levels and increased nicotinamide levels. As the deacetylase activity of SIRT1 is dependent on NAD⁺ availability and sensitive to nicotinamide production, it is feasible that poly(ADP-ribose) metabolism downregulates SIRT1.²⁶⁵ In fact, Vaziri *et al.*²⁴⁵ demonstrated that SIRT1 inhibition by nicotinamide enhances p53 acetylation. However, under normal conditions of high NAD⁺ levels, SIRT1 acts to downregulate p53 activity. It appears that the regulation of PARP activity and SIRT1 deacetylase activity may represent complementary therapeutic opportunities for the treatment of cancer. However, there is still a need for the design of selective sirtuin inhibitors in order to study the link between the poly(ADP-ribose) metabolic pathway and the protein acetylation/deacetylation pathway.

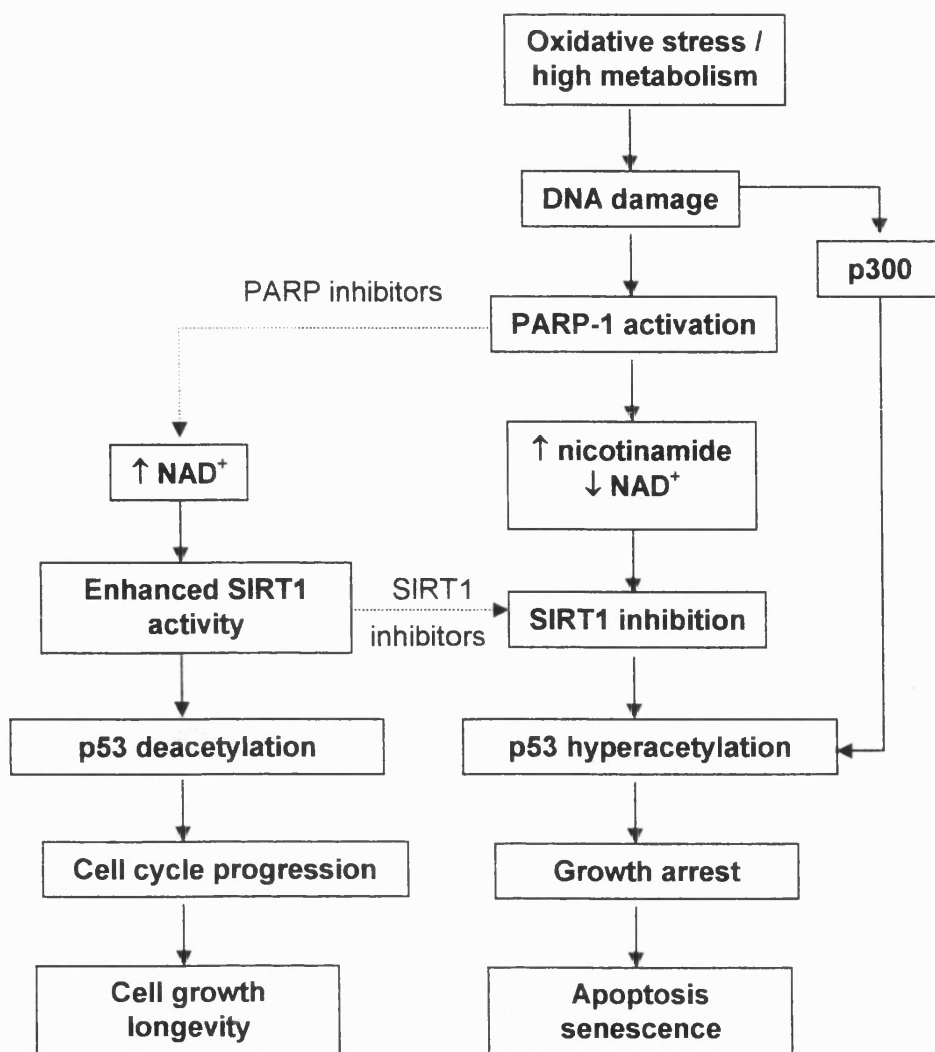


Figure 25. Proposed functional interplay between PARP-1 and SIRT1.²⁶⁵

Overall, we have successfully evaluated *in vitro* a series of 3-substituted and 2-substituted quinoline-8-carboxamides. Their potency against PARP-1 is comparable with our lead inhibitor 5-AIQ. 8-Carbamoyl-3-phenylquinoline-1-oxide **175** has been shown not to be a useful prodrug in this series against this target but may provide a new structural lead for PARP-1 inhibition.

5. Structural studies and molecular modelling

5.1 Structural studies of quinoline-8-carboxamides

Naphthalene-1-carboxamide has been synthesised previously in our laboratory. In the ^1H NMR spectrum of this primary amide, one N-H proton signal was observed at δ 7.74 and the other at δ 7.99. In this compound, intramolecular hydrogen-bonding is impossible and the NH_2 proton signals are only separated by ca. 0.25 ppm. In the ^1H NMR spectrum of quinoline-8-carboxamide **80**, one of the N-H protons resonates at δ 6.49 and the other at δ 10.95. Similarly, the signals for the NH_2 protons in 3-phenyl-quinoline-8-carboxamide **69** were observed at δ 6.17 and δ 10.95 (Figure 26). The difference of ca. 5 ppm between the signals of the NH_2 protons in both compounds **69** and **80** indicates that one proton is in a very strongly intramolecularly hydrogen-bonded environment (giving the downfield signals), while the other proton is not intramolecularly hydrogen-bonded. Interestingly, the ^1H - ^1H COSY spectrum of **69** in CDCl_3 showed a cross-peak between the two N-H signals of the carboxamide group (Figure 27), suggesting that they are in slow exchange and thus can couple to each other. Thus the ^1H NMR studies of **69** and **80** indicate that the carboxamide moiety is held in a conformation which is apposite for PARP-1 inhibitory activity.

Chloroform is a non-hydrogen-bonding solvent and the CDCl_3 NMR solvent promotes intramolecular hydrogen-bonding, giving rise to the ca. 5 ppm difference in the NH_2 signals in **69** and **80**. In contrast, DMSO is a powerful hydrogen-bond acceptor, with the potential to disrupt intramolecular hydrogen bonds. A ^1H NMR spectrum of compound **69** was taken in $(\text{CD}_3)_2\text{SO}$ (Figure 26); one of the N-H signals was evident at δ 7.99 whereas the other N-H proton signal was evident further downfield at δ 10.17. The difference in chemical shift of the two NH protons is diminished but is still significant at ca. 2.2 ppm. A similar $\Delta\delta$ was seen for 3-(3-(trifluoromethyl)phenyl)-quinoline-8-carboxamide **94** in $(\text{CD}_3)_2\text{SO}$ (Figure 28). This indicates that intramolecular hydrogen bonding is present even in this potentially powerfully disrupting solvent and points to the maintenance of the hydrogen bonds in aqueous biological media.

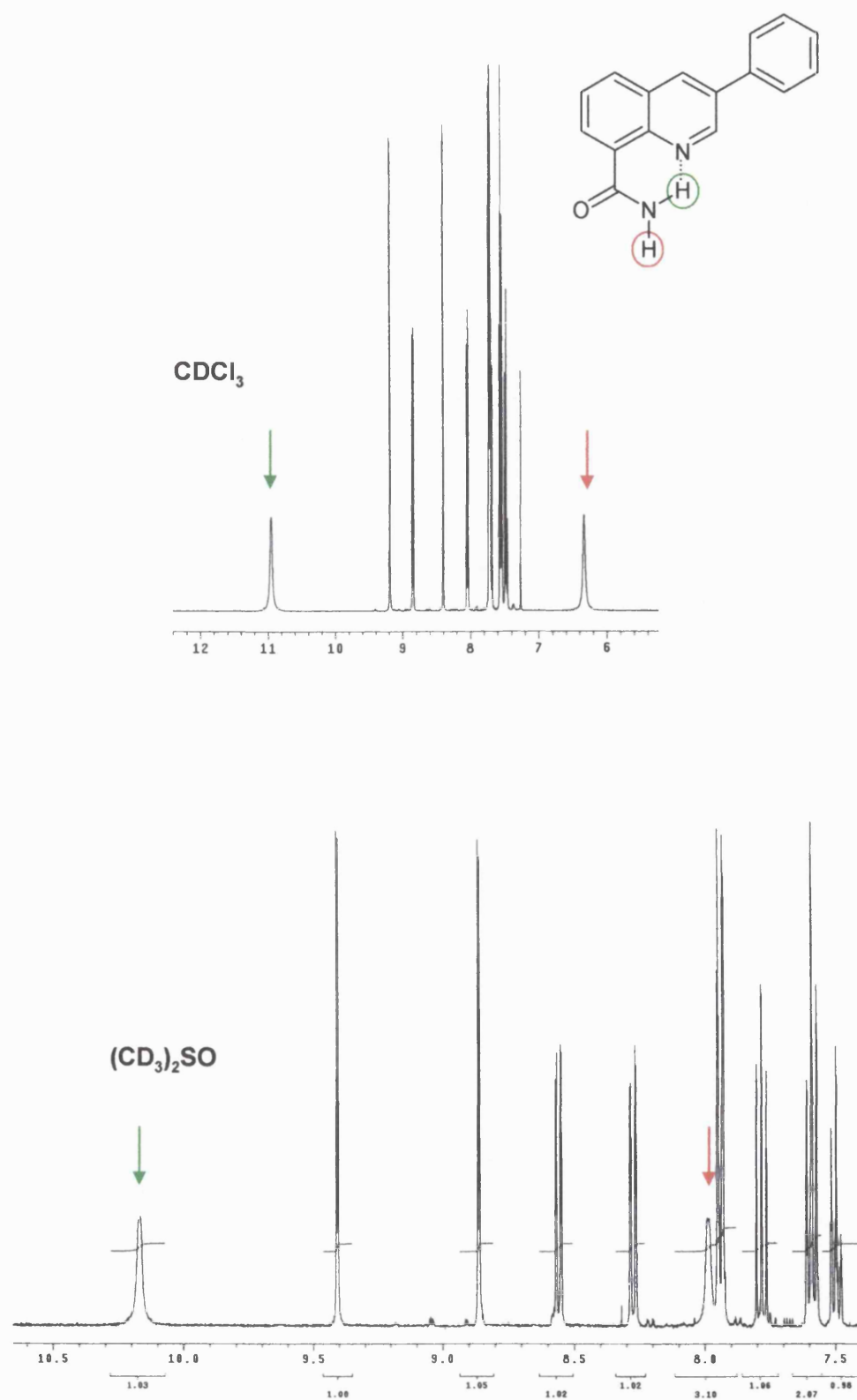


Figure 26. Comparison of the N-H signals of 3-phenylquinoline-8-carboxamide in CDCl₃ (top) and (CD₃)₂SO (bottom).

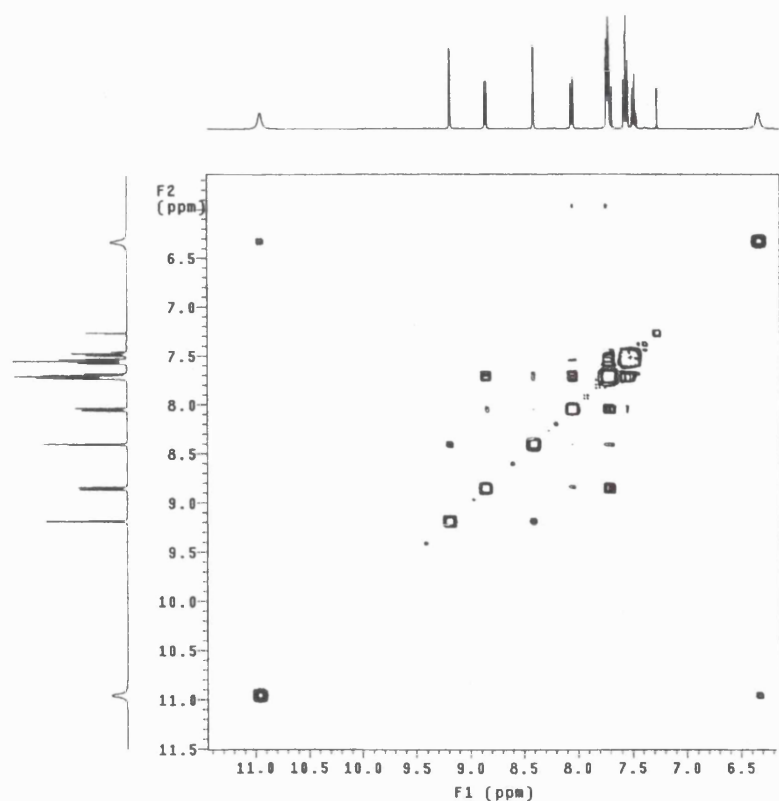


Figure 27. ^1H - ^1H COSY spectrum of 3-phenylquinoline-8-carboxamide **69**.

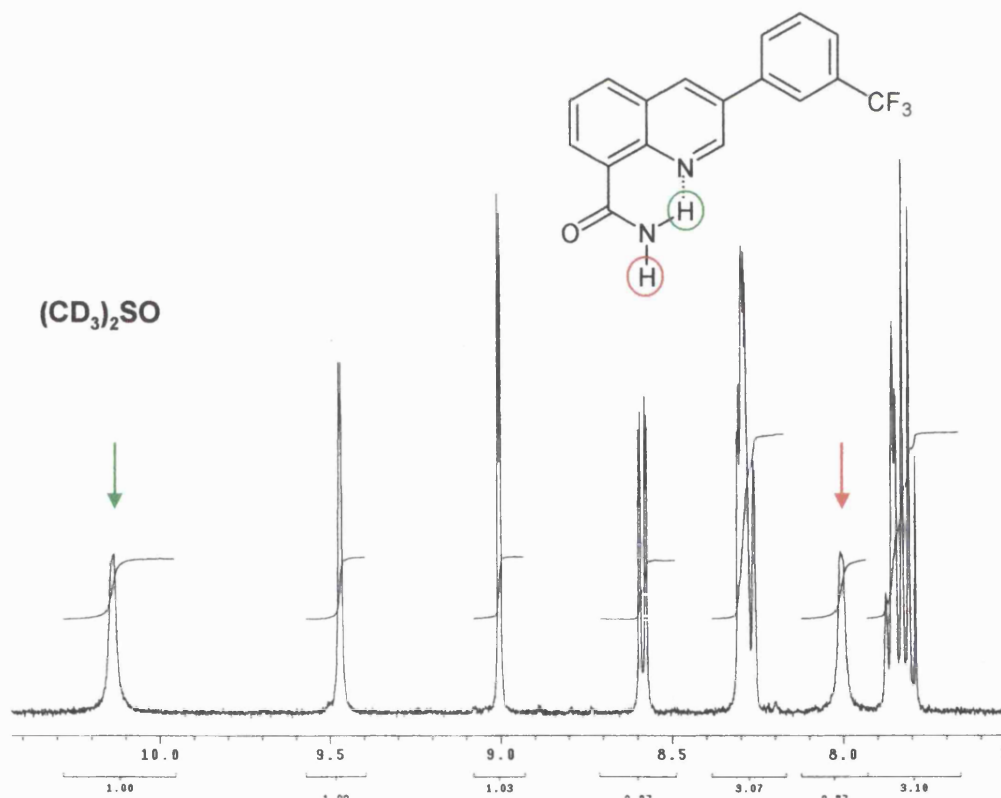


Figure 28. ^1H NMR spectrum of 3-(3-(trifluoromethyl)phenyl)quinoline-8-carboxamide **94** in $(\text{CD}_3)_2\text{SO}$.

From the examination of the ^1H NMR spectrum of 8-carbamoyl-3-phenylquinoline-1-oxide **175** in $(\text{CD}_3)_2\text{SO}$, it became apparent that the characteristic N-H peak usually found between δ 10.0 and δ 10.5 was not present (Figure 29). The ^1H NMR results suggest that the carboxamide moiety in **175** is not held in a restricted conformation as in its non-oxide analogue **69**.

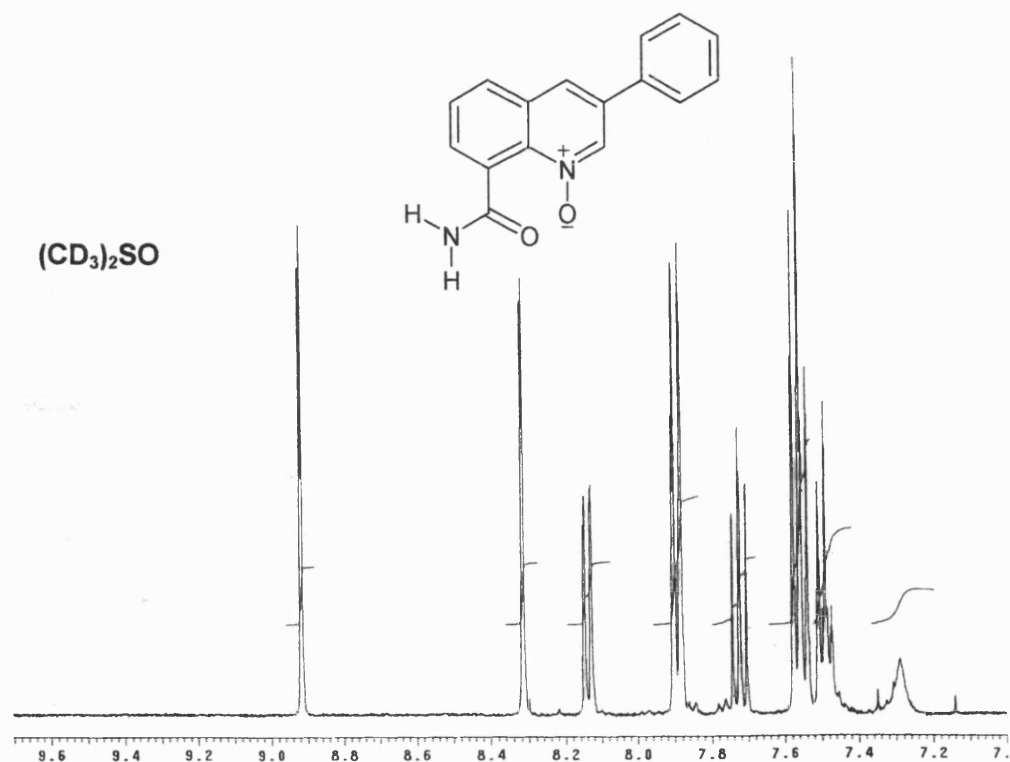


Figure 29. ^1H NMR spectrum of 8-carbamoyl-3-phenylquinoline-1-oxide **175** in $(\text{CD}_3)_2\text{SO}$.

5.2 X-ray crystallography of 3-phenylquinoline-8-carboxamide and 2-(3-(trifluoromethyl)phenyl)quinoline-8-carboxamide

Crystals of 3-phenylquinoline-8-carboxamide **69** were grown in an EtOAc/hexane system and the X-ray crystallographic structure is shown in Figures 30 and 31. The phenyl group in **69** is twisted out of the plane of the quinoline ring by 46.9° . In addition, the structure shows the presence of the predicted intramolecular hydrogen bond between the heterocyclic nitrogen and one of the NH groups of the carboxamide. This hydrogen bond holds the carboxamide in the plane of the aromatic quinoline, as required for the pharmacophore of inhibitors of PARP-1. This hydrogen bond was also demonstrated in solution in CDCl_3 and in $(\text{CD}_3)_2\text{SO}$ by NMR spectroscopy (see above). An additional (intermolecular) hydrogen bond is seen in the crystal between the carbonyl oxygen on one molecule and the "exocyclic" N-H of an adjacent molecule. Figure 30 illustrates these interactions between a pair of molecules whereas Figure 31 shows the longer range hydrogen-bonding and stacking arrangement of eight molecules.

X-ray crystallography of 3-(2-(trifluoromethyl)phenyl)quinoline-8-carboxamide **96** provided supporting evidence for the formation of the predicted intramolecular hydrogen bond. As with **69**, an intramolecular hydrogen-bond interaction was observed between the heterocyclic nitrogen and one of the N-H groups of the carboxamide, as shown in Figure 32. The steric bulk of the *ortho* substituent in **96** has a profound effect, in that the trifluoromethylphenyl group is twisted out of plane of the quinoline ring by 55.8° , a dihedral angle some 9° greater than that in **69**. The *ortho* substituent is prevented from being co-planar owing to the steric clash between the 3-substituent and the 2-H of the quinoline ring.

In compound **96**, the length of the proposed intramolecular hydrogen bond is 2.03 Å, with a bond angle (N-H-N) at hydrogen of 134.9° . Although the optimal angle for a hydrogen bond is 180° , hydrogen bonds in planar six-membered rings (e.g. enols of β -diketones) are common and relatively strong. This intramolecular hydrogen bond in **96** creates a planar six-membered ring and thus could be expected to be strong.

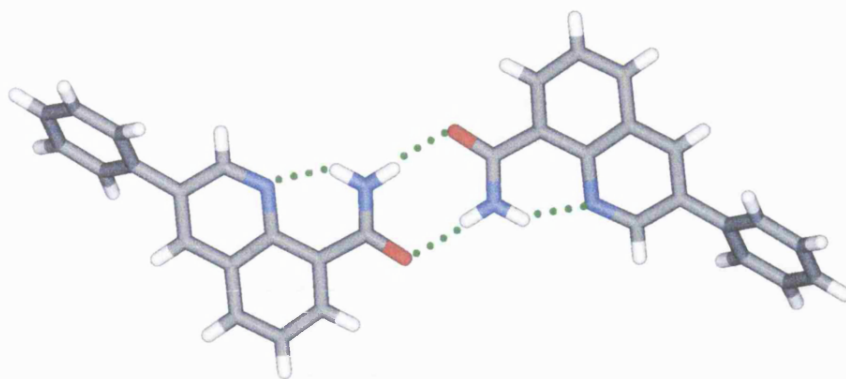


Figure 30. X-ray crystal structure of 3-phenylquinoline-8-carboxamide **69**. The red colour refers to oxygen, the blue refers to nitrogen, the white refers to hydrogen and the grey refers to carbon.

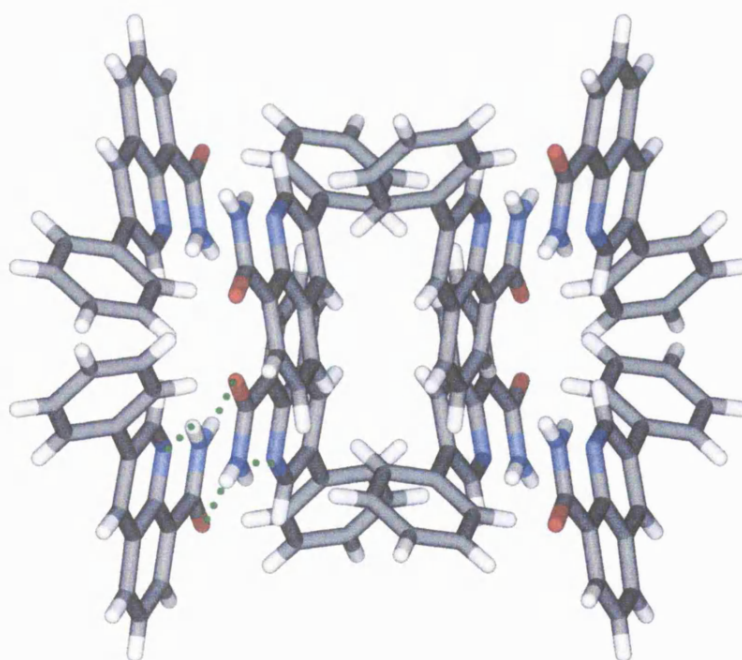


Figure 31. Intermolecular and intramolecular hydrogen bonding present in crystals of **69**. The red colour refers to oxygen, the blue refers to nitrogen, the white refers to hydrogen and the grey refers to carbon.

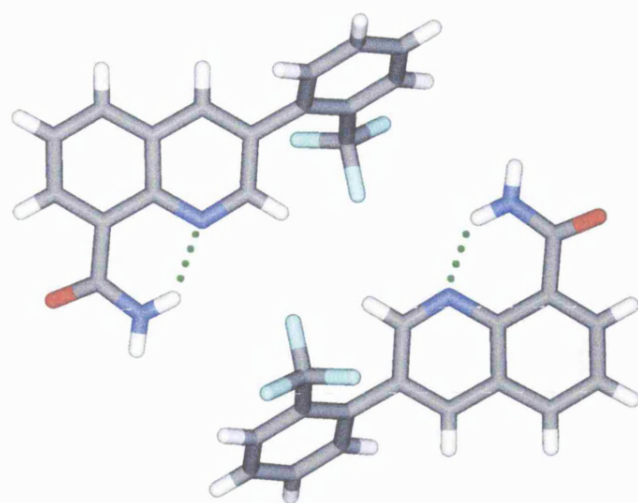


Figure 32. X-ray crystal structure of 3-(2-(trifluoromethyl)phenyl)quinoline-8-carboxamide **96**, showing intramolecular hydrogen-bonding interactions. The red colour refers to oxygen, the blue refers to nitrogen, the cyan refers to fluorine, the white refers to hydrogen and the grey refers to carbon.

5.3 Molecular modelling studies of 8-carbamoyl-3-phenylquinoline-1-oxide

In our original hypothesis, it was proposed that the quinoline-8-carboxamide N-oxide targets would act as hypoxia-selective prodrugs. It was thought that, in the presence of the N-oxide group, the carboxamide would be tipped out of the plane of the quinoline, thereby disrupting the pharmacophore required for PARP-1 inhibition. However, 8-carbamoyl-3-phenylquinoline-1-oxide **175** showed inhibitory activity approximately equal to that of its non-oxide analogue **69** (Section 4.1.3). This result indicates that the formation of the N-oxide may not twist the carboxamide out-of-plane as much as originally hypothesised. To understand this result better, molecular modelling of 8-carbamoyl-3-phenylquinoline-1-oxide **175** was undertaken. Models were built and modelled in Sybyl 7.3.3 and charged using Gasteiger-Marsilli and Gasteiger-Hückel methods. The models were minimised and subjected to five picoseconds of molecular dynamics. During the first picosecond, the temperature was raised from 0 to 450 K and then held at 450 K for the next four picoseconds. It was found that there were two low-energy conformations of the N-oxide **175** with the amide and phenyl twisted out of the plane of the quinoline (Figure 33). These low-energy conformations arise from either two clockwise twists of the substituents or two anticlockwise twists and are enantiomers.

When calculations were performed *in vacuo*, the structure adopted an intramolecular hydrogen bond between one of the carboxamide N-H protons and the N-oxide oxygen. The intramolecular hydrogen bond was occupied 90-95% of the time, depending on the calculated charge distribution within the molecule. When the above calculations were repeated using a ten-layer water shell (a hydrogen-bond-accepting and -donating solvent) the intramolecular hydrogen-bond occupancy significantly reduced as the carboxamide group formed transient hydrogen bonds to the solvent (water) shell. In this case, the intramolecular hydrogen-bond occupancy was calculated to be in the range of 60-70%, depending on the calculated charge distribution within the molecule.

The molecular modelling studies of **175** suggest that it may form a seven-membered hydrogen-bonded structure involving the N-oxide, causing the carboxamide moiety to twist only slightly out-of-plane and allowing binding to the active site of PARP-1.

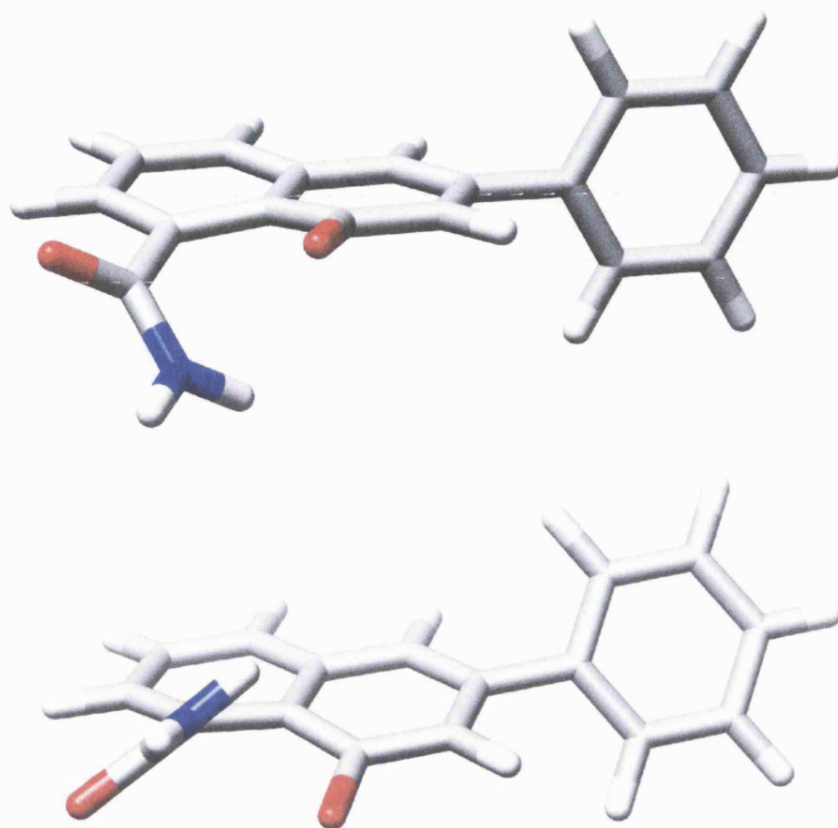


Figure 33. Calculated enantiomeric minimum-energy conformations of **175**. The upper structure corresponds to clockwise-clockwise rotation of the substituents and the lower to anticlockwise-anticlockwise rotations.

The postulated intramolecular hydrogen bond in the modelled structure of **175** contrasts with that in **96**, in that it forms a seven-membered non-planar ring. The hydrogen bond is long at 2.46 Å (*c.f.* 2.03 Å for **96**) and the bond angle (N-H-O) is unfavourable at 90.1°. These factors point to a much weaker intramolecular hydrogen bond in the N-oxide **175** than in the quinoline-8-carboxamides.

6. Conclusions

Several different approaches to the synthesis of 3-substituted quinoline-8-carboxamides were explored. In route (I), the use of 8-methylquinoline as a precursor for the introduction of an aromatic substituent into the 3-position was not a successful approach to give 3-substituted quinoline-8-carboxamides. Route (II) gave the first target molecule 3-phenylquinoline-8-carboxamide **69**, which was characterised by X-ray crystallography. Suzuki-Miyaura coupling of 3-iodo-8-nitroquinoline with phenylboronic acid gave 8-nitro-3-phenylquinoline **62**, for which the HMBC spectrum was fully assigned. Various methods were employed for the conversion of the nitro group in compound **62** to the amine, nitrile and finally carboxamide group. The intramolecular hydrogen bond in **69** was demonstrated in the X-ray crystal structure and in the ^1H NMR spectrum. The latter showed that one of the carboxamide N-H protons was hydrogen-bonded to the lone pair of the nitrogen of the quinoline, resulting in the signal being very downfield. However, route (II) is not an efficient synthetic strategy for the generation of libraries. An alternative route (III), which introduced diversity at the final stage in the sequence, was investigated. An 8-cyano group was formed early in the route for later hydration to the carboxamide group. 3-Phenylquinoline-8-carboxamide **69** was successfully synthesised but this route suffered from poor overall yield, owing to the difficult Sandmeyer step. A highly efficient route (IV) was finally developed to give a wide range of 3-substituted quinoline-8-carboxamides. The synthesis of 3-iodoquinoline-8-carboxamide **77** in route (IV) gave an ideal precursor for palladium-catalysed coupling reactions. Suzuki-Miyaura couplings of **77** with arylboronic acids proceeded well, giving a series of 3-arylquinoline-8-carboxamides. Varying Suzuki-Miyaura coupling conditions were investigated, with different conditions being optimum for different groups of arylboronic acids. Alkyl substituents could not be introduced by Suzuki-Miyaura coupling. However, a range of 3-alkylquinoline-8-carboxamides were synthesised by Stille coupling of **77** with alkyl stannane reagents. 3-alkynyl-quinoline-8-carboxamide derivatives were also obtained *via* Sonogashira coupling reactions. Therefore, we have developed synthetic methods that efficiently provide a diverse range of 3-substituted quinoline-8-carboxamides.

A series of 2-substituted quinoline-8-carboxamides was also explored. Attempts to convert 8-bromoquinolin-2(1*H*)-one to 2-oxo-1,2-dihydroquinoline-8-carbonitrile proved difficult using either palladium-catalysed methods, or more standard CuCN methods, thus preventing a sequence of palladium-catalysed coupling reactions to give the 2-

substituted quinoline-8-carboxamide targets. In an alternative route, the formation of the precursor 2,8-bromoquinoline **133** allowed for successful regioselective palladium-catalysed cross-coupling reactions. We have carried out effective regioselective Suzuki-Miyaura cross-couplings between 2,8-dibromoquinoline **133** and arylboronic acids that furnished 8-bromo-2-aryl substituted quinolines. In addition, we carried out a regioselective Stille cross-coupling reaction between 2,8-dibromoquinoline **133** and alkyl stannane reagents that furnished 8-bromo-2-alkyl substituted quinolines. HMBC analyses demonstrated that the C-Br bond at position 2 of the quinoline ring was more reactive towards palladium-catalysed coupling reactions than at the position 8. Lithium-bromine exchange and subsequent quenching with trimethylsilylisocyanate led to the target 2-substituted quinoline-8-carboxamides in good yields.

Several routes for the synthesis of quinoline-8-carboxamide N-oxides were investigated. The synthetic route for the reductive cyclisation of (*E*)-methyl 2-nitro-3-(3-oxo-2-phenylbut-1-enyl)benzoate proved long and low yielding and failed to provide the N-oxide target compounds. Direct N-oxidation of quinoline-8-carboxamide with various oxidants also failed, due to deactivation by the intramolecular hydrogen bond which was designed as part of the pharmacophore. We demonstrated that the presence of bulky and electron-withdrawing substituents in the 8-position of quinoline inhibited the N-oxidation reaction. Synthetic routes in which the 2- or 3- substituent was present in the N-oxidation step but the 8-position carried only a hydrogen atom were attempted. Owing to the solubility problems and poor reactivity of intermediates (1-oxido-2-phenylquinolin-8-yl)mercury(II) chloride and (1-oxido-3-phenylquinolin-8-yl)mercury(II) chloride, it was not possible to synthesise the N-oxide targets *via* these synthetic routes.

Finally, it was found that 3-phenylquinoline-8-carbonitrile **69** could be converted to the corresponding N-oxide using urea-hydrogen peroxide complex and trifluoroacetic anhydride as the oxidising agent, which generates peroxytrifluoroacetic acid *in situ* as the oxidant. Subsequent hydration with alkaline hydrogen peroxide gave the target 8-carbamoyl-3-phenylquinoline-1-oxide **175**.

In this project, we evaluated quinoline-8-carboxamide and representative 3-substituted and 2-substituted quinoline-8-carboxamides for their *in vitro* activity against human recombinant PARP-1. It was found that seven of the compounds had potency equal or better than our lead inhibitor 5-AIQ. Interestingly, the 2-substituted quinoline-8-carboxamides were slightly more potent than were quinoline-8-carboxamide or their 3-

substituted counterparts. 2-Methylquinoline-8-carboxamide was found to be the most potent PARP-1 inhibitor in the series with an IC_{50} value of 0.5 μ M. Biological evaluation of 8-carbamoyl-3-phenylquinoline-1-oxide **175** showed that it was not a useful prodrug strategy in this series against the PARP-1 target. 8-Carbamoyl-3-phenylquinoline-1-oxide **175** was found to have an IC_{50} of 23 μ M which was approximately equal to the inhibitory activity of its non-oxide analogue **69** (IC_{50} = 15 μ M). Molecular modelling studies on **175** suggested that it may form a seven-membered hydrogen-bonded structure involving the N-oxide, causing the carboxamide moiety to only twist slightly out of plane and allowing binding to the NAD^+ binding site. As constraining the carboxamide moiety into the *anti*-conformation by incorporation into a seven-membered ring is beneficial for PARP-1 inhibitory activity, the 8-carbamoyl-3-phenylquinoline-1-oxide **175** may provide a new structural lead for PARP-1 inhibition.

The quinoline-8-carboxamides were also tested against human recombinant SIRT1 for their *in vitro* activity. However, none of the quinoline-8-carboxamide compounds tested had an inhibitory effect on SIRT1 activity at the micromolar level.

During the course of the project several advances in quinoline chemistry have been made. In addition, the studies demonstrate the wide scope of the use of organometallic chemistry in the synthesis of libraries of compounds. Future work would involve the synthesis of 4-substituted quinoline-8-carboxamides and possibly disubstituted quinoline-8-carboxamides to further investigate the NAD^+ -binding pocket of PARP-1. Encouraged by the promising data for inhibition of PARP-1 *in vitro*, our main focus is to evaluate the quinoline-8-carboxamide compounds for their *in vivo* activity in various disease models.

7. Experimental

General Procedures

All melting points were determined using a Reichert-Jung Thermo Galen Kofler block and are uncorrected. IR spectra were recorded on a Perkin-Elmer RXI FT-IR spectrometer, either as a liquid (film) or as a KBr disc (KBr). ν_{\max} values are given in cm^{-1} . NMR spectra were recorded on either JEOL-Varian GX 270 (270.05 MHz ^1H ; 67.8 MHz ^{13}C) or Varian Mercury EX 400 (399.65 MHz ^1H ; 100.4 MHz ^{13}C ; 376.05 MHz ^{19}F) spectrometers. Tetramethylsilane was used as an internal standard for samples dissolved in CDCl_3 and $(\text{CD}_3)_2\text{SO}$. Multiplicities are indicated as follows; s (singlet), br (broad singlet), d (doublet), dd (doublet of doublets), t (triplet), q (quartet) and m (multiplet). Coupling constants (J) are expressed in Hz. Where indicated, 2-D experiments were used to assign ^1H NMR and ^{13}C NMR signals. Mass spectra were obtained by either Fast Atom Bombardment (FAB) (with 3-nitrobenzyl alcohol as the matrix) or Electrospray (ES) at the University of Bath Mass Spectrometry Service using a VG 7070 Mass Spectrometer, the University of Bath Department of Pharmacy and Pharmacology High Resolution Mass Spectrometry Service using a Bruker microOTOF™ and the EPSRC Mass Spectrometry Service, Swansea. Elemental analysis (CHN) was carried out at the School of Pharmacy, University of London, Microanalysis Service. Thin layer chromatography (TLC) was performed on silica gel 60 F₂₅₄-coated aluminium sheets (Merck) and visualisation was accomplished by UV light (254 nm). Flash column chromatography was performed using silica gel 60 (0.040-0.063 mm, Merck) as the stationary phase.

Boronic acids were purchased from Frontier Scientific, Inc. Other reagents were purchased from Aldrich, Lancaster or Acros chemical companies and were used without further purification. The Universal Colourimetric PARP Assay Kit was purchased from AMS biotechnology. The SIRT1 Fluorimetric Assay Kit was purchased from Biomol® International, LP. Milli-Q water was used in all the biological assays. THF and diisopropylamine were freshly distilled under nitrogen from sodium/benzophenone and calcium hydride respectively. Solutions in organic solvents were dried over magnesium sulfate and solvents were evaporated under reduced pressure. Experiments were conducted at ambient temperature, unless otherwise stated.

General Procedure 1 - Pd-Catalysed Suzuki-Miyaura coupling of heteroaryl halides with arylboronic acids.

The heteroaryl halide (1.0 mmol, 1 equiv.), Pd(PPh₃)₄ (10 mol %), Na₂CO₃ (1.2 mmol, 1.2 equiv.) and arylboronic acid (1.1 mmol, 1.1 equiv.) in toluene : EtOH : H₂O (10 mL : 1 mL : 1 mL) were heated at reflux at 80°C for 24 h under N₂. The evaporation residue, in EtOAc, was washed with water and brine. The organic layer was dried with MgSO₄ and the solvent was evaporated. The crude product was purified by chromatography.

General Procedure 2 - Pd-Catalysed Suzuki-Miyaura coupling of heteroaryl halides with 4-bromomethylphenylboronic and toluene-4-boronic acids.

The heteroaryl halide (1.0 mmol, 1 equiv.), K₂CO₃ (3 equiv.), Pd(PPh₃)₄ (10 mol %) and arylboronic acid (1.0 mmol, 1 equiv.) in THF / water (10 mL : 1 mL) were heated at reflux for 24 h under Ar. The evaporation residue, in EtOAc, was washed with water and brine. The organic layer was dried with MgSO₄ and the solvent was evaporated. The crude product was purified by chromatography.

General Procedure 3 - Pd-Catalysed Suzuki-Miyaura coupling of heteroaryl halides with arylboronic acids using the ligand SPhos.

The procedure of Buchwald and co-workers²⁰³ was adopted. A dried flask was charged with Pd(OAc)₂ (2.2 mg, 1.0 mol%), 2-(2',6'-dimethoxybiphenyl)dicyclohexylphosphine (8.2 mg, 2.0 mol %), arylboronic acid (1.5 mmol, 1.5 equiv.), powdered anhydrous K₃PO₄ (424 mg, 2.0 mmol, 2.0 equiv.), and heteroaryl halide (1.0 mmol, 1.0 equiv.). Dry toluene (2 mL) was added and the reaction mixture was heated at 100°C for 24 h under Ar. The reaction mixture was allowed to cool to ambient temperature, diluted with diethyl ether and filtered through a pad of silica gel (eluting with diethyl ether). The solvent was evaporated. The crude product was purified by chromatography.

General Procedure 4 - Pd-Catalysed Suzuki-Miyaura coupling of heteroaryl halides with pyridine boronic acids.

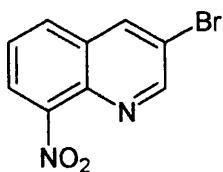
The heteroaryl halide (1.0 mmol, 1 equiv.), arylboronic acid (1.6 mmol, 1.6 equiv.), and Pd(PPh₃)₄ (5 mol%) were sequentially added to degassed DMF and the mixture was stirred for 30 min. Degassed aq. Na₂CO₃ (1 M) solution was added and the reaction mixture was heated under N₂ at 80°C until TLC monitoring showed that the reaction

was complete. The evaporation residue, in EtOAc, was washed with water and brine. The organic layer was dried with MgSO_4 and the solvent evaporated. The crude product was purified by chromatography.

General Procedure 5 - Stille coupling of heteroaryl halides with tetraalkyl stannane reagents.

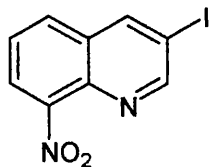
The heteroaryl halide (1.0 mmol, 1.0 equiv.), $\text{Pd}(\text{PPh}_3)_4$ (10 mol %) and tetraalkyl stannane reagent (2.0 mmol, 2.0 equiv.) in NMP (5 mL) were heated at 80°C for 24 h under N_2 . The mixture was extracted with EtOAc. The extract was washed with water and dried. The evaporation residue was purified by chromatography.

3-Bromo-8-nitroquinoline (60)



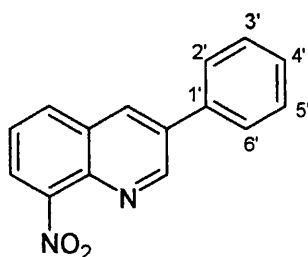
N-Bromosuccinimide (NBS, 356 mg, 2.0 mmol) was added in portions to 8-nitroquinoline **59** (348 mg, 2.0 mmol) in acetic acid (15 mL) during 1 h at 110°C. Heating under reflux was continued for 5 min and the mixture was stirred for 8 h at ambient temperature. The solution was poured into water with stirring and the pH was adjusted to 6 with aq. ammonia. The product was collected by filtration, washed with water and dried to give **60** (284 mg, 51%) as a pale yellow solid: $R_f = 0.4$ (hexane / EtOAc, 10:1); mp 119-120°C (lit.²⁶⁶ mp 123°C); ¹H NMR 270.05 MHz (CDCl₃) δ 7.65 (1 H, t, $J = 8.2$ Hz, 6-H), 7.95 (1 H, dd, $J = 8.2, 1.2$ Hz, 5-H), 8.06 (1 H, dd, $J = 8.2, 1.2$ Hz, 7-H), 8.43 (1 H, d, $J = 2.4$ Hz, 4-H), 9.05 (1 H, d, $J = 2.4$ Hz, 2-H); MS (FAB⁺) m/z 254.9604 (M + H) (C₉H₆⁸¹BrN₂O₂ requires 254.9592), 252.9607 (M + H) (C₉H₆⁷⁹BrN₂O₂ requires 252.9613), 206, 208 (M - NO₂).

3-Iodo-8-nitroquinoline (61)



8-Nitroquinoline **59** was treated with N-iodosuccinimide (NIS), as for the synthesis of **60**, to give **61** (71%) as a pale yellow solid: $R_f = 0.47$ (hexane / EtOAc, 10:1); mp 121-122°C (lit.²⁶⁷ mp 119-120°C); ¹H NMR 399.65 MHz (CDCl₃) δ 7.64 (1 H, t, $J = 8.1$ Hz, 6-H), 7.91 (1 H, dd, $J = 8.1, 1.2$ Hz, 5-H), 8.06 (1 H, dd, $J = 8.1, 1.2$ Hz, 7-H), 8.64 (1 H, d, $J = 2.0$ Hz, 4-H), 9.17 (1 H, d, $J = 2.0$ Hz, 2-H); MS (FAB⁺) m/z 301.9522 (M + H) (C₉H₆I₂N₂O₂ requires 301.9527), 255 (M - NO₂), 175 (M - I).

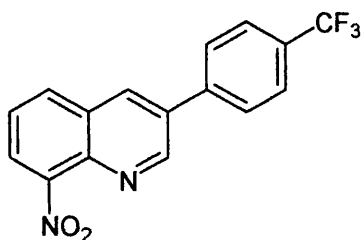
8-Nitro-3-phenylquinoline (62)



Method A: Compound **60** (506 mg, 2.0 mmol) was treated with phenylboronic acid (89.3 mg, 2.2 mmol) by General Procedure 1. Chromatography (hexane / EtOAc, 10:1) gave **62** (340 mg, 68%) as a white solid with properties as below.

Method B: Compound **61** was treated with phenylboronic acid and Pd(PPh₃)₄, as for the synthesis of **62** (Method A), to give **62** (97%) as a white solid: R_f = 0.18 (hexane / EtOAc, 10:1); mp 115-116°C (lit.²⁶⁸ mp 116-117°C); ¹H NMR 399.65 MHz (CDCl₃) δ 7.50 (1 H, tt, *J* = 8.2, 1.2 Hz, 4'-H), 7.56 (2 H, t, *J* = 8.2 Hz, 3',5'-H₂), 7.66 (1 H, t, *J* = 8.2 Hz, 6-H), 7.72 (2 H, dd, *J* = 8.2, 1.2 Hz, 2',6'-H₂), 8.06 (1 H, dd, *J* = 8.2, 1.2 Hz, 5-H), 8.11 (1 H, dd, *J* = 8.2, 1.2 Hz, 7-H), 8.39 (1 H, d, *J* = 2.3 Hz, 4-H), 9.34 (1 H, d, *J* = 2.3 Hz, 2-H); ¹³C NMR 399.65 MHz (HMBC) (CDCl₃) δ 123.7 (7-C), 125.8 (6-C), 127.5 (2',6'-C₂), 128.0 (4'-C), 129.0 (4a,8-C₂), 129.5 (3',5'-C₂), 132.5 (5-C), 133.0 (4-C), 135.7 (3-C), 136.7 (1'-C), 138.5 (8a-C), 152.3 (2-C).

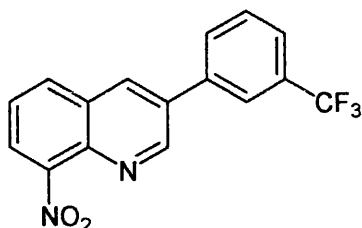
8-Nitro-3-(4-(trifluoromethyl)phenyl)quinoline (63)



Compound **61** (600 mg, 2.0 mmol) was treated with 4-trifluoromethylphenylboronic acid (418 mg, 2.2 mmol) by General Procedure 1. Chromatography (hexane / EtOAc, 10:1) gave **63** (470 mg, 74%) as a pale yellow solid: R_f = 0.24 (hexane / EtOAc, 10:1); mp 120-123°C; ¹H NMR 399.65 MHz (CDCl₃) δ 7.67 (1 H, t, *J* = 7.8 Hz, 6-H), 7.80 (4 H, s, 2',3',5',6'-H₄), 8.08 (1 H, dd, *J* = 7.8, 1.2 Hz, 5-H), 8.12 (1 H, dd, *J* = 7.8, 1.2 Hz, 7-H), 8.42 (1 H, d, *J* = 2.1 Hz, 4-H), 9.30 (1 H, d, *J* = 2.1 Hz, 2-H); ¹³C NMR 399.65 MHz

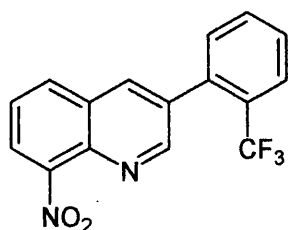
(HMBC) (CDCl₃) δ 123.9 (q, J = 271.4 Hz, CF₃), 124.2 (6-C), 126.1 (C-3), 126.4 (q, J = 3.8 Hz, 3',5'-C₂), 127.9 (2',6'-C₂), 128.7 (7-C), 130.9 (q, J = 32.9 Hz, 4'-C), 133.6 (5-C), 134.2 (4-C), 138.9 (8a-C), 140.2 (1'-C), 148.2 (8-C), 151.8 (2-C); ¹⁹F NMR (CDCl₃) δ -62.62 (s, CF₃); MS (ES⁺) m/z 319.0686 (M + H) (C₁₆H₁₀F₃N₂O₂ requires 319.0689), 249 (M - CF₃).

8-Nitro-3-(3-(trifluoromethyl)phenyl)quinoline (64)



Compound **61** (600 mg, 2.0 mmol) was treated with 3-trifluoromethylphenylboronic acid (418 mg, 2.2 mmol) by General Procedure 1. Chromatography (hexane / EtOAc, 10:1) gave **64** (620 mg, 97%) as a pale yellow solid: R_f = 0.26 (hexane / EtOAc, 10:1); mp 119-120°C; ¹H NMR 399.65 MHz (CDCl₃) δ 7.62-7.76 (3 H, m, 5',6',6-H₃), 7.88 (1 H, d, J = 7.4 Hz, 4'-H), 7.94 (1 H, s, 2'-H), 8.08 (1 H, dd, J = 7.4, 1.2 Hz, 5-H), 8.13 (1 H, dd, J = 7.4, 1.2 Hz, 7-H), 8.42 (1 H, d, J = 2.3 Hz, 4-H), 9.30 (1 H, d, J = 2.3 Hz, 2-H); ¹³C 399.65 MHz NMR (CDCl₃) δ 123.8 (q, J = 272.2 Hz, CF₃), 124.2 (CH), 124.3 (q, J = 3.8 Hz, CH), 125.5 (q, J = 3.8 Hz, CH), 126.1 (CH), 128.2 (q, J = 64.4 Hz, Cq), 128.7 (Cq), 130.0 (CH), 130.7 (CH), 132.3 (CH), 133.5 (CH), 134.2 (Cq), 137.5 (Cq), 138.8 (Cq), 148.1 (Cq), 151.7 (CH); ¹⁹F NMR (CDCl₃) δ -62.66 (s, CF₃); MS (ES⁺) m/z 319.0674 (M + H) (C₁₆H₁₀F₃N₂O₂ requires 319.0689).

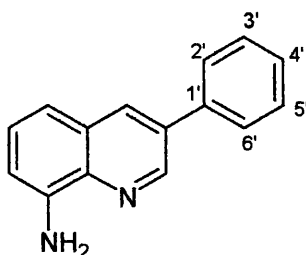
8-Nitro-3-(2-(trifluoromethyl)phenyl)quinoline (65)



Compound **61** (600 mg, 2.0 mmol) was treated with 2-trifluoromethylphenylboronic acid (418 mg, 2.2 mmol) by General Procedure 1. Chromatography (hexane / EtOAc, 10:1) gave **65** (420 mg, 66%) as a white solid: R_f = 0.27 (hexane / EtOAc, 10:1); mp 85-87°C; ¹H NMR 399.65 MHz (CDCl₃) δ 7.38 (1 H, d, J = 7.8 Hz, 6'-H), 7.60 (1 H, t, J =

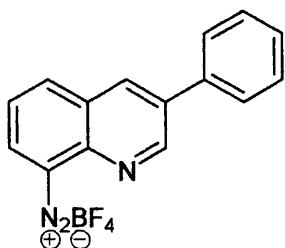
7.8 Hz, 4'-H), 7.58-7.72 (2 H, m, 5',6-H₂), 7.82 (1 H, d, *J* = 7.8 Hz, 3'-H), 8.08 (1 H, d, *J* = 7.4 Hz, 5-H), 8.10 (1 H, d, *J* = 7.4 Hz, 7-H), 8.22 (1 H, d, *J* = 1.8 Hz, 4-H), 9.03 (1 H, d, *J* = 1.8 Hz, 2-H), ¹³C NMR 399.65 MHz (HMBC) (CDCl₃) δ 123.8 (q, *J* = 273.7 Hz, CF₃), 124.2 (7-C), 125.9 (6-C), 126.5 (q, *J* = 5.3 Hz, 3'-C), 128.0 (3-C), 128.8 (4'-C), 129.0 (q, *J* = 29.9 Hz, 2'-C), 131.9 (5'-C), 132.1 (6'-C), 132.3 (5-C), 135.5 (4-C), 136.2 (8a-C), 138.6 (1'-C), 148.2 (4a,8-C₂), 152.8 (2-C); ¹⁹F NMR (CDCl₃) δ -56.63 (s, CF₃); MS (ES⁺) *m/z* 319.0673 (M + H) (C₁₆H₁₀F₃N₂O₂ requires 319.0689), 249 (M - CF₃).

3-Phenylquinolin-8-amine (66)



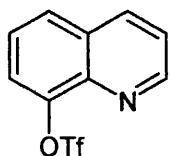
Anhydrous SnCl₂ (3.04 g, 16.0 mmol) was stirred with **62** (0.80 g, 3.2 mmol) in EtOH (50 mL) for 6 h. The mixture was poured into water and the solution was made alkaline with aq. NaOH. The precipitate, in EtOAc, was dried and the solvent was evaporated. Chromatography (hexane / EtOAc, 9:1) gave **66** (0.61 g, 82%) as a pale buff solid: *R_f* = 0.32 (hexane / EtOAc, 10:1); mp 74-76°C (lit.²⁶⁸ mp 74-75°C); ¹H NMR 399.65 MHz (CDCl₃) δ 4.96 (2 H, br, NH₂), 6.92 (1 H, dd, *J* = 7.7, 1.8 Hz, 7-H), 7.20 (1 H, dd, *J* = 7.7, 1.8 Hz, 5-H), 7.35 (1 H, t, *J* = 7.7 Hz, 6-H), 7.42 (1 H, tt, *J* = 8.1, 1.9 Hz, 4'-H), 7.51 (2 H, t, *J* = 8.1 Hz, 3',5'-H₂), 7.70 (2 H, dd, *J* = 8.1, 1.9 Hz, 2',6'-H₂), 8.20 (1 H, d, *J* = 2.4 Hz, 4-H), 9.02 (1 H, d, *J* = 2.4 Hz, 2-H).

3-Phenylquinoline-8-diazonium tetrafluoroborate (67)



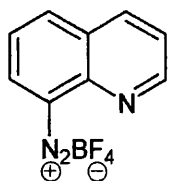
Compound **66** (500 mg, 2.3 mmol) in aq. HBF₄ (40%, 10 mL) was diazotised by slow addition of NaNO₂ (250 mg, 3.6 mmol) in iced water (2 mL) at 0°C and the mixture was stirred for 30 min. The diazonium salt was collected by filtration, washed once with cold aq. HBF₄, once with cold EtOH and four times with Et₂O to give **67** (300 mg, 41%) as a yellow solid: IR ν_{\max} (KBr) 2261 (N≡N⁺) cm⁻¹. This material was used without further purification or characterisation.

Quinolin-8-yl trifluoromethanesulfonate (82)



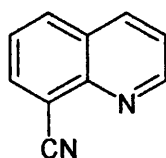
To quinolin-8-ol **81** (4.00 g, 27.6 mmol) in pyridine (10 mL) at 0°C was slowly added trifluoromethanesulfonic anhydride (9.32 g, 33.1 mmol). The mixture was stirred at 0°C for 5 min, then warmed to 23°C and stirred for 5 h. The mixture was poured into water and extracted with EtOAc. The organic extract was washed with water, 10% aq. HCl and water and dried. Evaporation and chromatography (hexane / EtOAc, 10:1) gave **82** (5.61 g, 73%) as a pale yellow solid: R_f = 0.38 (hexane / EtOAc, 10:1); mp 61-62°C (lit.²⁶⁹ mp 61-62°C); IR ν_{\max} (KBr) 1212 (CF), 1318 (SO₂) cm⁻¹; ¹H NMR 399.65 MHz (CDCl₃) δ 7.50 (1 H, dd, *J* = 8.4, 4.3 Hz, 3-H), 7.54 (1 H, t, *J* = 7.9 Hz, 6-H), 7.61 (1 H, dd, *J* = 7.9, 1.5 Hz, 7-H), 7.84 (1 H, dd, *J* = 7.9, 1.5 Hz, 5-H), 8.20 (1 H, dd, *J* = 8.4, 2.0 Hz, 4-H), 9.04 (1 H, dd, *J* = 4.3, 2.0 Hz, 2-H); ¹⁹F NMR (CDCl₃) δ -73.81 (s, CF₃).

Quinoline-8-diazonium tetrafluoroborate (71)



8-Aminoquinoline **70** (1.00 g, 6.9 mmol) in aq. HBF₄ (40%, 10 mL) was diazotised by slow addition of NaNO₂ (940 mg, 13.8 mmol) in iced water (2 mL) at 0°C and stirred for 20 min. The resulting diazonium salt was collected by filtration, washed once with cold aq. HBF₄, once with cold EtOH and four times with Et₂O to give **70** (910 mg, 54%) as a yellow solid: IR ν_{\max} (KBr) 2227 (N≡N⁺) cm⁻¹. This material was used without further purification or characterisation.

Quinoline-8-carbonitrile (72)



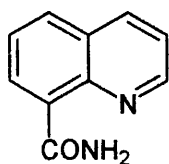
Method A: Compound **71** (300 mg, 1.2 mmol) was added to CuCN (421 mg, 4.8 mmol) and KCN (632 mg, 9.6 mmol) in water (10 mL). The mixture was heated at 50°C for 1 h, then stirred at ambient temperature for 8 h. The mixture was extracted with EtOAc. The extract was washed with water and dried and the solvent was evaporated. Chromatography (hexane / EtOAc, 10:1) gave **72** (170 mg, 92%) as a white solid with properties as described below.

Method B: Compound **82** (0.50 g, 1.8 mmol), CuI (34 mg, 0.18 mmol), KCN (0.23 g, 3.6 mmol) and Pd(PPh₃)₄ (0.10 g, 0.09 mmol) in dry MeCN (5 mL) were boiled under reflux for 25 h. The mixture was cooled to ambient temperature, diluted with EtOAc (10 mL), and then filtered through Celite[®]. The filtrate was washed with water and brine and dried. Evaporation and chromatography (hexane / EtOAc, 10:1) gave **72** (48 mg, 17%) as a white solid with properties as described below.

Method C: Compound **82** (3.00 g, 10.8 mmol), Zn(CN)₂ (0.78 g, 6.9 mmol) and Pd(PPh₃)₄ (1.28 g, 1.1 mmol) in DMF (30 mL) were heated at reflux for 2 h. The mixture was diluted with water (200 mL) and 2 M aq. sulfuric acid (20 mL) (CAUTION)

and extracted with EtOAc. The combined extracts were washed with brine and dried. Evaporation and recrystallisation (hexane / EtOAc) provided **72** (1.24 g, 73%) as a white solid: $R_f = 0.34$ (hexane / EtOAc, 10:1); mp 86-88°C (lit.¹⁹⁶ mp 87.5-88.5°C); IR ν_{\max} (KBr) 2232 (C≡N) cm^{-1} ; $^1\text{H NMR}$ 399.65 MHz (CDCl_3) δ 7.48-7.58 (2 H, m, 3,6- H_2), 8.02-8.08 (2 H, m, 5,7- H_2), 8.21 (1 H, dd, $J = 8.6, 1.6$ Hz, 4-H), 9.03 (1 H, dd, $J = 4.3, 1.6$ Hz, 2-H); MS (EI^+) m/z 154.0525 (M) ($\text{C}_{10}\text{H}_6\text{N}_2$ requires 154.0531), 128 (M - CN).

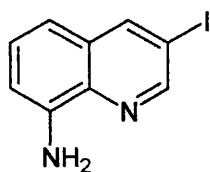
Quinoline-8-carboxamide (**80**)



Method A: Compound **72** (1.00 g, 6.5 mmol), in EtOH (10 mL), was treated with aq. 0.5 M NaOH (12.7 mL, 6.5 mmol) and 35% aq. H_2O_2 (2.2 mL, 23 mmol). The mixture was heated to 50°C for 1 h and allowed to cool and was neutralised with 10% w/v aq. sulfuric acid. The evaporation residue, in CH_2Cl_2 , was washed with water and brine. Drying and evaporation gave **80** (0.87 g, 78%) with properties as described below.

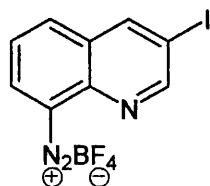
Method B: To 8-bromoquinoline **78** (500 mg, 2.4 mmol) in dry THF (2 mL) at -79°C was added $n\text{-BuLi}$ (1.6 M in hexanes, 1.7 mL, 2.6 mmol). After 30 min, trimethylsilylisocyanate (1 mL, 7.4 mmol) was added. The solution was stirred for a further 15 min at -79°C and for 12 h at 20°C. The evaporation residue, in CH_2Cl_2 , was washed with water and brine and was filtered. Evaporation and chromatography (CH_2Cl_2 / EtOAc, 1:2) gave **80** (200 mg, 48%) as a white solid: $R_f = 0.23$ (CH_2Cl_2 / EtOAc, 1:2); mp 170-172°C (lit.²⁷⁰ mp 171-173°C); IR ν_{\max} (KBr) 1593 (Amide II), 1654 (Amide I), 3330 & 3468 (NH_2) cm^{-1} ; $^1\text{H NMR}$ 399.65 MHz (CDCl_3) δ 6.49 (1 H, br, NH), 7.44 (1 H, dd, $J = 8.2, 4.4$ Hz, 3-H), 7.63 (1 H, t, $J = 7.9$ Hz, 6-H), 7.94 (1 H, dd, $J = 7.9, 2.2$ Hz, 5-H), 8.23 (1 H, dd, $J = 7.9, 2.2$ Hz, 7-H), 8.82 (1 H, dd, $J = 8.2, 2.3$ Hz, 4-H), 8.88 (1 H, dd, $J = 4.4, 2.3$ Hz, 2-H), 10.95 (1 H, br, NH); MS (FAB^+) m/z 173.0717 (M + H) ($\text{C}_{10}\text{H}_9\text{N}_2\text{O}$ requires 173.0715); Anal. Calcd. for $\text{C}_{10}\text{H}_9\text{N}_2\text{O}$: C, 69.76; H, 4.68; N, 16.27. Found: C, 69.62; H, 4.77; N, 16.12.

3-Iodoquinoline-8-amine (74)



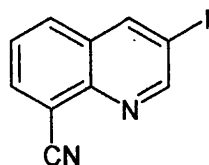
Anhydrous SnCl_2 (1.10 g, 5.8 mmol) in MeOH (5 mL) was stirred with **61** (0.50 g, 1.7 mmol) in CHCl_3 (25 mL) for 8 h. The solution was diluted with CH_2Cl_2 and washed with aq. NaOH (0.5 M). Drying, evaporation and chromatography (hexane / EtOAc, 4:1) gave **74** (0.21 g, 46%) as a pale yellow solid: $R_f = 0.51$ (hexane / EtOAc, 10:1); mp 125-128°C (lit.²⁶⁷ mp 129°C); $^1\text{H NMR}$ 270.05 MHz (CDCl_3) δ 4.95 (2 H, br, NH_2), 6.92 (1 H, dd, $J = 7.7, 1.2$ Hz, 7-H), 7.02 (1 H, dd, $J = 7.7, 1.2$ Hz, 5-H), 7.29 (1 H, t, $J = 7.7$ Hz, 6-H), 8.42 (1 H, d, $J = 2.0$ Hz, 4-H), 8.84 (1 H, d, $J = 2.0$ Hz, 2-H); MS (FAB⁺) m/z 271.9766 (M + H) ($\text{C}_9\text{H}_8\text{IN}_2$ requires 271.9766).

3-Iodoquinoline-8-diazonium tetrafluoroborate (75)



Compound **74** (600 mg, 2.2 mmol) in aq. HBF_4 (40%, 10 mL) was diazotised by slow addition of NaNO_2 (300 mg, 4.4 mmol) in iced water (2 mL) at 0°C and stirred for 20 min. The resulting diazonium salt was collected by filtration, washed once with cold aq. HBF_4 , once with cold EtOH and four times with Et_2O to give **75** (410 mg, 50%) as a yellow solid: IR ν_{max} (KBr) 2254 ($\text{N}\equiv\text{N}^+$) cm^{-1} . This material was used without further purification or characterisation.

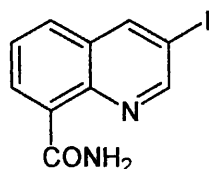
3-Iodoquinoline-8-carbonitrile (76)



Method A: Compound **75** (300 mg, 0.80 mmol) was added to CuCN (290 mg, 3.3 mmol) and KCN (420 mg, 6.7 mmol) in water (8 mL). The mixture was heated at 50°C for 1 h, then stirred at ambient temperature for 8 h. The mixture was extracted with EtOAc. The extract was washed with water and dried and the solvent was evaporated. Chromatography (hexane / EtOAc, 10:1) gave **76** (113 mg, 50%) as a pale buff solid with properties as described below.

Method B: Compound **72** (650 mg, 4.2 mmol) was treated with NIS (940 mg, 4.2 mmol) in AcOH (10 mL) and heated under reflux for 3 h. The mixture was extracted with EtOAc. The extract was washed with aq. NaHCO₃ and dried. Evaporation and chromatography (hexane / EtOAc, 2:3) gave **76** (412 mg, 35%) as a pale buff solid: R_f = 0.41 (EtOAc / hexane, 1:10); mp 82-84°C; IR ν_{\max} (KBr) 2250 (C≡N) cm⁻¹; ¹H NMR 399.65 MHz (CDCl₃) δ 7.62 (1 H, t, *J* = 7.5 Hz, 6-H), 7.96 (1 H, dd, *J* = 7.5, 1.2 Hz, 5-H), 8.13 (1 H, dd, *J* = 7.5, 1.2 Hz, 7-H), 8.62 (1 H, d, *J* = 2.0 Hz, 4-H), 9.19 (1 H, d, *J* = 2.0 Hz, 2-H); ¹³C NMR 399.65 MHz (HMBC) (CDCl₃) δ 91.9 (3-C), 113.4 (8-C), 116.7 (CN), 126.8 (6-C), 129.6 (4a-C), 131.7 (5-C), 135.9 (7-C), 144.1 (4-C), 145.6 (8a-C), 157.8 (2-C); MS (ES⁺) *m/z* 583 (2 M + Na), 280.9557 (M + H) (C₁₀H₆IN₂ requires 280.9570); Anal. Calcd. for C₁₀H₅IN₂: C, 42.89; H, 1.80; N, 10.00. Found: C, 42.83; H, 2.00; N, 9.78.

3-Iodoquinoline-8-carboxamide (77)

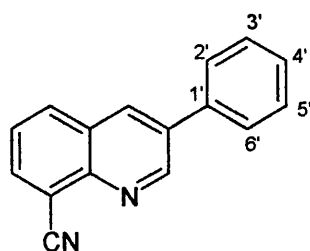


Method A: Compound **76** (50 mg, 0.20 mmol) in EtOH (1 mL), was treated with aq. NaOH (0.5 M, 3.5 mL, 1.8 mmol) and 35% w/v aq. H₂O₂ (0.2 mL). The mixture was heated to 50°C for 1 h, allowed to cool and neutralised with 10% w/v aq. sulfuric acid. The evaporation residue, in CH₂Cl₂, was washed with brine, dried and filtered.

Evaporation and chromatography (hexane / EtOAc, 3:2) gave **77** (23 mg, 43%) as a pale yellow solid with properties as below.

Method B: Compound **80** (700 mg, 4.1 mmol), NIS (910 mg, 4.1 mmol) in AcOH (7 mL) and FeCl₃ (5 mol%) were heated at reflux for 24 h. The mixture was then poured into water (100 mL) and extracted with CHCl₃. Washing (aq. NaHCO₃), drying, evaporation and chromatography (hexane / EtOAc, 3:2) gave **77** (0.48 g, 40%) as a pale yellow solid: R_f = 0.51 (hexane / EtOAc, 3:2); mp 211-214°C; IR ν_{\max} (KBr) 1562 (Amide II), 1668 (Amide I), 3302 & 3420 (NH₂) cm⁻¹; ¹H NMR 399.65 MHz (CDCl₃) δ 6.11 (1 H, br, NH), 7.72 (1 H, t, *J* = 8.0 Hz, 6-H), 7.89 (1 H, dd, *J* = 8.0, 1.5 Hz, 5-H), 8.64 (1 H, d, *J* = 2.2 Hz, 4-H), 8.86 (1 H, dd, *J* = 8.0, 1.5 Hz, 7-H), 9.05 (1 H, d, *J* = 2.2 Hz, 2-H), 10.53 (1 H, br, NH); ¹³C NMR 399.65 MHz (HMBC) (CDCl₃) δ 89.4 (3-C), 127.5 (6-C), 128.8 (4a-C or C-8), 130.2 (8-C or 4a-C), 131.4 (5-C), 134.8 (7-C), 143.8 (8a-C), 145.2 (5-C), 154.9 (2-C), 167.0 (CONH₂); MS (FAB⁺) *m/z* 298.9689 (M + H) (C₁₀H₇N₂O requires 298.9681).

3-Phenylquinoline-8-carbonitrile (**68**)

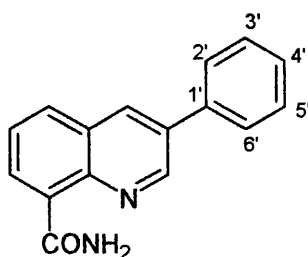


Method A: Compound **67** (200 mg, 0.60 mmol) was added to CuCN (203 mg, 2.0 mmol) and KCN (290 mg, 4.5 mmol) in water (8 mL). The mixture was heated at 50°C for 1 h, then stirred at ambient temperature for 8 h. The mixture was extracted with EtOAc. The extract was washed with water, dried and the solvent was evaporated. Chromatography (hexane / EtOAc, 10:1) gave **68** (110 mg, 78%) as a pale buff solid with properties as described below.

Method B: Compound **76** (557 mg, 2.0 mmol) was treated with phenylboronic acid (364 mg, 3.0 mmol) by General Procedure 3. Chromatography (hexane / EtOAc, 3:2) gave **68** (390 mg, 86%) as a white solid: R_f = 0.51 (hexane / EtOAc, 10:1); mp 122-124°C; IR ν_{\max} (KBr) 2230 (C≡N) cm⁻¹; ¹H NMR 399.65 MHz (CDCl₃) δ 7.47 (1 H, t, *J* = 7.4 Hz, 4'-H), 7.53 (2 H, t, *J* = 7.4 Hz, 3',5'-H₂), 7.64 (1 H, t, *J* = 7.5 Hz, 6-H), 7.71 (2 H, d, *J* = 7.4 Hz, 2',6'-H₂), 8.10 (1 H, dd, *J* = 7.5, 2.0 Hz, 5-H), 8.13 (1 H, dd, *J* = 7.5, 2.0

Hz, 7-H), 8.36 (1 H, d, $J = 2.4$ Hz, 4-H), 9.34 (1 H, d, $J = 2.4$ Hz, 2-H); ^{13}C NMR 399.65 MHz (HMBC) (CDCl_3) δ 113.0 (8-C), 117.2 (CN), 126.3 (6-C), 127.5 (2',6'-C₂), 128.0 (4a-C), 128.7 (4'-C), 129.4 (3',5'-C₂), 133.0 (5-C), 133.3 (4-C), 135.2 (7-C), 135.6 (3-C), 136.8 (1'-C), 146.5 (8a-C), 152.1 (2-C); MS (ES^+) m/z 483 (2 M + Na), 231.0909 (M + H) ($\text{C}_{16}\text{H}_{11}\text{N}_2$ requires 231.0917); Anal. Calcd. for $\text{C}_{16}\text{H}_{10}\text{N}_2$: C, 83.46; H, 4.38; N, 12.17. Found: C, 83.39; H, 4.39; N, 12.09.

3-Phenylquinoline-8-carboxamide (69)



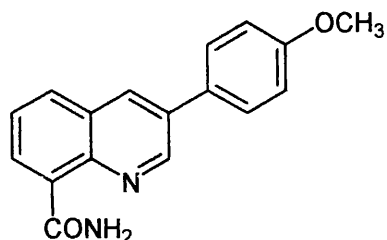
Method A: Compound **68** (50 mg, 0.20 mmol) in EtOH (1 mL), was treated with aq. 0.5 M NaOH (4.3 mL, 2.2 mmol) and 35% w/v aq. H_2O_2 (0.2 mL). The mixture was heated to 50°C for 1 h and allowed to cool; it was then neutralised with aq. H_2SO_4 (10%). The evaporation residue, in CH_2Cl_2 , was washed with water and brine. Drying and evaporation gave **69** (32 mg, 60%) as a pale yellow solid with properties as described below.

Method B: Compound **77** (100 mg, 0.34 mmol) was treated with phenylboronic acid (46 mg, 0.37 mmol) by General Procedure 1. Chromatography (hexane / EtOAc, 10:1) gave **69** (64 mg, 76%) as a pale yellow solid with properties as described below.

Method C: Compound **77** (149 mg, 0.50 mmol) was treated with phenylboronic acid (91 mg, 0.75 mmol) by General Procedure 3. Recrystallisation (hexane / EtOAc) gave **69** (115 mg, 93%) as a pale yellow solid: $R_f = 0.53$ (hexane / EtOAc, 2:3); mp 130-132°C; IR ν_{max} (KBr) 1600 (Amide II), 1674 (Amide I), 3270 & 3468 (NH_2) cm^{-1} ; ^1H NMR 399.65 MHz (CDCl_3) δ 6.17 (1 H, br, NH), 7.48 (1 H, t, $J = 8.0$ Hz, 4'-H), 7.56 (2 H, t, $J = 8.0$ Hz, 3',5'-H₂), 7.60 (1 H, t, $J = 7.5$ Hz, 6-H), 7.65-7.62 (2 H, m, 2',6'-H₂), 8.06 (1 H, dd, $J = 7.5, 1.4$ Hz, 5-H), 8.42 (1 H, d, $J = 2.3$ Hz, 4-H), 8.86 (1 H, dd, $J = 7.5, 1.4$ Hz, 7-H), 9.20 (1 H, d, $J = 2.3$ Hz, 2-H), 10.95 (1 H, br, NH); ^{13}C NMR 399.65 MHz (HMBC) (CDCl_3) δ 126.8 (8-C), 127.3 (6-C), 128.4 (2',6'-C₂), 128.4 (4a-C), 128.6 (3',5'-C₂), 129.3 (4'-C), 132.7 (4-C), 133.8 (5-C), 134.1 (7-C), 134.6 (3-C), 137.1 (1'-C), 144.7

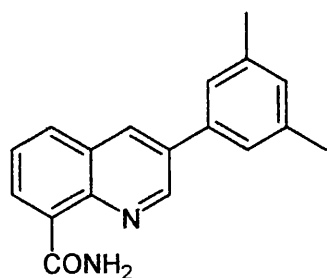
(8a-C), 149.0 (2-C), 167.6 (CONH₂); MS (FAB⁺) *m/z* 249.1030 (M + H) (C₁₆H₁₃N₂O requires 249.1028), 232 (M - NH₂).

3-(4-Methoxyphenyl)quinoline-8-carboxamide (91)



Compound **77** (158 mg, 0.53 mmol) was treated with 4-methoxyphenylboronic acid (88 mg, 0.58 mmol) by General Procedure 1. Chromatography (hexane / EtOAc, 10:1) gave **91** (140 mg, 95%) as a pale yellow solid: *R_f* = 0.30 (hexane / EtOAc, 10:1); mp 190-192°C; IR ν_{\max} (KBr) 1607 (Amide II) 1657 (Amide I), 3200 & 3468 (NH₂) cm⁻¹; ¹H NMR 399.65 MHz (CDCl₃) δ 3.88 (3 H, s, CH₃), 6.21 (1 H, br, NH), 7.06 (2 H, d, *J* = 8.6 Hz, 3',5'-H₂), 7.64 (2 H, d, *J* = 8.6 Hz, 2',6'-H₂), 7.66 (1 H, t, *J* = 8.0 Hz, 6-H), 8.00 (1 H, dd, *J* = 8.0, 1.4 Hz, 5-H), 8.33 (1 H, d, *J* = 2.3 Hz, 4-H), 8.80 (1 H, dd, *J* = 8.0, 1.4 Hz, 7-H), 9.16 (1 H, d, *J* = 2.3 Hz, 2-H), 10.96 (1 H, br, NH); ¹³C NMR 399.65 MHz (HMBC) (CDCl₃) δ 55.4 (CH₃), 114.8 (3',5'-C₂), 126.8 (6-C), 128.4 (2',6'-C₂), 128.3 (1'-C), 128.4 (4a-C or 8-C), 129.3 (8-C or 4a-C), 132.5 (5-C), 133.5 (3-C), 133.6 (7-C), 133.7 (4-C), 144.3 (8a-C), 148.8 (2-C), 160.4 (4'-C), 167.6 (CONH₂); MS (ES⁺) *m/z* 279.1129 (M + H) (C₁₇H₁₅N₂O₂ requires 279.1128), 261 (M + H - H₂O), 235 (M + H - CONH₂); Anal. Calcd. for C₁₇H₁₄N₂O₂: C, 73.37; H, 5.07; N, 10.07. Found: C, 72.92; H, 4.69; N, 9.63.

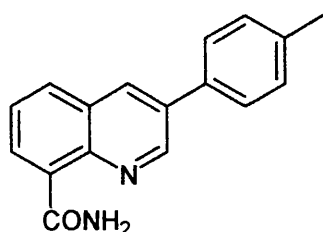
3-(3,5-Dimethylphenyl)quinoline-8-carboxamide (92)



Compound **77** (100 mg, 0.34 mmol) was treated with 3,5-dimethylphenylboronic acid (56 mg, 0.37 mmol) by General Procedure 1. Recrystallisation (hexane / EtOAc) gave

92 (61 mg, 65%) as a white solid: $R_f = 0.30$ (hexane / EtOAc, 3:2); mp 209-211°C; IR ν_{\max} (KBr) 1597 (Amide II), 1665 (Amide I), 3281 & 3468 (NH₂) cm⁻¹; ¹H NMR 399.65 MHz (CDCl₃) δ 2.43 (6 H, s, 2 x CH₃), 6.13 (1 H, br, NH), 7.11 (1 H, s, 4'-H), 7.32 (2 H, s, 2',6'-H₂), 7.70 (1 H, t, $J = 8.0$ Hz, 6-H), 8.04 (1 H, dd, $J = 8.0, 1.4$ Hz, 5-H), 8.39 (1 H, d, $J = 2.5$ Hz, 4-H), 8.84 (1 H, dd, $J = 8.0, 1.4$ Hz, 7-H), 9.17 (1 H, d, $J = 2.5$ Hz, 2-H), 10.98 (1 H, br, NH); ¹³C NMR 399.65 MHz (HMBC) (CDCl₃) δ 21.4 (2xCH₃), 125.2 (2',6'-C₂), 128.1 (4a-C or 8-C), 128.4 (8-C or 4a-C), 128.5 (6-C), 130.2 (4'-C), 132.6 (4-C), 133.9 (7-C), 134.0 (3-C), 134.5 (5-C), 136.1 (1'-C), 139.0 (3',5'-C₂), 144.6 (8a-C), 149.1 (2-C), 167.6 (CONH₂); MS (ES⁺) m/z 277.1334 (M + H) (C₁₈H₁₇N₂O requires 277.1335), 233 (M + H - CONH₂).

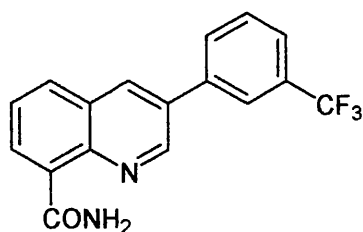
3-(4-Methylphenyl)quinoline-8-carboxamide (**93**)



Method A: Compound **77** (100 mg, 0.34 mmol) was treated with toluene-4-boronic acid (51 mg, 0.37 mmol) by General Procedure 2. Recrystallisation (hexane / EtOAc) gave **93** (43 mg, 48%) as a white solid with properties as described below.

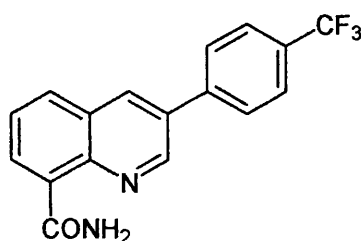
Method B: Compound **77** (447 mg, 3.0 mmol) was treated with toluene-4-boronic acid (306 mg, 2.3 mmol) by General Procedure 3. Recrystallisation (hexane / EtOAc) gave **93** (306 mg, 78%) as a white solid: $R_f = 0.35$ (hexane / EtOAc, 3:2); mp 176-177°C; IR ν_{\max} (KBr) 1599 (Amide II), 1675 (Amide I), 3283 & 3468 (NH₂) cm⁻¹; ¹H NMR 399.65 MHz (CDCl₃) δ 2.44 (3 H, s, CH₃), 6.17 (1 H, br, NH), 7.36 (2 H, d, $J = 8.0$ Hz, 3',5'-H₂), 7.63 (2 H, d, $J = 8.0$ Hz, 2',6'-H₂), 7.69 (1 H, t, $J = 8.0$ Hz, 6-H), 8.04 (1 H, dd, $J = 8.0, 1.5$ Hz, 5-H), 8.39 (1 H, d, $J = 2.0$ Hz, 4-H), 8.83 (1 H, dd, $J = 8.0, 1.5$ Hz, 7-H) 9.19 (1 H, d, $J = 2.0$ Hz, 2-H), 10.96 (1 H, br, NH); ¹³C NMR 399.65 MHz (HMBC) (CDCl₃) δ 21.2 (CH₃), 126.8 (6-C), 127.2 (3',5'-C₂), 128.4 (4a,8-C₂), 130.1 (2',6'-C₂), 132.6 (5-C), 133.7 (3-C or 1'-C), 133.8 (1'-C or 3-C), 134.1 (4-C), 134.2 (7-C), 138.6 (4'-C), 144.5 (8a-C), 149.0 (2-C), 167.6 (CONH₂); MS (ES⁺) m/z 263.1176 (M + H) (C₁₇H₁₅N₂O requires 263.1179), 219 (M + H - CONH₂); Anal. Calcd. for C₁₇H₁₄N₂O: C, 77.84; H, 5.38; N, 10.68. Found: C, 77.54; H, 5.21; N, 10.47.

3-(3-(Trifluoromethyl)phenyl)quinoline-8-carboxamide (94)



Compound **77** (158 mg, 0.53 mmol) was treated with 3-(trifluoromethyl)phenylboronic acid (111 mg, 0.58 mmol) by General Procedure 1. Chromatography (hexane / EtOAc, 10:1) gave **94** (73 mg, 43%) as a white solid: $R_f = 0.27$ (hexane / EtOAc, 10:1); mp 228-229°C; IR ν_{\max} (KBr) 1571 (Amide II), 1669 (Amide I), 3058 & 3466 (NH₂) cm⁻¹; ¹H NMR 399.65 MHz ((CD₃)₂SO) δ 7.78 (1 H, dd, $J = 7.9, 7.4$ Hz, 5'-H), 7.83 (1 H, d, $J = 7.4$ Hz, 6'-H), 7.86 (1 H, brd, $J = 7.9$ Hz, 4'-H), 8.00 (1 H, br, NH), 8.27 (1 H, d, $J = 4.3$ Hz, 2'-H), 8.29 (1 H, m, 6-H), 8.30 (1 H, dd, $J = 7.7, 1.9$ Hz, 5-H), 8.58 (1 H, dd, 7.7, 1.9 Hz, 7-H), 9.00 (1 H, d, $J = 2.3$ Hz, 4-H), 9.47 (1 H, d, $J = 2.3$ Hz, 2-H), 10.14 (1 H, br, NH); ¹³C NMR 399.65 MHz ((CD₃)₂SO) δ 123.9 (m), 125.1 (m), 127.0 (CH), 128.0 (CH), 129.5 (CH), 130.4 (CH), 131.3 (Cq), 131.4 (CH), 132.8 (CH), 133.1 (CH), 135.4 (CH), 137.6 (Cq), 144.2 (CH), 149.2 (CH), 166.3 (CONH₂); ¹⁹F NMR ((CD₃)₂SO) δ -62.56 (s, CF₃); MS (ES⁺) m/z 655 (2 M + Na), 317.0881 (M + H) (C₁₇H₁₂F₃N₂O requires 317.0896); Anal. Calcd. for C₁₇H₁₂F₃N₂O: C, 64.56; H, 3.51; N, 8.86. Found: C, 64.78; H, 3.49; N, 8.84.

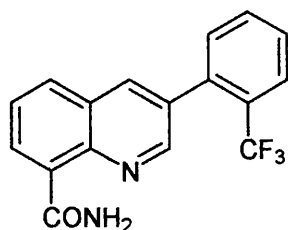
3-(4-(Trifluoromethyl)phenyl)quinoline-8-carboxamide (95)



Compound **77** (158 mg, 0.53 mmol) was treated with 4-(trifluoromethyl)phenylboronic acid (111 mg, 0.58 mmol) by General Procedure 1. Chromatography (EtOAc / hexane, 5:2) gave **95** (64 mg, 38%) as a white solid: $R_f = 0.27$ (hexane / EtOAc, 10:1); mp 184-185°C; IR ν_{\max} (KBr) 1572 (Amide II), 1671 (Amide I), 3120 & 3469 (NH₂) cm⁻¹; ¹H NMR 399.65 MHz (CDCl₃) δ 6.18 (1 H, br, NH), 7.73 (1 H, t, $J = 7.8$ Hz, 6-H), 7.80 (2 H, d, $J = 8.7$ Hz, 2',6'-H₂), 7.84 (2 H, d, $J = 8.7$ Hz, 3',5'-H₂), 8.09 (1 H, dd, $J = 7.8, 1.4$ Hz, 5-

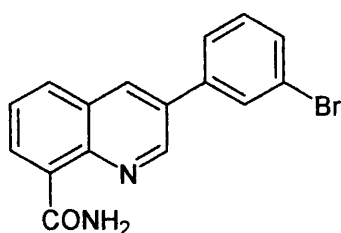
H), 8.45 (1 H, d, $J = 2.4$ Hz, 4-H), 8.89 (1 H, dd, $J = 7.8, 1.4$ Hz, 7-H), 9.20 (1 H, d, $J = 2.4$ Hz, 2-H), 10.86 (1 H, br, NH); ^{13}C NMR 399.65 MHz (HMBC) (CDCl_3) δ 124.0 (q, $J = 272.2$ Hz, CF_3), 126.3 (q, $J = 3.8$ Hz, 3',5'- C_2), 127.3 (6-C), 127.7 (2',6'- C_2), 128.2 (4a-C or 8-C), 128.5 (8-C or 4a-C), 130.6 (q, $J = 32.2$ Hz, 4'-C), 132.4 (1'-C), 132.8 (5-C), 134.7 (7-C), 135.2 (4-C), 140.6 (3-C), 145.0 (8a-C), 148.6 (2-C), 167.4 (CONH_2); ^{19}F NMR (CDCl_3) δ -60.92 (s, CF_3); MS (ES^+) m/z 317.0897 (M + H) ($\text{C}_{17}\text{H}_{12}\text{F}_3\text{N}_2\text{O}$ requires 317.0896), 299 (M + H - H_2O), 69 (CF_3), 273 (M + H - CONH_2).

3-(2-(Trifluoromethyl)phenyl)quinoline-8-carboxamide (96)



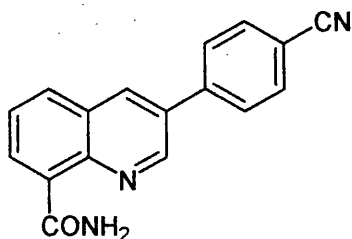
Compound **77** (158 mg, 0.53 mmol) was treated with 2-(trifluoromethyl)phenylboronic acid (111 mg, 0.58 mmol) by General Procedure 1. Chromatography (hexane / EtOAc, 10:1) gave **96** (46 mg, 27%) as a pale yellow solid: $R_f = 0.25$ (hexane / EtOAc, 10:1); mp 165-167°C, IR ν_{max} (KBr) 1571 (Amide II), 1669 (Amide I), 3468 & 3100 (NH_2) cm^{-1} ; ^1H NMR 399.65 MHz (CDCl_3) δ 6.21 (1 H, br, NH), 7.42 (1 H, d, $J = 7.6$ Hz, 6'-H), 7.60 (1 H, t, $J = 7.6$ Hz, 4'-H), 7.66 (1 H, t, $J = 7.6$ Hz, 5'-H), 7.73 (1 H, t, $J = 7.6$ Hz, 6-H), 7.85 (1 H, d, $J = 7.6$ Hz, 5-H), 8.03 (1 H, dd, $J = 7.6, 1.4$ Hz, 3'-H), 8.24 (1 H, dd, $J = 1.7$ Hz, 4-H), 8.88 (1 H, d, $J = 7.6$ Hz, 7-H), 8.90 (1 H, d, $J = 1.7$ Hz, 2-H), 10.91 (1 H, br, NH); ^{13}C NMR 399.65 MHz (HMBC) (CDCl_3) δ 126.5 (q, $J = 5.4$ Hz, 3'-C), 127.0 (6-C), 127.5 (4a-C or 8-C), 128.6 (4'-C), 128.9 (8-C or 4a-C), 129.1 (q, $J = 30.6$ Hz, 2'-C), 131.8 (6'-C), 132.0 (5'-C), 132.7 (5-C), 132.8 (3-C), 134.6 (7-C), 136.6 (q, $J = <2$ Hz, 1'-C), 137.0 (4-C), 144.7 (8a-C), 149.6 (2-C), 167.5 (CONH_2), CF_3 peak not observed; ^{19}F NMR (CDCl_3) δ -56.70 (s, CF_3); MS (ES^+) m/z 655 (2 M + Na), 317.0884 (M + H) ($\text{C}_{17}\text{H}_{12}\text{F}_3\text{N}_2\text{O}$ requires 317.0896).

3-(3-Bromophenyl)quinoline-8-carboxamide (97)



Compound **77** (158 mg, 0.53 mmol) was treated with 3-bromophenylboronic acid (116 mg, 0.58 mmol) by General Procedure 1. Recrystallisation (CHCl₃ / EtOAc) gave **97** (53 mg, 31%) as a white solid: *R*_f = 0.28 (hexane / EtOAc, 10:1); mp 178-180°C; IR ν_{\max} (KBr) 1597 (Amide II), 1665 (Amide I), 3282 & 3454 (NH₂) cm⁻¹; ¹H NMR 399.65 MHz (CDCl₃) δ 6.26 (1 H, br, NH), 7.42 (1 H, t, *J* = 7.8 Hz, 5'-H), 7.60 (1 H, dd, *J* = 7.8, 1.7 Hz, 4'-H), 7.64 (1 H, dd, *J* = 7.8, 1.7 Hz, 6'-H), 7.73 (1 H, t, *J* = 7.7 Hz, 6-H), 7.86 (1 H, t, *J* = 1.7 Hz, 2'-H), 8.06 (1 H, dd, *J* = 7.7, 1.6 Hz, 5-H), 8.40 (1 H, d, *J* = 2.3 Hz, 4-H), 8.85 (1 H, dd, *J* = 7.7, 1.6 Hz, 7-H), 9.14 (1 H, d, *J* = 2.3 Hz, 2-H) 10.92 (1 H, br, NH); ¹³C NMR 399.65 MHz (HMBC) (CDCl₃) δ 123.4 (3'-C), 125.9 (6'-C), 127.1 (6-C), 128.2 (4a-C or 8-C), 128.3 (8-C or 4a-C), 130.4 (5'-C), 131.5 (4'-C), 132.4 (3-C), 132.8 (2'-C), 134.5 (5-C), 134.9 (7-C), 135.2 (4-C), 139.1 (1'-C), 144.8 (8a-C), 148.6 (2-C), 167.5 (CONH₂); MS (FAB⁺) *m/z* 329.0102 (M + H) (C₁₆H₁₂⁸¹BrN₂O requires 329.0113), 327.0119 (M + H) (C₁₆H₁₂⁷⁹BrN₂O requires 327.0133); Anal. Calcd. for C₁₆H₁₁BrN₂O.0.75 CHCl₃: C, 48.28; H, 2.84; N, 6.02. Found: C, 48.55; H, 2.70; N, 6.03.

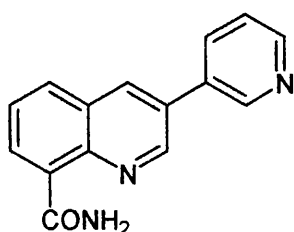
3-(4-Cyanophenyl)quinoline-8-carboxamide (98)



Compound **77** (158 mg, 0.53 mmol) was treated with 4-cyanophenylboronic acid (85 mg, 0.58 mmol) by General Procedure 1. Chromatography (petroleum ether / EtOAc, 3:2) gave **98** (58 mg, 40%) as white solid: *R*_f = 0.30 (petroleum ether / EtOAc, 3:2); mp 209-211°C; IR ν_{\max} (KBr) 1598 (Amide II), 1674 (Amide I), 2363 (C≡N), 3268 & 3467 (NH₂) cm⁻¹; ¹H NMR 399.65 MHz (CDCl₃) δ 6.20 (1 H, br, NH), 7.74 (1 H, t, *J* = 7.7 Hz, 6-H), 7.82 (4 H, s, 2',3',5',6'-H₄), 8.08 (1 H, dd, *J* = 7.7, 1.4 Hz, 5-H), 8.45 (1 H, d, *J* =

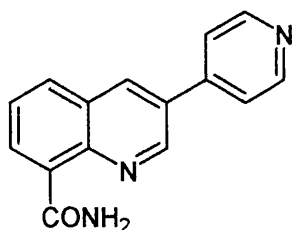
2.3 Hz, 4-H), 8.85 (1 H, dd, $J = 7.7, 1.4$ Hz, 7-H), 9.18 (1 H, d, $J = 2.3$ Hz, 2-H), 10.91 (1 H, br, NH); ^{13}C NMR 399.65 MHz (HMBC) (CDCl_3) δ 112.2 (4'-C), 118.4 (CN), 127.4 (2',6'-C₂), 127.9 (6-C), 128.0 (4a-C or 8-C), 128.3 (8-C or 4a-C), 131.8 (3',5'-C₂), 132.9 (7-C), 133.1 (4-C), 134.9 (5-C), 135.4 (3-C), 141.5 (1'-C), 145.1 (8a-C), 148.3 (2-C), 167.3 (CONH₂); MS (ES⁺) m/z 274.0974 (M + H) ($\text{C}_{17}\text{H}_{12}\text{N}_3\text{O}$ requires 274.0975), 230 (M + H - CONH₂)

3-(Pyridin-3-yl)quinoline-8-carboxamide (**99**)



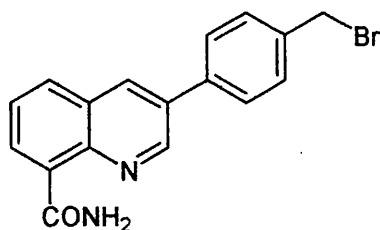
Compound **77** (312 mg, 1.1 mmol) was treated with pyridine-3-boronic acid (206 mg, 1.7 mmol) by General Procedure 4. Chromatography (petroleum ether / EtOAc, 3:2) gave **99** (68 mg, 26%) as a pale yellow solid: $R_f = 0.29$ (petroleum ether / EtOAc, 3:2); mp 136-137°C; IR ν_{max} (KBr) 1591 (Amide II), 1647 (Amide I), 3055 & 3436 (NH₂) cm^{-1} ; ^1H NMR 399.65 MHz (CDCl_3) δ 6.23 (1 H, br, NH), 7.48 (1 H, dd, $J = 7.9, 4.9$ Hz, 5'-H), 7.74 (1 H, t, $J = 8.0$ Hz, 6-H), 8.02 (1 H, dt, $J = 7.9, 1.5$ Hz, 4'-H), 8.07 (1 H, dd, $J = 8.0, 1.4$ Hz, 5-H), 8.44 (1 H, d, $J = 2.4$ Hz, 4-H), 8.71 (1 H, dd, $J = 4.9, 1.5$ Hz, 6'-H) 8.88 (1 H, dd, $J = 8.0, 1.4$ Hz, 7-H), 8.99 (1 H, d, $J = 1.5$ Hz, 2'-H), 9.17 (1 H, d, $J = 2.4$ Hz, 2-H), 10.83 (1 H, br, NH); ^{13}C NMR 399.65 MHz (HMBC) (CDCl_3) δ 124.0 (5'-C), 127.3 (6-C), 128.2 (4a-C or 8-C), 128.6 (8-C or 4a-C), 130.6 (1'-C), 132.7 (5-C), 132.8 (3-C), 134.6 (7,6'-C₂), 135.0 (4-C), 144.9 (8a-C), 148.4 (2',4'-C₂), 149.2 (2-C), 167.3 (CONH₂); MS (ES⁺) m/z 521 (2 M + Na), 250.0963 (M + H) ($\text{C}_{15}\text{H}_{12}\text{N}_3\text{O}$ requires 250.0975); Anal. Calcd. for $\text{C}_{15}\text{H}_{11}\text{N}_3\text{O}$: C, 72.28; H, 4.45; N, 16.86. Found: C, 72.38; H, 4.48; N, 16.41.

3-(Pyridin-4-yl)quinoline-8-carboxamide (100)



Compound **77** (104 mg, 0.35 mmol) was treated with pyridine-4-boronic acid (68 mg, 0.55 mmol) by General Procedure 4. Chromatography (hexane / EtOAc, 3:2) gave **100** (35, mg, 40%) as a pale yellow solid: $R_f = 0.37$ (hexane / EtOAc, 3:2); mp 190-193°C; IR ν_{\max} (KBr) 1591 (Amide II), 1654 (Amide I), 3055 & 3462 (NH₂) cm⁻¹; ¹H NMR 399.65 MHz (CD₃OD) δ 7.80 (1 H, t, $J = 8.1$ Hz, 6-H), 7.97 (2 H, d, $J = 5.9$ Hz, 2',6'-H₂), 8.28 (1 H, dd, $J = 8.1, 1.6$ Hz, 5-H), 8.71 (2 H, d, $J = 5.9$ Hz, 3',5'-H₂), 8.74 (1 H, dd, $J = 8.1, 1.6$ Hz, 7-H), 8.88 (1 H, d, $J = 2.4$ Hz, 4-H), 9.40 (1 H, d, $J = 2.4$ Hz, 2-H); ¹³C NMR 399.65 MHz (HMBC) (CD₃OD) δ 123.4 (2',6'-C₂), 128.2 (6-C), 129.7 (4a,8-C₂), 131.9 (3-C), 134.8 (5-C), 135.4 (7-C), 137.1 (4-C), 146.7 (8a-C), 146.8 (1'-C), 149.8 (3',5'-C₂), 151.0 (2-C); MS (ES⁺) m/z 521 (2 M + Na), 250.0965 (M + H) (C₁₅H₁₂N₃O requires 250.0975).

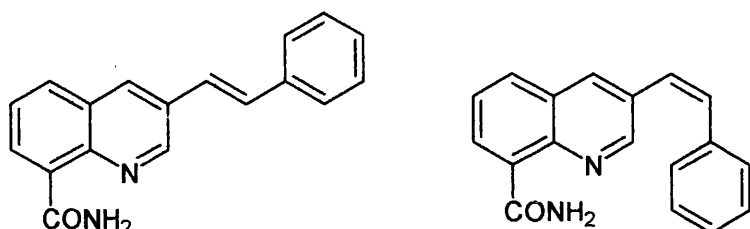
3-(4-Bromomethylphenyl)quinoline-8-carboxamide (101)



Compound **77** (80 mg, 0.27 mmol) was treated with 4-(bromomethyl)phenylboronic acid (58 mg, 0.27 mmol) by General Procedure 2. Chromatography (hexane / EtOAc, 3:2) gave **101** as a white solid (1.5 mg, 2%): $R_f = 0.60$ (hexane / EtOAc, 3:2); mp 178-181°C ¹H NMR 399.65 MHz (CD₃OD) δ 4.89 (2 H, s, CH₂), 7.56 (2 H, d, $J = 8.1$ Hz, 3',5'-H₂), 7.74 (1 H, t, $J = 7.7$ Hz, 6-H), 7.83 (2 H, $J = 8.1$ Hz, 2',6'-H₂), 8.22 (1 H, dd, $J = 7.7, 1.6$ Hz, 5-H), 8.66 (1 H, d, $J = 2.2$ Hz, 4-H), 8.68 (1 H, dd, $J = 7.7, 1.6$ Hz), 9.31 (1 H, d, $J = 2.2$ Hz, 2-H); ¹³C NMR 399.65 MHz (CD₃OD) δ 29.3 (CH₂), 127.4 (Cq), 131.9 (Cq), 132.0 (Cq), 132.5 (CH), 132.7 (CH), 134.0 (CH), 134.3 (CH), 134.5

(CH), 136.2 (Cq), 137.7 (CH), 144.6 (Cq), 149.5 (Cq), 149.0 (CH), 167.6 (CONH₂). Further elution gave recovered starting material **77** (26 mg, 33%).

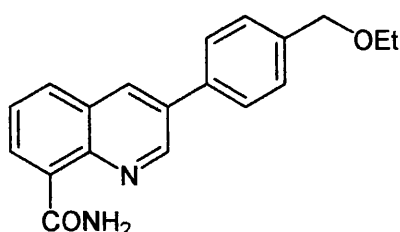
**(E)-3-(2-Phenylethenyl)quinoline-8-carboxamide 102a and
(Z)-3-(2-Phenylethenyl)quinoline-8-carboxamide 102b**



Compound **77** (100 mg, 0.34 mmol) was treated with (*E*)-2-phenylethenyl boronic acid (55 mg, 0.37 mmol) by General Procedure 1. Chromatography (hexane / EtOAc, 3:2) gave **102a** (48 mg, 52%) as a white solid: *R*_f = 0.33 (hexane / EtOAc, 3:2); mp 158-160°C; ¹H NMR 399.65 MHz **102a** (CDCl₃) δ 6.12 (1 H, br, NH), 7.28 (1 H, d, *J* = 19.8 Hz, 1' or 2'-H), 7.35 (1 H, d, *J* = 19.8 Hz, 2' or 1'-H), 7.38-7.59 (5 H, m, Ar 2',3',4',5',6'-H₅), 7.67 (1 H, t, *J* = 8.0 Hz, 6-H), 7.98 (1 H, dd, *J* = 8.0, 1.5 Hz, 5-H), 8.28 (1 H, d, *J* = 2.4 Hz, 4-H), 8.80 (1 H, dd, *J* = 8.0, 1.5 Hz, 7-H) 9.13 (1 H, d, *J* = 2.4 Hz, 2-H), 10.92 (1 H, br, NH).

Photoisomerisation reaction gave **102a,b** (4:1 *E:Z*); ¹H NMR 399.65 MHz **102b** 6.05 (1 H, br, NH), 6.80 (2 H, q, *J* = 10.8 Hz, 1',2'-H₂), 7.32-7.60 (5 H, m, Ar 2',3',4',5',6'-H₅), 7.65 (1 H, t, *J* = 8.1 Hz, 6-H), 7.83 (1 H, dd, *J* = 8.1, 1.6 Hz, 5-H), 8.08 (1 H, d, *J* = 2.0 Hz, 4-H), 8.74 (1 H, dd, *J* = 8.1, 1.6 Hz, 7-H), 8.76 (1 H, d, *J* = 2.0 Hz, 2-H), 10.91 (1 H, br, NH). MS (ES⁺) *m/z* 275.1179 (M + H) (C₁₈H₁₅N₂O requires 275.1179)

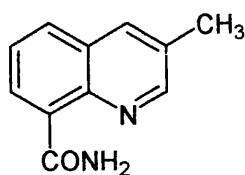
3-(4-Ethoxymethylphenyl)quinoline-8-carboxamide (103)



Compound **77** (100 mg, 0.34 mmol) was treated with 4-(bromomethyl)phenylboronic acid (80 mg, 0.37 mmol) by General Procedure 1. Chromatography (hexane / EtOAc,

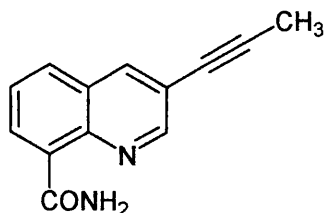
3:2) gave **103** as a white solid (32 mg, 31%): $R_f = 0.33$ (hexane / EtOAc, 3:2); mp 168-170°C; $^1\text{H NMR}$ 399.65 MHz (CDCl_3) δ 1.28 (3 H, t, $J = 7.0$ Hz, CH_3), 3.60 (2 H, q, $J = 7.0$ Hz, CH_2), 4.59 (2 H, s, OCH_2), 6.18 (1 H, br, NH), 7.55-7.40 (2 H, m, 3',5'- H_2), 7.72-7.60 (2 H, m, 2',6'- H_2), 7.99 (1 H, t, $J = 8.4$ Hz, 6-H), 8.04 (1 H, dd, $J = 8.4, 2.0$ Hz, 5-H), 8.28 (1 H, dd, $J = 8.4, 2.0$ Hz, 7-H), 8.93 (1 H, d, $J = 2.0$ Hz, 4-H), 9.18 (1, d, $J = 2.0$ Hz, 2-H), 10.95 (1 H, br, NH).

3-Methylquinoline-8-carboxamide (**106**)



Compound **77** (100 mg, 0.34 mmol) was treated with tetramethylstannane (122 mg, 0.68 mmol) by General Procedure 5. Chromatography (hexane / EtOAc, 3:2) gave **106** (25 mg, 40%) as a white solid: $R_f = 0.43$ (hexane / EtOAc, 3:2); mp 144-142°C; IR ν_{max} (KBr) 1570 (Amide II), 1665 (Amide I), 3019 & 3468 (NH_2) cm^{-1} ; $^1\text{H NMR}$ 399.65 MHz (CDCl_3) δ 2.53 (3 H, s, CH_3), 6.20 (1 H, br, NH), 7.62 (1 H, t, $J = 7.7$ Hz, 6-H), 7.88 (1 H, dd, $J = 7.7, 1.6$ Hz, 5-H), 8.01 (1 H, d, $J = 2.0$ Hz, 4-H), 8.73 (1 H, dd, $J = 7.7, 1.6$ Hz, 7-H), 8.75 (1 H, d, $J = 2.0$ Hz, 2-H), 10.99 (1 H, br, NH); $^{13}\text{C NMR}$ 399.65 MHz (CDCl_3) δ 18.5 (CH_3), 126.4 (6-C), 128.2 (4a-C or 8-C), 128.4 (8-C or 4a-C), 130.5 (3-C), 131.9 (7-C), 133.1 (5-C), 136.3 (4-C), 143.9 (8a-C), 151.4 (2-C), 167.9 (CONH_2); MS (ES^+) m/z 187.0866 ($\text{M} + \text{H}$) ($\text{C}_{11}\text{H}_{11}\text{N}_2\text{O}$ requires 187.0866), 143 ($\text{M} + \text{H} - \text{CONH}_2$); Anal. Calcd. for $\text{C}_{11}\text{H}_{10}\text{N}_2\text{O}$: C, 70.95; H, 5.41; N, 15.04. Found: C, 71.00; H, 5.69; N, 14.97.

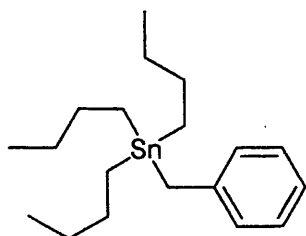
3-(Prop-1-ynyl)quinoline-8-carboxamide (**107**)



Compound **77** (100 mg, 0.34 mmol) was treated with tributyl(prop-1-ynyl)stannane (224 mg, 0.68 mmol) by General Procedure 5. Chromatography (hexane / EtOAc, 3:2) gave **107** (28 mg, 39%) as a buff solid: $R_f = 0.37$ (hexane / EtOAc, 3:2); mp 109-110°C; IR

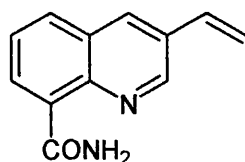
ν_{\max} (KBr) 1590 (Amide II), 1674 (Amide I), 2363 (C≡C), 3210 & 3470 (NH₂) cm⁻¹; ¹H NMR 399.65 MHz (CDCl₃) δ 2.13 (3 H, s, CH₃), 6.13 (1 H, br, NH), 7.68 (1 H, t, *J* = 7.8 Hz, 6-H), 7.90 (1 H, dd, *J* = 7.8, 1.6 Hz, 5-H), 8.24 (1 H, d, *J* = 2.3 Hz, 4-H), 8.84 (1 H, dd, *J* = 7.8, 1.6 Hz, 7-H), 9.05 (1 H, d, *J* = 2.3 Hz, 2-H), 10.75 (1 H, br, NH); ¹³C NMR 399.65 MHz (HMBC) (CDCl₃) δ 4.5 (CH₃), 90.6 (1'-C), 118.3 (2'-C), 127.0 (3-C), 127.7 (6-C), 128.2 (4a-C or 8-C), 128.5 (8-C or 4a-C), 132.1 (5-C), 134.4 (7-C), 139.3 (4-C), 143.8 (8a-C), 151.6 (2-C), 167.4 (CONH₂); MS (ES⁺) *m/z* 211.0873 (M + H) (C₁₃H₁₁N₂O requires 211.0866); Anal. Calcd. for C₁₃H₁₀N₂O: C, 74.27; H, 4.79; N, 13.33. Found: C, 74.25; H, 4.85; N, 13.31.

Tributylbenzylstannane (110)



To tributylstannyl chloride (0.96 mL, 1.16 g, 5.0 mmol) in dry THF (10 mL) was added benzylmagnesium chloride (2.5 mL), and the mixture was stirred for 2 h. The mixture was extracted with diethyl ether and washed with water. The organic layer was dried and the solvent was evaporated to give **111** (1.27 g, 66%) as a yellow oil (lit.²⁷¹ oil); ¹H NMR 270.05 MHz (CDCl₃) δ 0.90-0.94 (9 H, m, 3 x CH₃), 0.96-1.37 (18 H, m, 3 x CH₂CH₂CH₂), 2.34 (2 H, s, CH₂), 7.00-7.16 (4 H, m, 2',3',5',6'-H₄), 7.20 (1 H, t, *J* = 7.6 Hz, 4'-H).

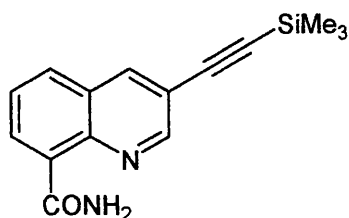
3-Ethenylquinoline-8-carboxamide (111)



Compound **77** (100 mg, 0.34 mmol), in degassed NMP (3 mL), was treated with triphenylphosphine (6.9 mg, 0.03 mmol), Pd₂dba₃ (3.0 mg, 0.005 mmol), CuI (3.6 mg, 0.019 mmol) and tributylethenylstannane (108 mg, 0.34 mmol) at 80°C for 24 h under Ar. The mixture was extracted with EtOAc. The extract was washed with brine and was

dried and filtered. Evaporation and chromatography (hexane / EtOAc, 10:1) gave **111** (37 mg, 55%) a pale yellow solid: $R_f = 0.47$ (hexane / EtOAc, 4:1); mp 174-176°C; ^1H NMR 399.65 MHz (CDCl_3) δ 5.50 (1 H, dd, $J = 11.0, 4.0$ Hz, 2'-H), 6.60 (1 H, dd, $J = 17.6, 4.0$ Hz, 2'-H), 6.13 (1 H, br, NH), 6.89 (1 H, dd, $J = 11.0, 17.6$ Hz, 1'-H), 7.68 (1 H, t, $J = 7.8$ Hz, 6-H), 7.96 (1 H, dd, $J = 7.8, 1.6$ Hz, 5-H), 8.17 (1 H, d, $J = 2.3$ Hz, 4-H), 8.78 (1 H, dd, $J = 7.8, 1.6$ Hz, 7-H), 9.03 (1 H, d, $J = 2.3$ Hz, 2-H), 10.90 (1 H, br, NH); ^{13}C NMR 399.65 MHz (HMBC) (CDCl_3) δ 117.3 (2'-C), 126.8 (6-C), 128.3 (4a-C or 8-C), 128.4 (8-C or 4a-C), 130.3 (3-C), 132.5 (5-C), 133.0 (1'-C), 133.8 (7-C), 133.9 (4-C), 144.9 (8a-C), 148.2 (2-C), 167.5 (CONH_2); MS (ES^+) m/z 199.0858 (M + H) ($\text{C}_{12}\text{H}_{11}\text{N}_2\text{O}$ requires 199.0866).

3-((Trimethylsilyl)ethynyl)quinoline-8-carboxamide (**120**)



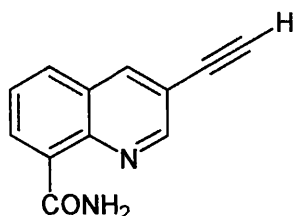
The Pd catalyst, $(\text{PPh}_3)_2\text{PdCl}_2$, used in this reaction was prepared as follows:

A mixture of PPh_3 (375 mg, 1.4 mmol) and PdCl_2 (130 mg, 0.70 mmol) in DMF (20 mL) was heated at 80°C for 24 h. Filtration and drying yielded $(\text{PPh}_3)_2\text{PdCl}_2$ as a yellow powder (450 mg, 90%).

Compound **77** (200 mg, 0.67 mmol) in dry THF (10 mL) was added to a suspension of $(\text{PPh}_3)_2\text{PdCl}_2$ (20 mg, 0.027 mmol) and CuI (27 mg, 0.14 mmol) in dry diisopropylamine (2.7 mL) and the mixture was stirred at 45°C for 30 min under Ar. Trimethylsilylethyne (72 mg, 0.72 mmol) was then added during 30 min and the mixture was stirred for another 2 h. Filtration (Celite[®]), evaporation and chromatography (hexane / EtOAc, 3:2) gave **120** (140 mg, 62%) as white crystals: $R_f = 0.78$ (hexane / EtOAc, 4:1); mp 152-155°C; IR ν_{max} (KBr) 1610 (Amide II), 1680 (Amide I), 2164 ($\text{C}\equiv\text{C}$), 3131 & 3276 (NH_2) cm^{-1} ; ^1H NMR 399.65 MHz (CDCl_3) δ 0.29 (9 H, s, 3 x CH_3), 6.21 (1 H, br, NH), 7.68 (1 H, t, $J = 7.6$ Hz, 6-H), 7.92 (1 H, dd, $J = 7.6, 1.6$ Hz, 5-H), 8.34 (1 H, d, $J = 2.1$ Hz, 4-H), 8.83 (1 H, dd, $J = 7.6, 1.6$ Hz, 7-H), 8.91 (1 H, d, $J = 2.1$ Hz, 2-H), 10.70 (1 H, br, NH); ^{13}C NMR 399.65 MHz (HMBC) (CDCl_3) δ 0.20 (3 x CH_3), 99.4 (2'-C), 101.0 (1'-C), 117.4 (3-C), 127.2 (6-C), 127.4 (4a-C or 8-C), 128.6 (4a-C or 8-C), 132.2 (5-C), 134.8 (7-C), 140.2 (4-C), 144.1 (8a-C), 151.5 (2-C), 167.2 (CONH_2); MS (ES^+) m/z 559 (2 M

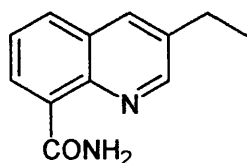
+ Na), 269.1097 (M + H) ($C_{15}H_{17}N_2OSi$ requires 269.1105); Anal. Calcd. for $C_{15}H_{16}N_2OSi$: C, 67.13; H, 6.01; N, 10.44. Found: C, 67.35; H, 5.81; N, 10.30.

3-Ethynylquinoline-8-carboxamide (114)



To a solution of **120** (100 mg, 0.34 mmol) in a mixture of $CHCl_3$ / MeOH / water (4:1:7) (20 mL), was added silver triflate (9.5 mg, 0.037 mmol). The mixture was heated at reflux for 3 d. A saturated aqueous solution of ammonium chloride was added to the mixture. The mixture was extracted with $CHCl_3$ and washed with water. Drying, evaporation and recrystallisation (hexane / EtOAc) gave **114** (72 mg, 99%) as pale buff crystals: R_f = 0.46 (hexane / EtOAc, 3:2); mp 252-255 °C; IR ν_{max} (KBr) 1639 (Amide II), 1687 (Amide I), 2099 ($C\equiv C$), 3190 & 3468 (NH_2) cm^{-1} ; 1H NMR 399.65 MHz ($CDCl_3$) δ 3.32 (1 H, s, 2'-H), 6.07 (1 H, br, NH), 7.71 (1 H, t, J = 8.2 Hz, 6-H), 7.96 (1 H, dd, J = 8.2, 1.6 Hz, 5-H), 8.40 (1 H, d, J = 2.0 Hz, 4-H), 8.86 (1 H, dd, J = 8.2, 1.6 Hz, 7-H), 8.96 (1 H, d, J = 2.0 Hz, 2-H), 10.67 (1 H, br, NH); ^{13}C NMR 399.65 MHz (HMBC) ($CDCl_3$) δ 80.0 (1'-C), 81.4 (2'-C), 116.4 (3-C), 127.3 (6-C), 127.4 (4a-C or 8-C), 128.7 (8-C or 4a-C), 132.2 (5-C), 135.1 (7-C), 140.7 (4-C), 144.3 (8a-C), 151.5 (2-C), 167.1 ($CONH_2$); MS (ES^+) m/z 197.0702 (M + H) ($C_{12}H_9N_2O$ requires 197.0709).

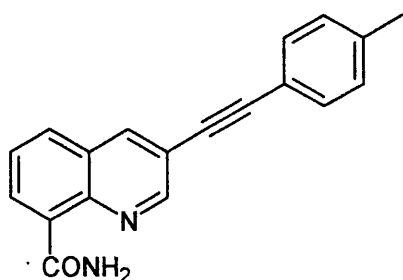
3-Ethylquinoline-8-carboxamide (123)



To **114** (70 mg, 0.36 mmol) in DMF/MeOH (1:1) (3 mL), a slurry of 10 % palladium on charcoal (0.05 g) in MeOH (1 mL) was added. The mixture was allowed to stir for 24 h. The mixture was filtered through Celite[®]. Recrystallisation (hexane / EtOAc) gave **123** (46 mg, 64%) as pale buff crystals: R_f = 0.31 (hexane / EtOAc, 3:2); mp 121-123°C; IR ν_{max} (KBr) 1600 (Amide II), 1666 (Amide I), 2928, 3350 (NH_2) cm^{-1} ; 1H NMR 399.65 MHz ($CDCl_3$) δ 1.37 (3 H, t, J = 7.8 Hz, CH_3), 2.88 (2 H, q, J = 7.9 Hz, CH_2), 6.08 (1 H,

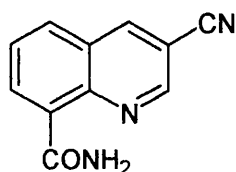
br, NH), 7.64 (1 H, t, $J = 7.9$ Hz, 6-H), 7.94 (1 H, dd, $J = 7.9, 1.6$ Hz, 5-H), 8.03 (1 H, d, $J = 2.3$ Hz, 4-H), 8.78 (1 H, dd, $J = 7.9, 1.6$ Hz, 7-H), 8.81 (1 H, d, $J = 2.3$ Hz, 2-H), 11.01 (1 H, br, NH); ^{13}C NMR 399.65 MHz (HMBC) (CDCl_3) δ 15.1 (CH_3), 26.0 (CH_2), 126.4 (6-C), 128.3 (4a-C or 8-C), 128.5 (8-C or 4a-C), 132.1 (7-C), 133.2 (4-C), 135.0 (5-C), 136.6 (3-C), 144.1 (8a-C), 150.9 (2-C), 167.8 (CONH_2); MS (ES^+) m/z 201.1020 ($\text{M} + \text{H}$) ($\text{C}_{12}\text{H}_{13}\text{N}_2\text{O}$ requires 201.1022).

3-(4-Methylphenyl)ethynylquinoline-8-carboxamide (124)



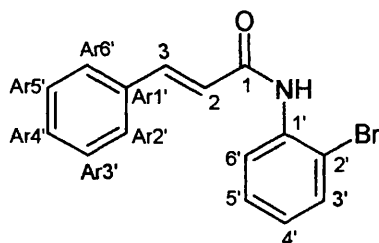
4-Iodotoluene (105 mg, 0.48 mmol) in dry THF (6 mL) was added to a suspension of $(\text{PPh}_3)_2\text{PdCl}_2$ (14 mg, 0.019 mmol) and CuI (19 mg, 0.10 mmol) in dry diisopropylamine (2.1 mL) and the mixture was stirred at 45°C for 30 min under Ar. Compound **114** (100 mg, 0.51 mmol) in dry THF (1 mL) was added and the mixture was stirred at 45°C for 24 h under Ar. Filtration (Celite[®]), evaporation and chromatography (CH_2Cl_2 / EtOAc, 2:1) gave **124** (17 mg, 12%) as buff solid: $R_f = 0.33$ (CH_2Cl_2 / EtOAc, 2:1); mp 109–110°C; IR ν_{max} (KBr) 1569 (Amide II), 1672 (Amide I), 2208 ($\text{C}\equiv\text{C}$), 3294 & 3468 (NH_2) cm^{-1} ; ^1H NMR 399.65 MHz (CDCl_3) δ 2.41 (3 H, s, CH_3), 6.14 (1 H, br, NH), 7.21 (2 H, d, $J = 8.0$ Hz, 3',5'- H_2), 7.50 (2 H, d, $J = 8.0$ Hz, 2',6'- H_2), 7.71 (1 H, t, $J = 7.7$ Hz, 6-H), 7.98 (1 H, dd, $J = 7.7, 1.4$ Hz, 5-H), 8.40 (1 H, d, $J = 2.2$ Hz, 4-H), 8.85 (1 H, dd, $J = 7.7, 1.4$ Hz, 7-H), 9.00 (1 H, d, $J = 2.2$ Hz, 2-H), 10.77 (1 H, br, NH); ^{13}C NMR 399.65 MHz (HMBC) (CDCl_3) δ 21.6 (CH_3), 85.1 (1'-C), 93.8 (2'-C), 117.9 (3-C), 119.1 (Ar 1'-C), 127.2 (6-C), 127.7 (4a-C or 8-C), 128.6 (8-C or 4a-C), 129.3 (Ar 3',5'- C_2), 131.7 (Ar 2',6'- C_2), 132.2 (7-C), 134.6 (5-C), 139.3 (Ar 4'-C), 139.4 (4-C), 144.0 (8a-C), 151.4 (2-C), 167.3 (CONH_2); MS (ES^+) m/z 309.1005 ($\text{M} + \text{Na}$) ($\text{C}_{19}\text{H}_{14}\text{N}_2\text{NaO}$ requires 309.0998).

3-Cyanoquinoline-8-carboxamide (125)



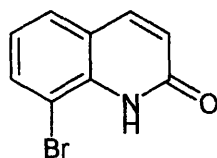
Compound **77** (100 mg, 0.34 mmol), in dry 1,4-dioxane (2 mL), was treated with CuCN (120 mg, 1.4 mmol), 1,1'-bis(diphenylphosphino)ferrocene (29 mg, 0.05 mmol) and Pd(dba)₃ (12 mg, 0.01 mmol). The reaction mixture was boiled under reflux for 24 h under Ar. The mixture was filtered through Celite[®] and extracted with EtOAc and washed with water. The organic layer was dried and the solvent was evaporated. Chromatography (hexane / EtOAc, 3:2) gave **125** (1.4 mg, 2%) as a white solid: R_f = 0.21 (hexane / EtOAc, 3:2); ¹H NMR 399.65 MHz (CDCl₃) δ 6.15 (1 H, br, NH), 7.87 (1 H, t, J = 7.7 Hz, 6-H), 8.09 (1 H, dd, J = 7.7, 1.6 Hz, 5-H), 8.67 (1 H, d, J = 2.2 Hz, 4-H), 9.04 (1 H, dd, J = 7.7, 1.6 Hz, 7-H), 9.10 (1 H, d, J = 2.2 Hz, 2-H), 10.32 (1 H, br, NH); MS (ES⁺) m/z 220.0485 (M + Na) (C₁₁H₇N₃NaO requires 220.0481).

E-N-(2-Bromophenyl)-3-phenylpropenamamide (128)



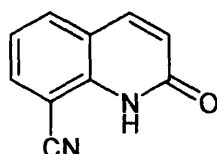
A mixture of *E*-3-phenylpropenoyl chloride (5.51 g, 33.2 mmol), 2-bromoaniline (5.67 g, 33.2 mmol) and K₂CO₃ (7.10 g, 51.5 mmol) in water (16.5 mL) and acetone (16 mL) was stirred vigorously at 0°C for 2 h. The mixture was then poured into ice-water (20 mL). The precipitate was collected. Recrystallisation (hexane) gave **128** (9.8 g, 97%) as white crystals: R_f = 0.85 (hexane / EtOAc, 3:2); mp 145-146°C (lit.²⁷² mp 148-149°C); ¹H NMR 399.65 MHz (CDCl₃) δ 6.58 (1 H, d, J = 15.5 Hz, 2-H), 6.98 (1 H, dt, J = 7.9, 1.5 Hz, 4'-H), 7.32-7.44 (3 H, m, Ar-3',Ar-4',Ar-5'-H₃), 7.53-7.60 (4 H, m, Ar-2',Ar-6',5',6'-H₄), 7.76 (1 H, d, J = 15.5 Hz, 3-H), 7.79 (1 H, br, NH), 8.50 (1 H, d, J = 8.2 Hz, 3'-H).

8-Bromoquinolin-2(1H)-one (129)



Compound **128** (9.78 g, 32.5 mmol) and AlCl_3 (26 g, 0.20 mol) in chlorobenzene (32 mL), were heated to 125°C for 24 h. At 50°C, the mixture was poured onto ice and the precipitate was filtered and collected. Recrystallisation (ethanol) gave **129** (3.0 g, 41%) as white crystals: $R_f = 0.43$ (petroleum ether / EtOAc, 3:2); mp 194-196°C (lit.²²¹ mp 196-198°C); $^1\text{H NMR}$ 399.65 MHz (CDCl_3) δ 6.63 (1 H, d, $J = 9.6$ Hz, 3-H), 7.07 (1 H, t, $J = 7.8$ Hz, 6-H), 7.48 (1 H, dd, $J = 7.8, 1.2$ Hz, 5-H), 7.71 (1 H, d, $J = 9.6$ Hz, 4-H), 7.71 (1 H, dd, $J = 7.8, 1.2$ Hz, 7-H), 9.08 (1 H, br, NH); $^{13}\text{C NMR}$ 399.65 MHz (CDCl_3) δ 109.1 (Cq), 121.0 (Cq), 123.0 (CH), 123.3 (CH), 124.4 (Cq), 127.5 (CH), 133.6 (CH), 140.4 (CH), 162.1 (C=O).

2-Oxo-1,2-dihydroquinoline-8-carbonitrile (130)

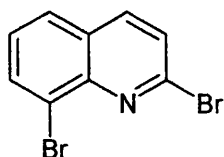


Method A: To **129** (97 mg, 0.43 mmol) in DMF (2 mL) were added $\text{Zn}(\text{CN})_2$ (30 mg, 0.27 mmol) and $\text{Pd}(\text{PPh}_3)_4$ (50 mg, 0.043 mmol). The mixture was heated to 150°C for 12 h. The mixture was filtered (Celite[®]) and extracted with EtOAc and washed with brine. Drying, evaporation and chromatography (hexane / EtOAc, 3:2) gave **130** (4.3 mg, 6%) as a white solid with properties as described below.

Method B: To **129** (200 mg, 0.89 mmol) in DMF (3 mL) was added CuCN (158 mg, 1.9 mmol) and the mixture was heated to 150°C for 12 h. The mixture was filtered through Celite[®] and extracted with EtOAc and washed with brine. Drying, evaporation and chromatography (hexane / EtOAc, 3:2) gave **130** (8.1 mg, 5%) as a white solid: $R_f = 0.44$ (hexane / EtOAc, 3:2); mp 155-157°C; $^1\text{H NMR}$ 399.65 MHz (CDCl_3) δ 6.73 (1 H, d, $J = 9.8$ Hz, 3-H), 7.06 (1 H, t, $J = 7.7$ Hz, 6-H), 7.74 (1 H, dd, $J = 7.7, 1.2$ Hz, 7-H), 7.78 (1 H, d, $J = 9.8$ Hz, 4-H), (1 H, dd, $J = 7.7, 1.2$ Hz, 5-H), 9.12 (1 H, br, NH); ^{13}C

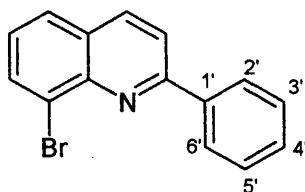
399.65 MHz NMR (HMBC) (CDCl₃) δ 98.4 (8-C), 114.9 (CN), 120.2 (4a-C), 122.4 (3-C), 123.9 (6-C), 132.9 (5-C), 134.1 (7-C), 139.4 (8a-C), 139.9 (4-C), 161.5 (2-C).

2,8-Dibromoquinoline (133)



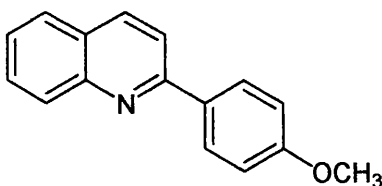
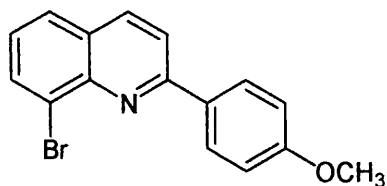
POBr₃ (1.07 g, 3.7 mmol) and **129** (0.41 g, 1.8 mmol) were heated at 140°C for 3 h. The mixture was then poured into ice-water. The precipitate was filtered and dried. Chromatography (CH₂Cl₂ / hexane, 1:1) gave **133** (0.43 g, 41%) as a pale buff solid: R_f = 0.24 (CH₂Cl₂ / hexane, 1:1); mp 118-119°C (lit.²²⁴ mp 118-119°C); ¹H NMR 399.65 MHz (CDCl₃) δ 7.41 (1 H, t, *J* = 7.8 Hz, 6-H), 7.57 (1 H, d, *J* = 8.6 Hz, 3-H), 7.76 (1 H, dd, *J* = 7.8, 1.2 Hz, 5-H), 7.98 (1 H, d, *J* = 8.6 Hz, 4-H), 8.05 (1 H, dd, *J* = 7.8, 1.2 Hz, 7-H); ¹³C NMR 399.65 MHz (HMBC) (CDCl₃) δ 123.6 (8-C), 126.9 (3-C), 127.5 (6-C), 127.6 (4a-C), 128.2 (5-C), 134.1 (7-C), 138.7 (4-C), 143.1 (8a-C), 145.2 (2-C).

8-Bromo-2-phenylquinoline (134)



Compound **133** (340 mg, 1.2 mmol) was treated with phenylboronic acid (162 mg, 1.3 mmol) by General Procedure 1. Chromatography (CH₂Cl₂ / hexane, 1:10) gave **134** (146 mg, 43%) as a pale brown oil (lit.²²⁴ oil): R_f = 0.28 (CH₂Cl₂ / hexane, 1:10); ¹H NMR 399.65 MHz (CDCl₃) δ 7.35 (1 H, t, *J* = 7.9 Hz, 6-H), 7.48 (2 H, t, *J* = 7.9 Hz, 3',5'-H₂), 7.54 (1 H, t, *J* = 7.9 Hz, 4'-H), 7.76 (1 H, dd, *J* = 7.9, 1.2 Hz, 5-H), 7.95 (1 H, d, *J* = 8.6 Hz, 3-H), 8.05 (1 H, d, *J* = 7.9, 1.2 Hz, 7-H), 8.18 (1 H, d, *J* = 8.6 Hz, 4-H), 8.31 (2 H, d, *J* = 7.9 Hz, 2',6'-H₂); ¹³C NMR 399.65 MHz (HMBC) (CDCl₃) δ 119.3 (3-C), 126.7 (6-C), 127.0 (4a-C or 8-C), 127.4 (5-C), 127.5 (8-C or 4a-C), 127.6 (1'-C), 127.7 (4'-C), 129.0 (2',6'-C₂), 129.9 (3',5'-C₂), 133.3 (4-C), 134.2 (8a-C), 137.3 (7-C), 156.8 (2-C).

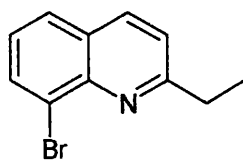
**8-Bromo-2-(4-methoxyphenyl)quinoline (135) and
2-(4-methoxyphenyl)quinoline (136)**



Compound **133** (350 mg, 1.2 mmol) was treated with 4-methoxyphenylboronic acid (244 mg, 1.4 mmol) by General Procedure 1. Chromatography (toluene) gave **135** (322 mg, 84%) as a pale orange oil: $R_f = 0.60$ (toluene); $^1\text{H NMR}$ 399.65 MHz (CDCl_3) δ 3.88 (3 H, s, CH_3), 7.04 (2 H, d, $J = 8.2$ Hz, 3',5'- H_2), 7.31 (1 H, t, $J = 7.9$ Hz, 6-H), 7.71 (1 H, dd, $J = 7.9, 1.2$ Hz, 5-H), 7.86 (1 H, d, $J = 8.8$ Hz, 3-H), 8.01 (1 H, dd, $J = 7.9, 1.2$ Hz, 7-H), 8.10 (1 H, d, $J = 8.8$ Hz, 4-H), 8.28 (2 H, d, $J = 8.2$ Hz, 2',6'- H_2); $^{13}\text{C NMR}$ 399.65 MHz (HMBC) (CDCl_3) δ 55.3 (CH_3), 114.2 (3',5'- C_2), 118.7 (3-C), 125.2 (8-C), 126.1 (6-C), 127.2 (5-C), 128.0 (4a-C), 129.0 (2',6'- C_2), 131.1 (4-C), 131.4 (1'-C), 137.0 (7-C), 145.0 (8a-C), 157.1 (2-C), 161.1 (4'-C); MS (ES^+) m/z 314.0163 ($\text{M} + \text{H}$) ($\text{C}_{16}\text{H}_{13}^{79}\text{BrNO}$ requires 314.0175).

Also isolated by chromatography was **136** (21 mg, 7%) as a pale buff solid: $R_f = 0.20$ (toluene); mp 118-119°C (lit.²⁷³ mp 122-123°C); $^1\text{H NMR}$ 399.65 MHz (CDCl_3) δ 3.88 (3 H, s, CH_3), 7.05 (2 H, d, $J = 8.0$ Hz, 3',5'- H_2), 7.49 (1 H, t, $J = 8.1$ Hz, 6-H), 7.71 (1 H, t, $J = 8.1$ Hz, 7-H), 7.81 (1 H, dd, $J = 8.1, 1.2$ Hz, 5-H), 7.83 (1 H, d, $J = 8.6$ Hz, 3-H) 8.12 (3 H, m, 2',6',8- H_3), 8.17 (1 H, $J = 8.6$ Hz, 4-H).

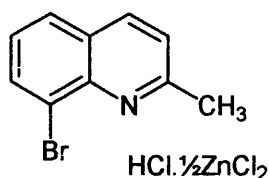
8-Bromo-2-ethylquinoline (138)



Compound **133** (150 mg, 0.53 mmol) was treated with tetraethylstannane (125 mg, 0.53 mmol) by General Procedure 5. Chromatography (hexane / EtOAc, 3:2) gave **138** (62 mg, 50%) as a pale brown oil: $R_f = 0.31$ (hexane / EtOAc, 3:2); $^1\text{H NMR}$ 399.65 MHz (CDCl_3) δ 1.43 (3 H, t, $J = 7.6$ Hz, CH_3), 3.08 (2 H, q, $J = 7.6$ Hz, CH_2), 7.30 (1 H, t, $J = 7.9$ Hz, 6-H), 7.34 (1 H, d, $J = 8.4$ Hz, 3-H), 7.73 (1 H, dd, $J = 7.9, 1.4$ Hz, 5-H),

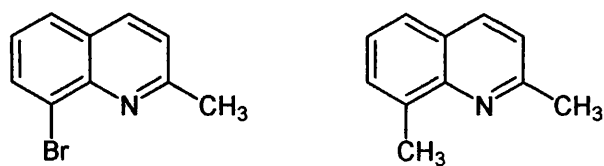
8.01 (1 H, dd, $J = 7.9, 1.4$ Hz, 7-H), 8.03 (1 H, d, $J = 8.4$ Hz, 4-H); ^{13}C NMR 399.65 MHz (HMBC) (CDCl_3) δ 13.5 (CH_3), 32.3 (CH_2), 121.7 (3-C), 124.5 (8-C), 126.0 (6-C), 127.41 (5-C), 128.0 (4a-C), 132.9 (7-C), 136.6 (4-C), 144.8 (8a-C), 165.1 (2-C); MS (EI^+) m/z 236 ($\text{M} - \text{H}$) ($\text{C}_{11}\text{H}_9^{81}\text{BrN}$), 233.9911 ($\text{M} - \text{H}$) ($\text{C}_{11}\text{H}_9^{79}\text{BrN}$ requires 233.9913).

8-Bromo-2-methylquinoline hydrochloride-ZnCl₂ complex (143)



(*E*)-But-2-enal (0.61 g, 8.7 mmol) was added to 2-bromoaniline (1.48 g, 8.7 mmol) in refluxing aq. HCl (6 M, 4 mL) during 30 min. After addition was complete, the mixture was heated for a further 30 min. The reaction mixture was cooled to ambient temperature and washed with diethyl ether. To the solution was added ZnCl₂ (1.20 g, 8.8 mmol) with vigorous stirring. The precipitate formed was filtered, washed with cold 3 M HCl, and dried in air. The solid was washed with Et₂O and dried to provide **143** (0.62 g, 73%) as a yellow crystalline solid. This material was used without further purification or characterisation.

8-Bromo-2-methylquinoline (139) and 2,8-Dimethylquinoline (140)

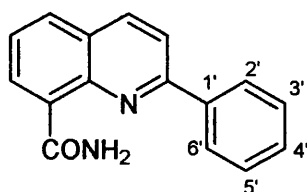


Method A: To a solution of compound **133** (108 mg, 0.38 mmol) and tetramethylstannane (67 mg, 0.37 mmol) in NMP (2 mL) was added Pd(PPh₃)₄ (43 mg, 0.04 mmol). The reaction was heated to 80°C for 8 h under Ar. The mixture was extracted with EtOAc and washed with water, brine, dried and filtered. Evaporation and chromatography (hexane / EtOAc, 10:1) gave a mixture (53 mg, pale brown oil) shown by ^1H NMR to comprise **139** (46% yield) and **140** (23% yield): ^1H NMR (270 MHz) **139** (CDCl_3) δ 2.73 (3 H, s, CH₃), 7.34 (1 H, d, $J = 8.2$ Hz, 3-H), 7.44 (1 H, t, $J = 8.0$ Hz, 6-H), 7.67 (1 H, dd, $J = 8.0, 1.2$ Hz, 5-H), 7.98 (1 H, d, $J = 8.0, 1.2$ Hz, 7-H), 7.99 (1 H, d, $J = 8.2$ Hz, 4-H); ^1H NMR (270 MHz) **140** (CDCl_3) δ 2.75 (3 H, s, CH₃), 2.81 (3 H, s,

CH₃), 7.27 (1 H, d, *J* = 8.2 Hz, 3-H), 7.32 (1 H, t, *J* = 7.9 Hz, 6-H), 7.72 (1 H, *J* = 7.9, 1.2 Hz, 5-H), 8.00 (1 H, dd, *J* = 7.9, 1.2 Hz, 7-H), 8.09 (1 H, d, 8.2 Hz, 4-H).

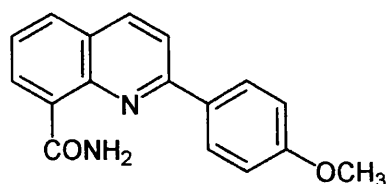
Method B: Compound **143** was placed in a separating funnel and shaken with cold water (15 mL). To this slurry was added conc. aq. ammonia (5 mL). The resulting oil was extracted with diethyl ether, dried and evaporated to give **139** (280 mg, 59%) as a pale yellow solid: *R_f* = 0.67 (hexane / EtOAc, 10:1) mp 63-65°C (lit.²²⁷ mp 67-68°C); ¹H NMR data as above.

2-Phenylquinoline-8-carboxamide (**144**)



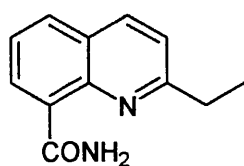
To **134** (110 mg, 0.39 mmol) in dry THF (0.5 mL) at -79°C was added *n*-BuLi (1.6 M in hexanes, 0.53 mL, 0.82 mmol). After 30 min, trimethylsilylisocyanate (0.15 mL, 1.2 mmol) was added. The solution was stirred for a further 15 min at -79°C and for 12 h at 20°C. The evaporation residue, in CH₂Cl₂, was washed with water and brine and dried. Evaporation and chromatography (CH₂Cl₂ / EtOAc, 2:1) gave **144** (33 mg, 34%) as a pale yellow solid: *R_f* = 0.68 (CH₂Cl₂ / EtOAc, 2:1); mp 209-210°C (lit.²⁷⁴ mp 210-212°C; IR ν_{\max} (KBr) 1600 (Amide II), 1674 (Amide I), 3270 & 3470 (NH₂) cm⁻¹; ¹H NMR 399.65 MHz (CDCl₃) δ 6.16 (1 H, br, NH), 7.52-7.58 (3 H, m, 3',5,5'-H₃), 7.66 (1 H, t, *J* = 7.6 Hz, 6-H), 7.92 (1 H, d, *J* = 8.6 Hz, 3-H), 7.99-8.04 (3 H, m, 2',4',6'-H₃), 8.34 (1 H, d, *J* = 8.6 Hz, 4-H), 8.87 (1 H, dd, *J* = 7.6, 1.6 Hz, 7-H), 11.20 (1 H, br, NH); ¹³C NMR 399.65 MHz (HMBC) (CDCl₃) δ 119.2 (3-C), 126.2 (6-C), 127.4 (4a-C or 8-C), 127.7 (2',6'-C₂), 128.4 (8-C or 4a-C), 129.2 (4'-C), 130.0 (3',5'-C₂), 132.2 (4-C), 134.6 (7-C), 138.5 (5-C), 139.2 (1'-C), 145.5 (8a-C), 157.3 (2-C), 167.8 (CONH₂).

2-(4-Methoxyphenyl)quinoline-8-carboxamide (145)



To **135** (100 mg, 0.32 mmol) in dry THF (0.5 mL) at -79°C was added *n*-BuLi (1.6 M in hexanes, 0.41 mL, 0.64 mmol). After 30 min, trimethylsilylisocyanate (0.12 mL, 0.96 mmol) was added. The solution was stirred for a further 15 min at -79°C and for 12 h at 20°C . The evaporation residue, in CH_2Cl_2 , was washed with water and brine and dried. Evaporation and chromatography (toluene) gave **145** (38 mg, 43%) as a pale yellow solid: $R_f = 0.37$ (hexane / EtOAc, 10:1); mp $221\text{--}224^{\circ}\text{C}$; IR ν_{max} (KBr) 1602 (Amide II), 1662 (Amide I), 3257 & 3448 (NH_2) cm^{-1} ; $^1\text{H NMR}$ 399.65 MHz (CDCl_3) δ 3.90 (3 H, s, CH_3), 6.27 (1 H, br, NH), 7.07 (2 H, d, $J = 8.0$ Hz, 3',5'- H_2), 7.63 (1 H, t, $J = 7.9$ Hz, 6-H), 7.87 (1 H, d, $J = 8.6$ Hz, 3-H), 7.96 (1 H, dd, $J = 7.9, 1.6$ Hz, 5-H), 7.98 (2 H, d, $J = 8.0$ Hz, 2',6'- H_2), 8.27 (1 H, d, $J = 8.6$ Hz, 4-H), 8.83 (1 H, dd, $J = 7.9, 1.6$ Hz, 7-H); 11.20 (1 H, br, NH), $^{13}\text{C NMR}$ 399.65 MHz (HMBC) (CDCl_3) δ 55.5 (CH_3), 114.6 (3',5'- C_2), 118.8 (3-C), 125.8 (6-C), 127.8 (4a-C or 8-C), 128.2 (8-C or 4a-C), 129.1 (2',6'- C_2), 131.6 (1'-C), 132.2 (7-C), 134.4 (5-C), 138.3 (4-C), 145.6 (8a-C), 156.9 (4'-C), 161.3 (2-C), 168.0 (CONH_2); MS (ES^+) m/z 279.1128 ($\text{M} + \text{H}$) ($\text{C}_{17}\text{H}_{15}\text{N}_2\text{O}_2$ requires 279.1128).

2-Ethylquinoline-8-carboxamide (146)



To **138** (50 mg, 0.21 mmol) in dry THF (0.34 mL) at -79°C was added *n*-BuLi (1.6 M in hexanes, 0.28 mL, 0.44 mmol). After 30 min, trimethylsilylisocyanate (0.09 mL, 0.63 mmol) was added. The solution was stirred for a further 15 min at -79°C and for 12 h at 20°C . The evaporation residue, in CH_2Cl_2 , was washed with water and brine and was dried. Evaporation and chromatography (hexane / EtOAc, 3:2) gave **146** (18 mg, 43%) as a pale yellow solid: $R_f = 0.68$ (hexane / EtOAc, 3:2); mp $172\text{--}175^{\circ}\text{C}$; IR ν_{max} (KBr) 1593 (Amide II), 1681 (Amide I), 3300 & 3469 (NH_2) cm^{-1} ; $^1\text{H NMR}$ 399.65 MHz (CDCl_3)

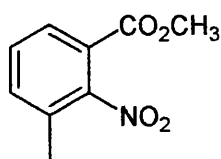
δ 1.41 (3 H, t, $J = 7.6$ Hz, CH₃), 3.03 (2 H, q, $J = 7.6$ Hz, CH₂), 6.47 (1 H, br, NH), 7.34 (1 H, d, $J = 8.6$ Hz, 3-H), 7.58 (1 H, t, $J = 7.8$ Hz, 6-H), 7.91 (1 H, dd, $J = 7.8, 1.4$ Hz, 5-H), 8.13 (1 H, d, $J = 8.6$ Hz, 4-H). 8.79 (1 H, dd, $J = 7.8, 1.4$ Hz, 7-H), 11.30 (1 H, br, NH); ¹³C NMR 399.65 MHz (HMBC) (CDCl₃) δ 13.0 (CH₃), 31.8 (CH₂), 121.0 (3-C), 125.4 (6-C), 126.9 (4a-C or 8-C), 127.7 (8-C or 4a-C), 132.2 (7-C), 133.9 (5-C), 137.6 (4-C), 145.1 (8a-C), 163.4 (2-C), 168.1 (CONH₂); MS (ES⁺) m/z 201.1016 (M + H) (C₁₂H₁₃N₂O requires 201.1022).

2-Methylquinoline-8-carboxamide (147)



To **139** (100 mg, 0.45 mmol) in dry THF (0.57 mL) at -79°C was added n-BuLi (1.6 M in hexanes, 0.61 mL, 0.94 mmol). After 30 min, trimethylsilylisocyanate (0.17 mL, 1.4 mmol) was added. The solution was stirred for a further 15 min at -79°C and for 12 h at 20°C. The evaporation residue, in CH₂Cl₂, was washed with water and brine and dried. Evaporation and chromatography (hexane / EtOAc, 3:2) gave **147** (44 mg, 52%) as a pale yellow solid: $R_f = 0.54$ (hexane / EtOAc, 3:2); mp 170-171°C (lit.²⁷⁵ mp 170-171°C); IR ν_{\max} (KBr) 1616 (Amide II), 1661 (Amide I), 3236 & 3480 (NH₂) cm⁻¹; ¹H NMR 399.65 MHz (CDCl₃) δ 2.77 (3 H, s, CH₃), 6.40 (1 H, br, NH), 7.35 (1 H, d, $J = 8.2$ Hz, 3-H), 7.60 (1 H, t, $J = 7.9$ Hz, 6-H), 7.93 (1 H, dd, $J = 7.9, 1.6$ Hz, 5-H), 8.15 (1 H, d, $J = 8.2$ Hz, 4-H), 8.82 (1 H, dd, $J = 7.9, 1.6$ Hz, 7-H), 11.25 (1 H, br, NH); ¹³C 399.65 MHz NMR (HMBC) (CDCl₃) δ 25.5 (CH₃), 121.8 (3-C), 125.4 (6-C), 126.7 (4a-C or 8-C), 127.7 (8-C or 4a-C), 132.2 (7-C), 133.2 (5-C), 137.6 (4-C), 145.2 (8a-C), 158.7 (2-C), 168.0 (CONH₂); MS (ES⁺) m/z 187.0857 (M + H) (C₁₁H₁₁N₂O requires 187.0866).

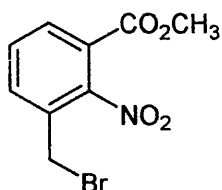
Methyl 3-methyl-2-nitrobenzoate (149)



3-Methyl-2-nitrobenzoic acid **148** (5.00 g, 27.6 mmol) was boiled under reflux in MeOH (500 mL) and conc. H₂SO₄ (5 mL) for 4 h. The evaporation residue, in CH₂Cl₂, was

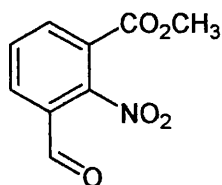
washed with aq. NaHCO₃ and dried and the solvent was evaporated to give **149** (2.79 g, 56%) as white crystals: R_f = 0.66 (EtOAc / hexane, 2:1); mp 71-73°C (lit.²⁷⁶ mp 72-73°C); ¹H NMR 270.05 MHz (CDCl₃) δ 2.35 (3 H, s, CH₃), 3.88 (3 H, s, OCH₃), 7.44-7.48 (2 H, m, 4,5-H₂), 7.83 (1 H, dd, J = 7.0, 2.2 Hz, 6-H).

Methyl 3-(bromomethyl)-2-nitrobenzoate (**150**)



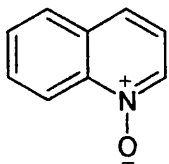
Compound **149** (392 mg, 2.2 mmol), dibenzoyl peroxide (24 mg, 0.10 mmol) and NBS (374 mg, 2.1 mmol) in CCl₄ (4 mL) were heated at 90°C for 24 h and irradiated using a 100W tungsten lamp. The mixture was washed with NaHCO₃, dried and concentrated. Chromatography (EtOAc / hexane, 1:19) gave **150** (301 mg, 53%) as a white solid: R_f = 0.57 (EtOAc / hexane, 2:1); mp 90-91°C (lit.²²⁸ mp 90-90.5°C); ¹H NMR 270.05 MHz (CDCl₃) δ 3.90 (3 H, s, OCH₃), 4.44 (2 H, s, CH₂Br), 7.57 (1 H, t, J = 7.9 Hz, 5-H), 7.72 (1 H, dd, J = 7.9, 1.5 Hz, 4-H), 7.94 (1 H, dd, J = 7.9, 1.5 Hz, 6-H).

Methyl 3-formyl-2-nitrobenzoate (**151**)



To **150** (0.73 g, 2.8 mmol) was added bis(tetrabutylammonium) dichromate (1.00 g, 1.4 mmol) in CHCl₃ (5 mL) and the mixture was heated under reflux for 1 h. The mixture was rapidly cooled in an ice-bath and filtered through a pad of silica (20 g); the silica was then washed with Et₂O (20 mL). The solvent was evaporated to give **151** (193 mg, 32%) as a pale yellow solid: R_f = 0.44 (EtOAc / hexane, 2:1); mp 94-96°C; ¹H NMR 399.65 MHz (CDCl₃) δ 3.87 (3 H, s, OCH₃), 7.72 (1 H, t, J = 7.9 Hz, 5-H), 8.11 (1 H, dd, J = 7.9, 1.6 Hz, 4-H), 8.20 (1 H, dd, J = 7.9, 1.6 Hz, 6-H), 9.90 (1 H, s, CHO); ¹³C NMR 399.65 MHz (CDCl₃) δ 53.5 (CH₃), 123.8 (1-C), 127.4 (3-C), 130.9 (4-C), 133.7 (5-C), 136.3 (6-C), 150.7 (2-C), 162.8 (C=O), 185.7 (CHO); MS (ES⁺) m/z 210.0397 (M + H) (C₉H₈NO₅ requires 210.0397), 178 (M - OCH₃)

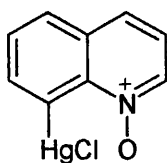
Quinoline-1-oxide (154)



Method A: To Na_2CO_3 (628 mg, 5.9 mmol) and urea hydrogen peroxide (628 mg, 6.7 mmol) in dry CH_2Cl_2 (10 mL) at 0°C was added dropwise trifluoroacetic anhydride (0.46 mL, 3.3 mmol). The solution was allowed to reach room temperature and quinoline (87 mg, 0.67 mmol) was added. The mixture was stirred overnight at 40°C . The mixture was extracted with CH_2Cl_2 and washed with water and brine. Evaporation and chromatography (EtOAc) gave **154** (60 mg, 62%) as a colourless hygroscopic oil with properties as described below.

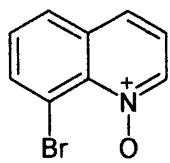
Method B: To quinoline (10.0 g, 0.080 mmol) was added aq. H_2O_2 35% (24 mL). The solution was boiled under reflux for 24 h. The evaporation residue, in EtOAc, was washed with aq. Na_2CO_3 and brine and dried. Evaporation and chromatography (EtOAc) gave **154** (3.23 g, 26%) as a colourless hygroscopic oil: $R_f = 0.15$ (EtOAc); lit.²⁷⁷ mp $61\text{--}62^\circ\text{C}$; $^1\text{H NMR}$ 399.65 MHz CDCl_3 δ 7.28 (1 H, dd, $J = 8.7, 6.0$ Hz, 3-H), 7.61 (1 H, ddd, $J = 8.2, 7.0, 1.4$ Hz, 6-H), 7.73 (1 H, d, $J = 8.7$ Hz, 4-H), 7.75 (1 H, ddd, $J = 8.7, 7.0, 1.4$ Hz, 7-H), 7.84 (1 H, d, $J = 8.2$ Hz, 5-H), 8.50 (1 H, d, $J = 6.0$ Hz, 2-H), 8.71 (1 H, d, $J = 8.7$ Hz, 8-H).

(1-Oxidoquinolin-8-yl)mercury(II) chloride (159)



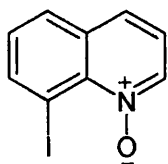
To **154** (1.00g, 6.9 mmol) in AcOH (1 mL) was added $\text{Hg}(\text{OAc})_2$ (2.20 g, 6.9 mmol). The mixture was boiled under reflux for 5 h. The residue was poured into brine (10 mL) and the solid formed was collected by filtration and washed with water to give **159** (2.26 g, 86%) as pale buff crystals: $R_f = 0.10$ (EtOAc); mp $236\text{--}237^\circ\text{C}$ (lit.²³⁵ mp 235°C); $^1\text{H NMR}$ 399.65 MHz $(\text{CD}_3)_2\text{SO}$ δ 7.57 (1 H, dd, $J = 8.3, 5.9$ Hz, 3-H), 7.78 (1 H, t, $J = 7.9$ Hz, 6-H), 8.03 (1 H, d, $J = 7.9$ Hz, 7-H), 8.06 (1 H, d, $J = 8.3$ Hz, 4-H), 8.11 (1 H, d, $J = 7.9$ Hz, 5-H), 8.74 (1 H, d, $J = 5.9$ Hz, 2-H).

8-Bromoquinoline-1-oxide (160)



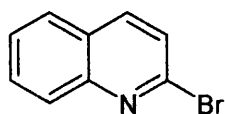
Bromine (0.51 g, 3.2 mmol), (1-oxidoquinolin-8-yl)mercury(II) chloride **159** (1.08 g, 2.9 mmol) and KBr (0.41 g, 3.4 mmol) in H₂O (2.0 mL) were ground into a paste using a pestle and mortar. The residue was then extracted with EtOAc and washed with brine. The organic layer was dried and concentrated. Chromatography (EtOAc) gave **160** (17 mg, 2%) as pale a buff solid: $R_f = 0.3$ (EtOAc); mp 97-99°C (lit.²³⁵ 102-104°C); ¹H NMR 270.05 MHz ((CD₃)₂SO) δ 7.57 (1 H, t, $J = 7.8$ Hz, 6-H), 7.65 (1 H, dd, $J = 8.3, 5.9$ Hz, 3-H), 8.05 (1 H, d, $J = 7.8$ Hz, 7-H), 8.16 (1 H, d, $J = 8.3$ Hz, 4-H), 8.47 (1 H, d, $J = 7.8$ Hz, 5-H), 9.03 (1 H, d, $J = 5.9$ Hz, 2-H).

8-Iodoquinoline-1-oxide (161)



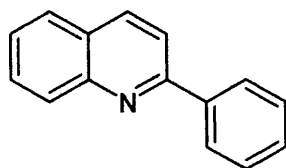
To **159** (1.18 g, 3.1 mmol) in NMP (1 mL) was added iodine (0.79 g, 3.1 mmol). The mixture was stirred for 24 h. Chromatography (acetone / EtOAc, 1:1) of the evaporation residue gave **161** (0.37 g, 44%) as a pale yellow solid: $R_f = 0.50$ (acetone / EtOAc, 1:1); mp 263-265°C; ¹H NMR 399.65 MHz ((CD₃)₂SO) δ 7.32 (1 H, t, $J = 7.9$ Hz, 6-H), 7.47 (1 H, dd, $J = 8.5, 6.2$ Hz, 3-H), 7.92 (1 H, d, $J = 8.5$ Hz, 4-H), 8.05 (1 H, dd, $J = 7.9, 1.1$ Hz, 5-H), 8.39 (1 H, dd, $J = 7.9, 1.1$ Hz, 7-H), 8.52 (1 H, dd, $J = 6.2, 0.8$ Hz, 2-H), ¹³C NMR 399.65 MHz (HMBC) ((CD₃)₂SO) δ 81.8 (8-C), 122.2 (3-C), 126.0 (6-C), 129.6 (4-C), 129.9 (5-C), 132.1 (4a-C), 136.4 (7-C), 138.6 (8a-C), 145.1 (2-C); MS (ES⁺) m/z 271.9567 (M + H) (C₉H₇INO requires 271.9494).

2-Bromoquinoline (163)



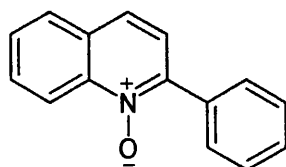
POBr₃ (2.08 g, 7.3 mmol) and quinoline-2-one (0.52 g, 3.6 mmol) were heated at 140°C for 3 h. The mixture was poured into ice-water. The precipitate was filtered and dried. Chromatography (CH₂Cl₂ / hexane, 1:1) gave **163** (526 mg, 34%) as a pale yellow solid: R_f = 0.36 (CH₂Cl₂ / hexane, 1:1); mp 49-51°C (lit.²⁷⁸ mp 50-51°C); ¹H NMR 270.05 MHz (CDCl₃) δ 7.33 (1 H, d, *J* = 8.5 Hz, 3-H), 7.42 (1 H, t, *J* = 8.1 Hz, 6-H), 7.60 (1 H, dd, *J* = 8.1, 1.8 Hz, 7-H), 7.62 (1 H, d, *J* = 8.1, 1.8 Hz, 5-H), 7.80 (1 H, d, *J* = 8.5 Hz, 4-H), 7.90 (1 H, d, *J* = 8.1 Hz, 8-H).

2-Phenylquinoline (164)



Compound **163** (4.12 g, 19.9 mmol) was treated with phenylboronic acid (3.64 g, 29.9 mmol) by General Procedure 3. Chromatography (EtOAc) gave **164** (4.03 g, 99%) as a pale yellow solid: R_f = 0.45 (EtOAc) mp 83-85°C (lit.²³⁷ mp 83-85°C); ¹H NMR 270.05 MHz (CDCl₃) δ 7.44-7.55 (4 H, m, 3,3',4',5'-H₄), 7.74 (1 H, t, *J* = 7.8 Hz, 6-H), 7.81 (1 H, d, *J* = 7.8 Hz, 7-H), 7.86 (1 H, d, *J* = 8.5 Hz, 4-H), 8.12-8.21 (4 H, m, 2',5,6',8-H₄).

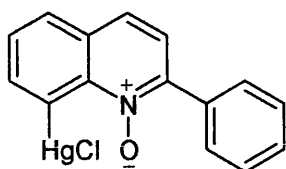
2-Phenylquinoline-1-oxide (165)



To **164** (0.95 g, 4.6 mmol) in CHCl₃ (8 mL) was added 77% 3-chloroperoxybenzoic acid (1.59 g, 9.3 mmol). The solution was stirred overnight. The insoluble 3-chlorobenzoic acid was filtered off and the filtrate was washed with NaHCO₃. The organic layer was dried and concentrated. Chromatography (hexane / EtOAc, 3:2) gave **165** (890 mg,

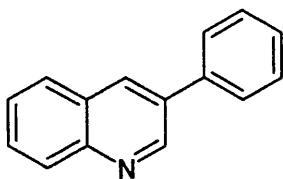
87%) as a pale yellow solid: $R_f = 0.31$ (hexane / EtOAc, 3:2); mp 141-142°C (lit.²⁷⁹ mp 142-143°C); $^1\text{H NMR}$ 270.05 MHz (CDCl_3) δ 7.47-7.52 (4 H, m, 3,3',4',5'-H₄), 7.62 (1 H, t, $J = 7.8$ Hz, 6-H), 7.76-7.92 (4 H, m, 2',5,6',8-H₄), 7.94 (1 H, dd, $J = 7.8, 1.7$ Hz, 7-H), 8.87 (1 H, d, $J = 8.6$ Hz, 4-H).

(1-Oxido-2-phenylquinolin-8-yl)mercury(II) chloride (166)



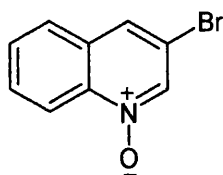
To **165** (150 g, 0.68 mmol) in glacial AcOH (1 mL) was added $\text{Hg}(\text{OAc})_2$ (216 mg, 0.68 mmol). The mixture was boiled under reflux for 5 h. The residue was poured into brine (5 mL) and the solid formed was collected by filtration and washed with water to give **166** (87 mg, 28%) as pale buff crystals: $R_f = 0.22$ (EtOAc); mp 235-237°C; IR ν_{max} (KBr) 1244 (N^+-O^-) cm^{-1} ; $^1\text{H NMR}$ 270.05 MHz ($(\text{CD}_3)_2\text{SO}$) δ 7.43-7.60 (3 H, m, 3',5',6-H₃), 7.66-7.89 (3 H, m, 2',4',6'-H₃), 8.01 (1 H, dd, $J = 8.0, 1.6$ Hz, 5-H), 8.13 (1 H, d, $J = 8.7$ Hz, 3-H), 8.64 (1 H, dd, $J = 8.0, 1.6$ Hz, 7-H), 8.85 (1 H, d, $J = 8.7$ Hz, 4-H). This material was used without further purification.

3-Phenylquinoline (170)



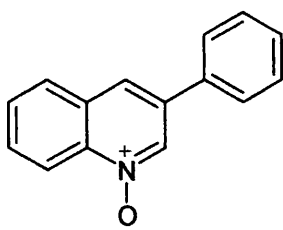
3-Bromoquinoline (310 mg, 1.5 mmol) was treated with phenylboronic acid (275 mg, 2.3 mmol) by General Procedure 3. Chromatography (EtOAc) gave **170** (230 mg, 75%) as a pale yellow oil (lit.²⁸⁰ oil): $R_f = 0.30$ (hexane / EtOAc, 3:2); $^1\text{H NMR}$ 270.05 MHz (CDCl_3) δ 7.42 (1 H, t, $J = 8.1$ Hz, 6-H), 7.46-7.49 (2 H, m, 3',5'-H₂), 7.51 (1H, t, $J = 7.7$ Hz, 4'-H), 7.64 (2 H, d, $J = 7.7$ Hz, 2',6'-H₂), 7.83 (1 H, d, $J = 8.1$ Hz, 5-H), 8.14-8.16 (2 H, m, 7,8-H₂), 8.25 (1 H, d, $J = 1.8$ Hz, 4-H), 8.83 (1 H, d, $J = 1.8$ Hz, 2-H).

3-Bromoquinoline-1-oxide (172)



To 3-bromoquinoline (4.53 g, 21.9 mmol) in CHCl_3 (40 mL) was added 77% 3-chloroperoxybenzoic acid (7.53 g, 43.8 mmol). The solution was stirred overnight. The insoluble 3-chlorobenzoic acid was filtered off and the filtrate was washed with NaHCO_3 . The organic layer was dried and the solvent was evaporated. Chromatography (hexane / EtOAc, 4:1) gave **172** (3.64 g, 75%) as a pale brown solid: $R_f = 0.46$ (hexane / EtOAc, 3:1); mp 97-99°C (lit.²⁸¹ mp 95-97°C); $^1\text{H NMR}$ 270.05 MHz (CDCl_3) δ 7.72 (1 H, t, $J = 7.5$ Hz, 6-H), 7.75 (2 H, m, 5,7-H₂), 7.77 (1 H, d, $J = 1.6$ Hz, 4-H), 8.62 (1 H, d, $J = 7.7$ Hz, 8-H), 8.65 (1 H, d, $J = 1.6$ Hz, 2-H).

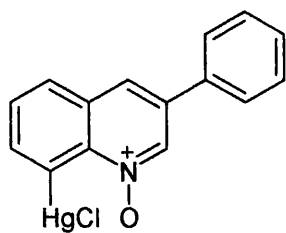
3-Phenylquinoline-1-oxide (171)



Method A: To **170** (0.95 g, 4.6 mmol) in CHCl_3 was added 77% 3-chloroperoxybenzoic acid (1.59 g, 9.3 mmol). The solution was stirred overnight. The insoluble 3-chlorobenzoic acid was filtered off and the filtrate was washed with NaHCO_3 . The organic layer was dried and concentrated. Chromatography (hexane / EtOAc, 1:1) gave **171** (223 mg, 22%) as a pale yellow solid with properties as described below.

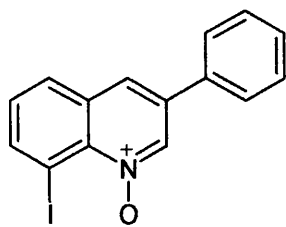
Method B: Compound **172** (3.34 g, 15.0 mmol) was treated with phenylboronic acid (2.74 g, 22.5 mmol) by General Procedure 3. Chromatography (EtOAc) gave **171** (2.47 g, 74%) as a pale yellow solid: $R_f = 0.38$ (EtOAc); mp 121-124°C (lit.²⁸² mp 123-124°C); $^1\text{H NMR}$ 270.05 MHz (CDCl_3) δ 7.47-7.51 (3 H, m, 3',6,5'-H₃), 7.63-7.66 (3 H, m, 2',4',6'-H₃), 7.74 (1 H, dd, $J = 7.9, 1.4$ Hz, 7-H), 7.89 (2 H, m, 4,5-H₂), 8.74 (1 H, d, $J = 8.8$ Hz, 8-H), 8.84 (1 H, d, $J = 1.9$ Hz, 2-H).

(1-Oxido-3-phenylquinolin-8-yl)mercury(II) chloride (173)



To **171** (3.48 g, 15.7 mmol) in glacial AcOH (15 mL) was added Hg(OAc)₂ (4.96 g, 15.7 mmol). The mixture was boiled under reflux for 5 h. The residue was poured into brine (50 mL) and the solid formed was collected by filtration and washed with water to give **173** (5.4 g, 75%) as pale buff crystals: *R*_f = 0.14 (EtOAc); mp 246-249°C; IR ν_{\max} (KBr) 1217 (N⁺-O⁻) cm⁻¹; ¹H NMR 399.65 MHz ((CD₃)₂SO) δ 7.48-7.59 (3 H, m, 3',5',6-H₃), 7.78-7.94 (3 H, m, 2',4',6'-H₃), 8.11 (1 H, d, *J* = 8.0 Hz, 7-H), 8.44 (1 H, d, *J* = 1.6 Hz, 4-H), 8.53 (1 H, d, *J* = 8.0 Hz, 5-H), 9.11 (1 H, d, *J* = 1.6 Hz, 2-H); ¹³C NMR 399.65 MHz ((CD₃)₂SO) δ 118.8 (Cq), 125.5 (Cq), 127.1 (CH), 128.8 (CH), 129.0 (CH), 129.1 (CH), 129.3 (CH), 129.4 (CH), 130.4 (Cq), 134.0 (Cq), 135.0 (CH), 140.1 (CH), 141.9 (Cq). This material was used without further purification.

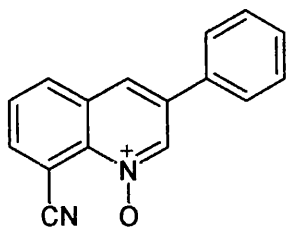
8-Iodo-3-phenylquinoline-1-oxide (174)



To **173** (400 mg, 0.88 mmol) in NMP (0.8 mL) was added iodine (116 mg, 0.88 mmol). The mixture was stirred for 24 h. Chromatography (hexane / EtOAc, 1:1) of the evaporation residue gave **174** (132 mg, 43%) as a pale yellow solid: *R*_f = 0.56 (hexane / EtOAc, 1:1); mp 162-165°C; IR ν_{\max} (KBr) 1240 (N⁺-O⁻) cm⁻¹; ¹H NMR 399.65 MHz (CDCl₃) δ 7.18 (1 H, t, *J* = 7.9 Hz, 6-H), 7.42-7.48 (2 H, m, 3',5'-H₂), 7.52 (1H, t, *J* = 8.2, 4'-H), 7.61 (2 H, dd, *J* = 8.2, 1.6 Hz, 2',6'-H₂), 7.82 (1 H, d, *J* = 1.6 Hz, 4-H), 7.84 (1 H, dd, *J* = 7.9, 1.4 Hz, 5-H), 8.36 (1 H, dd, *J* = 7.9, 1.4 Hz, 7-H); 8.76 (1 H, d, *J* = 1.6 Hz, 2-H); ¹³C NMR 399.65 MHz (HMBC) (CDCl₃) δ 109.9 (8-C), 123.8 (4-C), 126.9 (2',6'-C₂), 129.2 (5-C), 129.4 (4'-C), 129.5 (3',5'-C₂), 129.6 (4a-C), 132.4 (6-C), 135.0 (1'-C),

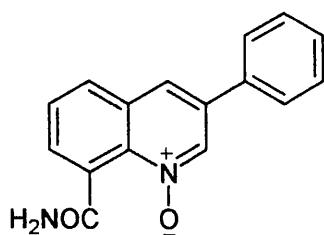
135.1 (8a-C), 135.8 (7-C), 138.2 (3-C), 145.3 (2-C); MS (ES⁺) *m/z* 347.9869 (M + H) (C₁₅H₁₁INO requires 347.9880), 221 (M + H - I⁺).

8-Cyano-3-phenylquinoline-1-oxide (176)



To Na₂CO₃ (280 mg, 2.6 mmol) and urea hydrogen peroxide complex (280 mg, 3.0 mmol) in dry CH₂Cl₂ (5 mL) at 0°C, was added dropwise trifluoroacetic anhydride (0.21 mL, 1.5 mmol). The solution was allowed to reach room temperature and compound **68** (70 mg, 0.30 mmol) was added. The mixture was stirred for 24 h at 40°C. The mixture was extracted with and CH₂Cl₂ washed with water and brine. Evaporation and chromatography (hexane / EtOAc, 1:1) gave **176** (10 mg, 14%) as a white solid: R_f = 0.47 (EtOAc); mp 212-214°C; IR ν_{max} (KBr) 1227 (N⁺-O⁻), 2364 (C≡N) cm⁻¹; ¹H NMR 399.65 MHz (CDCl₃) δ 7.48-7.56 (3 H, m, 3',6',5'-H₃), 7.64 (2 H, d, *J* = 7.8 Hz, 2',6'-H₂), 7.72 (1 H, t, *J* = 7.8 Hz, 4'-H), 7.91 (1 H, d, *J* = 1.6 Hz, 4-H), 8.13 (1 H, d, *J* = 7.4, 1.6 Hz, 5-H), 8.14 (1 H, dd, *J* = 7.4, 1.6 Hz, 7-H), 8.83 (1 H, d, *J* = 1.6 Hz, 2-H); ¹³C NMR 399.65 MHz (HMBC) (CDCl₃) δ 106.0 (8-C), 117.7 (CN), 122.9 (4-C), 127.1 (2',6'-C₂), 128.4 (6-C), 129.6 (3',4',5'-C₃), 131.1 (4a-C), 133.2 (5-C), 134.8 (1'-C), 136.2 (7-C), 136.9 (3-C), 138.9 (8a-C), 139.0 (2-C); MS (ES⁺) *m/z* 247.0865 (M + H) (C₁₆H₁₁N₂O requires 247.0866), 231 (M + H - O); Anal. Calcd. for C₁₆H₁₀N₂O: C, 78.03; H, 4.09; N, 11.38. Found: C, 78.05; H, 3.99; N, 11.12. Further elution gave recovered starting material **68** (22 mg, 31%).

8-carbamoyl-3-phenylquinoline-1-oxide (175)



Compound **176** (283 mg, 1.2 mmol) in EtOH (3.7 mL), was treated with aq. NaOH (0.5 M, 0.52 mL, 0.27 mmol) and aq. H₂O₂ (35%, 0.45 mL, 3.6 mmol). The mixture was heated to 50°C for 1 h and allowed to cool and was neutralised with aq. sulfuric acid (10%). The evaporation residue was purified by chromatography (EtOAc / MeOH, 5:1) to give **175** (43 mg, 14%) as a white solid: *R_f* = 0.19 (EtOAc / MeOH, 10:2); mp 264–265°C; IR ν_{\max} (KBr) 1219 (N⁺-O⁻), 3420 (NH₂) cm⁻¹; ¹H NMR 399.65 MHz ((CD₃)₂SO) δ 7.48 (1 H, t, *J* = 8.1 Hz, 6-H), 7.56 (2 H, t, *J* = 7.9 Hz, 3',5'-H₂), 7.72 (1 H, t, *J* = 7.9 Hz, 4'-H), 7.89 (2 H, d, *J* = 7.9 Hz, 2',6'-H₂), 8.13 (1 H, dd, *J* = 8.1, 1.2 Hz, 5-H), 8.15 (1 H, dd, *J* = 8.1, 1.2 Hz, 7-H), 8.31 (1 H, d, *J* = 1.8 Hz, 4-H), 8.92 (1 H, d, *J* = 1.8 Hz, 2-H); ¹³C NMR 399.65 MHz (HMBC) ((CD₃)₂SO) δ 122.2 (4-C), 127.2 (2',6'-C₂), 128.7 (6-C), 129.2 (4a-C or 8-C), 129.4 (8-C or 4a-C), 129.5 (3',5'-C₂), 129.7 (5-C), 130.9 (7-C), 131.8 (4'-C), 134.2 (3-C), 134.3 (2-C), 135.2 (1'-C), 136.2 (C-8a), 170.4 (CONH₂); MS (ES⁺) *m/z* 551 (2 M + Na), 265.0960 (M + H) (C₁₆H₁₃N₂O₂ requires 265.0972); Anal. Calcd. C₁₆H₁₂N₂O₂: C, 72.72; H, 4.58; N, 10.60. Found: C, 72.74; H, 4.46; N, 10.47.

Experimental Details for Chapter 4.0.

PARP-1 Colourimetric Assay

Materials and Method

Inhibitor constants were determined using the Universal PARP assay kit (Trevigen). The assays were performed in 96 strip-well plates pre-coated with histones. The potencies of novel quinoline-8-carboxamide PARP-1 inhibitors were compared with that of 5-aminoisoquinolin-1-(2*H*)-one, a known PARP-1 inhibitor.¹²⁹ Briefly, PARP inhibitor stock solutions (50 mM) were prepared by dissolving them in 100% DMSO. To generate inhibition curves, the PARP inhibitor stock solutions were diluted with 1 x PARP buffer to give seven different concentrations at 5 x stock solution such that the final concentrations in the assay were 100, 30, 10, 3, 1, 0.3, and 0.1 μM . The final concentration of DMSO in the assay was less than 0.2 % (v/v). A positive control (PARP enzyme with no inhibitor) and negative control (no PARP enzyme) were included in each assay. The PARP enzyme was diluted to 0.8 units / 15 μL with 1 x PARP buffer. Diluted PARP inhibitor (40 μL) was mixed with diluted PARP enzyme (60 μL), centrifuged and incubated for 10 min at ambient temperature. Then 25 μL of each solution was distributed into wells in triplicate. To initiate the reaction 25 μL of PARP cocktail [(10 x PARP cocktail, 10 x Activated DNA, 1 x PARP buffer (1:1:8) (v/v/v))] was added to each well using a multi-channel pipettor. In all cases the final reaction volume was 50 μL . The reaction was allowed to proceed for 1 h at ambient temperature. Plates were washed four times with PBS + 0.1 % (v/v) Triton X-100 (200 μL). Then 50 μL Strep-HRP (1000 fold with 1 x Strep diluent) was added to each well with a multi-channel pipettor, and the plate incubated for 30 min at ambient temperature before washing with PBS + 0.1 % (v/v) Triton X-100 (200 μL). Substrate TACS Sapphire (50 μL / well) was added with a multi-channel pipettor and the plates incubated in the dark for 30 min. Absorbance at 630 nm was measured using a Versamax microplate reader with SoftMax Pro 4.7.1 software. The colourimetric reaction was stopped by adding 0.2 M HCl (50 μL / well), and the absorbance read at 450 nm.

Data were analysed using GraphPad Prism 2.01 software. The IC_{50} values were calculated by plotting \log_{10} [inhibitor] versus absorbance for the replicant data. Quoted IC_{50} values are an average for the three replicant curves.

SIRT1 Fluorimetric Assay

Materials and Method

Inhibitor constants were determined using the SIRT1 fluorescent assay Biomol® kit. The assays were performed in black 96 strip-well plates. The potencies of novel quinoline-8-carboxamide inhibitors were compared with that of nicotinamide, a known Sirtuin inhibitor. The test inhibitor stock solutions (50mM) were prepared by dissolving them in 100% DMSO. To generate inhibition curves, the test inhibitor stock solutions were diluted with 1 x Sirtuin assay buffer (50 mM Tris / Cl, pH 8.0, 137 mM NaCl, 2.7 mM KCl, 1 mM MgCl₂, 1 mg / mL BSA) to give seven different concentrations at 5 x stock solution such that the final concentrations in the assay were 100, 30, 10, 3, 1, 0.3, and 0.1 μM. The final concentration of DMSO in the assay was less than 0.2 % (v/v). A positive control (Sirtuin enzyme with no inhibitor) and negative control (no Sirtuin enzyme) were included in each assay. The Sirtuin enzyme was diluted to 0.84 units / 15 μL with 1 x Sirtuin assay buffer. The diluted test inhibitor (40 μL) was mixed with diluted Sirtuin enzyme (60 μL) and kept on ice. Then 25 μL of each solution was distributed into wells in triplicate. To initiate the reaction 25 μL of 2 x substrate (*fluor de Lys-SIRT1*, NAD⁺ and 1 x Sirtuin assay buffer) was added to each well using a multi-channel pipettor (75 μM final concentration). In all cases the final reaction volume was 50 μL. The assay plate was incubated at 37°C for 1 h. Then fresh 1 x *fluor Lys*TM Developer II plus 2 mM nicotinamide (50 μL / well) was added to each well to quench the reaction and the plate incubated at 37°C for 35 min. Fluorescence at λ_{EX} 355 nm and λ_{ES} 460 nm was measured using a BMG Labtech Fluorostar Optima microplate reader with Optima version 5 software.

Data were analysed using GraphPad Prism 2.01 software. The IC₅₀ values were calculated by plotting log₁₀ [inhibitor] versus fluorescence for the replicant data. Quoted IC₅₀ values are an average for the three replicant curves.

References

- (1) Chabner, B. A.; Roberts, T. G. *Nat. Rev. Cancer* **2005**, *5*, 65-72.
- (2) Thomlinson, R. H.; Gray, L. H. *Br. J. Cancer* **1955**, *9*, 539-549.
- (3) Brown, J. M.; Wilson, W. R. *Nat. Rev. Cancer* **2004**, *4*, 437-447.
- (4) Brown, J. M.; Giaccia, A. J. *Cancer Res.* **1998**, *58*, 1408-1416.
- (5) Hockel, M.; Vaupel, P. *J. Natl. Cancer Inst.* **2001**, *93*, 266-276.
- (6) Sipkins, D. A.; Cheresch, D. A.; Kazemi, M. R.; Nevin, L. M.; Bednarski, M. D.; Li, K. C. P. *Nat. Med.* **1998**, *4*, 623-626.
- (7) Aboagye, E. O.; Kelson, A. B.; Tracy, M.; Workman, P. *Anti-Cancer Drug Des.* **1998**, *13*, 703-730.
- (8) Siim, B. G.; Laux, W. T.; Rutland, M. D.; Palmer, B. N.; Wilson, W. R. *Cancer Res.* **2000**, *60*, 4582-4588.
- (9) Coleman, C. N. *J. Natl. Cancer Inst.* **1988**, *80*, 310-317.
- (10) Henk, J. M.; Kunkler, P. B.; Smith, C. W. *Lancet* **1977**, *2*, 101-103.
- (11) Watson, E. R.; Halnan, K. E.; Dische, S.; Saunders, M. I.; Cade, I. S.; McEwen, J. B.; Wiemik, G.; Perrins, D. J. D.; Sutherland, M. A. *Br. J. Radiol.* **1978**, *51*, 879-887.
- (12) Adams, G. E.; Flockhart, I. R.; Smithen, C. E.; Stratford, I. J.; Wardman, P.; Watts, M. E. *Radiat. Res.* **1976**, *67*, 9-20.
- (13) Urtasun, R. C.; Band, P. R.; Chapman, J. D.; Feldstein, M. L. *N. Engl. J. Med* **1977**, *296*, 757-757.
- (14) Dische, S.; Saunders, M. I.; Lee, M. E.; Adams, G. E.; Flockhart, I. R. *Br. J. Cancer* **1977**, *35*, 567-579.
- (15) Brown, J. M.; Yu, N. Y.; Brown, D. M.; Lee, W. W. *Int. J. Radiat. Oncol. Biol. Phys.* **1981**, *7*, 695-703.
- (16) Lee, D. J.; Cosmatos, D.; Marcial, V. A.; Fu, K. K.; Rotman, M.; Cooper, J. S.; Ortiz, H. G.; Beitler, J. J.; Abrams, R. A.; Curran, W. J.; Coleman, C. N.; Wasserman, T. H. *Int. J. Radiat. Oncol. Biol. Phys.* **1995**, *32*, 567-576.
- (17) Teicher, B. A.; Crawford, J. M.; Holden, S. A.; Cathcart, K. N. S. *Cancer Res.* **1987**, *47*, 5036-5041.
- (18) Pallavicini, M. G.; Lalande, M. E.; Miller, R. G.; Hill, R. P. *Cancer Res.* **1979**, *39*, 1891-1897.
- (19) Walker, L. J.; Craig, R. B.; Harris, A. L.; Hickson, I. D. *Nucleic Acids Res.* **1994**, *22*, 4884-4889.
- (20) Adams, G. E.; Stratford, I. J. *Biochem. Pharm.* **1986**, *35*, 71-76.

- (21) Comerford, K. M.; Wallace, T. J.; Karhausen, J.; Louis, N. A.; Montalto, M. C.; Colgan, S. P. *Cancer Res.* **2002**, *62*, 3387-3394.
- (22) Hughes, C. S.; Shen, J. W.; Subject, J. R. *Cancer Res.* **1989**, *49*, 4452-4454.
- (23) Shen, J.; Hughes, C.; Chao, C.; Cai, J.; Bartels, C.; Gessner, T.; Subject, J. *Proc. Natl. Acad. Sci. USA* **1987**, *84*, 3278-3282.
- (24) Guillemin, K.; Krasnow, M. A. *Cell* **1997**, *89*, 9-12.
- (25) Huang, L. E.; Arany, Z.; Livingston, D. M.; Bunn, H. F. *J. Biol. Chem.* **1996**, *271*, 32253-32259.
- (26) Pugh, C. W.; Ratcliffe, P. J. *Nat. Med.* **2003**, *9*, 677-684.
- (27) Ravi, R.; Mookerjee, B.; Bhujwalla, Z. M.; Sutter, C. H.; Artemov, D.; Zeng, Q. W.; Dillehay, L. E.; Madan, A.; Semenza, G. L.; Bedi, A. *Genes Dev.* **2000**, *14*, 34-44.
- (28) Jiang, B. H.; Jiang, G. Q.; Zheng, J. Z.; Lu, Z. M.; Hunter, T.; Vogt, P. K. *Cell Growth Differ.* **2001**, *12*, 363-369.
- (29) Zhong, H.; De Marzo, A. M.; Laughner, E.; Lim, M.; Hilton, D. A.; Zagzag, D.; Buechler, P.; Isaacs, W. B.; Semenza, G. L.; Simons, J. W. *Cancer Res.* **1999**, *59*, 5830-5835.
- (30) Maxwell, P. H.; Wiesener, M. S.; Chang, G. W.; Clifford, S. C.; Vaux, E. C.; Cockman, M. E.; Wykoff, C. C.; Pugh, C. W.; Maher, E. R.; Ratcliffe, P. J. *Nature* **1999**, *399*, 271-275.
- (31) Stebbins, C. E.; Kaelin, W. G.; Pavletich, N. P. *Science* **1999**, *284*, 455-461.
- (32) Li, L. M.; Lin, X. Y.; Staver, M.; Shoemaker, A.; Semizarov, D.; Fesik, S. W.; Shen, Y. *Cancer Res.* **2005**, *65*, 7249-7258.
- (33) Welsh, S.; Williams, R.; Kirkpatrick, L.; Paine-Murrieta, G.; Powis, G. *Mol. Cancer Ther.* **2004**, *3*, 233-244.
- (34) Kong, D. H.; Park, E. J.; Stephen, A. G.; Calvani, M.; Cardellina, J. H.; Monks, A.; Fisher, R. J.; Shoemaker, R. H.; Melillo, G. *Cancer Res.* **2005**, *65*, 9047-9055.
- (35) Semenza, G. L. *Biochem. Pharmacol.* **2000**, *59*, 47-53.
- (36) Rapisarda, A.; Uranchimeg, B.; Sordet, O.; Pommier, Y.; Shoemaker, R. H.; Melillo, G. *Cancer Res.* **2004**, *64*, 1475-1482.
- (37) Yeo, E. J.; Chun, Y. S.; Cho, Y. S.; Kim, J. H.; Lee, J. C.; Kim, M. S.; Park, J. W. *J. Natl. Cancer Inst.* **2003**, *95*, 516-525.
- (38) Welsh, S. J.; Williams, R. R.; Birmingham, A.; Newman, D. J.; Kirkpatrick, D. L.; Powis, G. *Mol. Cancer Ther.* **2003**, *2*, 235-243.

- (39) Mabjeesh, N. J.; Escuin, D.; LaVallee, T. M.; Pribluda, V. S.; Swartz, G. M.; Johnson, M. S.; Willard, M. T.; Zhong, H.; Simons, J. W.; Giannakakou, P. *Cancer Cell* **2003**, *3*, 363-375.
- (40) Albert, A. *Nature* **1958**, *182*, 421-423.
- (41) Denny, W. A. *Lancet Oncol.* **2000**, *1*, 25-29.
- (42) Workman, P.; Stratford, I. J. *Cancer Metastasis Rev.* **1993**, *12*, 73-82.
- (43) Denny, W. A.; Wilson, W. R.; Hay, M. P. *Br. J. Cancer* **1996**, *74*, S32-S38.
- (44) Mohindra, J. K.; Rauth, A. M. *Br. J. Cancer* **1976**, *36*, 930-936.
- (45) Denny, W. A. *Eur. J. Med. Chem.* **2001**, *36*, 577-595.
- (46) Robertson, N.; Stratford, I. J.; Houlbrook, S.; Carmichael, J.; Adams, G. E. *Biochem. Pharmacol.* **1992**, *44*, 409-412.
- (47) Walton, M. I.; Workman, P. *Biochem. Pharmacol.* **1987**, *36*, 887-896.
- (48) Walton, M. I.; Workman, P. *Biochem. Pharmacol.* **1990**, *39*, 1735-1742.
- (49) Kayyali, U. S.; Donaldson, C.; Huang, H. L.; Abdelnour, R.; Hassoun, P. M. *J. Biol. Chem.* **2001**, *276*, 14359-14365.
- (50) López de Ceráin, A.; Marin, A.; Idoate, M. A.; Tunon, M. T.; Bello, J. *Eur. J. Cancer* **1999**, *35*, 320-324.
- (51) Ware, D. C.; Palmer, B. D.; Wilson, W. R.; Denny, W. A. *J. Med. Chem.* **1993**, *36*, 1839-1846.
- (52) Nishimoto, S.; Hatta, H.; Ueshima, H.; Kagiya, T. *J. Med. Chem.* **1992**, *35*, 2711-2712.
- (53) Kriste, A. G.; Tercel, M.; Stribbling, S. M.; Botting, K. J.; Wilson, W. R. *Br. J. Cancer* **2002**, *86*, S30-S31.
- (54) Jaffar, M.; Williams, K. J.; Stratford, I. J. *Adv. Drug Deliv. Rev.* **2001**, *53*, 217-228.
- (55) Denny, W. A.; Wilson, W. R. *J. Med. Chem.* **1986**, *29*, 879-887.
- (56) Jenkins, T. C.; Naylor, M. A.; O'Neill, P.; Threadgill, M. D.; Cole, S.; Stratford, I. J.; Adams, G. E.; Fielden, E. M.; Suto, M. J.; Stier, M. A. *J. Med. Chem.* **1990**, *33*, 2603-2610.
- (57) Lee, A. E.; Wilson, W. R. *Toxicol. Appl. Pharmacol.* **2000**, *163*, 50-59.
- (58) Everett, S. A.; Naylor, M. A.; Patel, K. B.; Stratford, M. R. L.; Wardman, P. *Bioorg. Med. Chem. Lett.* **1999**, *9*, 1267-1272.
- (59) Firestone, A.; Mulcahy, R. T.; Borch, R. F. *J. Med. Chem.* **1991**, *34*, 2933-2935.
- (60) Mulcahy, R. T.; Gipp, J. J.; Schmidt, J. P.; Joswig, C.; Borch, R. F. *J. Med. Chem.* **1994**, *37*, 1610-1615.

- (61) Sykes, B. M.; Atwell, G. J.; Hogg, A.; Wilson, W. R.; O'Connor, C. J.; Denny, W. A. *J. Med. Chem.* **1999**, *42*, 346-355.
- (62) Hicks, K. O.; Fleming, Y.; Siim, B. G.; Koch, C. J.; Wilson, W. R. *Int. J. Radiat. Oncol. Biol. Phys.* **1998**, *42*, 641-649.
- (63) Lee, D. J.; Trotti, A.; Spencer, S.; Rostock, R.; Fisher, C.; von Roemeling, R.; Harvey, E.; Groves, E. G. *Int. J. Radiat. Oncol. Biol. Phys.* **1998**, *42*, 811-815.
- (64) von Pawel, J.; von Roemeling, R.; Gatzemeier, U.; Boyer, M.; Elisson, L. O.; Ciark, P.; Talbot, D.; Rey, A.; Butler, T. W.; Hirsh, V.; Olver, I.; Bergman, B.; Ayoub, J.; Richrdson, G.; Dunlop, D.; Arcenas, A.; Vescio, R.; Viallet, J.; Treat, J. *J. Clin. Oncol.* **2000**, *18*, 1351-1359.
- (65) Monge, A.; Martínez-Crespo, F. J.; López de Ceráin, A.; Palop, J. A.; Narro, S.; Senador, V.; Marín, A.; Sainz, Y.; González, M.; Hamilton, E.; Barker, A. *J. Med. Chem.* **1995**, *38*, 4488-4494.
- (66) Naylor, M. A.; Adams, G. E.; Haigh, A.; Cole, S.; Jenner, T.; Robertson, N.; Siemann, D.; Stephens, M. A.; Stratford, I. J. *Anti-Cancer Drugs* **1995**, *6*, 259-269.
- (67) Barham, H. M.; Stratford, I. J. *Biochem. Pharmacol.* **1996**, *51*, 829-837.
- (68) Smith, P. J.; Blunt, N. J.; Desnoyers, R.; Giles, Y.; Patterson, L. H. *Cancer Chemother. Pharmacol.* **1997**, *39*, 455-461.
- (69) Raleigh, S. M.; Wanogho, E.; Burke, M. D.; McKeown, S. R.; Patterson, L. H. *Int. J. Radiat. Oncol. Biol. Phys.* **1998**, *42*, 763-767.
- (70) Patterson, L. H.; McKeown, S. R. *Br. J. Cancer* **2000**, *83*, 1589-1593.
- (71) Patterson, L. H.; McKeown, S. R.; Ruparella, K.; Double, J. A.; Bibby, M. C.; Cole, S.; Stratford, I. J. *Br. J. Cancer* **2000**, *82*, 1984-1990.
- (72) Friery, O. P.; Gallagher, R.; Murray, M. M.; Hughes, C. M.; Galligan, E. S.; McIntyre, I. A.; Patterson, L. H.; Hirst, D. G.; McKeown, S. R. *Br. J. Cancer* **2000**, *82*, 1469-1473.
- (73) Wilson, W. R.; van Zijl, P.; Denny, W. A. *Int. J. Radiat. Oncol. Biol. Phys.* **1992**, *22*, 693-696.
- (74) Lee, H. H.; Wilson, W. R.; Ferry, D. M.; van Zijl, P.; Pullen, S. M.; Denny, W. A. *J. Med. Chem.* **1996**, *39*, 2508-2517.
- (75) Lee, H. H.; Wilson, W. R.; Denny, W. A. *Anti-Cancer Drug Des.* **1999**, *14*, 487-497.
- (76) Yin, H.; Xu, Y.; Qian, X.; Li, Y.; Liu, J. *Bioorg. Med. Chem. Lett.* **2007**, *17*, 2166-2170.

- (77) Li, V. S.; Choi, D.; Wang, Z.; Jimenez, L. S.; Tang, M. S.; Kohn, H. J. *Am. Chem. Soc.* **1996**, *118*, 2326-2331.
- (78) Tomasz, M.; Lipman, R.; Chowdary, D.; Pawlak, J.; Verdine, G. L.; Nakanishi, K. *Science* **1987**, *235*, 1204-1208.
- (79) Haffty, B. G.; Wilson, L. D.; Son, Y. H.; Cho, E. I.; Papac, R. J.; Fischer, D. B.; Rockwell, S.; Sartorelli, A. C.; Ross, D. A.; Sasaki, C. T.; Fischer, J. J. *Int. J. Radiat. Oncol. Biol. Phys.* **2005**, *61*, 119-128.
- (80) Ross, D.; Beall, H. D.; Siegel, D.; Traver, R. D.; Gustafson, D. L. *Br. J. Cancer* **1996**, *74*, S1-S8.
- (81) Flader, C.; Liu, J. W.; Borch, R. F. *J. Med. Chem.* **2000**, *43*, 3157-3167.
- (82) Everett, S. A.; Naylor, M. A.; Barraja, P.; Swann, E.; Patel, K. B.; Stratford, M. R. L.; Hudnott, A. R.; Vojnovic, B.; Locke, R. J.; Wardman, P.; Moody, C. J. *J. Chem. Soc., Perkin Trans. 2* **2001**, 843-860.
- (83) Hendriks, H. R.; Pizao, P. E.; Berger, D. P.; Kooistra, K. L.; Bibby, M. C.; Boven, E.; Dreef-van der Meulen, H. C.; Henrar, R. E. C.; Fiebig, H. H.; Double, J. A.; Hornstra, H. W.; Pinedo, H. M.; Workman, P.; Schwartzmann, G. *Eur. J. Cancer* **1993**, *29A*, 897-906.
- (84) Dirix, L. Y.; Tonnesen, F.; Cassidy, J.; Epelbaum, R.; ten Bokkel Huinink, W. W.; Pavlidis, N.; Sorio, R.; Gamucci, T.; Wolff, I.; Te Velde, A.; Lan, J.; Verweij, J. *Eur. J. Cancer* **1996**, *32A*, 2019-2022.
- (85) Nguewa, P. A.; Fuentes, M. A.; Valladares, B.; Alonso, C.; Pérez, J. M. *Prog. Biophys. Mol. Biol.* **2005**, *88*, 143-172.
- (86) Shall, S. *Adv. Radiat. Biol.* **1984**, *11*, 1-69.
- (87) de Murcia, G.; Schreiber, V.; Molinete, M.; Saulier, B.; Poch, O.; Masson, M.; Niedergang, C.; Ménissier-de Murcia, J. *Mol. Cell. Biochem.* **1994**, *138*, 15-24.
- (88) Gradwohl, G.; Ménissier-de Murcia, J.; Molinete, M.; Simonin, F.; Koken, M.; Hoeijmakers, J. H. J.; de Murcia, G. *Proc. Natl. Acad. Sci. USA* **1990**, *87*, 2990-2994.
- (89) D'Amours, D.; Desnoyers, S.; D'Silva, I.; Poirier, G. G. *Biochem. J.* **1999**, *342*, 249-268.
- (90) Uchida, K.; Hanai, S.; Ishikawa, K.; Ozawa, Y.; Uchida, M.; Sugimura, T.; Miwa, M. *Proc. Natl. Acad. Sci. USA* **1993**, *90*, 3481-3485.
- (91) Bork, P.; Hofmann, K.; Bucher, P.; Neuwald, A. F.; Altschul, S. F.; Koonin, E. V. *FASEB J.* **1997**, *11*, 68-76.
- (92) Simonin, F.; Hofferer, L.; Panzeter, P. L.; Muller, S.; de Murcia, G.; Althaus, F. R. *J. Biol. Chem.* **1993**, *268*, 13454-13461.

- (93) Shall, S. *Biochimie* **1995**, *77*, 313-318.
- (94) Mendoz-Alvarez, H.; Alvarez-Gonzalez, R. *J. Biol. Chem.* **1993**, *268*, 22575-22580.
- (95) Griffin, R. J.; Curtin, N. J.; Newell, D. R.; Golding, B. T.; Durkacz, B. W.; Calvert, A. H. *Biochimie* **1995**, *77*, 408-422.
- (96) Oka, J.; Ueda, K.; Hayaishi, O.; Komura, H.; Nakanishi, K. *J. Biol. Chem.* **1984**, *259*, 986-995.
- (97) Chambon, P.; Weill, J. D.; Mandel, P. *Biochem. Biophys. Res. Commun.* **1963**, *11*, 39-43.
- (98) Shieh, W. M.; Amé, J. C.; Wilson, M. V.; Wang, Z. Q.; Koh, D. W.; Jacobson, M. K.; Jacobson, E. L. *J. Biol. Chem.* **1998**, *273*, 30069-30072.
- (99) Amé, J. C.; Spenlehauer, C.; de Murcia, G. *Bioessays* **2004**, *26*, 882-893.
- (100) Amé, J. C.; Rolli, V.; Schreiber, V.; Niedergang, C.; Apiou, F.; Decker, P.; Muller, S.; Höger, T.; Ménissier-de Murcia, J.; de Murcia, G. *J. Biol. Chem.* **1999**, *274*, 17860-17868.
- (101) Amé, J. C.; Schreiber, V.; Fraulob, V.; Dolle, P.; de Murcia, G.; Niedergang, C. P. *J. Biol. Chem.* **2001**, *276*, 11092-11099.
- (102) Ménissier-de Murcia, J.; Niedergang, C.; Trucco, C.; Ricoul, M.; Dutrillaux, B.; Mark, M.; Oliver, F. J.; Masson, M.; Dierich, A.; LeMeur, M.; Walztinger, C.; Chambon, P.; de Murcia, G. *Proc. Natl. Acad. Sci. USA* **1997**, *94*, 7303-7307.
- (103) Kanai, M.; Tong, W. M.; Sugihara, E.; Wang, Z. Q.; Fukasawa, K.; Miwa, M. *Mol. Cell. Biochem.* **2003**, *23*, 2451-2462.
- (104) Lange, B. M. H.; Gull, K. *J. Cell Biol.* **1995**, *130*, 919-927.
- (105) Augustin, A.; Spenlehauer, C.; Dumond, H.; Ménissier-de Murcia, J.; Piel, M.; Schmit, A. C.; Apiou, F.; Vonesch, J. L.; Kock, M.; Bornens, M.; de Murcia, G. *J. Cell Sci.* **2003**, *116*, 1551-1562.
- (106) Kickhoefer, V. A.; Vasu, S. K.; Rome, L. H. *Trends Cell Biol.* **1996**, *6*, 174-178.
- (107) Kickhoefer, V. A.; Rajavel, K. S.; Scheffer, G. L.; Dalton, W. S.; Scheper, R. J.; Rome, L. H. *J. Biol. Chem.* **1998**, *273*, 8971-8974.
- (108) Scheffer, G. L.; Wijngaard, P. L. J.; Flens, M. J.; Izquierdo, M. A.; Slovak, M. L.; Pinedo, H. M.; Meijer, C. J. L. M.; Clevers, H. C.; Scheper, R. J. *Nat. Med.* **1995**, *1*, 578-582.
- (109) De Rycker, M.; Venkatesan, R. N.; Wei, C.; Price, C. M. *Biochem. J.* **2003**, *372*, 87-96.

- (110) De Rycker, M.; Price, C. M. *Mol. Cell. Biol.* **2004**, *24*, 9802-9812.
- (111) Chi, N. W.; Lodish, H. F. *J. Biol. Chem.* **2000**, *275*, 38437-38444.
- (112) Smith, S.; Gariat, I.; Schmitt, A.; de Lange, T. *Science* **1998**, *282*, 1484-1487.
- (113) Kaminker, P. G.; Kim, S. H.; Taylor, R. D.; Zebarjadian, Y.; Funk, W. D.; Morin, G. B.; Yaswen, P.; Campisi, J. *J. Biol. Chem.* **2001**, *276*, 35891-35899.
- (114) Ma, Q.; Baldwin, K. T.; Renzelli, A. J.; McDaniel, A.; Dong, L. *Biochem. Biophys. Res. Commun.* **2001**, *289*, 499-506.
- (115) Kato, T.; Suzumura, Y.; Fukushima, M. *Anticancer Res.* **1988**, *8*, 239-243.
- (116) Chen, G.; Pan, Q. C. *Cancer Chemother. Pharmacol.* **1988**, *22*, 303-307.
- (117) Petrou, C.; Mourelatos, D.; Mioglou, E.; Dozi-Vassiliades, J.; Catsoulacos, P. *Teratog. Carcinog. Mutagen.* **1990**, *10*, 321-331.
- (118) Eliopoulos, P.; Mourelatos, D.; Dozi-Vassiliades, J. *Mutat. Res. Genet. Toxicol.* **1995**, *342*, 141-146.
- (119) Horsman, M. R.; Brown, D. M.; Hirst, D. G.; Brown, J. M. *Br. J. Cancer* **1986**, *53*, 247-254.
- (120) Miknyoczki, S. J.; Jones-Bolin, S.; Pritchard, S.; Hunter, K.; Zhao, H.; Wan, W. H.; Ator, M.; Bihovsky, R.; Hudkins, R.; Chatterjee, S.; Klein-Szanto, A.; Dionne, C.; Ruggeri, B. *Mol. Cancer Ther.* **2003**, *2*, 371-382.
- (121) Calabrese, C. R.; Almassy, R.; Barton, S.; Batey, M. A.; Calvert, A. H.; Canan-Koch, S.; Durkacz, B. W.; Hostomsky, Z.; Kumpf, R. A.; Kyle, S.; Li, J.; Maegley, K.; Newell, D. R.; Notarianni, E.; Stratford, I. J.; Skalitzky, D.; Thomas, H. D.; Wang, L. Z.; Webber, S. E.; Williams, K. J.; Curtin, N. J. *J. Natl. Cancer Inst.* **2004**, *96*, 56-67.
- (122) Griffin, R. J.; Pemberton, L. C.; Rhodes, D.; Bleasdale, C.; Bowman, K.; Calvert, A. H.; Curtin, N. J.; Durkacz, B. W.; Newell, D. R.; Porteous, J. K.; Golding, B. T. *Anti-Cancer Drug Des.* **1995**, *10*, 507-514.
- (123) Bowman, K. J.; Newell, D. R.; Calvert, A. H.; Curtin, N. J. *Br. J. Cancer* **2001**, *84*, 106-112.
- (124) Delaney, C. A.; Wang, L. Z.; Kyle, S.; White, A. W.; Calvert, A. H.; Curtin, N. J.; Durkacz, B. W.; Hostomsky, Z.; Newell, D. R. *Clin. Cancer Res.* **2000**, *6*, 2860-2867.
- (125) Tentori, L.; Portarena, I.; Graziani, G. *Pharmacol. Res.* **2002**, *45*, 73-85.

- (126) Tentori, L.; Leonetti, C.; Scarsella, M.; d'Amati, G.; Vergati, M.; Portarena, I.; Xu, W. Z.; Kalish, V.; Zupi, G.; Zhang, J.; Graziani, G. *Clin. Cancer Res.* **2003**, *9*, 5370-5379.
- (127) Horsman, M. R. *Acta Oncol.* **1995**, *34*, 571-587.
- (128) van der Maazen, R. W. M.; Thijssen, H. O. M.; Kaanders, J. H. A. M.; de koster, A.; Keyser, A.; Prick, M. J. J.; Grotenhuis, J. A.; Wesseling, P.; van der Kogel, A. J. *Radiother. Oncol.* **1995**, *35*, 118-122.
- (129) Suto, M. J.; Turner, W. R.; Arundel-Suto, C. M.; Werbel, L. M.; Sebolt-Leopold, J. S. *Anti-Cancer Drug Des.* **1991**, *6*, 107-117.
- (130) Brock, W. A.; Milas, L.; Bergh, S.; Lo, R.; Szabó, C.; Mason, K. A. *Cancer Lett.* **2004**, *205*, 155-160.
- (131) Farmer, H.; McCabe, N.; Lord, C. J.; Tutt, A. N. J.; Johnson, D. A.; Richardson, T. B.; Santarosa, M.; Dillon, K. J.; Hickson, I.; Knights, C.; Martin, N. M. B.; Jackson, S. P.; Smith, G. C. M.; Ashworth, A. *Nature* **2005**, *434*, 917-921.
- (132) Schroeijers, A. B.; Siva, A. C.; Scheffer, G. L.; de Jong, M. C.; Bolick, S. C. E.; Dukers, D. F.; Slootstra, J. W.; Meloen, R. H.; Wiemer, E.; Kickhoefer, V. A.; Rome, L. H.; Scheper, R. J. *Cancer Res.* **2000**, *60*, 1104-1110.
- (133) Faraoni, I.; Bonmassar, E.; Graziani, G. *Drug Resist. Update* **2000**, *3*, 161-170.
- (134) van Steensel, B.; de Lange, T. *Nature* **1997**, *385*, 740-743.
- (135) Cosi, C. *Expert Opin. Ther. Patents* **2002**, *12*, 1047-1071.
- (136) Thiemermann, C.; Bowes, J.; Myint, F. P.; Vane, J. R. *Proc. Natl. Acad. Sci. USA* **1997**, *94*, 679-683.
- (137) Halmosi, R.; Berente, Z.; Osz, E.; Toth, K.; Literati-Nagy, P.; Sumegi, B. *Mol. Pharmacol.* **2001**, *59*, 1497-1505.
- (138) Yang, Z. Q.; Zingarelli, B.; Szabó, C. *Shock* **2000**, *13*, 60-66.
- (139) Zingarelli, B.; Salzman, A. L.; Szabó, C. *Circ.Res.* **1998**, *83*, 85-94.
- (140) Szabó, G.; Bährle, S.; Stumpf, N.; Sonnenberg, K.; Szabó, T.; Pacher, P.; Csont, T.; Schulz, R.; Dengler, T. J.; Liaudet, L.; Jagtap, P. G.; Southan, G. J.; Vahl, C. F.; Hagl, S.; Szabó, C. *Circ.Res.* **2002**, *90*, 100-106.
- (141) Eliasson, M. J. L.; Sampei, K.; Mandir, A. S.; Hurn, P. D.; Traystman, R. J.; Bao, J.; Pieper, A.; Wang, Z. Q.; Dawson, T. M.; Snyder, S. H.; Dawson, V. L. *Nat. Med.* **1997**, *3*, 1089-1095.
- (142) Cosi, C.; Suzuki, H.; Skaper, S. D.; Milani, D.; Facci, L.; Menegazzi, M.; Vantini, G.; Kanai, Y.; Degryse, A.; Colpaert, F.; Koek, W.; Marien, M. R. *Ann. NY Acad. Sci.* **1997**, *825*, 366-379.

- (143) Cosi, C.; Marien, M. *Brain Res.* **1998**, *809*, 58-67.
- (144) Mandir, A. S.; Przedborski, S.; Jackson-Lewis, V.; Wang, Z. Q.; Simbulan-Rosenthal, C. M.; Smulson, M. E.; Hoffman, B. E.; Guastella, D. B.; Dawson, V. L.; Dawson, T. M. *Proc. Natl. Acad. Sci. USA* **1999**, *96*, 5774-5779.
- (145) Genovese, T.; Mazzon, E.; Muià, C.; Patel, N. S. A.; Threadgill, M. D.; Bramanti, P.; De Sarro, A.; Thiernemann, C.; Cuzzocrea, S. *J. Pharmacol. Exp. Ther.* **2005**, *312*, 449-457.
- (146) Liaudet, L.; Szabó, A.; Soriano, F. G.; Zingarelli, B.; Szabó, C.; Salzman, A. L. *Shock* **2000**, *14*, 134-141.
- (147) Mazzon, E.; Dugo, L.; De Sarro, A.; Li, J. H.; Caputi, A. P.; Zhang, J.; Cuzzocrea, S. *Shock* **2002**, *17*, 222-227.
- (148) Di Paola, R.; Genovese, T.; Caputi, A. P.; Threadgill, M. D.; Thiernemann, C.; Cuzzocrea, S. *Eur. J. Pharmacol.* **2004**, *492*, 203-210.
- (149) Chatterjee, P. K.; Chatterjee, B. E.; Pedersen, H.; Sivarajah, A.; McDonald, M. C.; Mota-Filipe, H.; Brown, P. A. J.; Stewart, K. N.; Cuzzocrea, S.; Threadgill, M. D.; Thiernemann, C. *Kidney Int.* **2004**, *65*, 499-509.
- (150) Ivanyi, Z.; Hauser, B.; Pittner, A.; Asfar, P.; Vassilev, D.; Nalos, M.; Altherr, J.; Bruckner, U. B.; Szabó, C.; Rademacher, P.; Froba, G. *Shock* **2003**, *19*, 415-421.
- (151) McDonald, M. C.; Mota-Filipe, H.; Wright, J. A.; Abdelrahman, M.; Threadgill, M. D.; Thompson, A. S.; Thiernemann, C. *Br. J. Pharmacol.* **2000**, *130*, 843-850.
- (152) Lam, T. T. *Res. Commun. Mol. Pathol. Pharmacol.* **1997**, *95*, 241-252.
- (153) Oliver, F. J.; Ménissier-de Murcia, J.; Nacci, C.; Decker, P.; Andriantsitohaina, R.; Muller, S.; de la Rubia, G.; Stoclet, J. C.; de Murcia, G. *EMBO J.* **1999**, *18*, 4446-4454.
- (154) Szabó, A.; Hake, P.; Salzman, A. L.; Szabó, C. *Shock* **1998**, *10*, 347-353.
- (155) Pieper, A. A.; Brat, D. J.; Krug, D. K.; Watkins, C. C.; Gupta, A.; Blackshaw, S.; Verma, A.; Wang, Z. Q.; Snyder, S. H. *Proc. Natl. Acad. Sci. USA* **1999**, *96*, 3059-3064.
- (156) Miesel, R.; Kurpisz, M.; Kroger, H. *Inflammation* **1995**, *19*, 379-387.
- (157) Jijon, H. B.; Churchill, T.; Malfair, D.; Wessler, A.; Jewell, L. D.; Parsons, H. G.; Madsen, K. L. *Am. J. Physiol. Gastroint. Liver Physiol.* **2000**, *279*, G641-G651.
- (158) Ratnam, K.; Low, J. A. *Clin. Cancer Res.* **2007**, *13*, 1383-1388.

- (159) Kummar, S.; Kinders, R.; Rubinstein, L.; Parchment, R. E.; Murgo, A. J.; Collins, J.; Pickeral, O.; Low, J.; Steinberg, S. M.; Gutierrez, M.; Yang, S.; Helman, L.; Wiltrout, R.; Tomaszewski, J. E.; Doroshow, J. H. *Nat. Rev. Cancer* **2007**, *7*, 131-139.
- (160) Plummer, R.; Middleton, M.; Wilson, R.; Jones, C.; Evans, J.; Robson, L.; Steinfeldt, H.; Kaufman, R.; Reich, S.; Calvert, A. H. *Proc. Am. Soc. Clin. Oncol.* **2005**, *24*, A3065.
- (161) Plummer, R.; Lorigan, P.; Evans, J.; Steven, N.; Middleton, M.; Wilson, R.; Snow, K.; Dewji, R.; Calvert, H. *Proc. Am. Soc. Clin. Oncol.* **2006**, *25*, A8013.
- (162) Fong, P. C.; Spicer, J.; Reade, S.; Reid, A.; Vidal, L.; Schellens, J. H.; Tutt, A.; Harris, P. A.; Kaye, S.; De Bono, J. S. *Proc. Am. Soc. Clin. Oncol.* **2006**, *25*, A3022.
- (163) Wang, C.; Bedikian, A. Y.; Kim, K.; Papadopoulos, N. E.; Hwu, W.; Hwu, P. *Proc. Am. Soc. Clin. Oncol.* **2006**, *25*, A12015.
- (164) Lapidus, R. G.; Xu, W.; Spicer, E.; Hoover, R.; Zhang, J. *Proc. Am. Assoc. Cancer Res.* **2006**, *47*, A2141.
- (165) Iwashita, A.; Yamazaki, S.; Mihara, K.; Hattori, K.; Yamamoto, H.; Ishida, J.; Matsuoka, N.; Mutoh, S. *J. Pharmacol. Exp. Ther.* **2004**, *309*, 1067-1078.
- (166) Shall, S. *J. Biochem. (Tokyo)* **1975**, *77*, P2-P2.
- (167) Purnell, M. R.; Whish, W. J. D. *Biochem. J.* **1980**, *185*, 775-777.
- (168) Hong, L.; Goldstein, B. M. *J. Med. Chem.* **1992**, *35*, 3560-3567.
- (169) Banasik, M.; Komura, H.; Shimoyama, M.; Ueda, K. *J. Biol. Chem.* **1992**, *267*, 1569-1575.
- (170) White, A. W.; Almassy, R.; Calvert, A. H.; Curtin, N. J.; Griffin, R. J.; Hostomsky, Z.; Maegley, K.; Newell, D. R.; Srinivasan, S.; Golding, B. T. *J. Med. Chem.* **2000**, *43*, 4084-4097.
- (171) Skalitzky, D. J.; Marakovits, J. T.; Maegley, K. A.; Ekker, A.; Yu, X. H.; Hostomsky, Z.; Webber, S. E.; Eastman, B. W.; Almassy, R.; Li, J. K.; Curtin, N. J.; Newell, D. R.; Calvert, A. H.; Griffin, R. J.; Golding, B. T. *J. Med. Chem.* **2003**, *46*, 210-213.
- (172) Cockcroft, X. L.; Dillon, K. J.; Dixon, L.; Drzewiecki, J.; Kerrigan, F.; Loh, V. M.; Martin, N. M. B.; Menear, K. A.; Smith, G. C. M. *Bioorg. Med. Chem. Lett.* **2006**, *16*, 1040-1044.

- (173) Griffin, R. J.; Srinivasan, S.; Bowman, K.; Calvert, A. H.; Curtin, N. J.; Newell, D. R.; Pemberton, L. C.; Golding, B. T. *J. Med. Chem.* **1998**, *41*, 5247-5256.
- (174) Ishida, J.; Yamamoto, H.; Kido, Y.; Kamijo, K.; Murano, K.; Miyake, H.; Ohkubo, M.; Kinoshita, T.; Warizaya, M.; Iwashita, A.; Mihara, K.; Matsuoka, N.; Hattori, K. *Bioorg. Med. Chem.* **2006**, *14*, 1378-1390.
- (175) Rice, W. G.; Schaeffer, C. A.; Harten, B.; Villinger, F.; South, T. L.; Summers, M. F.; Henderson, L. E.; Bess, J. W.; Arthur, L. O.; McDougal, J. S.; Orloff, S. L.; Mendeleyev, J.; Kun, E. *Nature* **1993**, *361*, 473-475.
- (176) Bauer, P. I.; Mendeleyeva, J.; Kirsten, E.; Comstock, J. A.; Hakam, A.; Buki, K. G.; Kun, E. *Biochem. Pharmacol.* **2002**, *63*, 455-462.
- (177) Ruf, A.; Ménissier de Murcia, J.; de Murcia, G. M.; Schulz, G. E. *Proc. Natl. Acad. Sci. USA* **1996**, *93*, 7481-7485.
- (178) Kinoshita, T.; Nakanishi, I.; Warizaya, M.; Iwashita, A.; Kido, Y.; Hattori, K.; Fujii, T. *FEBS Lett.* **2004**, *556*, 43-46.
- (179) Berry, J. M.; Watson, C. Y.; Whish, W. J. D.; Threadgill, M. D. *J. Chem. Soc., Perkin Trans. 1* **1997**, 1147-1156.
- (180) Parveen, I.; Naughton, D. P.; Whish, W. J. D.; Threadgill, M. D. *Bioorg. Med. Chem. Lett.* **1999**, *9*, 2031-2036.
- (181) Ferrer, S.; Naughton, D. P.; Threadgill, M. D. *Tetrahedron* **2003**, *59*, 3437-3444.
- (182) Ferrer, S.; Naughton, D. P.; Threadgill, M. D. *Tetrahedron* **2003**, *59*, 3445-3454.
- (183) Kouznetsov, V. V.; Méndez, L. Y. V.; Gómez, C. M. M. *Curr. Org. Chem.* **2005**, *9*, 141-161.
- (184) Parveen, I. PhD thesis, Univeristy of Bath, 2001.
- (185) Howitz, J.; Schwenk, W. *Chem. Ber.* **1906**, *39*, 2705-2711.
- (186) Nakashima, T.; Suzuki, I. *Chem. Pharm. Bull.* **1969**, *17*, 2293-2298.
- (187) Miyaura, N.; Suzuki, A. *Chem. Rev.* **1995**, *95*, 2457-2483.
- (188) Suzuki, H.; Watanabe, T.; Yokoyama, Y.; Murakami, Y. *Heterocycles* **2002**, *56*, 515-518.
- (189) Price, C. C.; Guthrie, D. B. *J. Am. Chem. Soc.* **1946**, *68*, 1592-1593.
- (190) Wade, L. G. *Organic chemistry*; Prentice Hall International: New Jersey, 1999.
- (191) Fieser, L. F.; Hershberg, E. B. *J. Am. Chem. Soc.* **1940**, *62*, 1640-1645.
- (192) Roe, A.; Hawkins, G. F. *J. Am. Chem. Soc.* **1949**, *71*, 1785-1786.

- (193) Baik, W.; Han, J. L.; Lee, K. C.; Lee, N. H.; Kim, B. H.; Hahn, J. T. *Tetrahedron Lett.* **1994**, *35*, 3965-3966.
- (194) Suggs, J. W.; Pearson, G. D. N. *J. Org. Chem.* **1980**, *45*, 1514-1515.
- (195) Li, H. C.; Chou, P. T.; Hu, Y. H.; Cheng, Y. M.; Liu, R. S. *Organometallics* **2005**, *24*, 1329-1335.
- (196) Anderson, B. A.; Bell, E. C.; Ginah, F. O.; Harn, N. K.; Pagh, L. M.; Wepsiec, J. P. *J. Org. Chem.* **1998**, *63*, 8224-8228.
- (197) Takagi, K.; Okamoto, T.; Sakakibara, Y.; Ohno, A.; Oka, S.; Hayama, N. *Bull. Chem. Soc. Jpn.* **1976**, *49*, 3177-3180.
- (198) Marcantonio, K. M.; Frey, L. F.; Liu, Y.; Chen, Y.; Strine, J.; Phenix, B.; Wallace, D. J.; Chen, C. Y. *Org. Lett.* **2004**, *6*, 3723-3725.
- (199) Sundermeier, M.; Zapf, A.; Beller, M. *Eur. J. Inorg. Chem.* **2003**, 3513-3526.
- (200) Johnsson, R.; Meijer, A.; Ellervik, U. *Tetrahedron* **2005**, *61*, 11657-11663.
- (201) Castanet, A. S.; Colobert, F.; Broutin, P. E. *Tetrahedron Lett.* **2002**, *43*, 5047-5048.
- (202) Suzuki, A. *J. Organomet. Chem.* **1999**, *576*, 147-168.
- (203) Barder, T. E.; Walker, S. D.; Martinelli, J. R.; Buchwald, S. L. *J. Am. Chem. Soc.* **2005**, *127*, 4685-4696.
- (204) Yang, Y. H.; Martin, A. R. *Heterocycles* **1992**, *34*, 1395-1398.
- (205) Shao, B.; Victory, S.; Ilyin, V. I.; Goehring, R. R.; Sun, Q.; Hogenkamp, D.; Hodges, D. D.; Islam, K.; Sha, D.; Zhang, C.; Nguyen, P.; Robledo, S.; Sakellaropoulos, G.; Carter, R. B. *J. Med. Chem.* **2004**, *47*, 4277-4285.
- (206) Sicre, C.; Alonso-Gómez, J. L.; Cid, M. M. *Tetrahedron* **2006**, *62*, 11063-11072.
- (207) Bumagin, N. A.; Bykov, V. V.; Sukhomlinova, L. I.; Tolstaya, T. P.; Beletskaya, I. P. *J. Organomet. Chem.* **1995**, *486*, 259-262.
- (208) Sato, M.; Miyaura, N.; Suzuki, A. *Chem. Lett.* **1989**, 1405-1408.
- (209) Wright, S. W.; Hageman, D. L.; McClure, L. D. *J. Org. Chem.* **1994**, *59*, 6095-6097.
- (210) Guiles, J. W.; Johnson, S. G.; Murray, W. V. *J. Org. Chem.* **1996**, *61*, 5169-5171.
- (211) Zou, G.; Reddy, Y. K.; Falck, J. R. *Tetrahedron Lett.* **2001**, *42*, 7213-7215.
- (212) Stille, J. K. *Angew. Chem., Int. Edit. Engl.* **1986**, *25*, 508-523.

- (213) Farina, V.; Kapadia, S.; Krishnan, B.; Wang, C.; Liebeskind, L. S. *J. Org. Chem.* **1994**, *59*, 5905-5911.
- (214) Gulykina, N. S.; Dolgina, T. M.; Bondarenko, G. N.; Beletskaya, I. P. *Russ. J. Org. Chem.* **2003**, *39*, 797-806.
- (215) Bertus, P.; Fecourt, F.; Bauder, C.; Pale, P. *New J. Chem.* **2004**, *28*, 12-14.
- (216) Crouch, R. D. *Tetrahedron* **2004**, *60*, 5833-5871.
- (217) Jackson, W. P.; Ley, S. V. *J. Chem. Soc., Perkin Trans. 1* **1981**, 1516-1519.
- (218) Orsini, A.; Viterisi, A.; Bodlenner, A.; Weibel, J. M.; Pale, P. *Tetrahedron Lett.* **2005**, *46*, 2259-2262.
- (219) Woon, E. C. Y.; Dhami, A.; Mahon, M. F.; Threadgill, M. D. *Tetrahedron* **2006**, *62*, 4829-4837.
- (220) Sakamoto, T.; Ohsawa, K. *J. Chem. Soc., Perkin Trans. 1* **1999**, 2323-2326.
- (221) Cottet, F.; Marull, M.; Lefebvre, O.; Schlosser, M. *Eur. J. Org. Chem.* **2003**, 1559-1568.
- (222) Handy, S. T.; Zhang, Y. N. *Chem. Commun.* **2006**, 299-301.
- (223) Fauvarque, J. F.; Pflüger, F.; Troupel, M. *J. Organomet. Chem.* **1981**, *208*, 419-427.
- (224) Mao, L. S.; Moriuchi, T.; Sakurai, H.; Fujii, H.; Hirao, T. *Tetrahedron Lett.* **2005**, *46*, 8419-8422.
- (225) Nolan, J. M.; Comins, D. L. *J. Org. Chem.* **2003**, *68*, 3736-3738.
- (226) Pereira, R.; Iglesias, B.; de Lera, A. R. *Tetrahedron* **2001**, *57*, 7871-7881.
- (227) Leir, C. M. *J. Org. Chem.* **1977**, *42*, 911-913.
- (228) Söderberg, B. C.; Shriver, J. A. *J. Org. Chem.* **1997**, *62*, 5838-5845.
- (229) Mohan, R.; Katzenellenbogen, J. A. *J. Org. Chem.* **1984**, *49*, 1238-1246.
- (230) Baik, W.; Kim, D. I.; Lee, H. J.; Chung, W. J.; Kim, B. H.; Lee, S. W. *Tetrahedron Lett.* **1997**, *38*, 4579-4580.
- (231) Abramovitch, R. A.; Obach, A. *Can. J. Chem.* **1959**, *37*, 502-504.
- (232) Couturier, M.; Le, T. *Org. Process Res. Dev.* **2006**, *10*, 534-538.
- (233) Zhong, P.; Guo, S. R.; Song, C. S. *Synth. Commun.* **2004**, *34*, 247-253.
- (234) Fieser, L. F.; Martin, E. L. *J. Am. Chem. Soc.* **1935**, *57*, 1840-1844.
- (235) Ukai, T.; Yamamoto, Y.; Ito, Y.; Yanagi, A.; Yotsuka, M. *J. Pharm. Soc. Japan* **1955**, *75*, 490-493.
- (236) Mongin, F.; Queguiner, G. *Tetrahedron* **2001**, *57*, 4059-4090.

- (237) Butler, D. E.; Bass, P.; Nordin, I. C.; Hauck, F. P.; L'Italien, Y. J. *J. Med. Chem.* **1971**, *14*, 575-579.
- (238) Jain, S. L.; Joseph, J. K.; Sain, B. *Synlett* **2006**, 2661-2663.
- (239) Phillips, V. A. PhD thesis, University of Bradford, 2003.
- (240) Schraufstatter, I. U.; Hyslop, P. A.; Hinshaw, D. B.; Spragg, R. G.; Sklar, L. A.; Cochrane, C. G. *Proc. Natl. Acad. Sci. USA* **1986**, *83*, 4908-4912.
- (241) Kiehlbauch, C. C.; Aboulela, N.; Jacobson, E. L.; Ringer, D. P.; Jacobson, M. K. *Anal. Biochem.* **1993**, *208*, 26-34.
- (242) Decker, P.; Miranda, E. A.; de Murcia, G.; Muller, S. *Clin. Cancer Res.* **1999**, *5*, 1169-1172.
- (243) Gasser, S. M.; Cockell, M. M. *Gene* **2001**, *279*, 1-16.
- (244) Tanner, K. G.; Landry, J.; Sternglanz, R.; Denu, J. M. *Proc. Natl. Acad. Sci. USA* **2000**, *97*, 14178-14182.
- (245) Vaziri, H.; Dessain, S. K.; Eagon, E. N.; Imai, S. I.; Frye, R. A.; Pandita, T. K.; Guarente, L.; Weinberg, R. A. *Cell* **2001**, *107*, 149-159.
- (246) Bouras, T.; Fu, M. F.; Sauve, A. A.; Wang, F.; Quong, A. A.; Perkins, N. D.; Hay, R. T.; Gu, W.; Pestell, R. G. *J. Biol. Chem.* **2005**, *280*, 10264-10276.
- (247) Yeung, F.; Hoberg, J. E.; Ramsey, C. S.; Keller, M. D.; Jones, D. R.; Frye, R. A.; Mayo, M. W. *EMBO J.* **2004**, *23*, 2369-2380.
- (248) Brunet, A.; Sweeney, L. B.; Sturgill, J. F.; Chua, K. F.; Greer, P. L.; Lin, Y. X.; Tran, H.; Ross, S. E.; Mostoslavsky, R.; Cohen, H. Y.; Hu, L. S.; Cheng, H. L.; Jedrychowski, M. P.; Gygi, S. P.; Sinclair, D. A.; Alt, F. W.; Greenberg, M. E. *Science* **2004**, *303*, 2011-2015.
- (249) Porcu, M.; Chiarugi, A. *Trends Pharmacol. Sci.* **2005**, *26*, 94-103.
- (250) Anekonda, T. S.; Reddy, P. H. *J. Neurochem.* **2006**, *96*, 305-313.
- (251) Pagans, S.; Pedal, A.; North, B. J.; Kaehlcke, K.; Marshall, B. L.; Dorr, A.; Hetzer-Egger, C.; Henklein, P.; Frye, R.; McBurney, M. W.; Hruby, H.; Jung, M.; Verdin, E.; Ott, M. *PLoS. Biol.* **2005**, *3*, 210-220.
- (252) Dryden, S. C.; Nahhas, F. A.; Nowak, J. E.; Goustin, A. S.; Tainsky, M. A. *Mol. Cell. Biol.* **2003**, *23*, 3173-3185.
- (253) Hiratsuka, M.; Inoue, T.; Toda, T.; Kimura, N.; Shirayoshi, Y.; Kamitani, H.; Watanabe, T.; Ohama, E.; Tahimic, C. G. T.; Kurimasa, A.; Oshimura, M. *Biochem. Biophys. Res. Commun.* **2003**, *309*, 558-566.
- (254) Frye, R. *Br. J. Cancer* **2002**, *87*, 1479-1479.
- (255) Hallows, W. C.; Lee, S.; Denu, J. M. *Proc. Natl. Acad. Sci. USA* **2006**, *103*, 10230-10235.

- (256) Haigis, M. C.; Mostoslavsky, R.; Haigis, K. M.; Fahie, K.; Christodoulou, D. C.; Murphy, A. J.; Valenzuela, D. M.; Yancopoulos, G. D.; Karow, M.; Blander, G.; Wolberger, C.; Prolla, T. A.; Weindruch, R.; Alt, F. W.; Guarente, L. *Cell* **2006**, *126*, 941-954.
- (257) Finnin, M. S.; Donigian, J. R.; Pavletich, N. P. *Nat. Struct. Biol.* **2001**, *8*, 621-625.
- (258) Hoff, K. G.; Avalos, J. L.; Sens, K.; Wolberger, C. *Structure* **2006**, *14*, 1231-1240.
- (259) Min, J. R.; Landry, J.; Sternglanz, R.; Xu, R. M. *Cell* **2001**, *105*, 269-279.
- (260) Huhtiniemi, T.; Wittekindt, C.; Laitinen, T.; Leppanen, J.; Salminen, A.; Poso, A.; Lahtela-Kakkonen, M. *J. Comput. Aided Mol. Des.* **2006**, *20*, 589-599.
- (261) Napper, A. D.; Hixon, J.; McDonagh, T.; Keavey, K.; Pons, J. F.; Barker, J.; Yau, W. T.; Amouzegh, P.; Flegg, A.; Hamelin, E.; Thomas, R. J.; Kates, M.; Jones, S.; Navia, M. A.; Saunders, J. O.; DiStefano, P. S.; Curtis, R. *J. Med. Chem.* **2005**, *48*, 8045-8054.
- (262) Grozinger, C. M.; Chao, E. D.; Blackwell, H. E.; Moazed, D.; Schreiber, S. L. *J. Biol. Chem.* **2001**, *276*, 38837-38843.
- (263) Bedalov, A.; Gatabonton, T.; Irvine, W. P.; Gottschling, D. E.; Simon, J. A. *Proc. Natl. Acad. Sci. USA* **2001**, *98*, 15113-15118.
- (264) Avalos, J. L.; Bever, K. M.; Wolberger, C. *Mol. Cell* **2005**, *17*, 855-868.
- (265) Zhang, J. *Bioessays* **2003**, *25*, 808-814.
- (266) Hauser, C. R.; Bloom, M. S.; Breslow, D. S.; Adams, J. T.; Amore, S. T.; Weiss, M. J. *J. Am. Chem. Soc.* **1946**, *68*, 1544-1546.
- (267) Gershon, H.; Clarke, D. D.; McMahan, J. J.; Gershon, M. *Monatsh. Chem.* **2002**, *133*, 1325-1330.
- (268) Case, F. H.; Sasin, R. *J. Org. Chem.* **1955**, *20*, 1330-1336.
- (269) Echavarren, A. M.; Stille, J. K. *J. Am. Chem. Soc.* **1987**, *109*, 5478-5486.
- (270) Prijs, B.; Gall, R.; Hinderling, R.; Erlenmeyer, H. *Helv. Chim. Acta* **1954**, *37*, 90-94.
- (271) Cooper, M. S.; Fairhurst, R. A.; Heaney, H.; Papageorgiou, G.; Wilkins, R. F. *Tetrahedron* **1989**, *45*, 1155-1166.
- (272) Evindar, G.; Batey, R. A. *J. Org. Chem.* **2006**, *71*, 1802-1808.
- (273) Kundu, N. G.; Mahanty, J. S.; Das, P.; Das, B. *Tetrahedron Lett.* **1993**, *34*, 1625-1628.
- (274) Elderfield, R. C.; Gensler, W. J.; Bembry, T. H.; Williamson, T. A.; Weisl, H. *J. Am. Chem. Soc.* **1946**, *68*, 1589-1591.

- (275) Browning, C.; Cohen, J.; Ashley, J.; Gulbransen, R. *Proc. R. Soc. London, Ser. B* **1932**, *110*, 249-260.
- (276) Somei, M.; Saida, Y.; Komura, N. *Chem. Pharm. Bull.* **1986**, *34*, 4116-4125.
- (277) Tolstiko, G. A.; Jemilev, U. M.; Jurjev, V. P.; Gershano, F. B.; Rafikov, S. R. *Tetrahedron. Lett.* **1971**, 2807.
- (278) Schlosser, M.; Cottet, F. *Eur. J. Org. Chem.* **2002**, 4181-4184.
- (279) Endo, T.; Saeki, S.; Hamana, M. *Chem. Pharm. Bull.* **1981**, *29*, 3105-3111.
- (280) Cadogan, J. I. G. *J. Chem. Soc.* **1962**, 4257.
- (281) Blank, B.; Ditullio, N. W.; Owings, F. F.; Deviney, L.; Miao, C. K.; Saunders, H. L. *J. Med. Chem.* **1977**, *20*, 572-576.
- (282) Kaslow, C. E.; Buchner, B. *J. Org. Chem.* **1958**, *23*, 271-276.

Appendices

Appendix 1. Raw data for PARP-1 colourimetric activity assay

3-Ethynylquinoline-8-carboxamide (114)

Log [μM]	Absorbance reading (450nm)			
	Data Set A	Data Set B	Data Set C	Mean
2.0	0.0700	0.0630	0.0700	0.06766666
1.5	0.1090	0.0930	0.0610	0.08766667
1.0	0.0950	0.1140	0.1390	0.1160000
0.5	0.1770	0.1700	0.1820	0.1763333
0.0	0.2320	0.2400	0.2320	0.2346667
-0.5	0.3240	0.3320	0.3060	0.3206667
-1.0	0.3850	0.3050	0.3490	0.3463333

3-(4-Methylphenyl)quinoline-8-carboxamide (93)

Log [μM]	Absorbance reading (450nm)			
	Data Set A	Data Set B	Data Set C	Mean
2.0	0.2600	0.1530	0.1690	0.194000
1.5	0.2800	0.2010	0.2420	0.241000
1.0	0.3290	0.2680	0.4070	0.3346667
0.5	0.3410	0.3190	0.2780	0.3126667
0.0	0.4240	0.4230	0.3660	0.4043333
-0.5	0.4950	0.3870	0.4380	0.440000
-1.0	0.4730	0.5150	0.5020	0.4966667

3-Phenylquinoline-8-carboxamide (69)

Log [μM]	Absorbance reading (450nm)			
	Data Set A	Data Set B	Data Set C	Mean
2.0	0.0570	0.0540	0.0490	0.05333333
1.5	0.0840	0.0990	0.0980	0.09366667
1.0	0.1690	0.2290	0.1820	0.1933333
0.5	0.2240	0.2750	0.3000	0.2663333
0.0	0.3750	0.3150	0.3690	0.3530000
-0.5	0.3490	0.2530	0.2990	0.3003333
-1.0	0.2530	0.3410	0.3070	0.3003333

Quinoline-8-carboxamide (80)

Log [μM]	Absorbance reading (450nm)			
	Data Set A	Data Set B	Data Set C	Mean
2.0	0.0550	0.0460	0.0500	0.050300
1.5	0.0510	0.0570	0.0530	0.052800
1.0	0.0870	0.1030	0.0820	0.090700
0.5	0.1750	0.1960	0.2000	0.190300
0.0	0.2350	0.2770	0.2570	0.256300
-0.5	0.3240	0.3610	0.3370	0.340600
-1.0	0.3860	0.4050	0.4280	0.406300

3-(3-(Trifluoromethyl)phenyl)quinoline-8-carboxamide (94)

Log [μM]	Absorbance reading (450nm)			
	Data Set A	Data Set B	Data Set C	Mean
2.0	0.1800	0.2150	0.2230	0.206000
1.5	0.2470	0.3190	0.2660	0.2773333
1.0	0.2960	0.3470	0.3160	0.3196667
0.5	0.3910	0.4300	0.3440	0.3883333
0.0	0.4180	0.3970	0.5490	0.4546667
-0.5	0.4650	0.5000	0.4220	0.4623333
-1.0	0.4920	0.4280	0.4670	0.4623333

3-(4-Methoxyphenyl)quinoline-8-carboxamide (91)

Log [μM]	Absorbance reading (450nm)			
	Data Set A	Data Set B	Data Set C	Mean
2.0	0.1260	0.1960	0.1650	0.1623333
1.5	0.1990	0.2270	0.2530	0.2263333
1.0	0.2890	0.2700	0.2930	0.284000
0.5	0.2540	0.3140	0.2940	0.2873333
0.0	0.3570	0.4200	0.3150	0.364000
-0.5	0.3380	0.3590	0.3980	0.365000
-1.0	0.3450	0.3980	0.3550	0.366000

3-(4-Cyanophenyl)quinoline-8-carboxamide (98)

Log [μM]	Absorbance reading (450nm)			
	Data Set A	Data Set B	Data Set C	Mean
2.0	0.1670	0.1130	0.0940	0.1246667
1.5	0.2360	0.1920	0.1590	0.1956667
1.0	0.3090	0.3000	0.2620	0.2903333
0.5	0.3550	0.3270	0.3120	0.3313333
0.0	0.4280	0.3900	0.4070	0.4083333
-0.5	0.4000	0.3720	0.3400	0.3706667
-1.0	0.4920	0.4230	0.4160	0.4436667

3-Ethylquinoline-8-carboxamide (123)

Log [μM]	Absorbance reading (450nm)			
	Data Set A	Data Set B	Data Set C	Mean
2.0	0.1030	0.0730	0.0820	0.086000
1.5	0.1980	0.1470	0.1710	0.172000
1.0	0.4320	0.3900	0.4350	0.419000
0.5	0.7540	0.6870	0.7060	0.715700
0.0	1.1060	0.9770	0.8984	0.992333
-0.5	1.3680	1.2580	1.0540	1.226700
-1.0	1.3800	1.2030	1.2390	1.274000

3-Ethenylquinoline-8-carboxamide (111)

Log [μM]	Absorbance reading (450nm)			
	Data Set A	Data Set B	Data Set C	Mean
2.0	0.0900	0.0860	0.0860	0.087300
1.5	0.2210	0.2330	0.2040	0.219000
1.0	0.5660	0.4100	0.5030	0.493000
0.5	0.7430	0.7930	0.8240	0.786700
0.0	1.0440	1.2060	1.2890	1.179670
-0.5	1.2200	1.1970	1.1610	1.192670
-1.0	1.1880	1.2510	1.3000	1.246300

3-Methylquinoline-8-carboxamide (106)

Log [μM]	Absorbance reading (450nm)			
	Data Set A	Data Set B	Data Set C	Mean
2.0	0.0500	0.0490	0.0520	0.050300
1.5	0.0710	0.0550	0.0570	0.061000
1.0	0.1380	0.1270	0.1180	0.127700
0.5	0.2130	0.2490	0.2290	0.230300
0.0	0.3100	0.3110	0.3210	0.314000
-0.5	0.3770	0.3620	0.3640	0.368000
-1.0	0.4220	0.4040	0.4350	0.420300

3-(Prop-1-ynyl)quinoline-8-carboxamide (107)

Log [μM]	Absorbance reading (450nm)			
	Data Set A	Data Set B	Data Set C	Mean
2.0	0.0500	0.0490	0.0550	0.051300
1.5	0.0580	0.0580	0.0590	0.058300
1.0	0.1330	0.1450	0.1090	0.129000
0.5	0.2130	0.2020	0.2250	0.213000
0.0	0.2840	0.2910	0.3250	0.300000
-0.5	0.4110	0.4490	0.4400	0.433000
-1.0	0.4500	0.4200	0.4550	0.442000

2-Ethylquinoline-8-carboxamide (146)

Log [μM]	Absorbance reading (450nm)			
	Data Set A	Data Set B	Data Set C	Mean
2.0	0.0810	0.1760	0.0950	0.1173333
1.5	0.1360	0.1280	0.1510	0.1383333
1.0	0.3320	0.2170	0.6210	0.390000
0.5	0.5740	0.6210	0.7260	0.6240333
0.0	1.0400	1.4710	1.9620	1.491000
-0.5	2.9730	2.7680	2.6060	2.782333
-1.0	3.1500	3.1700	2.5020	2.940667

2-Methylquinoline-8-carboxamide (147)

Log [μM]	Absorbance reading (450nm)			
	Data Set A	Data Set B	Data Set C	Mean
2.0	0.0820	0.1800	0.0830	0.115000
1.5	0.1360	0.1080	0.0990	0.1143333
1.0	0.4580	0.1700	0.1200	0.2493333
0.5	0.7730	0.6580	0.1580	0.5296667
0.0	1.2950	1.0600	0.7640	1.039667
-0.5	2.5170	2.0870	2.2860	2.296667
-1.0	2.9140	2.7470	2.6970	2.786000

2-Phenylquinoline-8-carboxamide (144)

Log [μM]	Absorbance reading (450nm)			
	Data Set A	Data Set B	Data Set C	Mean
2.0	0.1310	0.0990	0.1040	0.1113667
1.5	0.1250	0.1130	0.1350	1.243333
1.0	0.2130	0.2040	0.2520	0.223000
0.5	0.8740	0.8500	0.8890	0.871000
0.0	1.8930	1.7440	1.4340	1.690333
-0.5	2.5460	2.8490	2.6870	2.694000
-1.0	2.0880	2.2900	2.4930	2.903333

2-(4-Methoxyphenyl)quinoline-8-carboxamide (145)

Log [μM]	Absorbance reading (450nm)			
	Data Set A	Data Set B	Data Set C	Mean
2.0	0.1810	0.1420	0.1450	0.156000
1.5	0.1940	0.2060	0.1940	0.198000
1.0	0.2560	0.2460	0.2100	0.237300
0.5	0.3310	0.3930	0.3570	0.360300
0.0	0.7100	0.5550	0.5080	0.591000
-0.5	0.8260	0.9370	0.7480	0.837000
-1.0	0.9380	1.0870	0.9660	0.997000

5-AIQ

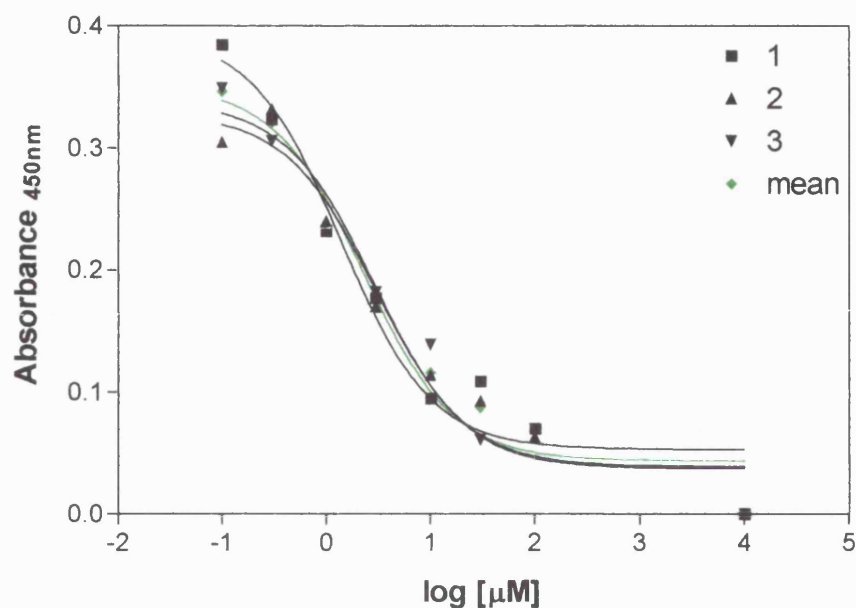
Log [μM]	Absorbance reading (450nm)			
	Data Set A	Data Set B	Data Set C	Mean
2.0	0.1410	0.1620	0.0900	0.131000
1.5	0.3290	0.3060	0.2970	0.3106667
1.0	0.5720	0.5490	0.4340	0.5183334
0.5	1.0620	0.9940	1.0060	1.020667
0.0	1.3340	1.3150	1.1480	1.265667
-0.5	2.0220	2.0330	2.0100	2.021667
-1.0	2.3310	1.9850	2.1020	2.139333

8-Carbamoyl-3-phenylquinoline-1-oxide (175)

Log [μM]	Absorbance reading (450nm)			
	Data Set A	Data Set B	Data Set C	Mean
2.0	0.0800	0.0630	0.0700	0.071000
1.5	0.3640	0.4280	0.3630	0.385000
1.0	2.0630	1.8350	2.2230	2.040333
0.5	2.4100	2.4180	2.2170	2.348333
0.0	2.2550	2.1580	2.1720	2.195000
-0.5	2.1590	2.0970	1.8490	2.035000
-1.0	2.0110	2.1190	2.0170	2.049000

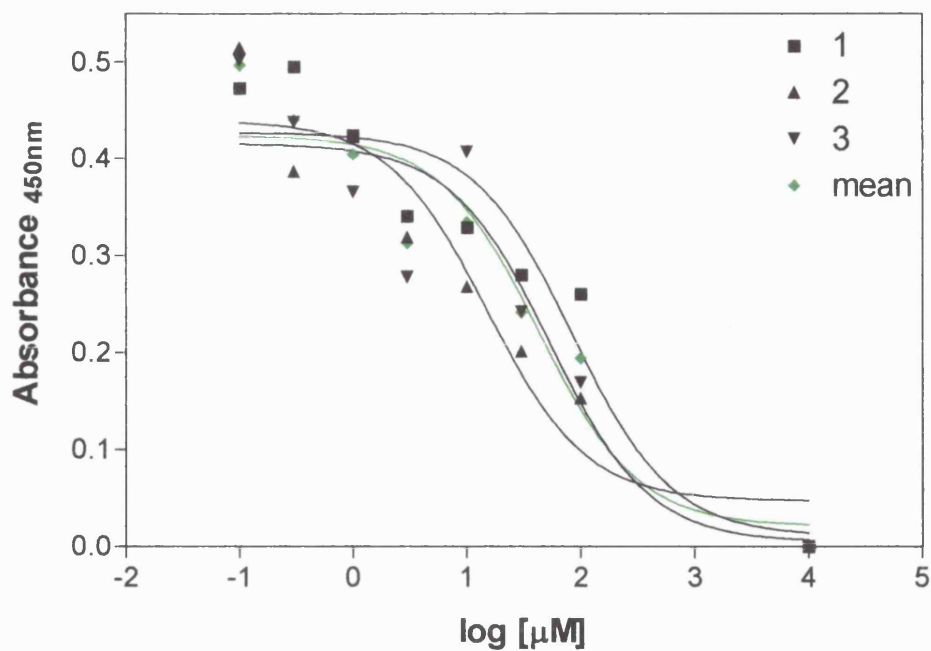
Appendix 2. IC₅₀ Data analysis for PARP-1 inhibitors

3-Ethynylquinoline-8-carboxamide (114)



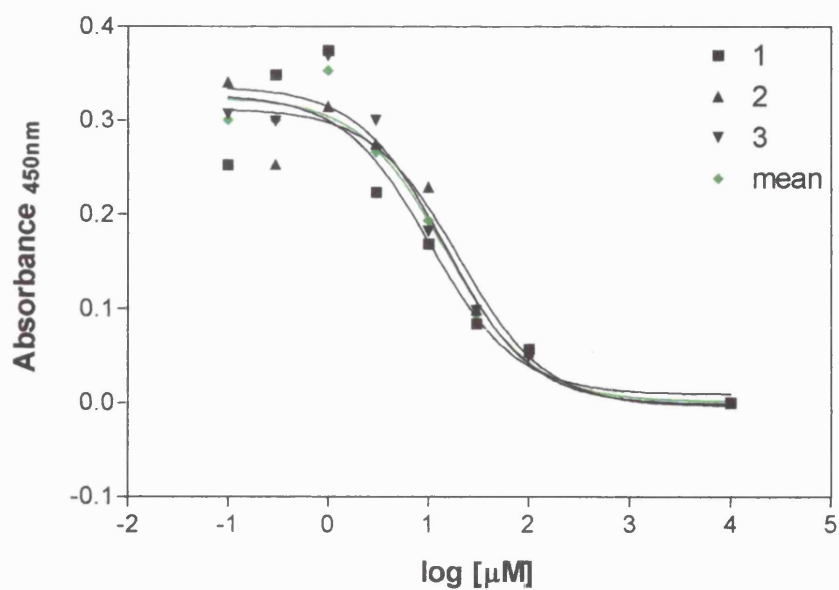
	Data Set-A	Data Set-B	Data Set-C	Data Set-D
Best-fit values				
BOTTOM	0.05313	0.03888	0.03737	0.04368
TOP	0.3947	0.3285	0.3384	0.3519
LOGEC50	0.1417	0.4745	0.4651	0.3560
EC50	1.386	2.982	2.918	2.270
Std. Error				
BOTTOM	0.01949	0.01871	0.01934	0.01663
TOP	0.03653	0.02474	0.02581	0.02473
LOGEC50	0.1968	0.1863	0.1861	0.1650
95% Confidence Intervals				
BOTTOM	0.003025 to 0.1032	-0.009231 to 0.08699	-0.01236 to 0.08710	0.0009220 to 0.08643
TOP	0.3007 to 0.4886	0.2649 to 0.3922	0.2721 to 0.4048	0.2884 to 0.4155
LOGEC50	-0.3644 to 0.6477	-0.004493 to 0.9534	-0.01349 to 0.9436	-0.06823 to 0.7802
EC50	0.4321 to 4.443	0.9897 to 8.983	0.9694 to 8.782	0.8546 to 6.029
Goodness of Fit				
Degrees of Freedom	5	5	5	5
R ²	0.9545	0.9580	0.9581	0.9669
Absolute Sum of Squares	0.005551	0.004142	0.004455	0.003545
Sy.x	0.03332	0.02878	0.02985	0.02663
Data				
Number of X values	8	8	8	8
Number of Y replicates	1	1	1	1
Total number of values	8	8	8	8
Number of missing values	0	0	0	0

3-(4-Methylphenyl)quinoline-8-carboxamide (93)



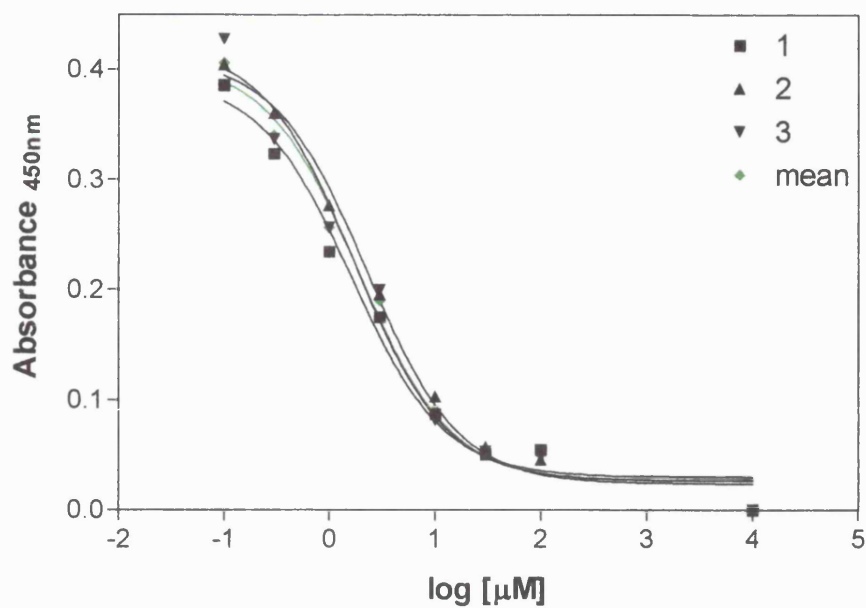
	Data Set-A	Data Set-B	Data Set-C	Data Set-D
Best-fit values				
BOTTOM	0.01066	0.04686	0.004526	0.02085
TOP	0.4267	0.4396	0.4153	0.4237
LOGEC50	1.928	1.179	1.729	1.629
EC50	84.65	15.10	53.64	42.61
Std. Error				
BOTTOM	0.06442	0.04986	0.07363	0.05627
TOP	0.03152	0.03598	0.03866	0.03088
LOGEC50	0.2679	0.2639	0.3127	0.2484
95% Confidence Intervals				
BOTTOM	-0.1550 to 0.1763	-0.08134 to 0.1751	-0.1848 to 0.1938	-0.1238 to 0.1655
TOP	0.3457 to 0.5078	0.3471 to 0.5321	0.3159 to 0.5147	0.3443 to 0.5031
LOGEC50	1.239 to 2.616	0.5006 to 1.858	0.9255 to 2.534	0.9908 to 2.268
EC50	17.33 to 413.4	3.167 to 72.04	8.423 to 341.6	9.790 to 185.4
Goodness of Fit				
Degrees of Freedom	5	5	5	5
R ²	0.8835	0.9091	0.8516	0.9041
Absolute Sum of Squares	0.02012	0.01722	0.02770	0.01679
Sy.x	0.06344	0.05869	0.07443	0.05795
Data				
Number of X values	8	8	8	8
Number of Y replicates	1	1	1	1
Total number of values	8	8	8	8
Number of missing values	0	0	0	0

3-Phenylquinoline-8-carboxamide (69)



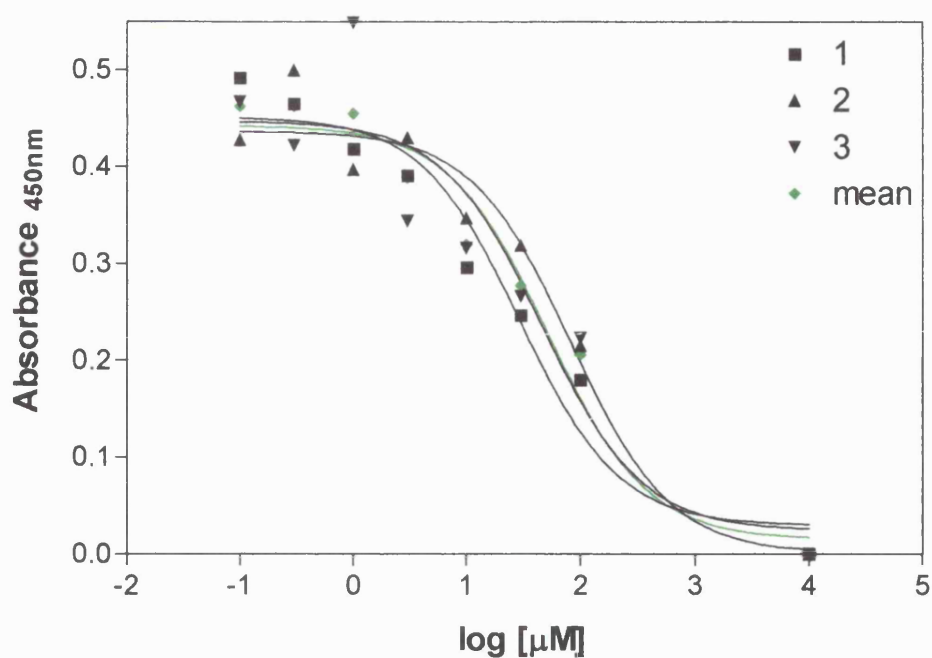
	Data Set-A	Data Set-B	Data Set-C	Data Set-D
Best-fit values				
BOTTOM	0.008868	-0.003737	-0.001511	0.001397
TOP	0.3278	0.3127	0.3362	0.3247
LOGEC50	1.018	1.304	1.163	1.166
EC50	10.43	20.15	14.55	14.66
Std. Error				
BOTTOM	0.04114	0.02893	0.02810	0.02246
TOP	0.03357	0.01913	0.02052	0.01636
LOGEC50	0.2880	0.1805	0.1742	0.1452
95% Confidence Intervals				
BOTTOM	-0.09691 to 0.1146	-0.07811 to 0.07064	-0.07376 to 0.07074	-0.05635 to 0.05914
TOP	0.2415 to 0.4141	0.2635 to 0.3619	0.2834 to 0.3889	0.2826 to 0.3668
LOGEC50	0.2777 to 1.759	0.8402 to 1.768	0.7152 to 1.611	0.7928 to 1.539
EC50	1.896 to 57.36	6.922 to 58.68	5.190 to 40.81	6.205 to 34.62
Goodness of Fit				
Degrees of Freedom	5	5	5	5
R ²	0.8983	0.9533	0.9585	0.9708
Absolute Sum of Squares	0.01323	0.005311	0.005534	0.003527
Sy.x	0.05143	0.03259	0.03327	0.02656
Data				
Number of X values	8	8	8	8
Number of Y replicates	1	1	1	1
Total number of values	8	8	8	8
Number of missing values	0	0	0	0

Quinoline-8-carboxamide (80)



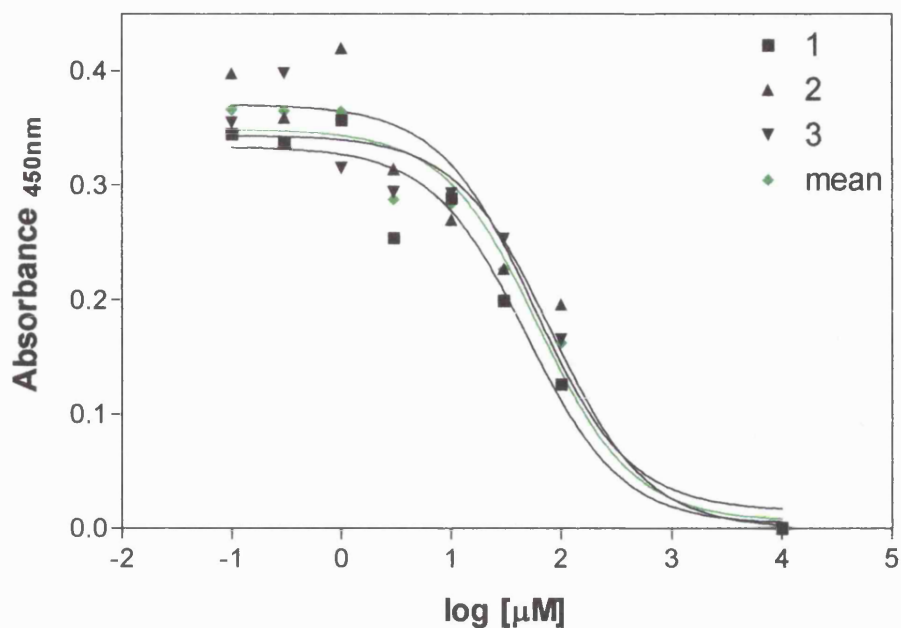
	Data Set-A	Data Set-B	Data Set-C	Data Set-D
Best-fit values				
BOTTOM	0.02995	0.02382	0.02654	0.02648
TOP	0.3920	0.4110	0.4226	0.4077
LOGEC50	0.2115	0.3540	0.2381	0.2728
EC50	1.627	2.259	1.730	1.874
Std. Error				
BOTTOM	0.01297	0.009869	0.01642	0.01275
TOP	0.02247	0.01471	0.02763	0.02068
LOGEC50	0.1185	0.07805	0.1351	0.1069
95% Confidence Intervals				
BOTTOM	-0.003392 to 0.06329	-0.001551 to 0.04920	-0.01568 to 0.06875	-0.006309 to 0.05927
TOP	0.3342 to 0.4497	0.3732 to 0.4488	0.3516 to 0.4937	0.3546 to 0.4609
LOGEC50	-0.09322 to 0.5162	0.1533 to 0.5546	-0.1092 to 0.5854	-0.002150 to 0.5477
EC50	0.8068 to 3.282	1.423 to 3.586	0.7776 to 3.850	0.9951 to 3.530
Goodness of Fit				
Degrees of Freedom	5	5	5	5
R ²	0.9828	0.9924	0.9778	0.9859
Absolute Sum of Squares	0.002360	0.001250	0.003723	0.002199
Sy.x	0.02173	0.01581	0.02729	0.02097
Data				
Number of X values	8	8	8	8
Number of Y replicates	1	1	1	1
Total number of values	8	8	8	8
Number of missing values	0	0	0	0

3(3-(Trifluoromethyl)phenyl)quinoline-8-carboxamide (94)



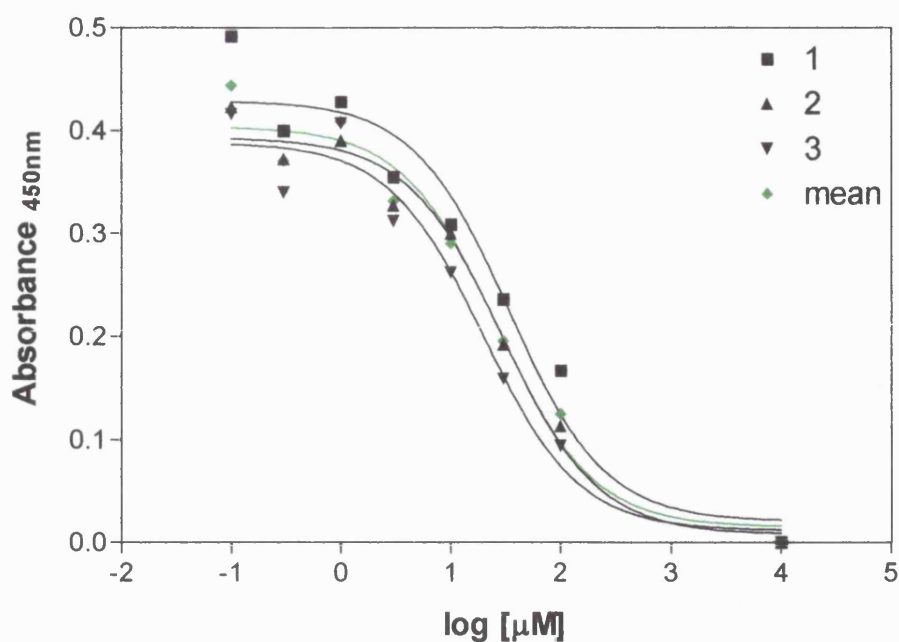
	Data Set-A	Data Set-B	Data Set-C	Data Set-D
Best-fit values				
BOTTOM	0.02969	0.001136	0.02445	0.01525
TOP	0.4515	0.4366	0.4471	0.4424
LOGEC50	1.471	1.915	1.665	1.712
EC50	29.61	82.29	46.20	51.53
Std. Error				
BOTTOM	0.04021	0.03971	0.07246	0.03836
TOP	0.02398	0.01951	0.03914	0.02029
LOGEC50	0.1772	0.1576	0.3027	0.1571
95% Confidence Intervals				
BOTTOM	-0.07370 to 0.1331	-0.1010 to 0.1032	-0.1619 to 0.2107	-0.08337 to 0.1139
TOP	0.3899 to 0.5131	0.3865 to 0.4868	0.3465 to 0.5477	0.3902 to 0.4945
LOGEC50	1.016 to 1.927	1.510 to 2.321	0.8865 to 2.443	1.308 to 2.116
EC50	10.37 to 84.55	32.37 to 209.2	7.700 to 277.2	20.33 to 130.6
Goodness of Fit				
Degrees of Freedom	5	5	5	5
R ²	0.9519	0.9563	0.8625	0.9581
Absolute Sum of Squares	0.009261	0.007667	0.02746	0.007561
Sy,x	0.04304	0.03916	0.07411	0.03889
Data				
Number of X values	8	8	8	8
Number of Y replicates	1	1	1	1
Total number of values	8	8	8	8
Number of missing values	0	0	0	0

3-(4-Methoxyphenyl)quinoline-8-carboxamide (91)



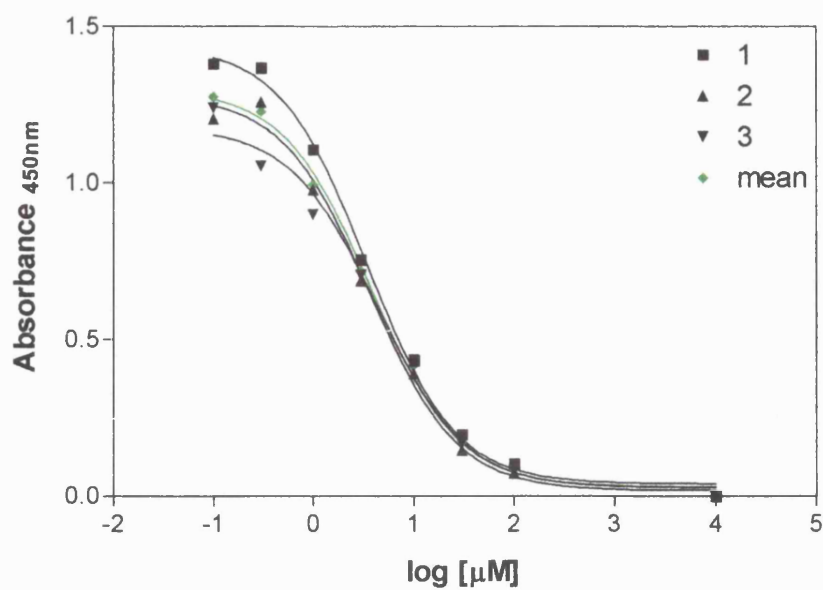
	Data Set-A	Data Set-B	Data Set-C	Data Set-D
Best-fit values				
BOTTOM	0.003711	0.01522	8.9100e-005	0.006144
TOP	0.3335	0.3705	0.3437	0.3489
LOGEC50	1.688	1.758	1.915	1.791
EC50	48.77	57.34	82.25	61.75
Std. Error				
BOTTOM	0.03164	0.04694	0.03372	0.02912
TOP	0.01691	0.02436	0.01656	0.01493
LOGEC50	0.1685	0.2296	0.1696	0.1471
95% Confidence Intervals				
BOTTOM	-0.07763 to 0.08506	-0.1055 to 0.1359	-0.08660 to 0.08678	-0.06872 to 0.08101
TOP	0.2900 to 0.3770	0.3079 to 0.4331	0.3011 to 0.3862	0.3105 to 0.3872
LOGEC50	1.255 to 2.121	1.168 to 2.349	1.479 to 2.351	1.412 to 2.169
EC50	17.98 to 132.3	14.73 to 223.2	30.13 to 224.5	25.85 to 147.5
Goodness of Fit				
Degrees of Freedom	5	5	5	5
R ²	0.9525	0.9135	0.9497	0.9622
Absolute Sum of Squares	0.005188	0.01115	0.005529	0.004251
Sy.x	0.03221	0.04723	0.03325	0.02916
Data				
Number of X values	8	8	8	8
Number of Y replicates	1	1	1	1
Total number of values	8	8	8	8
Number of missing values	0	0	0	0

3-(4-Cyanophenyl)quinoline-8-carboxamide (98)



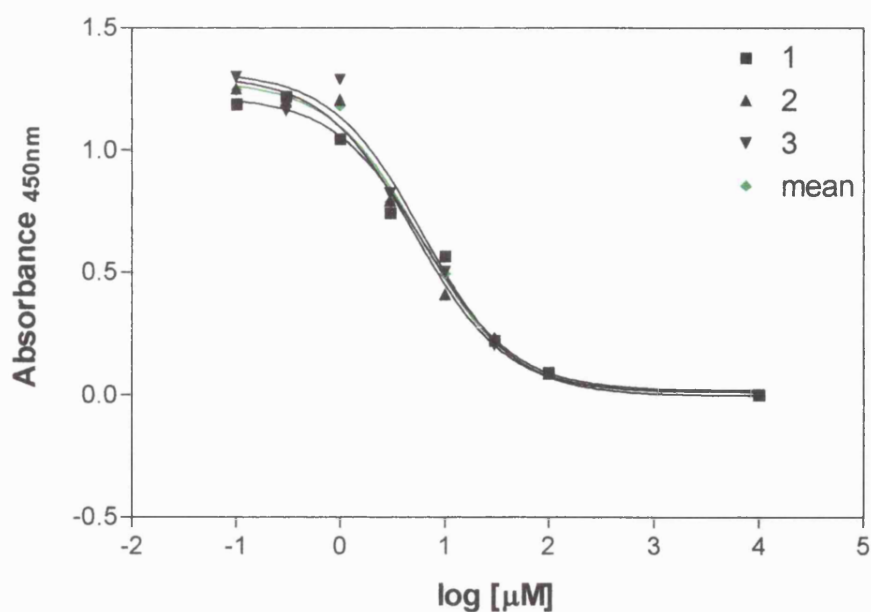
	Data Set-A	Data Set-B	Data Set-C	Data Set-D
Best-fit values				
BOTTOM	0.02046	0.007823	0.01158	0.01488
TOP	0.4291	0.3931	0.3885	0.4038
LOGEC50	1.532	1.469	1.299	1.426
EC50	34.07	29.41	19.92	26.69
Std. Error				
BOTTOM	0.04162	0.02187	0.02893	0.02938
TOP	0.02399	0.01306	0.01920	0.01799
LOGEC50	0.1859	0.1056	0.1519	0.1426
95% Confidence Intervals				
BOTTOM	-0.08655 to 0.1275	-0.04840 to 0.06404	-0.06280 to 0.08595	-0.06065 to 0.09042
TOP	0.3674 to 0.4907	0.3595 to 0.4267	0.3391 to 0.4378	0.3576 to 0.4501
LOGEC50	1.055 to 2.010	1.197 to 1.740	0.9088 to 1.690	1.060 to 1.793
EC50	11.34 to 102.4	15.74 to 54.97	8.105 to 48.94	11.47 to 62.07
Goodness of Fit				
Degrees of Freedom	5	5	5	5
R ²	0.9461	0.9824	0.9666	0.9689
Absolute Sum of Squares	0.009608	0.002743	0.005329	0.005073
Sy.x	0.04384	0.02342	0.03265	0.03185
Data				
Number of X values	8	8	8	8
Number of Y replicates	1	1	1	1
Total number of values	8	8	8	8
Number of missing values	0	0	0	0

3-Ethylquinoline-8-carboxamide (123)



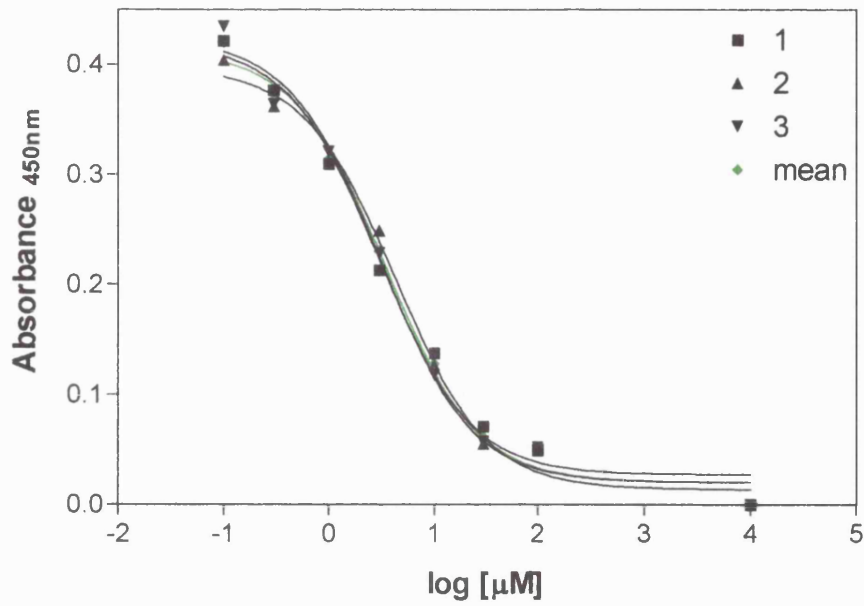
	Data Set-A	Data Set-B	Data Set-C	Data Set-D
Best-fit values				
BOTTOM	0.03926	0.01759	0.02745	0.02927
TOP	1.439	1.279	1.178	1.299
LOGEC50	0.5361	0.5614	0.6417	0.5731
EC50	3.437	3.642	4.383	3.742
Std. Error				
BOTTOM	0.02445	0.03088	0.04202	0.02201
TOP	0.03046	0.03757	0.04743	0.02649
LOGEC50	0.04891	0.06770	0.09731	0.04770
95% Confidence Intervals				
BOTTOM	-0.02359 to 0.1021	-0.06180 to 0.09699	-0.08058 to 0.1355	-0.02733 to 0.08587
TOP	1.360 to 1.517	1.183 to 1.376	1.056 to 1.299	1.231 to 1.367
LOGEC50	0.4104 to 0.6619	0.3873 to 0.7354	0.3915 to 0.8919	0.4505 to 0.6958
EC50	2.573 to 4.591	2.439 to 5.438	2.463 to 7.797	2.822 to 4.963
Goodness of Fit				
Degrees of Freedom	5	5	5	5
R ²	0.9970	0.9942	0.9881	0.9971
Absolute Sum of Squares	0.006763	0.01059	0.01847	0.005337
Sy,x	0.03678	0.04603	0.06078	0.03267
Data				
Number of X values	8	8	8	8
Number of Y replicates	1	1	1	1
Total number of values	8	8	8	8
Number of missing values	0	0	0	0

3-Ethenylquinoline-8-carboxamide (111)



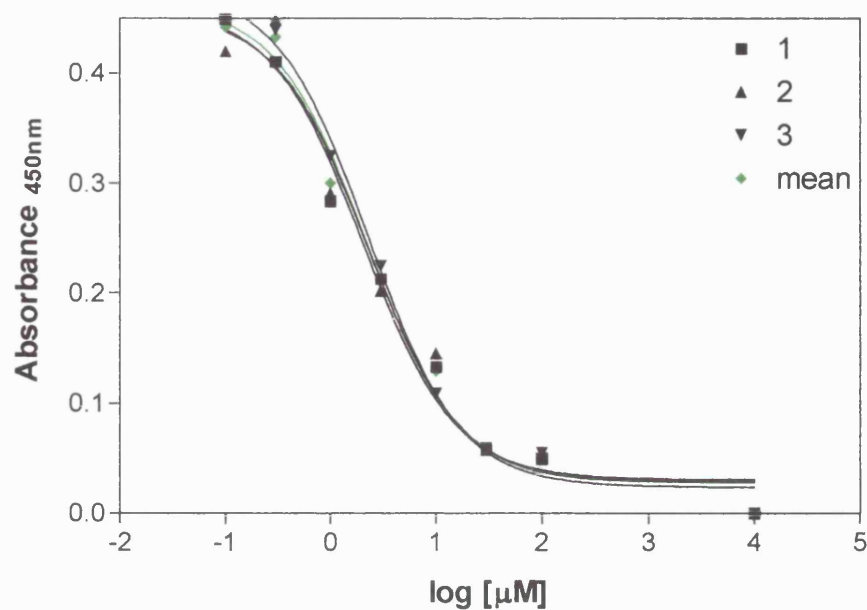
	Data Set-A	Data Set-B	Data Set-C	Data Set-D
Best-fit values				
BOTTOM	0.01758	0.01237	-0.003473	0.009695
TOP	1.219	1.305	1.320	1.282
LOGEC50	0.8013	0.7103	0.7876	0.7635
EC50	6.328	5.133	6.132	5.801
Std. Error				
BOTTOM	0.04484	0.04362	0.06341	0.03599
TOP	0.04386	0.04626	0.06277	0.03639
LOGEC50	0.09218	0.08704	0.1192	0.07116
95% Confidence Intervals				
BOTTOM	-0.09771 to 0.1329	-0.09977 to 0.1245	-0.1665 to 0.1595	-0.08283 to 0.1022
TOP	1.107 to 1.332	1.186 to 1.424	1.158 to 1.481	1.188 to 1.375
LOGEC50	0.5643 to 1.038	0.4866 to 0.9341	0.4812 to 1.094	0.5805 to 0.9464
EC50	3.667 to 10.92	3.066 to 8.593	3.029 to 12.41	3.807 to 8.840
Goodness of Fit				
Degrees of Freedom	5	5	5	5
R ²	0.9891	0.9904	0.9819	0.9935
Absolute Sum of Squares	0.01860	0.01889	0.03758	0.01234
Sy.x	0.06099	0.06146	0.08670	0.04967
Data				
Number of X values	8	8	8	8
Number of Y replicates	1	1	1	1
Total number of values	8	8	8	8
Number of missing values	0	0	0	0

3-Methylquinoline-8-carboxamide (106)



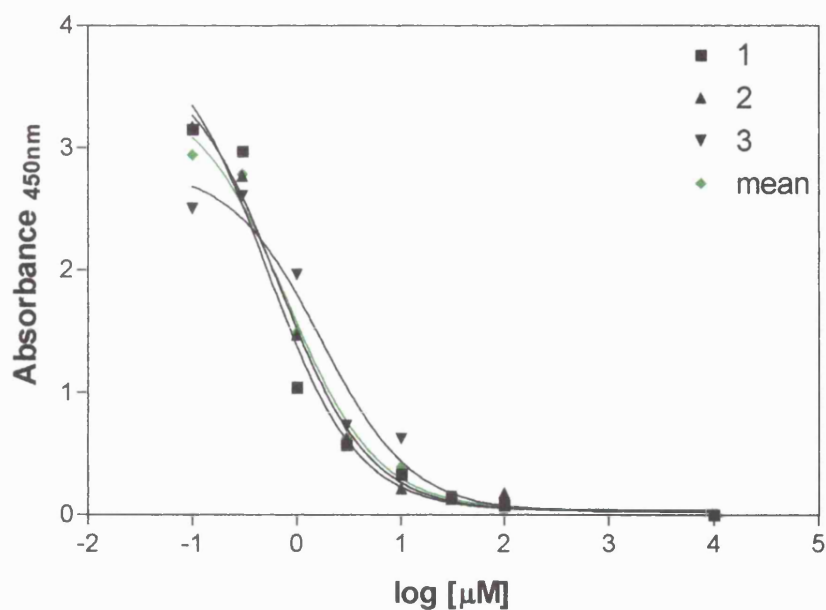
	Data Set-A	Data Set-B	Data Set-C	Data Set-D
Best-fit values				
BOTTOM	0.02707	0.01378	0.02019	0.02030
TOP	0.4204	0.3977	0.4247	0.4137
LOGEC50	0.4726	0.6272	0.4868	0.5311
EC50	2.969	4.238	3.068	3.397
Std. Error				
BOTTOM	0.01255	0.01085	0.01303	0.01103
TOP	0.01662	0.01241	0.01702	0.01381
LOGEC50	0.09210	0.07576	0.09231	0.07871
95% Confidence Intervals				
BOTTOM	-0.005192 to 0.05934	-0.01410 to 0.04167	-0.01330 to 0.05368	-0.008059 to 0.04867
TOP	0.3776 to 0.4631	0.3658 to 0.4296	0.3810 to 0.4685	0.3782 to 0.4492
LOGEC50	0.2359 to 0.7094	0.4324 to 0.8219	0.2495 to 0.7242	0.3287 to 0.7334
EC50	1.721 to 5.122	2.706 to 6.637	1.776 to 5.299	2.132 to 5.413
Goodness of Fit				
Degrees of Freedom	5	5	5	5
R ²	0.9894	0.9927	0.9893	0.9922
Absolute Sum of Squares	0.001865	0.001244	0.001989	0.001382
Sy.x	0.01931	0.01577	0.01995	0.01663
Data				
Number of X values	8	8	8	8
Number of Y replicates	1	1	1	1
Total number of values	8	8	8	8
Number of missing values	0	0	0	0

3-(Prop-1-ynyl)quinoline-8-carboxamide (107)



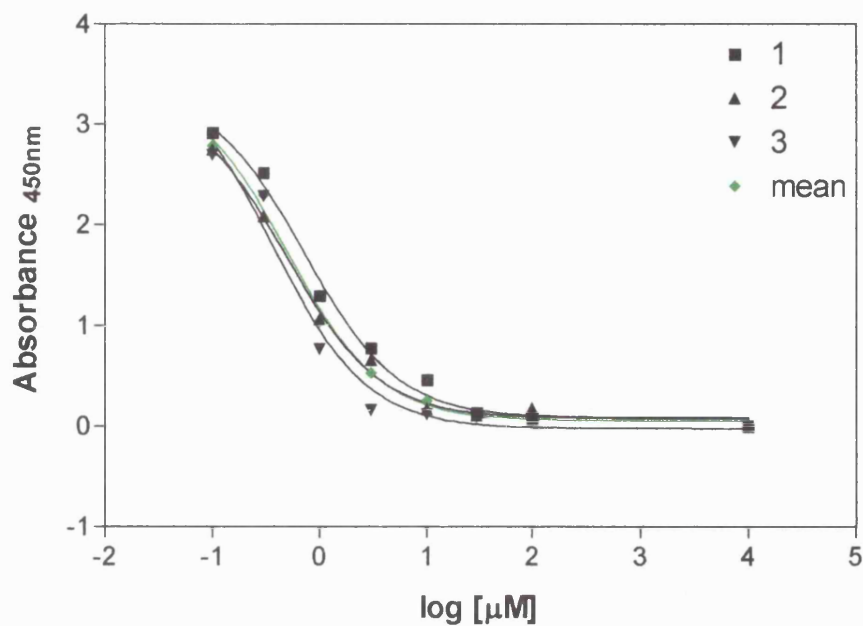
	Data Set-A	Data Set-B	Data Set-C	Data Set-D
Best-fit values				
BOTTOM	0.03064	0.02896	0.02373	0.02771
TOP	0.4606	0.4566	0.4791	0.4653
LOGEC50	0.3070	0.3500	0.3572	0.3388
EC50	2.028	2.239	2.276	2.182
Std. Error				
BOTTOM	0.01593	0.02121	0.01080	0.01447
TOP	0.02491	0.03173	0.01605	0.02190
LOGEC50	0.1163	0.1521	0.07252	0.1021
95% Confidence Intervals				
BOTTOM	-0.01031 to 0.07158	-0.02556 to 0.08348	-0.004047 to 0.05150	-0.009502 to 0.06491
TOP	0.3965 to 0.5246	0.3751 to 0.5382	0.4378 to 0.5204	0.4090 to 0.5216
LOGEC50	0.008154 to 0.6059	-0.04111 to 0.7412	0.1708 to 0.5437	0.07642 to 0.6012
EC50	1.019 to 4.036	0.9097 to 5.511	1.482 to 3.497	1.192 to 3.992
Goodness of Fit				
Degrees of Freedom	5	5	5	5
R ²	0.9833	0.9717	0.9934	0.9871
Absolute Sum of Squares	0.003356	0.005788	0.001495	0.002716
Sy,x	0.02591	0.03402	0.01729	0.02330
Data				
Number of X values	8	8	8	8
Number of Y replicates	1	1	1	1
Total number of values	8	8	8	8
Number of missing values	0	0	0	0

2-Ethylquinoline-8-carboxamide (146)



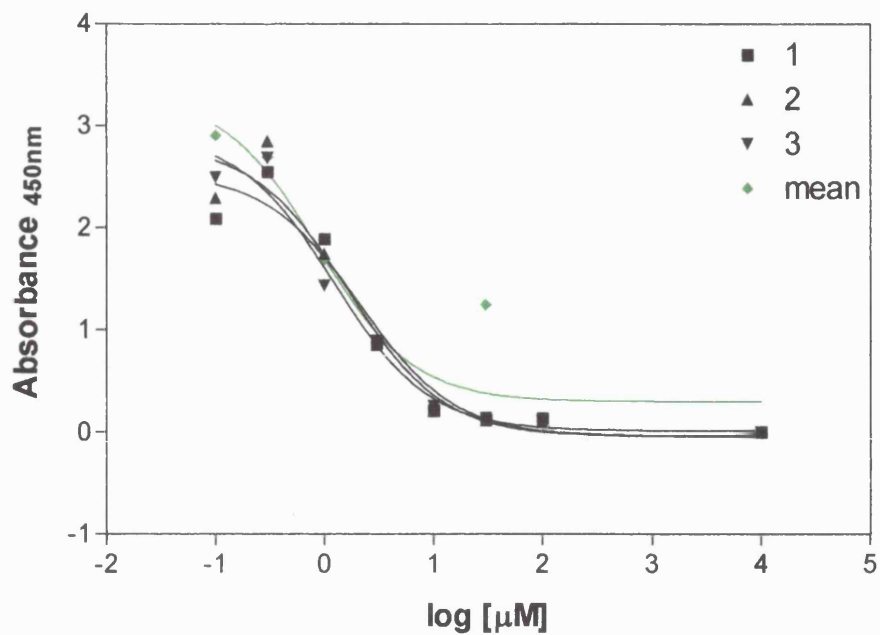
	Data Set-A	Data Set-B	Data Set-C	Data Set-D
Best-fit values				
BOTTOM	0.03320	0.03137	0.02640	0.04094
TOP	3.983	3.748	2.839	3.458
LOGEC50	-0.2862	-0.1755	0.2323	-0.09292
EC50	0.5174	0.6675	1.707	0.8074
Std. Error				
BOTTOM	0.1416	0.06208	0.1296	0.08562
TOP	0.4838	0.1773	0.2195	0.2165
LOGEC50	0.1734	0.07282	0.1507	0.1019
95% Confidence Intervals				
BOTTOM	-0.3308 to 0.3972	-0.1282 to 0.1910	-0.3068 to 0.3596	-0.1792 to 0.2611
TOP	2.740 to 5.227	3.293 to 4.204	2.275 to 3.403	2.902 to 4.015
LOGEC50	-0.7319 to 0.1596	-0.3627 to 0.01169	-0.1551 to 0.6197	-0.3549 to 0.1691
EC50	0.1854 to 1.444	0.4338 to 1.027	0.6996 to 4.165	0.4416 to 1.476
Goodness of Fit				
Degrees of Freedom	5	5	5	5
R ²	0.9691	0.9941	0.9725	0.9881
Absolute Sum of Squares	0.3619	0.06623	0.2329	0.1212
Sy.x	0.2690	0.1151	0.2158	0.1557
Data				
Number of X values	8	8	8	8
Number of Y replicates	1	1	1	1
Total number of values	8	8	8	8
Number of missing values	0	0	0	0

2-Methylquinoline-8-carboxamide (147)



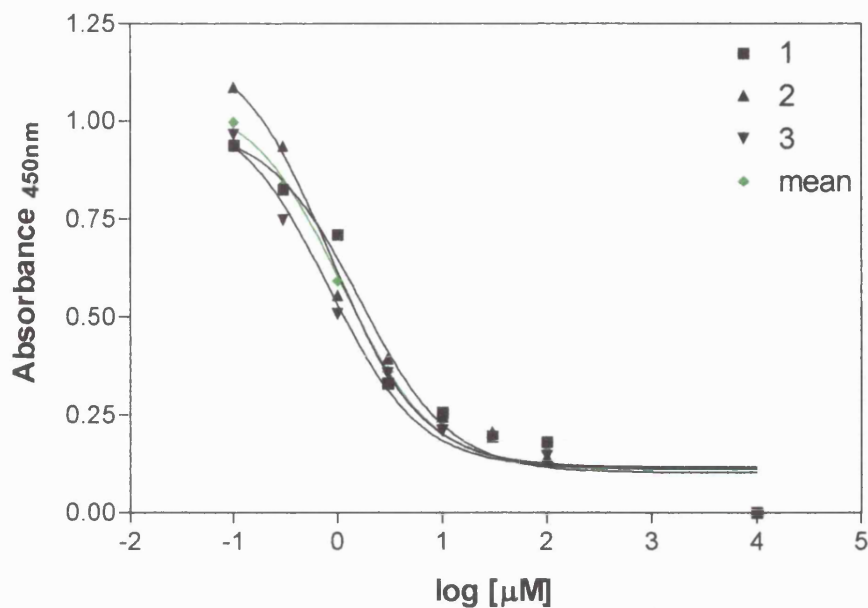
	Data Set-A	Data Set-B	Data Set-C	Data Set-D
Best-fit values				
BOTTOM	0.08290	0.07714	-0.02522	0.05160
TOP	3.362	3.291	3.596	3.413
LOGEC50	-0.1443	-0.3090	-0.4325	-0.3037
EC50	0.7172	0.4909	0.3694	0.4969
Std. Error				
BOTTOM	0.06763	0.04675	0.1050	0.05194
TOP	0.1842	0.1661	0.4692	0.1828
LOGEC50	0.08752	0.07200	0.1645	0.07606
95% Confidence Intervals				
BOTTOM	-0.09097 to 0.2568	-0.04306 to 0.1973	-0.2952 to 0.2448	-0.08192 to 0.1851
TOP	2.888 to 3.836	2.864 to 3.718	2.390 to 4.802	2.943 to 3.883
LOGEC50	-0.3694 to 0.08068	-0.4941 to -0.1239	-0.8554 to -0.009578	-0.4992 to -0.1081
EC50	0.4272 to 1.204	0.3205 to 0.7518	0.1395 to 0.9782	0.3168 to 0.7796
Goodness of Fit				
Degrees of Freedom	5	5	5	5
R ²	0.9914	0.9946	0.9746	0.9940
Absolute Sum of Squares	0.07746	0.03984	0.2114	0.04905
Sy.x	0.1245	0.08927	0.2056	0.09905
Data				
Number of X values	8	8	8	8
Number of Y replicates	1	1	1	1
Total number of values	8	8	8	8
Number of missing values	0	0	0	0

2-Phenylquinoline-8-carboxamide (144)



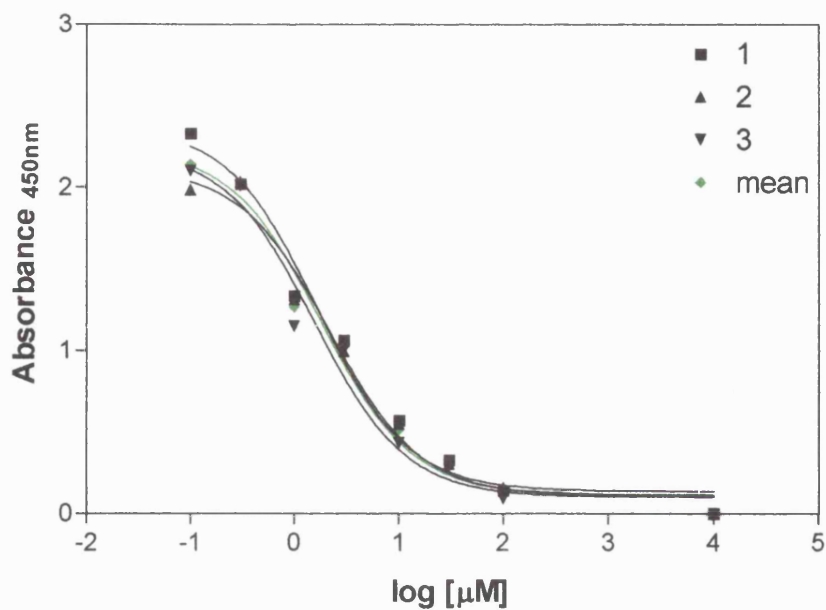
	Data Set-A	Data Set-B	Data Set-C	Data Set-D
Best-fit values				
BOTTOM	-0.04404	-0.04681	0.008908	0.2935
TOP	2.540	2.818	2.915	3.311
LOGEC50	0.3243	0.2169	0.08665	-0.06008
EC50	2.110	1.648	1.221	0.8708
Std. Error				
BOTTOM	0.1587	0.1703	0.1153	0.2503
TOP	0.2438	0.2932	0.2307	0.6046
LOGEC50	0.1910	0.1961	0.1418	0.3288
95% Confidence Intervals				
BOTTOM	-0.4521 to 0.3640	-0.4847 to 0.3911	-0.2876 to 0.3054	-0.3500 to 0.9371
TOP	1.913 to 3.166	2.064 to 3.572	2.322 to 3.508	1.757 to 4.866
LOGEC50	-0.1668 to 0.8154	-0.2873 to 0.7211	-0.2778 to 0.4511	-0.9054 to 0.7853
EC50	0.6810 to 6.537	0.5161 to 5.261	0.5275 to 2.826	0.1243 to 6.099
Goodness of Fit				
Degrees of Freedom	5	5	5	5
R ²	0.9562	0.9543	0.9761	0.8875
Absolute Sum of Squares	0.3297	0.4058	0.2005	1.019
Sy x	0.2568	0.2849	0.2002	0.4514
Data				
Number of X values	8	8	8	8
Number of Y replicates	1	1	1	1
Total number of values	8	8	8	8
Number of missing values	0	0	0	0

2-(4-Methoxyphenyl)quinoline-8-carboxamide (145)



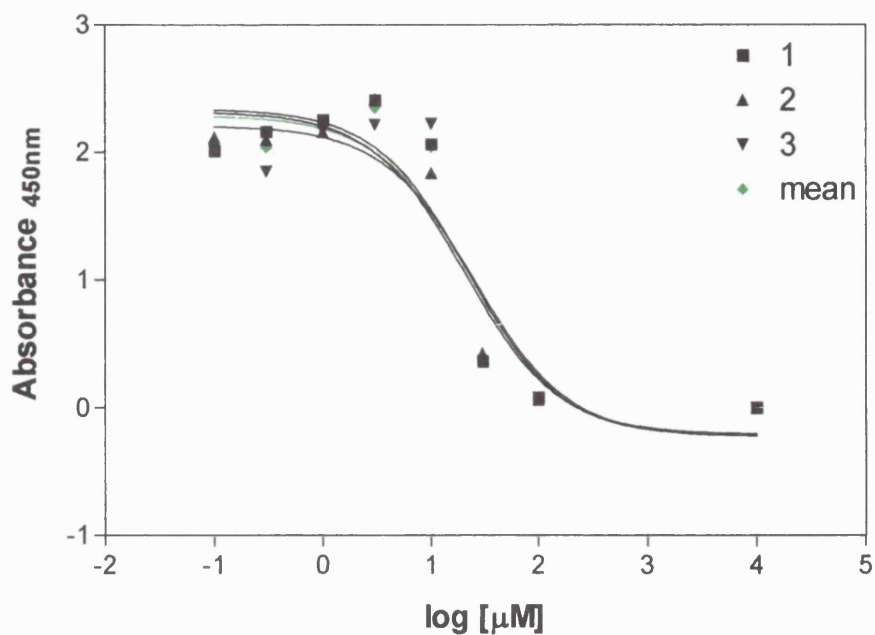
	Data Set-A	Data Set-B	Data Set-C	Data Set-D
Best-fit values				
BOTTOM	0.1019	0.1164	0.1141	0.1099
TOP	0.9871	1.200	1.034	1.061
LOGEC50	0.2093	-0.06940	-0.08082	0.03425
EC50	1.619	0.8523	0.8302	1.082
Std. Error				
BOTTOM	0.04510	0.03888	0.03693	0.03442
TOP	0.07834	0.09514	0.09180	0.07345
LOGEC50	0.1688	0.1432	0.1618	0.1339
95% Confidence Intervals				
BOTTOM	-0.01409 to 0.2178	0.01640 to 0.2163	0.01914 to 0.2090	0.02139 to 0.1984
TOP	0.7857 to 1.188	0.9558 to 1.445	0.7976 to 1.270	0.8720 to 1.250
LOGEC50	-0.2247 to 0.6433	-0.4376 to 0.2988	-0.4968 to 0.3352	-0.3101 to 0.3786
EC50	0.5960 to 4.398	0.3651 to 1.990	0.3185 to 2.164	0.4897 to 2.391
Goodness of Fit				
Degrees of Freedom	5	5	5	5
R ²	0.9658	0.9766	0.9704	0.9789
Absolute Sum of Squares	0.02859	0.02470	0.02241	0.01836
Sy,x	0.07562	0.07029	0.06694	0.06060
Data				
Number of X values	8	8	8	8
Number of Y replicates	1	1	1	1
Total number of values	8	8	8	8
Number of missing values	0	0	0	0

5-AIQ



	Data Set-A	Data Set-B	Data Set-C	Data Set-D
Best-fit values				
BOTTOM	0.1381	0.1090	0.1023	0.1159
TOP	2.377	2.121	2.235	2.240
LOGEC50	0.2225	0.3419	0.1977	0.2564
EC50	1.669	2.198	1.577	1.805
Std. Error				
BOTTOM	0.08561	0.07864	0.09635	0.08178
TOP	0.1465	0.1186	0.1695	0.1349
LOGEC50	0.1257	0.1204	0.1506	0.1242
95% Confidence Intervals				
BOTTOM	-0.08204 to 0.3582	-0.09317 to 0.3112	-0.1454 to 0.3500	-0.09439 to 0.3261
TOP	2.000 to 2.754	1.816 to 2.426	1.800 to 2.671	1.893 to 2.586
LOGEC50	-0.1007 to 0.5457	0.03231 to 0.6516	-0.1896 to 0.5850	-0.06298 to 0.5758
EC50	0.7931 to 3.514	1.077 to 4.483	0.6462 to 3.846	0.8650 to 3.765
Goodness of Fit				
Degrees of Freedom	5	5	5	5
R ²	0.9807	0.9821	0.9726	0.9811
Absolute Sum of Squares	0.1022	0.08003	0.1313	0.09135
Sy.x	0.1430	0.1265	0.1621	0.1352
Data				
Number of X values	8	8	8	8
Number of Y replicates	1	1	1	1
Total number of values	8	8	8	8
Number of missing values	0	0	0	0

8-Carbamoyl-3-phenylquinoline-1-oxide (175)



	Data Set-A	Data Set-B	Data Set-C	Data Set-D
Best-fit values				
BOTTOM	-0.2252	-0.2093	-0.2271	-0.2232
TOP	2.342	2.319	2.209	2.288
LOGEC50	1.347	1.313	1.406	1.359
EC50	22.23	20.56	25.47	22.85
Std. Error				
BOTTOM	0.3736	0.3050	0.4258	0.3603
TOP	0.2398	0.2004	0.2629	0.2305
LOGEC50	0.2822	0.2372	0.3312	0.2779
95% Confidence Intervals				
BOTTOM	-1.186 to 0.7353	-0.9935 to 0.5749	-1.322 to 0.8678	-1.150 to 0.7032
TOP	1.725 to 2.959	1.804 to 2.834	1.533 to 2.885	1.695 to 2.880
LOGEC50	0.6214 to 2.073	0.7034 to 1.923	0.5545 to 2.257	0.6444 to 2.074
EC50	4.182 to 118.2	5.051 to 83.73	3.585 to 180.9	4.409 to 118.5
Goodness of Fit				
Degrees of Freedom	5	5	5	5
R ²	0.8914	0.9218	0.8531	0.8941
Absolute Sum of Squares	0.8597	0.5863	1.075	0.7968
Sy.x	0.4147	0.3424	0.4636	0.3992
Data				
Number of X values	8	8	8	8
Number of Y replicates	1	1	1	1
Total number of values	8	8	8	8
Number of missing values	0	0	0	0

Appendix 3. Raw data for SIRT1 fluorometric activity assay

Nicotinamide

Log [μM]	Fluorescence reading (460 nm)		
	Data Set A	Data Set B	Data Set C
2.0	971	803	1106
1.5	1151	1512	1074
1.0	1092	1525	779
0.5	1256	1138	1364
0.0	1495	1551	1314
-0.5	1241	1202	1017
-1.0	1046	909	1189

5-AIQ

Log [μM]	Fluorescence reading (460 nm)		
	Data Set A	Data Set B	Data Set C
2.0	1949	1661	1895
1.5	1153	1618	1711
1.0	1501	1037	1532
0.5	1017	1191	943
0.0	1473	1249	803
-0.5	928	1260	912
-1.0	1282	301	1231

Quinoline-8-carboxamide (80)

Log [μM]	Fluorescence reading (460 nm)		
	Data Set A	Data Set B	Data Set C
2.0	896	781	894
1.5	1101	1144	1003
1.0	949	921	909
0.5	1100	1143	1061
0.0	1506	1012	895
-0.5	1020	1227	1177
-1.0	1363	1373	1173

3-AB

Log [μM]	Fluorescence reading (460 nm)		
	Data Set A	Data Set B	Data Set C
2.0	991	712	527
1.5	1154	1146	597
1.0	1289	985	1176
0.5	1119	1186	1212
0.0	1291	1358	1089
-0.5	1264	993	1009
-1.0	1324	1279	1206

3-Methylquinoline-8-carboxamide (106)

Log [μ M]	Fluorescence reading (460 nm)		
	Data Set A	Data Set B	Data Set C
2.0	960	885	980
1.5	1077	1309	957
1.0	1039	966	1188
0.5	1501	1370	743
0.0	1497	1644	1119
-0.5	1202	1475	1504
-1.0	1398	1313	1435

2-Phenylquinoline-8-carboxamide (144)

Log [μ M]	Fluorescence reading (460 nm)		
	Data Set A	Data Set B	Data Set C
2.0	835	1140	876
1.5	1211	842	1233
1.0	806	1455	992
0.5	1039	1401	1406
0.0	1206	1295	893
-0.5	1256	1133	1505
-1.0	1148	1476	1411

2-Methylquinoline-8-carboxamide (147)

Log [μ M]	Fluorescence reading (460 nm)		
	Data Set A	Data Set B	Data Set C
2.0	1048	895	634
1.5	1054	1156	702
1.0	1443	618	1142
0.5	871	1390	989
0.0	1303	1239	1197
-0.5	1619	1577	1416
-1.0	1313	1479	1140

Appendix 4. X-ray crystallography data for compound 69

Table A. Crystal data and structure refinement for 69.

Identification code	Compound 69
Empirical formula	C ₁₆ H ₁₂ N ₂ O
Formula weight	248.28
Temperature	150(2) K
Wavelength	0.71073 Å
Crystal system	Monoclinic
Space group	C2/c
Unit cell dimensions	a = 16.2950(4) Å α = 90° b = 11.1110(3) Å β = 108.069(1)° c = 14.3230(4) Å γ = 90°
Volume	2465.34(11) Å ³
Z	8
Density (calculated)	1.338 Mg/m ³
Absorption coefficient	0.085 mm ⁻¹
F(000)	1040
Crystal size	0.50 x 0.50 x 0.13 mm
Theta range for data collection	3.67 to 27.49 °
Index ranges	-21 ≤ h ≤ 21; -14 ≤ k ≤ 14; -18 ≤ l ≤ 18
Reflections collected	17583
Independent reflections	2827 [R(int) = 0.0610]
Reflections observed (>2σ)	2037
Data Completeness	0.995
Absorption correction	None
Refinement method	Full-matrix least-squares on F ²
Data / restraints / parameters	2827 / 2 / 181
Goodness-of-fit on F ²	1.036
Final R indices [I > 2σ(I)]	R ¹ = 0.0471 wR ₂ = 0.1141
R indices (all data)	R ¹ = 0.0712 wR ₂ = 0.1300
Largest diff. peak and hole	0.221 and -0.247 eÅ ⁻³

Table B. Atomic coordinates ($\times 10^4$) and equivalent isotropic displacement parameters ($\text{\AA}^2 \times 10^3$) for **69**.

Atom	x	y	z	U(eq)
O(10)	2768(1)	4066(1)	4685(1)	63(1)
N(1)	3363(1)	2378(1)	2323(1)	35(1)
N(10)	2806(1)	2318(1)	3924(1)	45(1)
C(2)	3552(1)	1912(1)	1570(1)	35(1)
C(3)	3914(1)	2556(1)	938(1)	32(1)
C(4)	4066(1)	3757(1)	1131(1)	33(1)
C(5)	3957(1)	5562(1)	2090(1)	37(1)
C(6)	3748(1)	6073(1)	2854(1)	40(1)
C(7)	3421(1)	5349(1)	3460(1)	37(1)
C(8)	3290(1)	4136(1)	3314(1)	32(1)
C(9)	3502(1)	3585(1)	2511(1)	31(1)
C(10)	2926(1)	3487(1)	4024(1)	36(1)
C(30)	4114(1)	1925(1)	122(1)	32(1)
C(31)	3517(1)	1154(1)	-499(1)	36(1)
C(32)	3713(1)	559(1)	-1251(1)	43(1)
C(33)	4515(1)	703(2)	-1375(1)	47(1)
C(34)	5114(1)	1461(2)	-766(1)	47(1)
C(35)	4915(1)	2084(2)	-25(1)	40(1)
C(4A)	3850(1)	4313(1)	1910(1)	31(1)

Table C. Bond lengths [Å] and angles [°] for **69**.

O(10)-C(10)	1.2366(17)	N(1)-C(2)	1.3160(17)
N(1)-C(9)	1.3724(18)	N(10)-C(10)	1.314(2)
C(2)-C(3)	1.4182(19)	C(3)-C(4)	1.370(2)
C(3)-C(30)	1.4830(18)	C(4)-C(4A)	1.4126(18)
C(5)-C(6)	1.366(2)	C(5)-C(4A)	1.412(2)
C(6)-C(7)	1.404(2)	C(7)-C(8)	1.371(2)
C(8)-C(9)	1.4368(18)	C(8)-C(10)	1.5089(19)
C(9)-C(4A)	1.4206(19)	C(30)-C(31)	1.392(2)
C(30)-C(35)	1.395(2)	C(31)-C(32)	1.383(2)
C(32)-C(33)	1.383(2)	C(33)-C(34)	1.376(3)
C(34)-C(35)	1.388(2)		
C(2)-N(1)-C(9)	118.63(12)	N(1)-C(2)-C(3)	125.02(13)
C(4)-C(3)-C(2)	116.58(12)	C(4)-C(3)-C(30)	123.28(12)
C(2)-C(3)-C(30)	120.14(12)	C(3)-C(4)-C(4A)	120.78(12)
C(6)-C(5)-C(4A)	120.46(13)	C(5)-C(6)-C(7)	119.62(14)
C(8)-C(7)-C(6)	122.67(13)	C(7)-C(8)-C(9)	118.44(13)
C(7)-C(8)-C(10)	116.27(12)	C(9)-C(8)-C(10)	125.29(13)
N(1)-C(9)-C(4A)	120.65(12)	N(1)-C(9)-C(8)	120.48(12)
C(4A)-C(9)-C(8)	118.87(13)	O(10)-C(10)-N(10)	122.49(13)
O(10)-C(10)-C(8)	119.08(14)	N(10)-C(10)-C(8)	118.42(12)
C(31)-C(30)-C(35)	118.89(13)	C(31)-C(30)-C(3)	120.84(12)
C(35)-C(30)-C(3)	120.26(13)	C(32)-C(31)-C(30)	120.46(13)
C(33)-C(32)-C(31)	120.10(15)	C(34)-C(33)-C(32)	120.12(14)
C(33)-C(34)-C(35)	120.14(14)	C(34)-C(35)-C(30)	120.27(15)
C(5)-C(4A)-C(4)	121.80(13)	C(5)-C(4A)-C(9)	119.92(12)
C(4)-C(4A)-C(9)	118.28(13)		

Table D. Anisotropic displacement parameters ($\text{\AA}^2 \times 10^3$) for **69**.

Atom	U11	U22	U33	U23	U13	U12
O(10)	104(1)	46(1)	57(1)	-13(1)	53(1)	-10(1)
N(1)	42(1)	31(1)	35(1)	-2(1)	17(1)	0(1)
N(10)	64(1)	39(1)	43(1)	-8(1)	32(1)	-9(1)
C(2)	41(1)	30(1)	35(1)	-1(1)	15(1)	1(1)
C(3)	31(1)	35(1)	29(1)	1(1)	9(1)	3(1)
C(4)	31(1)	36(1)	30(1)	2(1)	8(1)	-1(1)
C(5)	40(1)	33(1)	34(1)	2(1)	8(1)	-4(1)
C(6)	48(1)	28(1)	39(1)	-5(1)	7(1)	-2(1)
C(7)	39(1)	37(1)	32(1)	-6(1)	7(1)	3(1)
C(8)	32(1)	33(1)	29(1)	-2(1)	7(1)	1(1)
C(9)	29(1)	32(1)	29(1)	-1(1)	6(1)	2(1)
C(10)	38(1)	40(1)	32(1)	-5(1)	12(1)	-1(1)
C(30)	36(1)	31(1)	29(1)	5(1)	11(1)	7(1)
C(31)	41(1)	31(1)	37(1)	1(1)	15(1)	2(1)
C(32)	60(1)	31(1)	37(1)	-1(1)	14(1)	2(1)
C(33)	66(1)	43(1)	38(1)	2(1)	25(1)	15(1)
C(34)	46(1)	56(1)	47(1)	8(1)	25(1)	12(1)
C(35)	38(1)	47(1)	37(1)	1(1)	13(1)	3(1)
C(4A)	30(1)	33(1)	28(1)	0(1)	5(1)	0(1)

Table E. Hydrogen coordinates ($\times 10^4$) and isotropic displacement parameters ($\text{\AA}^2 \times 10^3$) for **69**.

Atom	x	y	z	U(eq)
H(2)	3437	1080	1441	42
H(4)	4319	4222	735	39
H(5)	4176	6050	1677	44
H(6)	3824	6912	2974	48
H(7)	3285	5716	3993	44
H(31)	2970	1035	-405	43
H(32)	3296	50	-1682	51
H(33)	4654	277	-1882	56
H(34)	5665	1558	-853	57
H(35)	5325	2620	384	48
H(10A)	2914(12)	1947(16)	3416(12)	55(5)
H(10B)	2615(11)	1888(14)	4342(12)	46(5)

Appendix 5. X-ray crystallography data for compound 96.

Table A. Crystal data and structure refinement for 96.

Identification code	Compound 96
Empirical formula	C ₁₇ H ₁₁ F ₃ N ₂ O
Formula weight	316.28
Temperature	150(2) K
Wavelength	0.71073 Å
Crystal system	Triclinic
Space group	P-1
Unit cell dimensions	a = 8.0440(3)Å α = 83.548(1)° b = 9.1370(3)Å β = 81.155(2)° c = 9.8910(4)Å γ = 76.326(2)°
Volume	695.77(4) Å ³
Z	2
Density (calculated)	1.510 Mg/m ³
Absorption coefficient	0.123 mm ⁻¹
F(000)	324
Crystal size	0.35 x 0.20 x 0.15 mm
Theta range for data collection	3.86 to 28.33°
Index ranges	-10 ≤ h ≤ 10; -12 ≤ k ≤ 12; -13 ≤ l ≤ 13
Reflections collected	10349
Independent reflections	3395 [R(int) = 0.0360]
Reflections observed (>2σ)	2602
Data Completeness	0.979
Refinement method	Full-matrix least-squares on F ²
Data / restraints / parameters	3395 / 2 / 217
Goodness-of-fit on F²	1.030
Final R indices [>2σ(I)]	R ¹ = 0.0432 wR ₂ = 0.1093
R indices (all data)	R ¹ = 0.0629 wR ₂ = 0.1202
Largest diff. peak and hole	0.365 and -0.386 eÅ ⁻³

Table B. Atomic coordinates ($\times 10^4$) and equivalent isotropic displacement parameters ($\text{\AA}^2 \times 10^3$) for **96**.

Atom	x	y	z	U(eq)
C(2)	6260(2)	3862(1)	2441(1)	28(1)
C(3)	7359(2)	2423(1)	2225(1)	26(1)
C(4)	8412(2)	2291(1)	993(1)	27(1)
C(4A)	8394(2)	3537(1)	15(1)	25(1)
C(5)	9435(2)	3422(1)	-1275(1)	29(1)
C(6)	9427(2)	4661(2)	-2182(1)	31(1)
C(7)	8400(2)	6073(1)	-1823(1)	29(1)
C(8)	7336(2)	6244(1)	-594(1)	26(1)
C(8A)	7291(2)	4947(1)	355(1)	24(1)
C(9)	6334(2)	7829(1)	-332(1)	29(1)
C(31)	7288(2)	1076(1)	3210(1)	25(1)
C(32)	7018(2)	-197(1)	2688(1)	28(1)
C(33)	6913(2)	-1510(1)	3511(1)	30(1)
C(34)	7060(2)	-1580(1)	4892(1)	31(1)
C(35)	7339(2)	-342(1)	5441(1)	30(1)
C(36)	7461(2)	976(1)	4616(1)	27(1)
C(37)	7777(2)	2257(2)	5288(1)	33(1)
O(1)	6766(1)	8907(1)	-1066(1)	42(1)
N(1)	6219(1)	5065(1)	1576(1)	28(1)
N(2)	5015(2)	8008(1)	660(1)	32(1)
F(1)	8853(1)	3019(1)	4502(1)	40(1)
F(2)	6317(1)	3296(1)	5635(1)	47(1)
F(3)	8465(1)	1789(1)	6454(1)	51(1)

Table C. Bond lengths [Å] and angles [°] for **96**.

C(2)-N(1)	1.3118(16)	C(2)-C(3)	1.4184(17)
C(3)-C(4)	1.3726(17)	C(3)-C(31)	1.4879(16)
C(4)-C(4A)	1.4076(17)	C(4A)-C(5)	1.4141(17)
C(4A)-C(8A)	1.4231(16)	C(5)-C(6)	1.3624(17)
C(6)-C(7)	1.4078(18)	C(7)-C(8)	1.3756(17)
C(8)-C(8A)	1.4306(16)	C(8)-C(9)	1.5103(17)
C(8A)-N(1)	1.3712(15)	C(9)-O(1)	1.2420(15)
C(9)-N(2)	1.3224(17)	C(31)-C(32)	1.3978(17)
C(31)-C(36)	1.4095(17)	C(32)-C(33)	1.3842(17)
C(33)-C(34)	1.3816(18)	C(34)-C(35)	1.3863(18)
C(35)-C(36)	1.3916(17)	C(36)-C(37)	1.4976(18)
C(37)-F(3)	1.3383(15)	C(37)-F(1)	1.3396(15)
C(37)-F(2)	1.3499(16)		
N(1)-C(2)-C(3)	124.99(11)	C(4)-C(3)-C(2)	116.49(11)
C(4)-C(3)-C(31)	120.57(11)	C(2)-C(3)-C(31)	122.72(11)
C(3)-C(4)-C(4A)	120.89(11)	C(4)-C(4A)-C(5)	121.98(11)
C(4)-C(4A)-C(8A)	118.17(11)	C(5)-C(4A)-C(8A)	119.85(11)
C(6)-C(5)-C(4A)	120.51(11)	C(5)-C(6)-C(7)	119.78(11)
C(8)-C(7)-C(6)	122.15(11)	C(7)-C(8)-C(8A)	118.81(11)
C(7)-C(8)-C(9)	116.51(11)	C(8A)-C(8)-C(9)	124.65(11)
N(1)-C(8A)-C(4A)	120.62(11)	N(1)-C(8A)-C(8)	120.58(11)
C(4A)-C(8A)-C(8)	118.79(11)	O(1)-C(9)-N(2)	122.69(11)
O(1)-C(9)-C(8)	118.77(11)	N(2)-C(9)-C(8)	118.53(11)
C(32)-C(31)-C(36)	117.48(11)	C(32)-C(31)-C(3)	116.78(10)
C(36)-C(31)-C(3)	125.74(11)	C(33)-C(32)-C(31)	121.87(12)
C(34)-C(33)-C(32)	119.85(12)	C(33)-C(34)-C(35)	119.81(11)
C(34)-C(35)-C(36)	120.52(12)	C(35)-C(36)-C(31)	120.45(11)
C(35)-C(36)-C(37)	117.13(11)	C(31)-C(36)-C(37)	122.42(11)
F(3)-C(37)-F(1)	106.12(11)	F(3)-C(37)-F(2)	105.70(10)
F(1)-C(37)-F(2)	105.75(10)	F(3)-C(37)-C(36)	112.16(11)
F(1)-C(37)-C(36)	113.72(10)	F(2)-C(37)-C(36)	112.76(11)
C(2)-N(1)-C(8A)	118.76(10)		

Table D. Anisotropic displacement parameters ($\text{\AA}^2 \times 10^3$) for **96**.

Atom	U11	U22	U33	U23	U13	U12
C(2)	31(1)	26(1)	26(1)	-1(1)	1(1)	-7(1)
C(3)	28(1)	24(1)	26(1)	0(1)	-5(1)	-7(1)
C(4)	30(1)	22(1)	28(1)	-3(1)	-4(1)	-5(1)
C(4A)	28(1)	25(1)	25(1)	-1(1)	-5(1)	-8(1)
C(5)	34(1)	26(1)	27(1)	-4(1)	-1(1)	-6(1)
C(6)	37(1)	34(1)	22(1)	-3(1)	0(1)	-10(1)
C(7)	33(1)	28(1)	26(1)	2(1)	-7(1)	-10(1)
C(8)	27(1)	25(1)	26(1)	0(1)	-7(1)	-7(1)
C(8A)	26(1)	25(1)	23(1)	-2(1)	-5(1)	-7(1)
C(9)	33(1)	26(1)	27(1)	2(1)	-8(1)	-5(1)
C(31)	24(1)	24(1)	26(1)	-1(1)	0(1)	-4(1)
C(32)	29(1)	27(1)	26(1)	-1(1)	-3(1)	-5(1)
C(33)	30(1)	24(1)	34(1)	-1(1)	-2(1)	-6(1)
C(34)	30(1)	26(1)	34(1)	6(1)	-3(1)	-6(1)
C(35)	29(1)	32(1)	26(1)	2(1)	-2(1)	-5(1)
C(36)	25(1)	27(1)	26(1)	-1(1)	-1(1)	-4(1)
C(37)	38(1)	33(1)	27(1)	-1(1)	-3(1)	-8(1)
O(1)	53(1)	26(1)	40(1)	6(1)	6(1)	-4(1)
N(1)	31(1)	25(1)	26(1)	0(1)	-2(1)	-5(1)
N(2)	36(1)	23(1)	34(1)	0(1)	-3(1)	-3(1)
F(1)	46(1)	41(1)	38(1)	-2(1)	-4(1)	-22(1)
F(2)	46(1)	39(1)	54(1)	-20(1)	5(1)	-6(1)
F(3)	79(1)	48(1)	33(1)	0(1)	-22(1)	-24(1)

Table E. Hydrogen coordinates ($\times 10^4$) and isotropic displacement parameters ($\text{\AA}^2 \times 10^3$) for **96**.

Atom	x	y	z	U(eq)
H(2)	5495	3963	3276	34
H(4)	9162	1346	797	32
H(5)	10145	2473	-1511	35
H(6)	10112	4572	-3054	37
H(7)	8443	6935	-2449	35
H(32)	6904	-160	1743	33
H(33)	6740	-2362	3128	36
H(34)	6971	-2473	5462	37
H(35)	7449	-393	6389	36
H(2A)	4840(20)	7207(14)	1222(15)	49(5)
H(2B)	4416(19)	8942(12)	766(16)	46(4)